Dublin City University
Ollscoil Chathair Bhaile Átha Cliath

DEVELOPMENT OF A POINT-OF-CARE BREATH AMMONIA DEVICE AND ITS APPLICATION TO NON-INVASIVE MONITORING OF HAEMODIALYSIS PATIENTS

by
Mr. Troy Hibbard

Supervisors:
Prof. Anthony J. Killard
& Prof. Malcolm R. Smyth

Thesis submitted for the Degree of Doctor of Philosophy (Ph.D.)
August 2012

Biomedical Diagnostics Institute
School of Chemical Sciences
National Centre for Sensor Research

DECLARATION OF WORK

"I hereby certify that this material, which I now submit for assessment on the programme of study leading to the award of Ph.D. is entirely my own work, that I have exercised reasonable care to ensure that the work is original, and does not to the best of my knowledge breach any law of copyright, and has not been taken from the work of others save and to the extent that such work has been cited and acknowledged within the text of my work".

Candidate Signature (Troy Hibbard)

_____

Student ID Number (57210806)

_____

Submission Date (August 2012)

_____

DEDICATION

This thesis is dedicated to my family.

You have always been by my side and I am eternally grateful!

ACKNOWLEDGEMENTS

For as long as I can remember, I have always had a love for science. It is because of this that I am deeply grateful to my supervisors Anthony J. Killard and Malcolm R. Smyth for providing me with an opportunity to make a contribution to the world of science. Without their guidance, this journey would not have been possible. During this time, I seemed to have new questions every day. Luckily, Karl Crowley was always available to share his expertise in the areas of chemistry and physics. Furthermore, I am thankful to Leanne Harris who always gave time to answer my day-to-day questions on scientific technique. With the engineering, I would like to thank Zahra Shahbazian, Stephen Beirne, and Brendan Heery for their input and unique perspectives. Thank you to the Masters students, Orla Smith and Ihuoma Osuji, who assisted me in the lab during their time at DCU. I am thankful to Aoife Morrin for helping me to understand how to strengthen my thesis during the mid-viva examination. Also, I would like to thank Norman Ratcliffe and Fiona Regan for taking the time to examine my research and discuss it with me during my final viva examination. It was truly enjoyable to meet all of the staff from the Biomedical Diagnostics Institute and the School of Chemical Sciences. Their interests in my research and kind words were motivational. The help given by the team at St. Vincent's University Hospital was essential to organising the clinical trials, and I am appreciative of the effort they put in to this work. I wish to express my gratitude to all of the people who supplied the equipment necessary to complete this project, and to Enterprise Ireland for supporting this project under grant number TD/2008/0140. To my friends, Robby Strotman, Tim Fox, Karl Egan, Andrea Minari, and Ann-Marie Dolan, I always knew I could count on you when I needed to talk. To Melanie Koch and her family, you have always been supportive and made me feel at home here. To my family, Donna, Michael, Jennifer, Jean, and Pappa, you have always believed in me. I would never have made it this far without you. I cannot begin to thank you enough.

TABLE OF CONTENTS (1)

TABLE OF CONTENTS (2)

TABLE OF CONTENTS (3)

TABLE OF CONTENTS (4)

TABLE OF CONTENTS (5)

TABLE OF CONTENTS (6)

TABLE OF CONTENTS (7)

GLOSSARY OF ABBREVIATIONS (1)

AmBeR = Ammonia Breath Monitor

APCI-MS = Atmospheric Pressure Chemical Ionisation – Mass Spectrometry

BUN = Blood Urea Nitrogen

CAPD = Continuous Ambulatory Peritoneal Dialysis

CRDS = Cavity Ring Down Spectroscopy

EBC = Exhaled Breath Condensate

GC-IMS = Gas Chromatography – Ion Mobility Spectrometry

GCS = Glasgow Coma Scale

GFR = Glomerular Filtration Rate

Kt/V = Dialysis Clearance Ratio

IDE = Inter-digitated Electrode

IDMS = Isotope Dilution Mass Spectrometry

IMS = Ion Mobility Spectrometry

LIF = Laser Induced Fluorescence

MCC = Multi Capillary Column

MWCNT = Multi Wall Carbon Nano Tubes

μCP = Micro-contact Printing

NIST = National Institute of Standards and Technology

OFC-CEAS = optical frequency comb cavity – enhanced absorption spectroscopy

PALS = Photoacoustic Laser Spectroscopy

PC = Plasma Chromatography

PET = Polyethylene Terephthalate

PPB = Parts-Per-Billion

PPBV = Parts-Per-Billion by Volume

PPM = Parts-Per-Million

PPT = Parts-Per-Trillion

PTFE = Polytetrafluoroethylene

PTR-MS = Proton Transfer Reaction – Mass Spectrometry

QCM = Quartz Crystal Microbalance

RH = Relative Humidity

SIFT-MS = Selected Ion Flow Tube – Mass Spectrometry

GLOSSARY OF ABBREVIATIONS (2)

SPME = Solid Phase Micro Extraction

SWCNT = Single Wall Carbon Nano Tubes

TDLAS = Tunable Diode Laser Absorption Spectroscopy

TMT = Trail Making Test

UBT = Urea Breath Test

URR = Urea Reduction Ratio

USRDS = United States Renal Data System

VIPA = Virtually Imaged Phase Array

VC = Volatile Compound

VSC = Volatile Sulphur Compound

WHC = West Haven Criteria

PRESENTATIONS AND PUBLICATIONS (1)

Oral Presentations

- **MSc Biomedical Diagnostics - Lecture on Advances in Diagnostic Technology**
  Electrochemical Sensors and the Essentials of Biomedical Research
  School of Chemical Sciences, X146, DCU, Ireland on March 29, 2012

- **Centre for Talented Youth – Lecture on Biomedical Diagnostics**
  Electrochemical Sensors and the Essentials of Biomedical Research
  School of Chemical Sciences, X146, DCU, Ireland on July 6, 2011

- **BDI Annual Retreat**
  Electrochemical Sensors for the Detection of Ammonia in Breath
  Castleknock Hotel, Dublin, Ireland on April 1, 2011

- **MSc Biomedical Diagnostics Module – Thesis in Three Minutes**
  Every Breath You Take… Towards Analysis of Health Dysfunction
  School of Chemical Sciences, X146, DCU, Ireland on February 24, 2011

- **Innovation Dublin, Thesis in Three: Elevator Pitch for your Ph.D.**
  Every Breath You Take… Towards Analysis of Health Dysfunction
  Sugar Club, Dublin, Ireland on November 17, 2010*

  *1st place presentation winner for novel commercialisation aspects

- **Engineering Conferences International (ECI), Exhaled Breath Analysis: From Sensors to Devices and Applications**
  Electrochemical Sensors for the Detection of Ammonia in Breath
  Il Ciocco Hotel and Conference Centre, Barga, Italy from October 24 to 29, 2010

Poster Presentations

- **The 2nd International Conference on Bio-Sensing Technology**
  Printed Polyaniline-Modified Interdigitated Electrodes for Detection and Quantification of Ammonia in Breath
  NH Grand Hotel Krasnapolsky, Amsterdam, the Netherlands from October 10 to 12, 2011

- **Printed Functional Materials 2011**
  Printing of Polyaniline Nanoparticle Electrodes for Detection and Quantification of Ammonia in Breath
  National Centre for Sensor Research, DCU, Ireland on September 12, 2011

- **Eirelec '11: Electrochemistry – The Future?**
  Electrochemical Sensors for the Monitoring of Ammonia in Human Breath
  Dunraven Arms Hotel, Co. Limerick, Ireland from May 16 to 18, 2011

PRESENTATIONS AND PUBLICATIONS (2)

- **The 6th Conference on Analytical Sciences in Ireland (CASi)**
  Electrochemical Sensors for the Monitoring of Ammonia in Human Breath
  The Helix, DCU, Ireland from February 21 to 22, 2011

- **International Society of Electrochemistry (ISE), 61st Annual Meeting**
  Investigation of an Ink-jet Printed Gas Sensor for Detection and Quantification of Ammonia in Human Breath
  Nice, France from September 26 to October 1, 2010

Technology Showcase Presentations

- **Organic Electronics Association**
  BDI, Dublin City University, Dublin, Ireland on September 13, 2011

- **Labour Party Press Release**
  BDI, Dublin City University, Dublin, Ireland on February 7, 2011

- **Best Practice in the Translation of Medical Technology Research**
  Helix, Dublin City University, Dublin, Ireland on November 23 to 25, 2010

- **Big Ideas Technology Showcase**
  Croke Park, Dublin, Ireland on October 20, 2010

Publications

- Hibbard, T.; Crowley, K.; Shahbazian, Z.; and Killard, A.J. (2012) "A system for the continuous generation of simulated human breath supplemented with trace gases", *Analytical Methods*, Vol. 4 (Issue 7) Pp. 2172 – 2176.

- Hibbard, T. and Killard, A.J. (2011) "Breath ammonia levels in a normal human population study as determined by photoacoustic laser spectroscopy", *The Journal of Breath Research*, Vol. 5 (Issue 3) P. 037101*

  *Special Issue: Exhaled Breath Analysis: From Sensors to Devices and Applications

- Hibbard, T. and Killard, A. J. (2011) "Breath Ammonia Analysis: Clinical Application and Measurement", *Critical Reviews in Analytical Chemistry*, Vol. 41 (Issue 1) Pp. 21 – 35.

ABSTRACT

Initial investigation into diagnostic breath ammonia monitoring, and the current status of technology, indicated that breath analysis would have great potential as a non-invasive means of diagnosis. The ideal breath ammonia monitoring device would be one that is sensitive to the specific gas and capable of detecting it at the physiologically relevant concentrations in the ppb range with (1) good precision and accuracy, (2) insensitivity to interferences, (3) is ideally portable for point-of-care use, (4) provides ease-of-use to the user, (5) displays real-time measurements, and (6) is of low cost. To begin assessment, the normal range of human breath ammonia was defined via photoacoustic laser spectroscopy (PALS) which identified baseline concentrations to be from 29 to 688 ppb. Following this, a system was developed to simulate breath interferents such as humidity and temperature over a human range encompassing normal and abnormal breath ammonia concentrations (18 to 2,993 ppb). This instrumentation assisted in evaluating the performance of an ammonia sensitive electrode based on print-fabrication technology and polyaniline nanoparticles. The electrodes displayed an intra-variability from 0.05 to 1.67%, and generated a 0.99 correlation across a range of 40 to 2,175 ppbv ammonia (LOD=6.3 ppbv) fulfilling the analytical and biomedical requirements necessary for sensing ammonia in exhaled breath. Having optimised the ammonia sensor, a breath sampling system (AmBeR) was engineered and optimised which was capable of performing measurement of breath ammonia at the point-of-care. Observations of breath from a healthy population demonstrated a 0.97 correlation between AmBeR and PALS. Clinical evaluation followed in a haemodialysis patient cohort. While the clinical results did not show strong population correlations with measures of blood nitrogen (r=0.64 BUN, r=0.62 creatinine, $p<0.01$), it did show strong significant intra-individual correlations (range 0.86 - 0.96 with BUN, 0.78 - 0.97 with creatinine) which may indicate potential for clinical application.

LIST OF FIGURES (1)

LIST OF FIGURES (2)

LIST OF FIGURES (3)

LIST OF TABLES

CHAPTER 1

INTRODUCTION TO BREATH AMMONIA ANALYSIS: CLINICAL APPLICATION AND MEASUREMENT

1.1 Current status of clinical breath analysis

The diagnostic potential of clinical breath analysis has been recognised for centuries. It is said that the original research can be found within the writings of Hippocrates [1]. However, the dynamics of oxygen inhalation and absorption via the lungs followed by exhalation of carbon dioxide were not pieced together until 1784 when Lavoisier examined respiration via calorimetry [2]. By the 1950s, separation of individual gas molecules became possible with gas chromatography [3]. Since then, more and more compounds found in human breath have been linked to physiological conditions. For example, acetone has been linked to diabetes, whereas ammonia is indicative of liver and/or kidney dysfunction. Human breath is a highly complex substance with numerous variables that can interfere with one another. Each human breath contains over 1,000 trace volatile compounds (VCs) [4]. On average, exhaled human breath is a mixture of 78.6% (w/v) nitrogen, 16% (w/v) oxygen, 4.5% (w/v) carbon dioxide, and 0.9% (w/v) inert gases and VCs [5]. This mixture is exhaled at temperatures between 34^{o}C [6] and 37^{o}C [7] while relative humidity may range from 91% to 96% in oral exhalations, and from 82% to 85% in nasal exhalations [8]. Human breath cannot have a relative humidity above 99% since 100% implies that the water has gone from the vapour to the condensed phase [9]. Additional respiratory variables such as flow rate and lung volume must also be considered when making measurements of trace gases in breath, and these can vary according to an individual's height, weight, age, and body surface area [10]. Essentially, larger volumes have the potential for a greater mass of gas. Flow rates are required in order to calculate the concentration of gas present. Several parameters are important for exhaled flow rate and volume analysis:

- **Forced vital capacity** is a volume measurement where the full volume of inhaled air is added to the full volume of forced exhaled breath [5].
- **Minute volume** (or maximum voluntary ventilation - MVV) is a volume-to-rate measurement of the litres of breath exhaled over a period of one minute [5].
- **Peak expiratory flow** is a rate measurement performed by calculating how fast the breath volume can be forced out of the lungs [5].

Calculations and values can be found in any number of spirometry related articles such as those published by the American Thoracic Society [21], Bass [22], Tomlinson [23], and Quanjer [24]. Within the 0.9% (w/v) of breath which constitutes inert gases and VCs, the individual gas concentrations can range between parts-per-million (ppm) and parts-per-trillion (ppt). Some of the gases that have been detected so far down to parts-per-billion (ppb) levels are shown in Table 1.1. Of these gases, ammonia has attracted increasing interest for clinical diagnostics such as in haemodialysis monitoring [16], asthma assessment [25], diagnosis of hepatic encephalopathy [26], detection of *Helicobacter pylori* [27], and analysis of halitosis [28]. The physiological range expected for human breath ammonia is in the region of 50 to 2,000 ppb [27]. To be effective, analytical techniques for breath ammonia quantification must be capable of a limit of detection of some 50 ppb. While there are several analytical technologies capable of this, they also possess many limitations for application in clinical settings. While it is true that these techniques are moving from invasive to non-invasive, most detection methods are still extremely complex instrumental systems and require special training to use. Aside from breath analysis, other non-invasive techniques based on the analysis of urine, saliva, hair, and nails may also offer potential solutions [1]. With regard to breath analysis, however, development of breath monitors that are simple and portable for point-of-care use is a critical next step. Furthermore, the possibility of performing real-time analysis of breath has recently become a reality. Originally, breath analysis depended on collection of exhaled breath condensate (EBC) which was placed within the detection region of a device [14]. However, by collecting breath samples into containers such as balloons, samples undergo

Table 1.1 Concentrations of Gases in Human Breath

Breath gas	Concentration range (ppb)	Reference
Acetaldehyde	2 - 5	[11]
	6 - 33	[12]
Acetone	293 - 870	[11]
	200 - 2,000	[12]
Ammonia	50 - 2,000	[13]
	559 - 639	[14]
	425 - 1,800	[15]
	422 - 2,389	[11]
	200 - 2,000	[12]
(Pre-dialysis)	1,500 - 2,000	[16]
(Post-dialysis)	200 - 300	[16]
Carbon dioxide	30 - 40,000,000	[17, 18]
Ethanol	27 - 153	[11]
	100 - 3,358	[12]
Hydrogen cyanide	2 - 12	[12]
Isoprene	55 - 121	[11]
Methanol	32 – 1,684	[19]
Nitric oxide	6 - 31	[6, 20]
Propanol	0 - 135	[19]

significant losses and contamination [29]. Typically, collection of EBC is only recommended if pH analysis of breath compounds is necessary [30].

1.2 Ammonia metabolism and the urea cycle

When food is ingested, a fine balance of nutritional absorption and toxin removal takes place. The body must be specific about how amino acids are processed, or nitrogenous compound concentrations could prove fatal. Initially, the stomach and intestines break down food into amino acids, nucleotide bases, and other nitrogenous compounds which diffuse into the blood [31]. These excess nitrogenous compounds are then absorbed from the blood into the liver. The liver converts them into less toxic soluble forms which can be safely removed in relatively low volumes of water. In mammals, this less toxic form is urea. The urea cycle, as it applies to humans, is the pathway upon which amino acids are effectively broken down (Fig. 1.1).

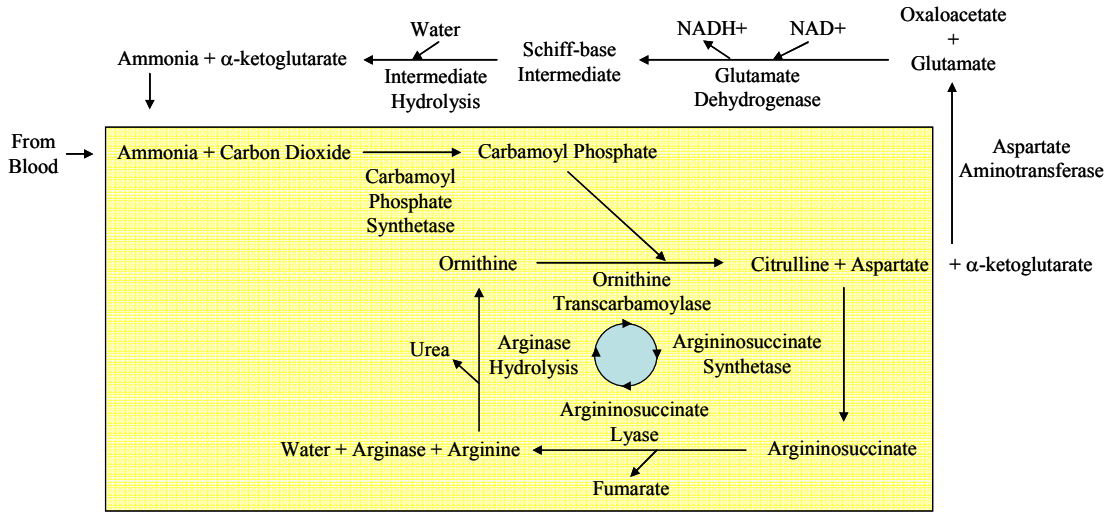

Figure 1.1 The urea cycle. Taking place in the liver (yellow box), the urea cycle breaks down nitrogenous compounds such as ammonia into the less toxic form of urea. The processes of transamination and oxidative deamination also allow for the conversion of aspartate into free ammonia [32]**.**

Ammonia is first absorbed into the liver and combined with carbon dioxide to form carbamoyl phosphate. This enters the urea cycle and combines with ornithine to form citrulline. Amino acids are fed into the cycle via their transamination by aspartate which combines with citrulline to form argininosuccinate [33]. Aspartate also acts to drive the availability of free ammonia which is used in the initial steps with carbon dioxide [32].

Argininosuccinate is then split into fumarate (which is fed into the citric acid cycle) and arginine. Arginine then reacts with arginase and water to produce urea and regenerated ornithine [31]. As the liver finishes processing, the urea is excreted into the bloodstream among excess ammonia and is absorbed by the kidneys via the glomerulus. The typical glomerular filtration rate (GFR) is about 0.125 L/min creating 1 to 2 Litres of urine a day [32], while excess water is recycled back into the body. However, this rate decreases if the concentration of materials is high enough to impede absorption. Kidneys serve the purpose of filtering the blood urea and excess ammonia out of the body in the form of urine [33]. Normal concentrations of ammonia in blood range between 120 ppb (12 μg/dl) and 660 ppb (66 μg/dl) [34]. However, if the liver loses the ability to enzymatically break down nitrogenous compounds, or the kidneys can no longer remove them from the blood, then complications such as hyperammonaemia [31], hepatic encephalopathy [35], and / or uraemia [32] can arise. In order to monitor these levels, current methods depend on invasively measuring the nitrogen concentration found within the urea in the blood (i.e. blood urea nitrogen, BUN) [16].

1.3 Current and potential clinical applications for breath ammonia monitoring

Clinically, several conditions are related to changes of blood nitrogen levels and consequently ammonia levels. These are impairments in relation to the liver, brain, kidneys, stomach, duodenum, oral cavity, and lungs. In all cases, if ammonia levels in the blood are of a higher concentration than those found in the air, then ammonia can diffuse out of the blood and into the lungs [36]. Doing so allows for potential clinical measurements of blood ammonia from a non-invasive perspective.

1.3.1 Hepatic encephalopathy

With reference to the organs involved in nitrogen metabolism, the liver and kidneys are central to the proper removal of ammonia from the body. If there is a problem associated with either of these, ammonia levels in the blood may escalate to toxic levels. With liver dysfunction, the result is hyperammonaemia (i.e. increased ammonia in blood) which has further consequences including damage to brain tissue (i.e. hepatic encephalopathy) [31]. Studies have shown a 0.61 correlation between arterial ammonia levels and severity of hepatic encephalopathy [37]. Normally, the brain is protected by a blood-brain barrier that prevents toxins from entering. However, if there is an obstruction in the synthesis of the

urea cycle, components are created that can modify the permeability of the blood-brain barrier. An example of a compound that can do this is glutamine. During the transamination process of the urea cycle, glutamate is capable of joining with excess ammonia via glutamine synthetase to create glutamine. Glutamine in elevated levels is then able to change the osmotic tendencies around brain tissue resulting in swelling of the brain [31]. This swelling is due to higher concentrations of toxins outside the barrier flowing into the lower concentrated area of the brain. Included in this flow would be ammonia if levels in the blood were high. By entering the brain, ammonia is capable of modifying the gene expression and signal transmission of astrocytes and neurons. Such modifications primarily induce type 2 Alzheimer's disease. Though glutamine production can cause damage to the brain, its production may also be able to prevent cell damage. Astrocytes can generate glutamine synthetase which catalyses the reaction of ammonia with glutamate so as to reduce the ammonia levels. However, this would not reduce the swelling nor assist much with the already effected neurons [35]. Methods for analysis involve taking blood measurements for ammonia levels and correlating the data against known neuropsychiatric standards such as the Trail Making Test (TMT) [38], the West Haven Criteria (WHC), and the Glasgow Coma Scale (GCS) [26]. The potential for measuring breath ammonia could replace the need for such invasive methods.

1.3.2 Haemodialysis

Assuming the liver is functioning properly, kidney failure can also result in harmful conditions such as uraemia (i.e. increased urea in the blood) [39], acidosis (i.e. elevated H^+ levels), and edema (i.e. extreme water retention) [32]. Furthermore, hormones become imbalanced, bones lose strength, blood pressure increases, and fewer red blood cells are produced [40]. In the case where the filtration rate from the blood into the renal tubules is hindered or blocked, solutes that are normally filtered out of the body begin to build up in the blood. Urea reaches toxic levels and hydrogen compounds turn the blood acidic. This increase in solute concentration forces the body to retain as much water as possible to maintain equilibrium [32]. In time, the same consequences arise that result from liver dysfunction. Currently, the primary method for assisting renal failure is haemodialysis (Fig. 1.2). This begins by removing aliquots of blood from the body which then go through a dialyser to filter the toxins. Dialysers are re-usable pieces of equipment that must be sterilised between uses. Within the dialyser, the blood is filtered by way of thousands of

small fibre membranes. Blood passes through the fibres leaving the toxins trapped behind [40]. The rate at which toxins are removed from the blood is dependent upon blood flow rate due to solute concentrations, mass, and the area of diffusion [41]. To determine the individual filtration requirements, toxins are isolated according to Fick's Law:

$$J = - DA\ (dc/dx) = - DA\ (\Delta c/\Delta x) \quad \textbf{(1)}$$

where the flux of toxins J flowing over a distance of dx is proportional to the difference in concentration dc and the area of diffusion A. Diffusivity D is a constant value with units of cm^2/sec that results from balancing the rest of the equation at a given temperature [41]. Once the toxins are isolated by diffusion, a cleaning solution known as dialysate flushes the waste material away from the dialyser fibres [40]. Dialysate is a solution made specific to individual needs, and hence the concentrations of solute vary. However, the general composition consists of sodium, potassium, calcium, magnesium, chloride, acetate, bicarbonate, and glucose [42]. Once the waste material is removed, the dialyser returns the clean blood to the body [40].

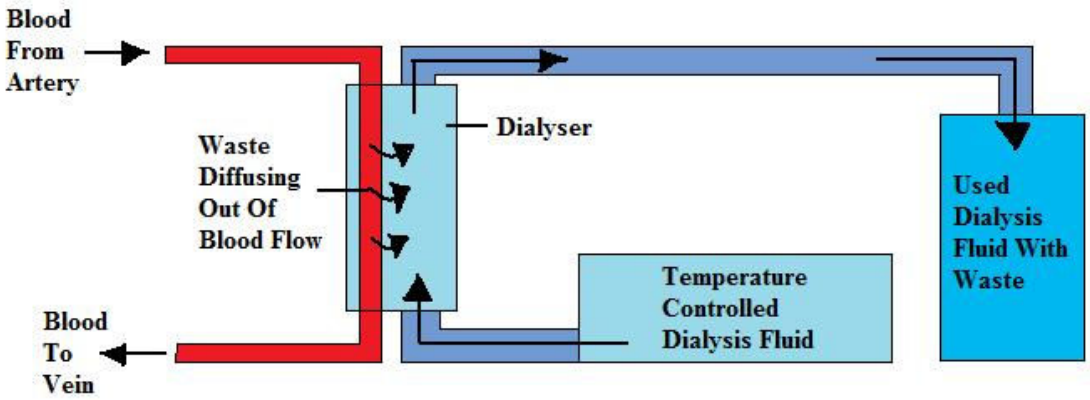

Figure 1.2 Haemodialysis. Nitrogenous waste products of the blood are diffusing across the dialysis membrane and into the dialyser. From there, the dialysis fluid carries the waste away allowing filtered blood to return to the body [40]**.**

This is a time- consuming technique that requires most patients to visit a clinic about three times a week for six or more hours at a time [39]. While a patient is undergoing haemodialysis, a calculation is performed that shows how well urea is being filtered from the body. This is known as the urea reduction ratio (URR):

URR = ((BUN before treatment – BUN after treatment) / BUN before treatment) X 100% **(2)**

A URR of at least 65% is necessary for effective haemodialysis [16]. By focusing on blood urea nitrogen (BUN) and creatinine levels, a standard of excess nitrogen in the blood can be compared. Literature has shown a potential 0.95 correlation between breath ammonia and BUN, and 0.83 between breath ammonia and creatinine [16] suggesting that breath ammonia analysis has the potential to be an effective surrogate for BUN for monitoring haemodialysis efficacy.

1.3.3 Peptic ulcers

Aside from liver and kidney dysfunction, ammonia concentrations in breath can also be used to diagnose peptic ulcers affecting either the stomach or duodenum. The causal link between these ulcers and breath ammonia is a bacterium known as *Helicobacter pylori*. Currently, about 40% of adults are infected with *H. pylori* [43]. It is assumed that the infection is contracted through food or water, but the origin is still unclear. Stomach acids have little effect on the bacteria since *H. pylori* secrete urease enzymes that neutralise acids and weaken the surrounding tissue. By weakening the lining of the stomach and/or duodenum, *H. pylori* allows biological acids to deteriorate the tissue and form ulcers [44]. The current method of diagnosis is the urea breath test (UBT) which involves measuring the urease activity of the organism via the ingestion of ^{13}C or ^{14}C labelled urea [45]. If *H.pylori* is present in the stomach, the high levels of urease excreted by *H. pylori* are detected by monitoring the breakdown of the labelled urea into radioactive carbon dioxide and ammonia as follows [46]:

$$(NH_2)_2CO + H_2O \longrightarrow CO_2 + 2NH_3 \quad \textbf{(3)}$$

The compounds then pass through the blood, diffuse into the lungs, and can be measured in the breath which is detected using a scintillation counter [47]. Since initial ammonia baseline levels can vary from individual to individual, the rate of ammonia increase upon urea absorption is monitored. It has been shown graphically that the ammonia concentration of *H. pylori* negative individuals increases by approximately 0.12 ppm while *H. pylori* positive individuals increases by approximately 0.40 ppm over the same time range [27]. Ammonia breath monitoring has the potential to play a role in measuring urease breakdown

without the need for radioactive labels if the low detection limits of breath ammonia generated can be reached.

1.3.4 Halitosis

H. pylori is a urease positive bacteria which is specific to the stomach and duodenum. However, there are bacteria which can generate ammonia in the oral cavity. In the mouth, anaerobic bacteria metabolise food debris and create numerous byproducts which are the cause of the smells associated with halitosis [28]. About 90% of breath odour originates from the oral cavity as a result of orolaryngeal and/or gastrointestinal disorders [48]. Studies show that halitosis is primarily due to volatile sulphur compounds (VSC) in the oral cavity causing tissue damage and malodour. VSCs can be measured using a gas chromatograph in conjunction with a flame photometric detector system. Of the VSCs that develop, methyl mercaptan has been shown to have a correlation with ammonia [28]. Furthermore, the relationship between VSCs and ammonia has been shown to have a 0.39 correlation [49]. Normal concentrations of oral ammonia are usually too low to measure. However, as methyl mercaptan levels change, ammonia levels show a proportional change. Furthermore, an increase in the bacterial load of the oral region correlates with increase in ammonia. Hence, by measuring the ammonia concentration from the bacteria that grow within the tongue coating and dental plague, and relating it to the methyl mercaptan levels associated with VSC measurements, ammonia in the oral cavity has the potential for assessing halitosis and oral hygiene [28].

1.3.5 Pulmonary dysfunction

Lung dysfunction or impairment such as asthma also has potential links with breath ammonia. It has been shown that individuals with asthma have lower levels of ammonia in their breath than healthy individuals. It is speculated that concentrations of ammonia produced by glutaminase may be directly affected by the levels of corticosteroids and cytokines produced by asthma patients. The methods used for analysis rely on collecting exhaled breath condensate in a lamellar condenser followed by measurement with a solid state ion selective electrode [50]. However, examining breath in gaseous form may simplify this technique.

1.4 Techniques for quantifying ammonia gas in breath

When it comes to quantifying ammonia gas, being able to isolate them from complex gaseous mixtures is important. Since the 1950's, techniques such as chemical ionisation, gas chromatography, laser spectroscopy, and chemical detection have emerged as the key methods. Their sensitivity, precision and accuracy have proven suitable for selectively detecting and identifying low molecular weight species in gaseous form. Furthermore, combining these methods with each other in various ways (e.g. with mass spectrometry) shows potential for strengthening their detection capabilities. The techniques that follow and their detection limits for ammonia are summarised in Table 1.2.

1.4.1 Techniques based on chemical ionisation

Chemical ionisation uses the charge of a molecule to control how it reacts with other molecules. Under various pressures, the molecular reaction rate can also be controlled [51]. By combining atmospheric pressure chemical ionisation with mass spectrometry (APCI-MS), a spectral image displaying the mass-to-charge ratio can be obtained. APCI-MS was first developed as a method for analyzing trace gases in breath. However, due to interference problems with breath ammonia, an improvement was devised using protonated water clusters formed from ion-molecule reactions (Fig. 1.3) [8]. It was later confirmed that the proton transfer reactions of APCI were capable of increasing the sensitivity of the detection of compounds by several orders of magnitude [52]. Furthermore, data indicated that higher humidity levels decreased fragmentation of ionization gases and, therefore, increased overall sensitivity. Since normal human breath has an average relative humidity of around 84% from the nose, and 94% from the mouth, this is a variable that must be considered [8]. This technique shows strong potential for analysis of ammonia in human breath since protonated analyte-water clusters of $(H_2O)nNH_3^+$ have shown stability with other techniques [53].

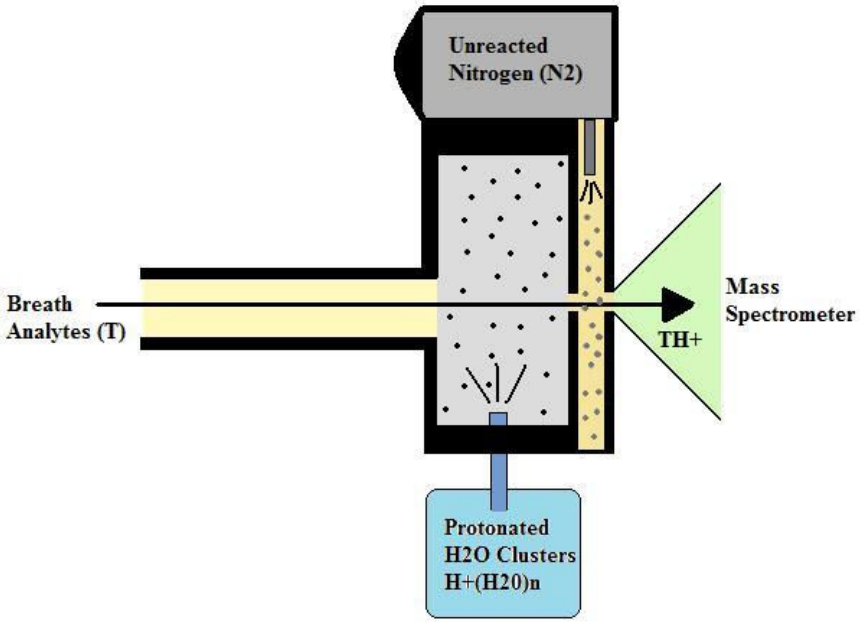

Figure 1.3 Atmospheric Pressure Chemical Ionisation–Mass Spectroscopy (APCI-MS). By reacting protonated water clusters $H^+(H_20)n$ with analyte *T*, a proton-transfer reaction takes place forming protonated analyte-water clusters $TH^+(H_20)n$ of varying sizes. From here, unreacted nitrogen N_2 molecules are forced to collide with the weakly bound water molecules of the cluster, thereby separating the water molecules $(H_20)n$ from the cluster and leaving only the protonated analyte TH^+. The structure of the analyte is then analysed by mass spectrometry [54]**.**

Two chemical ionisation techniques that are capable of ammonia detection are proton transfer reaction – mass spectrometry (PTR-MS) and selected ion flow tube – mass spectrometry (SIFT-MS). PTR-MS (Fig. 1.4) has been used mostly for air analysis and environmental studies where atmospheric ammonia gas can be detected between 90 and 270 ppt [55]. However, PTR-MS has shown potential for analysing VCs from exhaled breath as well [56]. Primarily, the precursor ion H_3O^+ is used to initiate proton transfer with trace gases (*T*) such as VCs, because H_3O^+ will react with most VCs found in air. The majority of VCs have a proton affinity higher than that of water, and will therefore transfer protons with almost every interaction [56]. Furthermore, only one ion species (TH^+) will emerge from each collision along with the dissociation of water [57]. Using a flow-drift tube to control ion movement prevents cluster ions from forming which, in return, results in

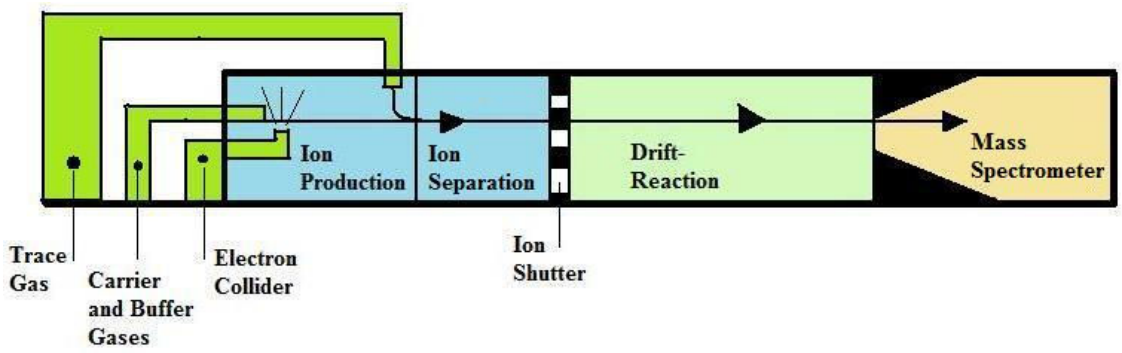

Figure 1.4 Proton Transfer Reaction – Mass Spectrometry (PTR-MS). The initial section known as the "ion production section" collides electrons with carrier gas molecules so as to assert an ionic charge upon them. This ionised carrier gas, known as the precursor ion H_3O^+, reacts with trace gases which are added downstream. These reactants are carried to the "ion separation section" by gas flow, typically in the form of a buffer gas such as helium, to maintain a neutral atmosphere within the tube. Since the "ion shutter" only interacts with one ion charge at a time, specificity is high. Depending on what factors are being examined in the "drift-reaction section", the shutter can be set to open at pulse intervals or simply remain open continuously. If set to pulse, then drift velocities can be analysed. In continuous flow, the reaction rates can be focused on [58]**.**

a clear spectrum for analysis [12]. Cluster ions do not form since the ion separation section uses an electric field to send negative and positive ions in different directions [58]. However, the disadvantage of using an electric field is that ionic-molecular reaction times are unpredictable. PTR-MS has the advantage of being able to select for specific molecules via precursor ions. However, there is still a problem with separating compounds of similar pressure, mass, or density due to the use of H_3O^+ precursor ions alone [12]. With SIFT-MS, the initial concept was used to investigate the kinetic behaviour of gas phase ion-neutral reactions. Since then, thousands of gas reactions ranging from environmental to clinical have been studied using the SIFT-MS technique. It can be seen from Fig. 1.5 that SIFT-MS is similar to PTR-MS in that it uses helium as the buffer gas at a given flow rate in the flow tube. However, unlike PTR-MS, three precursor ions (H_3O^+, NO^+ and O_2^+) are available allowing for additional proton transfer reactions [59]. Having more precursor ions allows for multiple ion spectra and greater quantification in mixed samples [60].

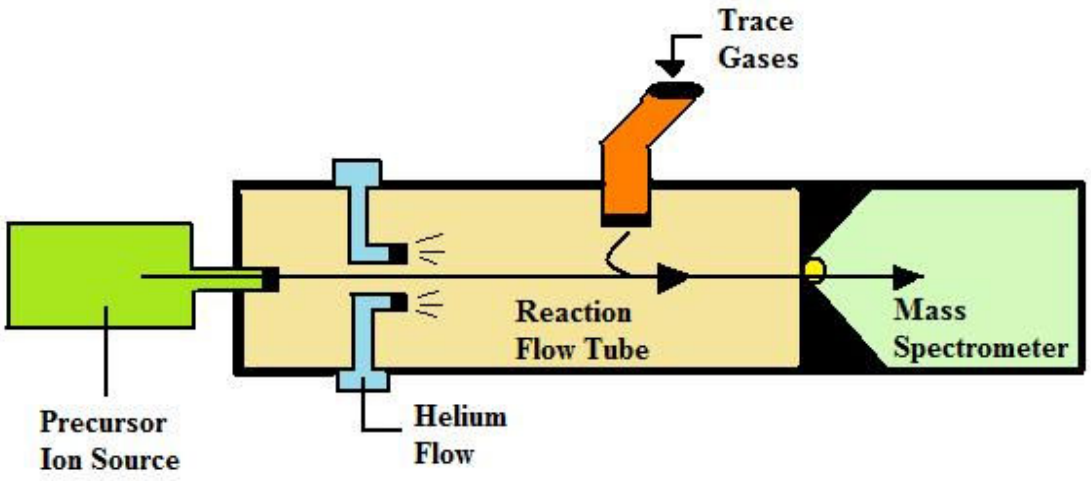

Figure 1.5 Selected Ion Flow Tube – Mass Spectrometry (SIFT-MS). The ions are introduced into the helium flow from an ion source at the beginning of the tube. Upon which, a gas sample (e.g. breath) is introduced directly and reactions take place. Adding breath samples to the system directly reduces the uncertainties that tend to arise with collection methods [11]**. Once the protonated analyte flows to the end of the tube, the ions are selected by a sampling orifice and directed into the mass spectrometer for analysis** [61]**.**

With SIFT-MS, analysis of breath VCs (including ammonia) is achieved in about 10 ms with a sensitivity as low as 10 ppb [15]. Furthermore, water vapour and metabolite condensation are prevented by heating the tubing [12]. With real-time measurements and high sensitivities possible for clinical measurement of human breath, the SIFT-MS is being modified into a more portable version known as the *Profile 3*. The key benefits of this system are that it is smaller and more sensitive than previous versions [61].

1.4.2 Gas Chromatography

Another technique which has been widely used in quantifying breath gases is gas chromatography. This has been combined with sampling methods such as solid phase micro extraction (SPME) to collect the breath prior to their addition to the chromatographic column [4]. As the breath sample flows through the column, the individual gas molecules separate by their affinity for either the carrier gas or the liquid coating on the column [62]. However, since gas chromatography is reliant on first collecting a sample, quantification is

not performed in real-time. Furthermore, SPME provides greater sensitivity, but concentration accuracy decreases due to possible loss during the collection process [12]. Chromatographic columns can also be damaged by moisture such as that found in humid breath. Hence, an additional drying method could be used to remove any water vapour that is present or the accuracy of readings could be effected [63]. The rate at which a species flows through the column is dependent upon the nature, amount, and surface area of the individual molecules being examined at a specific temperature [64]. In conjunction with gas chromatography, ion mobility spectrometry (GC-IMS) is capable of analysing the concentrations of ammonia found in human breath as low as 14 ppt [65]. Initially termed plasma chromatography (PC), the adaptation of IMS to GC first took place in the 1970s [53] and is capable of identifying breath gases by their mobility and drift velocity in an electric field at atmospheric pressure [4]. To calculate the mobility (K) of ions under the conditions of the electric field (E), the following equation can be used:

$$K = (V_d)(E^{-1}) \quad \textbf{(4)}$$

where V_d is the velocity of the drift ion [53]. The difference in mobility and drift velocity are dependent upon the differences in the unique mass and geometry of the specific gas particles [12]. However, due to IMS originally being designed for detection of chemical warfare agents, explosives and drugs, it relies heavily on known ion-molecular reactions [66]. This means GC-IMS spectrometers have limited sensitivity and cannot directly analyse breath samples. Hence, the trace gases from breath must be separated by way of column chromatography before the ion mobility can be deduced in the drift tube (Fig. 1.6). In some cases, the use of multi-capillary columns (MCC) have been recommended over a single narrow column because MCCs allow for a higher flow rate and sample capacity [65]. Furthermore, results can be obtained from 20 ms to a few minutes depending on the number of spectra being studied. Using IMS spectrum peaks to identify differences between the breath of patients and healthy people has already been found to provide fast and accurate ammonia concentrations [66].

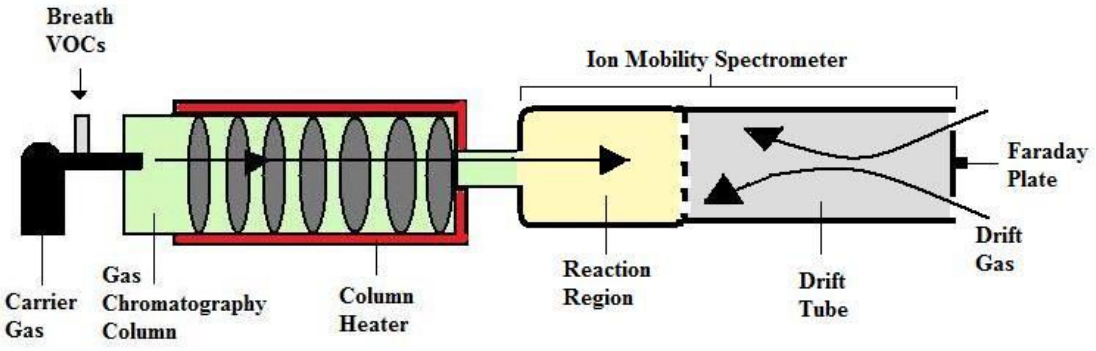

Figure 1.6 Gas Chromatography – Ion Mobility Spectrometry (GC-IMS). While separation is taking place in the capillary column, reactant ions are being produced in the "reaction region". Once separation is complete, the analytes from the column are introduced into the reaction region where protonation takes place. The protonated gases then enter the electric field of the drift tube and head towards the detector at a constant velocity. Since there is a counter-flow of drift gas, the opposing ions collide with each other causing separation based on the individual charges and masses. From here, a spectrum based upon unique ion mobility is generated from impact intervals with the Faraday plate [67]**.**

1.4.3 Laser Spectroscopy

Laser spectroscopy utilises the characteristic absorption or emission of energy by matter (in this case gas particles) at specific wavelengths when excited by a laser energy source [68]. Use of laser spectroscopy has shown high selectivity, high sensitivity, and real time potential for clinical breath ammonia analysis [25]. Specific techniques used for ammonia quantification are laser induced fluorescence (LIF), cavity ring down spectroscopy (CRDS), tunable diode laser absorption spectroscopy (TDLAS), photoacoustic spectroscopy (PAS), and optical frequency comb cavity – enhanced absorption spectroscopy (OFC-CEAS). With LIF, detection of breath molecules as low as 10 ppt has been demonstrated with gases such as nitric oxide [69]. Recently, however, LIF has shown the capability for making qualitative measurements of ammonia [70]. Ammonia detection is currently qualitative because of the typical problem of collisional quenching which results in no radiation from the fluorescing state during transition [71]. Using fluorescence techniques, ammonia molecules were originally detected at an excited state between 220 and 115 nm by way of a Nd:YAG-based dye laser source [70]. However, it has since been discovered that ammonia has multiple

excitation states and investigation is underway to define these. Using the LIF technique of double-photon excitation, it is possible to excite ammonia molecules between the regions of 300 and 310 nm. Doing so enables ammonia gas to fluoresce at wavelengths as high as 565 nm (Fig. 1.7). Furthermore, LIF provides the advantage of being able to detect more than one species of gas at a time using a single laser emission. This would enable multiple gases to be measured simultaneously [70]. LIF is also considered to be a "background-free" technique implying that spectral images are not impeded by overwhelming emission light [71].

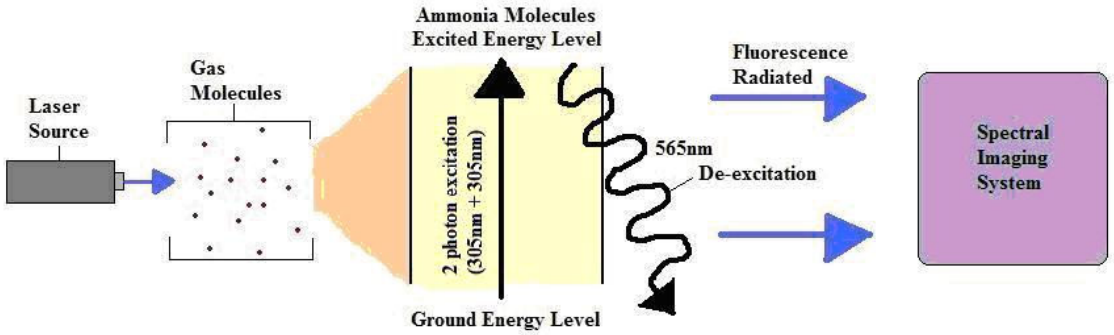

Figure 1.7 Laser Induced Fluorescence (LIF). Initially, the laser interacts with the gas molecules (e.g. ammonia) at a specific wavelength. The molecules increase in energy from their original ground state to an excited level. To get back to the ground state, the molecules release the energy (de-excitation). This energy is radiated in the form of fluorescence which is detected and analysed by spectroscopy [70]**.**

In CRDS, the molecules in breath are quantified according to the absorption rate of pulsed light within an optical cavity (Fig. 1.8) [72]. The rate of absorption is directly related to the amount of time required for light to leave the cavity. It is expected that the decay rate will be shorter if the absorption is larger [71]. This information can then be used to calculate the decay rate. The decay rate indicates the amount of photons lost, which in turn, defines the species of gases in the cavity [73].

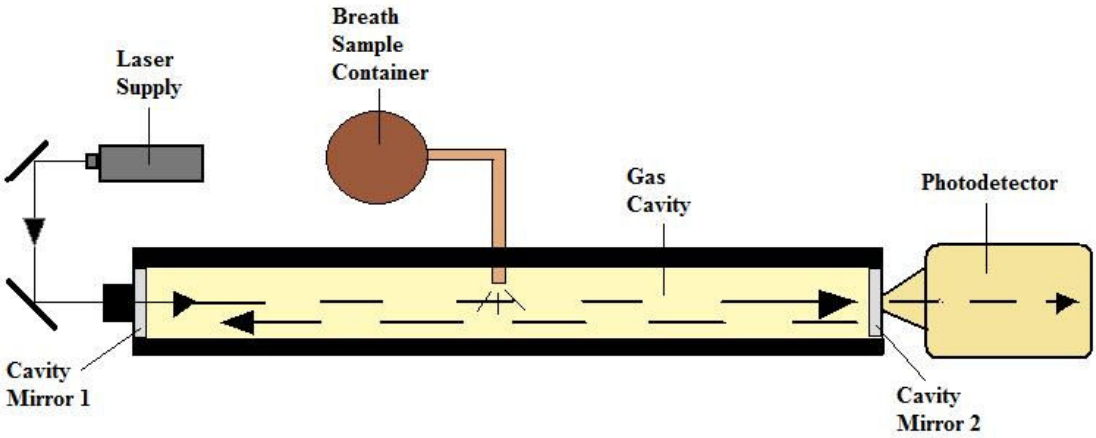

Figure 1.8 Cavity Ring Down Spectroscopy (CRDS). The collected breath sample is first placed into the cavity between two mirrors. Once the sample has been added, a single laser pulse is transmitted into the cavity at which point it bounces back and forth between the two mirrors. With each reflected hit, a fraction of the laser leaks out of the cavity and is detected by a photodetector [73]**.**

The following equation shows how the decay rate (τ^{-1}) decreases according to the rate at which the breath sample absorbs light:

$$\tau^{-1} = (c\ (1 - R) / d) + c\alpha \qquad \textbf{(5)}$$

where c is the speed of light, d is the length of the cavity, R is the reflectivity of the mirrors, and α is the absorption coefficient of the medium between the mirrors [73]. With CRDS, breath ammonia can be detected as low as 25 ppb over a period of 20 seconds. Using a mid-IR Quantum Cascade laser at 967.35 cm^{-1}, ammonia coincides with its strongest spectral region [74]. This method is highly sensitive, but due to the noisy transmitted intensity required from the laser, the accuracy is limited [75]. In the case of TDLAS (Fig. 1.9), its typical use has been to provide high-resolution spectra for gases from industrial pollution. However, due to its ability to detect various trace gases at low levels with little interference, it has also shown potential for clinical breath analysis [76]. TDLAS is capable of detecting breath ammonia at concentrations as low as 1 ppm in approximately 10 s [77]. However, breath samples must be pre-collected using such techniques as exhaling into a container [78] which, in turn, removes the possibility for real-time analysis.

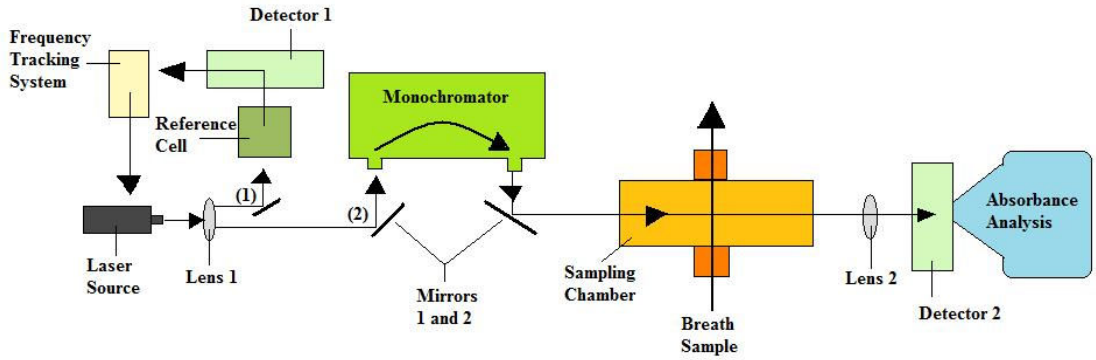

Figure 1.9 Tunable Diode Laser Absorption Spectroscopy (TDLAS). The process begins with an infrared laser being introduced to the first lens. The lens divides the laser light into two beams. One beam is sent through a reference cell that contains the gas species that is being searched for in the breath sample. By doing this, an absorbance reference is provided to detector one for analysis comparison. The second beam is focused into and out of a monochromator by two mirrors. Monochromators serve the purpose of characterizing spectrums and wavelength calibrations. This is the half point of the laser beams full distance. Beyond the monochromator, the laser passes through the breath sampling chamber and intersects with detector two. Using the reference of beam one, beam two is then able to lock on to specific sample gases according to their unique absorbances [77]**.**

The TDLAS gas measurement is based on the Beer-Lambert relationship using an infrared laser to measure the transmitted intensity, *Iv*:

$$I_v = I_{v,0}\, exp[-\, S(T)g(V\text{-}V_o)NL] \qquad \textbf{(6)}$$

where $I_{v,0}$ is the initial laser intensity, $S(T)$ is the temperature-dependent absorption line strength, $g(V\text{-}V_o)$ is the frequency dependence of the line strength, N is the target gas number density, and L is the optical path length through the gas [79]. PALS (Fig. 1.10) differs from other laser-based techniques in that it uses acoustics to measure gas concentrations. After a CO_2 laser excites a molecule in the photoacoustic chamber, the light energy converts to heat [16]. As the molecule de-excites, the vibrational energy is emitted and the pressure is monitored by a microphone [25]. This photoacoustic measurement (P) can be calculated as follows:

$$P = P_o e^{-\sigma Nl} \longrightarrow (P_o\text{-}P) \approx P_o \sigma Nl \qquad \textbf{(7)}$$

where (P_o-P) is the absorbed laser intensity which is converted to acoustic energy, σ is the area of absorption per molecule, N is the number of absorbing molecules, and l is the absorption path length [80]. In the case of breath ammonia, the gas molecules can be detected at a wavelength of 1,531.68 nm [81]. PALS is capable of detecting breath ammonia at concentrations as low as 10 ppb in approximately 13 s [82]. This technique has high sensitivity, but requires a strong power source such as a CO_2 laser to accommodate the detection requirements [81].

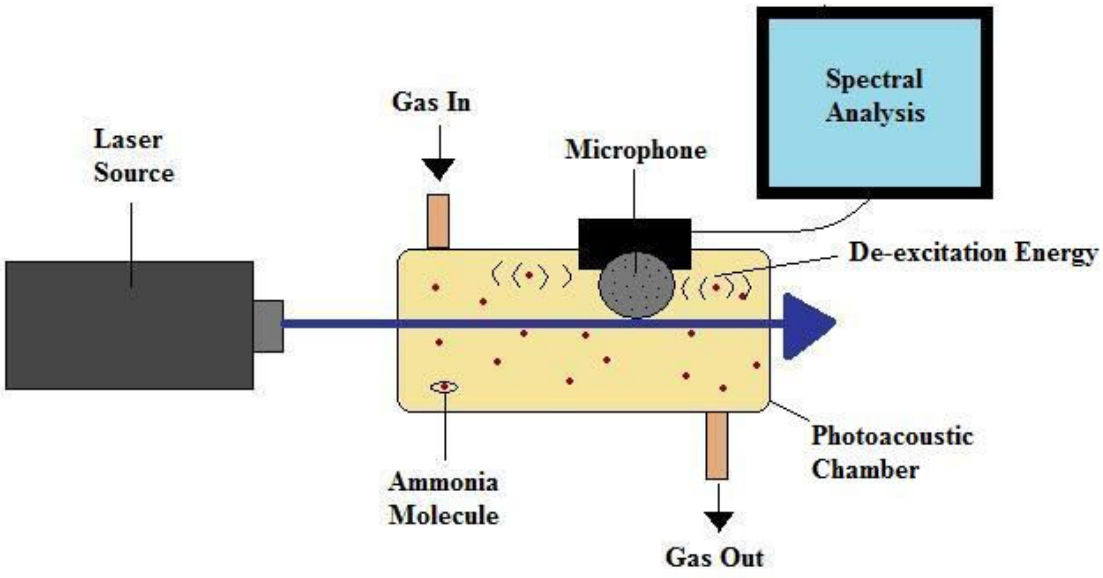

Figure 1.10 Photoacoustic Laser Spectroscopy (PALS). The laser enters the chamber filled with ammonia gas and excites the molecules. Upon de-excitation, the energy released is picked up by the microphone and relayed to the spectroscopic analysis system [25]**.**

OFC-CEAS is a technique capable of monitoring numerous molecules at the same time. To do this, a mode-locked fibre laser adjusted to a wide spectrum interacts with the breath compounds contained in an enhancement cavity [83]. Doing so allows for an increase in detection sensitivity and molecular absorption of light energy [84]. The light reflects in the chamber with a large number of round trips so as to ensure the molecules are enhanced to levels providing high peak intensities [25]. This makes characterization by way of the virtually imaged phase array (VIPA) spectrometer clear enough for a camera (InGaAs) to record the spectra (Fig. 1.11) [83]. Breath ammonia concentrations have been detected by OFC-CEAS as low as 4.4 ppm. Using the mode-locked fibre laser, ammonia is detected

between the wavelengths of 1.5 to 1.55μm. However, this range overlaps with that of water making the specificity of the spectra difficult [84].

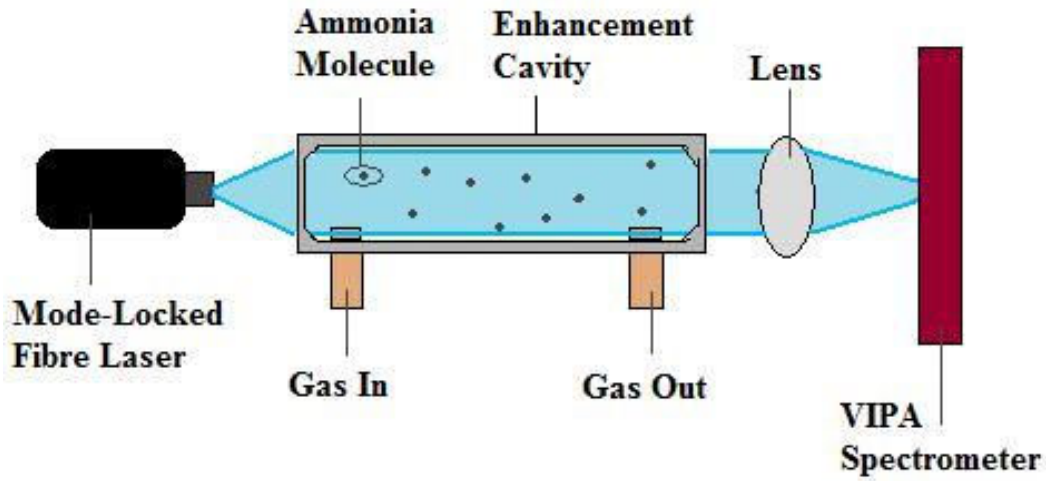

Figure 1.11 Optical Frequency Comb - Cavity Enhanced Absorption Spectroscopy (OFC-CEAS). A laser source excites the ammonia molecules to high peak levels so as to ensure that a clear spectra can be seen within the VIPA spectrometer [84]**.**

1.4.4 Chemical Sensors

Since the 1980s, chemical sensors have evolved from being monitors in the food industry to analysers of breath gases [4]. Among these, the electronic nose has been given primary recognition for clinical breath monitoring research. Electronic noses focus on the variations in surface conductivity when a material is introduced to different gas compounds. Since these devices have to be "trained" to recognize a range of specific odours, they are more qualitative than quantitative. Hence, current devices would have difficulty with analyzing concentrations of complex mixtures such as moist human breath [12]. Some chemical sensors that are in development for potential breath ammonia monitoring are the quartz crystal microbalance (QCM) and the liquid-film conductivity sensor. In a comparison with photoacoustic techniques, studies have shown that QCM (Fig. 1.12) with a zirconium phosphate coating is capable of measuring breath ammonia concentrations as low as 0.1 to 10 ppm with an accuracy of +/- 0.1 ppm [82].

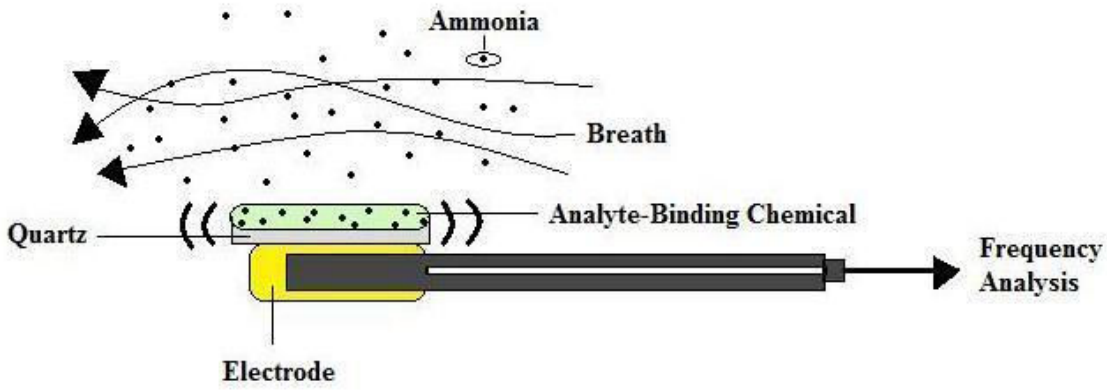

Figure 1.12 Quartz Crystal Microbalance (QCM). A gold electrode is attached to a quartz crystal. The quartz is coated with a chemical that is made sensitive to analytes flowing through the system. When an analyte appears, it is bound to the quartz by way of the chemical coating. Furthermore, the gold electrode gives off a current that causes the quartz to fluctuate at specific frequencies. Changes in frequency are proportional to the mass of the deposited analyte providing distinction between gases [85]**.**

Assuming that the film coating on the quartz crystal is homogeneous, the change in frequency (Δf) can be calculated as follows:

$$\Delta f = (-2.3 \times 10^{6})(f^{2}_{o})(\Delta M_s/A) \quad \textbf{(8)}$$

where f^{2}_{o} is the frequency of quartz crystal, ΔM_s is the mass of the analyte being bound, and A is the area being coated [85]. However, build up of condensed water vapour in the sampling tube from exhaled breath may absorb some of the ammonia. This could reduce the accuracy of the actual ammonia be collected [82]. Similarly, the liquid-film conductivity sensor (Fig. 1.13) has proven to be capable of measuring breath gas responses of ammonia as low as 18 ppb [86]. Using a film consisting of dilute sulphuric acid, a conductimetric measurement is monitored as breath ammonia is titrated into the liquid. As ammonia is absorbed, the conductivity decreases proportionally. Hence, the rate of decrease is directly related to ammonia concentration.

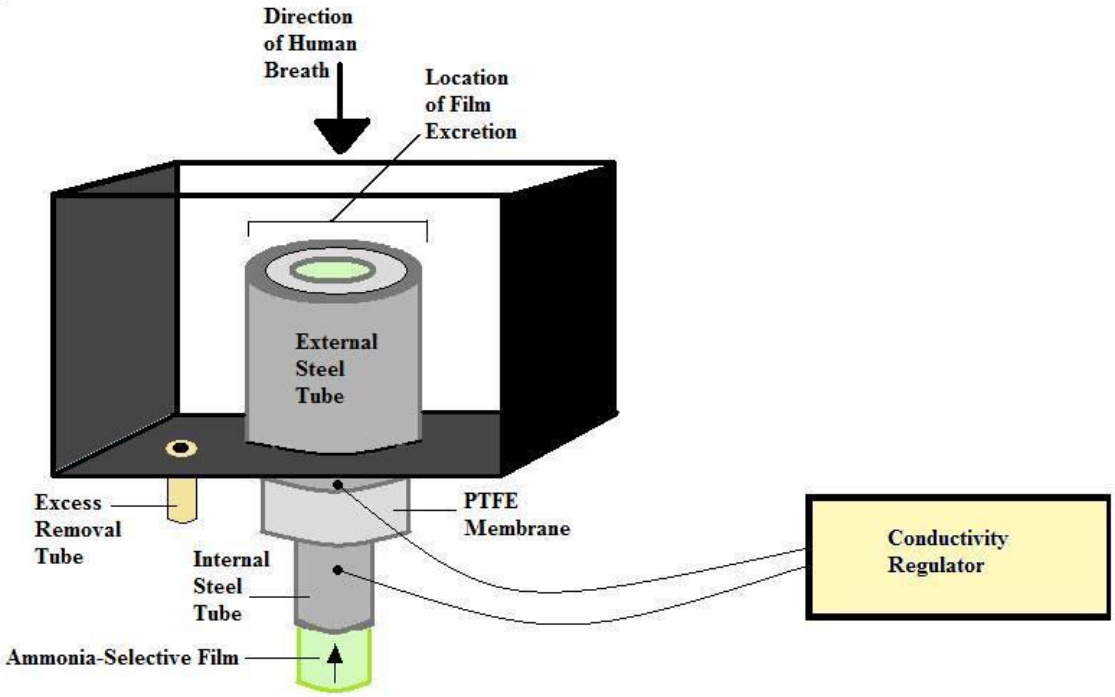

Figure 1.13 Liquid-Film Conductivity Sensor. The device consists of an internal and external steel tube that sandwich a polytetrafluoroethylene (PTFE) membrane between them. At the location of film excretion, an acidic film consisting of H_2SO_4 is created. The external area of the tube is coated with a hydrophilic solution in order to prevent the film from spilling over the sides [86]**. Figure reproduced from reference** [86]**.**

As the acidity is completely neutralized by ammonia, the time taken for full neutralization (T_{nutr}) can be directly calculated:

$$T_{nutr} = 2vx / I \quad \textbf{(9)}$$

where the initial titratable acidity ($2vx$) is divided by the rate of ammonia absorption (I) [86]. As the humidity of breath can cause problems where ammonia absorbs into condensed water, use of a dehumidifying agent such as NaOH was recommended.

1.4.5 Techniques with the potential for breath ammonia detection

Additional techniques that may prove useful for breath ammonia detection are absorption spectroscopy and micro-plasmas. Absorption techniques have been used to detect breath acetone at 14 ppb via reaction with alkaline salicylaldehyde to form a coloured product.

The reaction can be detected using GaN-based light emitting diodes for excitation of the molecule, with detection at 465 nm in blue absorption. Though ammonia has not yet been analysed, the potential for detection of other specific compounds found in breath could be possible as well. However, absorption spectroscopy is limited by its ability to monitor only one compound at a time [87]. The concept of using micro-plasmas (i.e. microdischarges), is also being considered as a means of detection enhancement for gases. A micro-plasma is a highly energetic gas capable of increasing the energy levels of other molecules [4]. These charged particles can be produced by three-body collisions, and their energy can be modified by using pulsed excitation over a microsecond scale [88]. When using techniques such as Penning ionization and energy transfer, the micro-plasma can excite species in a way that provides unique spectra for each compound. With various spectra available, unknown samples can be analysed without the need for separating them by methods such as chromatography. Currently, breath acetone has been detected at sub-ppb levels by comparing micro-plasma enhanced emission peaks against those of industrial grade acetone [4]. This research is still in the early stages, but shows that the detection limit of breath gases could be increased for adaptation to other technologies.

1.5 Conclusions

Breath analysis is attracting increasing interest as a non-invasive means of diagnosis. In particular, detection of ammonia in human breath has the potential to probe several processes including those involving the kidneys, liver, and bacterial infection of either the stomach or mouth. Several instrumental and non-instrumental methods exist which are capable of measuring breath ammonia. However, most of these systems were originally developed for environmental monitoring applications. The ideal breath ammonia monitoring device is one that is sensitive to the specific gas and capable of detecting it at the physiologically relevant concentrations in the ppb range with good precision and accuracy, insensitivity to interference (particularly temperature and humidity effects), is ideally portable for point-of-care use, provides ease-of-use to the user, displays real-time measurements, and is of low cost. These demanding set of criteria mean that no ideal technique yet exists for effectively measuring breath ammonia in the clinical setting. In the case of several techniques, these are still not yet capable of reaching the necessary limit of detection of 50 ppb to make them applicable for diagnostic application. For some of those

that can reach the ppb range, a collection or pre-concentration method is often required which removes the possibility for real-time measurements. Furthermore, these pre-analytical steps are likely to introduce errors in the measurement. Devices based on laser spectroscopy can provide real-time measurements, but are still too complex to be considered low cost or portable point-of-care technologies. Chemical sensors are also capable of generating real-time data, but may also have reduced precision and accuracy compared to instrumental techniques. In conclusion, there still remains a challenge to develop simple devices that are capable of the real-time analysis of human breath ammonia for diagnostic applications.

Table 1.2 Analytical techniques for measuring ammonia in human breath.

Technique	Limit of detection for ammonia	Remarks	Reference
Proton Transfer Reaction - Mass Spectrometry (PTR-MS)	90 ppt (atmospheric)	Reaction times in electric field are undefined. However, use of a precursor ion allows for high accuracy of specific molecule detection.	[55]
Selected Ion Flow Tube-Mass Spectrometry (SIFT-MS)	10 ppb	Uses multiple precursor ions which allows for greater quantification in mixed samples. A more portable version is in development.	[15]
Gas Chromatography-Ion Mobility Spectrometry (GC-IMS)	14 ppt	Relies on known reactions, and gases must be separated by gas chromatography before quantification can take place.	[65]
Laser Induced Fluorescence (LIF)	Qualitative	Capable of detecting more than one species of gas via a single laser emission. Occasionally, collisional quenching can result in no radiation.	[70]
Cavity Ring Down Spectroscopy (CRDS)	25 ppb	Use of a laser allows for high sensitivity of gas detection, but the transmission intensity required can be noisy causing limited accuracy.	[74]
Tunable Diode Laser Absorption Spectroscopy (TDLAS)	1 ppm	Use of a laser allows for high sensitivity of gas detection. However, since samples must be pre-collected, readings are not real-time.	[77]
Photoacoustic Spectroscopy (PAS)	10 ppb	Highly sensitive to gas detection. Although, the balance of signal-to-noise can prove difficult resulting in a weak signal.	[82][80]
Optical Frequency Comb-Cavity Enhanced Absorption Spectroscopy (OFC-CEAS)	4.4 ppm	Capable of monitoring several molecules simultaneously. Specificity decreases, though, between gases of similar spectra ranges.	[84]
Quartz Crystal Microbalance (QCM)	0.1 ppm	Has potential for real-time measurements. Accuracy can be decreased by a build up of condensation on the sensor.	[82]
Liquid Film Conductivity Sensor	18 ppb	Has potential for real-time measurements. Accuracy can be decreased by a build up of condensation on the sensor.	[86]

THESIS AIMS AND OBJECTIVES

- Investigate the background of diagnostic breath ammonia monitoring and the challenges associated with current technology
- Establish the normal range of human breath ammonia by way of currently established technology to define baseline analytical requirements
- Develop a system to simulate potential breath interferents such as humidity and temperature over the known human range for controlled ammonia sensor characterisation studies
- Evaluate the performance of the ammonia sensing element (nanoPANI interdigitated electrode) to ensure that it fulfils the analytical requirements for sensing ammonia in exhaled breath over the range necessary for biomedical applications
- Engineer and optimise a breath sampling system (AmBeR) compatible with the requirements of breath ammonia monitoring while satisfying the needs for (1) non-invasive analysis, (2) point-of-care testing, (3) real-time data acquisition, (4) increased ease of use for patient comfort and safety, (5) low cost production, and (6) mass manufacturability
- Perform clinical assessment of the AmBeR prototype with haemodialysis patients, and define relationship between breath ammonia and blood metabolites (e.g. urea and creatinine)

1.6 References

[1] Risby, T.H.and Solga, S.F., (2006), "Current Status of Clinical Breath Analysis", *Applied Physics B,* Vol.85 (2-3), pp. 421-426.

[2] Shaw, R., (2003), "Antoine Laurent Lavoisier", in *Curriculum Corporation, ed., Great Scientists and Discoveries,* (1st ed.), 1, Curriculum Corporation, Australia, pp. 60.

[3] Morgan, D.J. (1961), "Construction and Operation of a Simple Flame-Ionization Detector for Gas Chromatography", *Journal of Scientific Instruments,* Vol.38 (12), pp. 501-503.

[4] Cao, W.and Duan, Y., (2007), "Current Status of Methods and Techniques for Breath Analysis", *Critical Reviews in Analytical Chemistry,* Vol.37 (1), pp. 3-13.

[5] Tortora, G.J., (2006), "Lung Volumes and Capacities; Exchange of Oxygen and Carbon Dioxide", *in AnonymousPrinciples of Anatomy and Physiology,* (11th ed.), John Wiley & Sons, Inc., New Jersey, pp. 868-870.

[6] Paredi, P., Kharitonov, S.A.and Barnes, P.J., (2002), "Faster Rise of Exhaled Breath Temperature in Asthma: A Novel Marker of Airway Inflammation?", *American Journal of Respiratory and Critical Care Medicine,* Vol.165 (2), pp. 181-184.

[7] Nodelman, V., Ben-Jebria, A.and Ultman, J.S., (1998), "Fast-Responding Thermionic Chlorine Analyzer For Respiratory Applications", *Review of Scientific Instruments,* Vol.69 (11), pp. 3978-3983.

[8] Zehentbauer, G., Krick, T.and Reineccius, G.A., (2000), "Use of Humidified Air in Optimizing APCI-MS Response in Breath Analysis", *Journal of Agricultural and Food Chemistry,* Vol.48 (11), pp. 5389-5395.

[9] Holloway, A.M.and Wayne, R.P., (2010), "Life and the atmosphere", *Atmospheric Chemistry,* pp. 80-98.

[10] Hankinson, J.L., Odencrantz, J.R.and Fedan, K.B., (1999), "Spirometric Reference Values from a Sample of the General U.S. Population", *American Journal of Respiratory and Critical Care Medicine,* Vol.159 (1), pp. 179-187.

[11] Diskin, A.M., Spanel, P.and Smith, D., (2003), "Time Variation of Ammonia, Acetone, Isoprene and Ethanol in Breath: A Quantitative SIFT-MS Study Over 30 Days", *Physiological Measurement,* Vol.24 (1), pp. 107-119.

[12] Smith, D.and Spanel, P., (2007), "The Challenge of Breath Analysis for Clinical Diagnosis and Therapeutic Monitoring", *Analyst,* Vol.132 (5), pp. 390-396.

[13] Aguilar, A.D., et al., (2008), "A Breath Ammonia Sensor Based on Conducting Polymer Nanojunctions", *IEEE Sensors Journal,* Vol.8 (3), pp. 269-273.

[14] Brooks, S.M., Haight, R.R.and Gordon, R.R., (2006), "Age Does Not Affect Airway pH and Ammonia as Determined by Exhaled Breath Measurements", *Lung,* Vol.184 pp. 195-200.

[15] Davies, S., Spanel, P.and Smith, D., (1997), "Quantitative Analysis of Ammonia on the Breath of Patients in End-Stage Renal Failure", *Kidney International,* Vol.52 (1), pp. 223-228.

[16] Narasimhan, L.R., Goodman, W.and Patel, C.K.N., (2001), "Correlation of Breath Ammonia with Blood Urea Nitrogen and Creatinine During Hemodialysis", *Proceedings of the National Academy of Sciences of the United States of America,* Vol.98 (8), pp. 4617-4621.

[17] Timmer, B.H., et al., (2004), "Miniaturized Measurement System for Ammonia in Air", *Analytica Chimica Acta,* Vol.507 (1), pp. 137-143.

[18] Rudnick, S.N.and Milton, D.K., (2003), "Risk of Indoor Airborne Infection Transmission Estimated from Carbon Dioxide Concentration", *Indoor Air,* Vol.13 (3), pp. 237-245.

[19] Turner, C., Španěl, P.and Smith, D., (2006), "A Longitudinal Study of Methanol in the Exhaled Breath of 30 Healthy Volunteers Using Selected Ion Flow Tube Mass Spectrometry, SIFT-MS", *Physiological Measurement,* Vol.27 (7), pp. 637-648.

[20] Schmetterer, L., et al., (1997), "Exhaled NO During Graded Changes in Inhaled Oxygen in Man", *Thorax,* Vol.52 (8), pp. 736-738.

[21] American Thoracic Society. (1995), "Standardization of Spirometry - 1994 Update", *American Journal of Respiratory and Critical Care Medicine,* Vol.152 (3), pp. 1107-1136.

[22] Bass, H. (1973), "The Flow Volume Loop: Normal Standards and Abnormalities in Chronic Obstructive Pulmonary Disease", *Chest,* Vol.63 (2), pp. 171-176.

[23] Tomlinson, S.P., Tilley, D.G.and Burrows, C.R., (1994), "Computer Simulation of the Human Breathing Process", *IEEE Engineering in Medicine and Biology,* Vol.13 (1), pp. 115-124.

[24] Quanjer, P.H., et al., (1993), "Lung Volumes and Forced Ventilary Flows - Report Working Party Standardization of Lung-Function Tests European-Community For Steel and Coal - Official Statement of the European Respiratory Society", *European Respiratory Journal,* Vol.6 (16), pp. 5-40.

[25] Wang, C.and Sahay, P., (2009), "Breath Analysis Using Laser Spectroscopic Techniques: Breath Biomarkers, Spectral Fingerprints, and Detection Limits", *Sensors,* Vol.9 (10), pp. 8230-8262.

[26] DuBois, S., et al., (2005), "Breath Ammonia Testing for Diagnosis of Hepatic Encephalopathy", *Digestive Diseases and Sciences,* Vol.50 (10), pp. 1780-1784.

[27] Kearney, D.J., Hubbard, T.and Putnam, D., (2002), "Breath Ammonia Measurement in *Helicobacter pylori* Infection", *Digestive Diseases and Sciences,* Vol.47 (11), pp. 2523-2530.

[28] Amano, A., et al., (2002), "Monitoring Ammonia to Assess Halitosis", *Oral Surgery Oral Medicine Oral Pathology,* Vol.94 (6), pp. 692-696.

[29] Smith, D., et al., (2008), "A Selected Ion Flow Tube Mass Spectrometry Study of Ammonia in Mouth- and Nose- Exhaled Breath and in the Oral Cavity", *Rapid Communications in Mass Spectrometry,* Vol.22 (6), pp. 783-789.

[30] Wells, K., et al., (2005), "Exhaled Breath Condensate pH Assays Are Not Influenced by Oral Ammonia", *Thorax,* Vol.60 (1), pp. 27-31.

[31] Berg, J.M., Tymoczko, J.L.and Stryer, L.(2002), "Protein Turnover and Amino Acid Catabolism", *in AnonymousBiochemistry,* (5th ed.), W.H. Freeman and Company, New York, pp. 633-659.

[32] Tate, P., (2009), "Protein Metabolism", *in AnonymousSeeley's Principles of Anatomy and Physiology,* McGraw-Hill Companies, Inc., New York, pp. 704-706, 723-734, 742-743.

[33] Voet, D., Voet, J.G.and Pratt, C.A.(1999), "The Urea Cycle", *in AnonymousFundamentals of Biochemistry,* Chichester-Wiley, pp. 620-624.

[34] Wakabayashi, H., et al., (1997), "Measurement of the Expiratory Ammonia Concentration and its Clinical Significance", *Metabolic Brain Disease,* Vol.12 (2), pp. 161-169.

[35] Butterworth, R.F. (2003), "Hepatic Encephalopathy", *Alcohol Research and Health,* Vol.27 (3), pp. 240-246.

[36] Timmer, B., Olthuis, W.and Berg, A.v.d., (2005), "Ammonia Sensors and Their Applications – A Review", *Sensors and Actuators B,* Vol.107 (2), pp. 666-677.

[37] Ong, J.P., et al., (2003), "Correlation Between Ammonia Levels and the Severity of Hepatic Encephalopathy", *The American Journal of Medicine,* Vol.114 (3), pp. 188-193.

[38] Reitan, R.M. (1955), "The Relation of the Trail Making Test to Organic Brain Damage", *Journal of Consulting Psychology,* Vol.Volume 19 (5), pp. 393-394.

[39] Blake, P., (1996), "Quantification and Prescription General Principles", *in AnonymousReplacement of Renal Function by Dialysis,* (4th ed.), Kluwer Academic Publishers, Boston, pp. 619-621.

[40] National Institutes of Health, The. (2006), "Treatment Methods for Kidney Failure", *National Kidney and Urologic Diseases Information Clearinghouse,* pp. 1-28.

[41] Sargent, J.A., (1996), "Principles and Biophysics of Dialysis", *in AnonymousReplacement of Renal Function by Dialysis,* (4th ed.), Kluwer Academic Publishers, Boston, pp. 34-35.

[42] Ronco, C., (1996), "Hemodialysis Fluid Composition", *in AnonymousReplacement of Renal Function by Dialysis,* (4th ed.), Kluwer Academic Publishers, Boston, pp. 256-260.

[43] Neithercut, W.D., et al., (1993), "Effect of *Helicobacter pylori* Infection on Intragastric Urea and Ammonium Concentrations in Patients with Chronic Renal Failure", *Journal of Clinical Pathology,* Vol.46 (6), pp. 544-547.

[44] National Institutes of Health, The. (2010), "*H. pylori* and Peptic Ulcer", *National Digestive Diseases Information Clearinghouse,* Vol.07 (4225), pp. 1-6.

[45] Cao, W.and Duan, Y., (2006), "Breath Analysis: Potential for Clinical Diagnosis and Exposure Assessment", *Clinical Chemistry,* Vol.52 (5), pp. 800-811.

[46] Balon, H.R., et al., (2001), "C-14 Urea Breath Test", *Society of Nuclear Medicine Procedure Guidelines Manual, Version 3.0,* pp. 37-39.

[47] Atherton, J.C.and Spiller, R.C., (1994), "The Urea Breath Test for *Helicobacter pylori*", *Gut,* Vol.35 (6), pp. 723-725.

[48] Henker, J., Schuster, F.and Nissler, K., (2001), "Successful Treatment of Gut-Caused Halitosis With A Suspension of Living Non-pathogenic *Escherichia coli* Bacteria - A Case Report", *European Journal of Pediatrics,* Vol.160 (10), pp. 592-594.

[49] Van den Broek, Annemiek M.W.T., Feenstra, L.and Baat, C.d., (2007), "A Review of the Current Literature on Aetiology and Measurement Methods of Halitosis", *Journal of Dentistry,* Vol.35 (8), pp. 627-635.

[50] MacGregor, G., et al., (2005), "Breath Condensate Ammonium is Lower in Children with Chronic Asthma", *European Respiratory Journal,* Vol.26 (2), pp. 271-276.

[51] Munson, B. (2000), "Development of Chemical Ionization Mass Spectrometry", *International Journal of Mass Spectrometry,* Vol.200 (1-3), pp. 243-251.

[52] Sunner, J., Nicol, G.and Kebarle, P., (1988), "Factors Determining Relative Sensitivity of Analytes in Positive Mode Atmospheric Pressure Ionization Mass Spectrometry", *Analytical Chemistry,* Vol.60 (13), pp. 1300-1307.

[53] Kanu, A.B.and Hill Jr., H.H., (2008), "Ion Mobility Spectrometry Detection for Gas Chromatography", *Journal of Chromatography,* Vol.1177 (1), pp. 12-27.

[54] Benoit, F., et al., (1983), "Breath Analysis By Atmospheric Pressure Ionization Mass Spectrometry", *Analytical Chemistry,* Vol.55 (4), pp. 805-807.

[55] Norman, M., et al., (2009), "Intercomparison of Ammonia Measurement Techniques at an Intensively Managed Grassland Site (Oensingen, Switzerland)", *Atmospheric Chemistry and Physics,* Vol.9 (8), pp. 2635-2645.

[56] Moser, B., et al., (2005), "Mass Spectrometric Profile of Exhaled Breath – Field Study by PTR-MS", *Respiratory Physiology & Neurobiology,* Vol.145 (2-3), pp. 295-300.

[57] Lindinger, W., Hansel, A.and Jordan, A., (1998), "Proton-Transfer-Reaction Mass Spectrometry (PTR-MS): On-line Monitoring of Volatile Organic Compounds at PPTV Levels", *Chemical Society Reviews,* Vol.27 (5), pp. 347-354.

[58] McFarland, M., et al., (1973), "Flow-Drift Technique for Ion Mobility and Ion-Molecule Reaction Rate Constant Measurements. I. Apparatus and Mobility Measurements", *The Journal of Chemical Physics,* Vol.59 (12), pp. 6610-6619.

[59] Smith, D.and Spanel, P., (2005), "Selected Ion Flow Tube Mass Spectrometry (SIFT-MS) for On-Line Trace Gas Analysis", *Mass Spectrometry,* Vol.24 (5), pp. 661-700.

[60] Turner, C., Španěl, P.and Smith, D., (2006), "A Longitudinal Study of Ammonia, Acetone and Propanol in the Exhaled Breath of 30 Subjects Using Selected Ion Flow Tube Mass Spectrometry, SIFT-MS", *Physiological Measurement,* Vol.27 (4), pp. 321-337.

[61] Smith, D., Pysanenko, A.and Spanel, P., (2009), "Ionic Diffusion and Mass Discrimination Effects in the New Generation of Short Flow Tube SIFT-MS Instruments", *International Journal of Mass Spectrometry,* Vol.281 (1-2), pp. 15-23.

[62] Grob, R.L. and Barry, E.F., (2004)*, Modern Practice of Gas Chromatography,* , John Wiley & Sons, Inc.,.

[63] Manolis, A. (1983), "The Diagnostic Potential of Breath Analysis", *Clinical Chemistry,* Vol.29 (1), pp. 5-15.

[64] Joint FAO/WHO Expert Committee on Food Additives. (2006), "Combined Compendium of Food Additive Specifications", *FAO JECFA Monographs,* Vol.4 pp. 17-19.

[65] Ruzsanyi, V., et al., (2005), "Detection of Human Metabolites Using Multi-Capillary Columns Coupled to Ion Mobility Spectrometers", *Journal of Chromatography A,* Vol.1084 (1-2), pp. 145-151.

[66] Baumbach, J. (2006), "Process Analysis Using Ion Mobility Spectrometry", *Analytical and Bioanalytical Chemistry,* Vol.384 (5), pp. 1059-1070.

[67] Jünger, M., Bödeker, B.and Baumbach, J.I., (2010), "Peak Assignment in Multi-Capillary Column-Ion Mobility Spectrometry Using Comparative Studies with Gas Chromatography-Mass Spectrometry for VOC Analysis", *Analytical and Bioanalytical Chemistry,* Vol.396 (1), pp. 471-482.

[68] Banwell, C.N. and McCash, E.M., (1994), *Fundamentals of Molecular Spectroscopy,* (4th ed.), McGraw-Hill,.

[69] Mitscherling, C., et al., (2009), "Laser-induced Fluorescence Spectroscopy of 14N18O and its Application to Breath Analysis", *Isotopes in Environmental and Health Studies,* Vol.45 (1), pp. 59-67.

[70] Westblom, U.and Alden, M., (1990), "Laser-Induced Fluorescence Detection of NH3 in Flames with the Use of Two-Photon Excitation", *Applied Spectroscopy,* Vol.44 (5), pp. 881-886.

[71] Berden, G., Peeters, R.and Meijer, G., (2000), "Cavity Ring-Down Spectroscopy: Experimental Schemes and Applications", *International Reviews in Physical Chemistry,* Vol.19 (4), pp. 565-607.

[72] Wang, C.and Surampudi, A.B., (2008), "An Acetone Breath Analyzer Using Cavity Ringdown Spectroscopy: An Initial Test With Human Subjects Under Various Situations", *Measurement Science and Technology,* Vol.19 (10), pp. 1-10.

[73] Mürtz, M., Frech, B.and Urban, W., (1999), "High-Resolution Cavity Leak-Out Absorption Spectroscopy in the 10-mm Region", *Applied Physics B,* Vol.68 (2), pp. 243-249.

[74] Manne, J., et al., (2006), "Pulsed Quantum Cascade Laser-Based Cavity Ring-Down Spectroscopy for Ammonia Detection in Breath", *Applied Optics,* Vol.45 (36), pp. 9230-9237.

[75] O'Keefe, A.and Deacon, D.A.G., (1988), "Cavity Ring-Down Optical Spectrometer for Absorption Measurements Using Pulsed Laser Sources", *Review of Scientific Instruments,* Vol.59 (12), pp. 2544-2551.

[76] Stepanov, E.V.and Moskalenko, K.L., (1993), "Gas Analysis of Human Exhalation by Tunable Diode Laser Spectroscopy", *Optical Engineering,* Vol.32 (2), pp. 361-367.

[77] Lachish, U., et al., (1987), "Tunable Diode Laser Based Spectroscopic System for Ammonia Detection in Human Respiration", *Review of Scientific Instruments,* Vol.58 (6), pp. 923-927.

[78] Giubileo, R.S., et al., (2001), "A TDLAS System for the Diagnosis of *Helicobacter pylori* Infection in Humans", *Laser Physics,* Vol.11 (1), pp. 154-157.

[79] Frish, M.B., et al., (2007), "The Next Generation of TDLAS Analyzers", *Society of Photo-Optical Instrumentation Engineers Optics East,* Vol.6765 pp. 76506-76517.

[80] Harren, F.J.M., et al., (2000), "Photoacoustic Spectroscopy in Trace Gas Monitoring", *in AnonymousEncyclopedia of Analytical Chemistry,* John Wiley & Sons Ltd, pp. 2203-2226.

[81] Webber, M.E., Pushkarsky, M.and Patel, C.K.N., (2003), "Fiber-Amplifier-Enhanced Photoacoustic Spectroscopy with Near-Infrared Tunable Diode Lasers", *Applied Optics,* Vol.42 (12), pp. 2119-2126.

[82] Ishida, H., et al., (2008), "The Breath Ammonia Measurement of the Hemodialysis with a QCM-NH3 Sensor", *Bio-medical Materials and Engineering,* Vol.18 (2), pp. 99-106.

[83] Balslev-Clauson, D. , (2007), "Broad Band Cavity Enhance Direct Frequency Comb Spectroscopy", Masters, University of Copenhagen,.

[84] Thorpe, M.J., et al., (2008), "Cavity-enhanced Optical Frequency Comb Spectroscopy: Application to Human Breath Analysis", *Optics Express,* Vol.16 (4), pp. 2387-2397.

[85] James, D., et al., (2004), "Chemical Sensors for Electronic Nose Systems", *Michrochimica Acta,* Vol.149 (1-2), pp. 1-17.

[86] Toda, K., Li, J.and Dasgupta, P.K., (2006), "Measurement of Ammonia in Human Breath with a Liquid-Film Conductivity Sensor", *Analytical Chemistry,* Vol.78 (20), pp. 7284-7291.

[87] Teshima, N., et al., (2005), "Determination of Acetone in Breath", *Analytica Chimica Acta,* Vol.535 (1-2), pp. 189-199.

[88] Becker, K.H., Schoenbach, K.H.and Eden, J.G., (2006), "Microplasmas and Applications", *Journal of Physics D: Applied Physics,* Vol.39 (3), pp. R55-R70.

CHAPTER 2

DETERMINATION OF BREATH AMMONIA LEVELS IN A NORMAL HUMAN POPULATION

2.1 Introduction

The focus of this chapter was to determine the concentration range of the common breath metabolite ammonia from the exhaled breath of a healthy human cohort. In previous work with healthy volunteers, Diskin *et al* [1], Endre *et al* [2], and Smith *et al* [3] performed studies with either five or six volunteers. To obtain a larger concentration range per population, 30 volunteers assisted with the current research. Identification of the normal ranges of ammonia in exhaled breath allows for recognition of abnormally high concentrations related to states of physiological dysfunction. Furthermore, this recognition will allow for proper assessment of the sensor performance during the development stages of AmBeR. The found ammonia concentrations were further correlated against biometric data including gender, age, body mass index (BMI), and breath carbon dioxide levels since previous studies have suggested that a relationship may exist among healthy people. The effects of daily routine were also investigated followed by a quick comparison of nasal and oral sampling routes. The short study of nasal exhalations was performed to see if it may bear potential for future works, but oral exhalations were examined more extensively in this preliminary work since they have shown a strong correlation with blood urea levels in previous literature [4].

This chapter outlines the application of a photoacoustic laser spectroscopy (PALS) device known as the Nephrolux^{TM} to quantify the ammonia metabolites in breath. By removing the need for sample collection into bags, PALS provides real-time analysis. Photoacoustic spectroscopy is a well-known technique that has the advantage of being relatively simple while still capable of high sensitivity detection. Previous literature has explained the process of PALS in depth [5][6]. To summarise, as ammonia (NH_3) and carbon dioxide (CO_2) breath gases enter the photoacoustic chamber of the Nephrolux^{TM}, the tunable CO_2-laser [7] excites the gas molecules. The light energy used for absorption is then converted to heat [4]. Pressure from this temperature change is detected by the chamber microphone during the de-excitation process [8]. The photoacoustic signal, S, provided a magnitude in arbitrary units displayed as:

$$S = S_m P C \alpha \quad \textbf{(1)}$$

where S_m is the sensitivity of the microphone (in units volts per pascal), P is the power of incident laser radiation (in units of watts), C is a constant for the cell-geometry, measurement conditions, and modulation frequency (in units of pascal centimetres per

watt), and α is the absorption cross-section of the transition being interrogated (in units of inverse centimetres) [9]. The CO_2-laser used by PALS is tuneable for gas selectivity allowing for ammonia detection as low as 1 ppb ±10% and carbon dioxide down to 0.1% ±5% (of reading) to generate results within 120 seconds. Once the breath is analysed by the signal processor, the data is transmitted through the single-board computer system of the Nephrolux™ and saved to an external lap-top (Fig. 2.1).

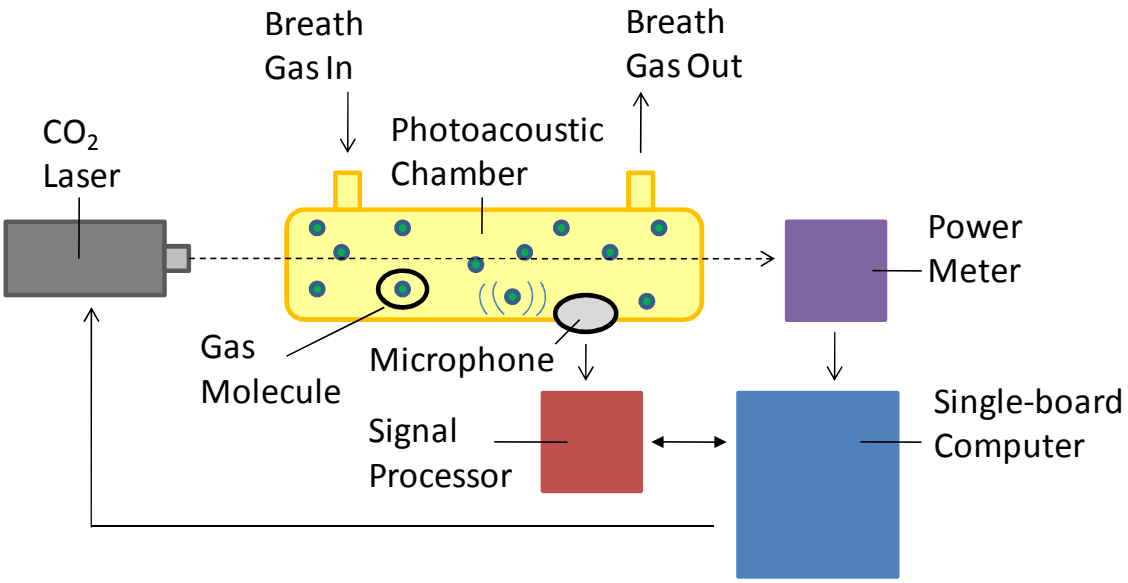

Figure 2.1 Ammonia gas molecule measurement using photoacoustic spectroscopy. Schematic of the PALS system. The CO_2 laser enters the photoacoustic chamber and excites the gas molecules. As de-excitation occurs, the pressure is released and detected by the microphone where it is transmitted to the signal processor [8]**. Figure reproduced from reference** [10]**.**

2.2 Materials and methods

2.2.1 Instrumentation

The PALS (Nephrolux™, Pranalytica Inc., CA, USA) (Fig. 2.2) underwent a multipoint ammonia calibration during development at Pranalytica which generated a strong R^2 of 0.99.

Figure 2.2 Breath ammonia measurement using photoacoustic spectroscopy. The typical procedure for volunteer breath collection using PALS.

2.2.2 Oral breath ammonia and biometric parameters

A cohort of 30 normal healthy human volunteers was locally recruited following institutional ethical approval (Appendix 1). Following a questionnaire, only those with no breathing abnormalities or related medical conditions were entered into the study population. Breath ammonia, breath carbon dioxide, gender, ethnicity, age and BMI were recorded. For breath sampling, volunteers were asked to sit in a relaxed position while breathing into a face mask which was connected to a breath delivery tube. All volunteers were asked to breathe using either oral or nasal respiration. A breath sample was defined as a relaxed full exhalation from the volunteer after a relaxed full inhalation. Over a period of 10 minutes, breath measurements were pulled into the photoacoustic chamber every 41 seconds by way of a vacuum flow. For the purpose of clinical analysis, it was useful to define whether whole breath averaged concentrations or peak alveolar concentrations were being observed. When focusing specifically on the alveolar concentrations, the compounds exclusively from within the lungs are monitored. With this study, however, whole breath

examination took place which provided samples consisting of both the alveolar region and dead space (e.g. trachea) within the respiratory system [11]. Furthermore, previous literature has described ammonia as being a sticky substance which could potentially adhere to the walls of the system [9]. To prevent this adsorption, the tubing of the Nephrolux^{TM} was constantly heated while breath consistently flowed into the system. Each sample was an average of five breath measurements.

2.2.3 Daily variation in oral breath ammonia concentrations

A single male and female volunteer from the 30 healthy volunteers were studied for five consecutive days to observe daily variation in their oral ammonia breath concentrations. Using PALS, the sampling technique was the same as previously specified. The volunteers fasted from midnight to 10:00 am at which point they were sampled. They were again sampled at 13:00 pm (post-prandial), and at 16:00 pm following a normal daily routine. Food intake by the volunteers was recorded in a diary in case cross-examination was found to be necessary.

2.2.4 Oral breath ammonia and nasal breath ammonia

Three comparisons were made between the mean oral and mean nasal breath ammonia concentrations of two volunteers. The comparisons were made following a similar timeline to the previous daily variation section, and the sampling technique was the same as discussed previously using PALS.

2.3 Results and discussion

2.3.1 Oral breath ammonia and statistical confidence

The survey population had a mean age of 34 years. There were 19 female and 11 male volunteers, and the average body mass index was 25.18 kg/m^2. Of these volunteers, 20 identified themselves as ethnically Irish, with several Europeans, two Americans and one Asian. The biometric data, mean oral breath ammonia, and mean oral breath carbon dioxide concentrations from the 30 volunteers are compiled in Table 2.1. The mean breath ammonia range was calculated by averaging five breath samples per individual. The mean oral breath ammonia of the 30 volunteers was 264.9 ppb with a standard deviation of

±182.8 ppb while the intra-individual (i.e. averaged five breath samples) deviation was ±43 ppb.

Table 2.1 Compilation of biometrics, mean oral breath ammonia, and mean oral breath carbon dioxide concentrations for 30 volunteers (mean = average of five breath samples per person).

Volunteer (number)	Gender (M/F)	Age (years)	Body Mass Index (kg/m^2)	Mean NH_3 (ppb)	Mean CO_2 (%)
1	Female	23	24.08	157 ±11	3.1 ±0.2
2	Male	29	23.10	458 ±84	3.1 ±0.5
3	Female	27	17.51	397 ±24	2.8 ±0.3
4	Male	33	25.83	308 ±35	3.2 ±0.9
5	Female	30	20.81	59 ±4	3.2 ±0.2
6	Female	58	28.38	194 ±9	3.7 ±0.3
7	Female	54	23.83	283 ±43	3.2 ±0.4
8	Male	41	28.96	264 ±44	2.1 ±0.2
9	Female	33	N/A	688 ±42	2.9 ±0.5
10	Male	25	29.35	237 ±27	2.9 ±0.5
11	Female	46	35.02	503 ±111	2.4 ±0.1
12	Male	33	31.08	356 ±68	3.5 ±0.9
13	Female	26	35.15	326 ±28	3.2 ±0.3
14	Female	27	24.38	89 ±10	3.3 ±0.4
15	Female	43	36.23	442 ±99	2.7 ±1.2
16	Female	51	28.47	244 ±61	2.4 ±0.5
17	Female	N/A	21.97	57 ±6	2.5 ±0.4
18	Male	36	20.33	327 ±29	2.1 ±0.5
19	Female	26	20.81	118 ±22	2.5 ±0.8
20	Female	30	21.22	421 ±47	2.3 ±0.5
21	Female	38	26.49	99 ±16	3.5 ±0.5
22	Female	44	18.28	104 ±13	2.9 ±1.2
23	Female	45	20.38	467 ±52	2.8 ±1.0
24	Male	38	20.76	84 ±24	3.4 ±0.6
25	Male	25	22.86	81 ±41	2.2 ±0.9
26	Male	23	22.86	448 ±238	2.6 ±1.1
27	Male	24	24.17	598 ±58	2.3 ±0.5
28	Male	27	30.93	29 ±21	3.8 ±0.2
29	Female	30	24.42	45 ±6	2.8 ±0.2
30	Female	28	22.68	67 ±8	2.6 ±0.5

Mean oral breath ammonia concentrations recorded from this test population ranged from approximately 29 to 688 ppb. Previous literature has shown that oral breath ammonia ranges for healthy populations of different sample sizes can vary. Research using selected ion flow mass spectrometry (SIFT-MS) observed oral breath ammonia concentrations of 220 to 550 ppb from a population of five healthy volunteers [2], and 200 ppb to 1,800 ppb from a separate cohort of six volunteers [3] whereas, a larger group of 30 volunteers produced an oral breath ammonia range of 248 to 2,935 ppb [12], and another of 200 volunteers gave 112 to 2,865 ppb [13]. Understanding the significance of the sample size is helpful in relating the resulting breath ammonia ranges to the rest of the human population. In other words, larger sample sizes are more likely to generate results that are closely related to the target population as well as produce a smaller margin of error [14]. In population statistics in which a sample is used, a measure of confidence is needed in order to know if the sample results can be related to the larger population. Assuming that the sample studied here was not statistically abnormal, it is safe to claim that the results of a confidence interval calculation for the sample will be true 95% of the time [15]. In calculation of the confidence interval for the given sample size and oral breath ammonia concentrations, it can be claimed that there is 95% confidence that the interval of 196.7 ppb to 333.2 ppb contains the true mean of the local population. There was a standard error of 33.3 ppb as well as a skewness of 0.48 and a kurtosis of -0.70. It should be recognised that the population sample (n=30) examined in this study was of a small group where metabolic ammonia concentrations could be related to local factors such as ethnicity, diet and localised environmental factors, and may result in a mean and range distinct from those of other research.

2.3.2 Oral breath ammonia and gender

The 19 female volunteers ranged from a mean minimum of 45 ppb to a mean maximum of 688 ppb, with an average of 250 ±189 ppb. The 11 male volunteers had a mean minimum of 29 ppb and a mean maximum of 598 ppb, with an average of 290 ±177ppb showing that the female standard deviation was slightly higher than that of the males. To compare the breath ammonia levels of females against males, a box plot analysis was used (Fig. 2.3). From the box plot, the oral breath ammonia of females and males combined gave a median of 254 ppb where the upper quartile (*Q3*) was 415 ppb and the lower quartile (*Q1*) was 91

ppb. The upper quartile represents the median of the top half of the data set. Hence, the upper 25% of the total ammonia concentrations exist between Q3 and the Max Limit. The

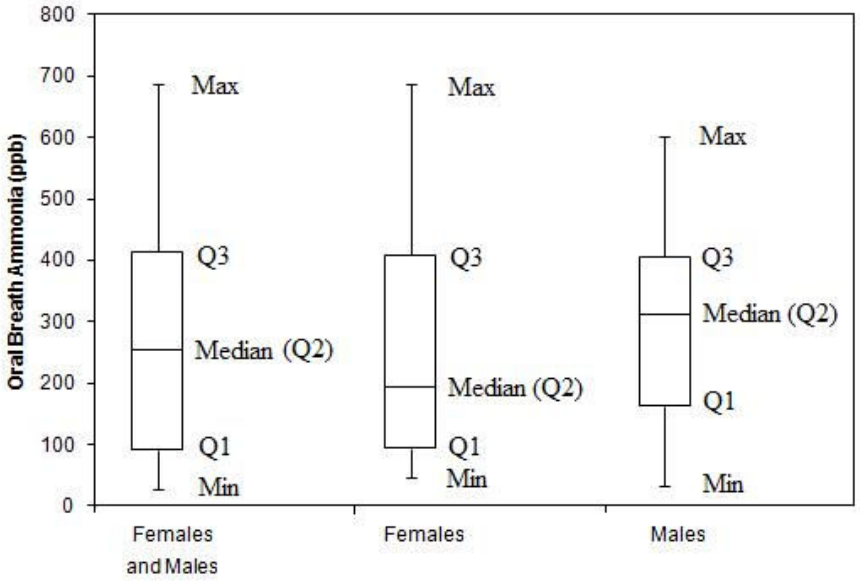

Figure 2.3 Box plot comparison of mean oral breath ammonia levels from female and male populations. Centre line shows median, box shows upper and lower quartiles, and whiskers give maximum and minimum range. Total sample population, n=30 total; n=ll male, n=19 female.

lower quartile is indicated by the median of the bottom half of the box data. This area between Q1 and the Min Limit contains the lower 25% of the total concentrations. The breath ammonia of the females was skewed towards a lower median of 194 ppb (*Q1* = 94 ppb, *Q3* = 409 ppb) while the males leaned more towards a higher median concentration of 308 ppb (*Q1* = 160 ppb, *Q3* = 402 ppb). Further comparison of the ammonia levels between females and males via a *t*-test indicated a *p*-value of 0.57. For the *t*-test, a null hypothesis was used stating that the two populations will produce similar breath ammonia, and any differences were due to chance. With no predictions or expectations of a difference being made, a two-tailed *p*-value was sought. Furthermore, since the two variables were independent of each other and a slightly different standard deviation was observed, an unequal type-2 measurement took place. Since the resulting *p*-value was greater than 0.05, there was no significant difference between the female and male breath ammonia concentrations of this cohort. Two other studies from literature using selected ion flow tube mass spectrometry (SIFT-MS) also provided comparisons between oral breath ammonia

and gender. In one, 95 females were compared against 105 males. The concentrations of breath ammonia were found to be significantly different (p<0.01) between the two genders [13]. In contrast, the other study involving 11 female and 19 male subjects showed no significant difference (p>0.05) among the genders [12]. The fact that the cohort sizes of these studies were quite different from each other must be acknowledged. Such differences make comparisons difficult and imply that more research is necessary in this area.

2.3.3 Oral breath ammonia and oral breath carbon dioxide

The relationship between oral breath ammonia and oral breath carbon dioxide was also studied (Fig. 2.4). Mean CO_2 levels were recorded as being between 2.1% and 3.8% among the 30 volunteers with an average of 2.9 ±0.5%. Literature has shown that the approximate amount of CO_2 found in exhaled oral breath can reach as high as 4.5% [16], but this concentration can differ from individual to individual resulting in a high level of variation [17]. A correlation coefficient of 0.08 indicated an absence of a correlation (p>0.05). With a lack of literature comparing human oral breath ammonia against oral breath carbon dioxide, comparisons with previous breath ammonia work could not be made.

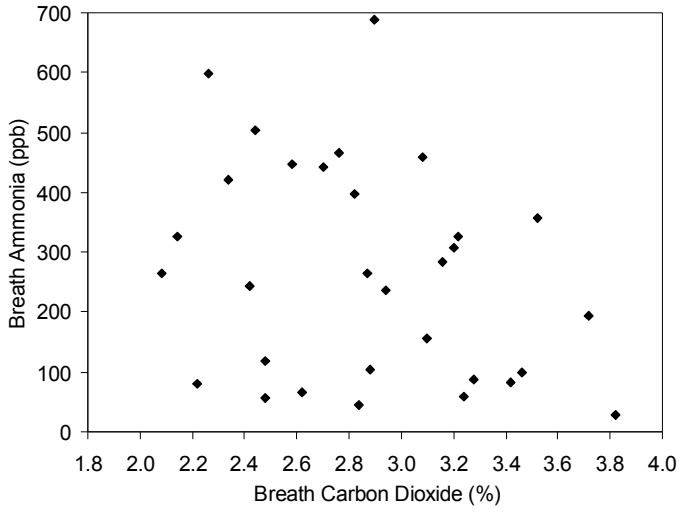

Figure 2.4 Relationship between mean oral breath carbon dioxide (n=5) and mean oral breath ammonia (n=5) in a population of 30 normal healthy human volunteers.

However, similar comparisons based on the blood work of 17 volunteers with hepatic cirrhosis have shown that inhalation of CO_2 up to five percent led to a decrease in blood NH_3 [18]. When CO_2 concentrations in blood decrease, the blood's pH increases possibly

indicating that metabolic alkalosis has taken place. In such instances of lower CO_2, renal venous blood NH_3 concentrations are expected to increase as well [19]. Since it has been stated in previous works that high concentrations of blood NH_3 are capable of diffusing into the lungs [20], perhaps future work could be performed comparing the link between exhaled NH_3 and CO_2 respiration.

2.3.4 Oral breath ammonia and age

The correlation between mean oral breath ammonia and age was examined (Fig. 2.5). The sample age range was between 23 and 58 years with an average of 34 ±10 years. It is believed that liver volume and portal blood flow decrease in function with increasing age [21]. The correlation was found to be insignificant given an R^2 of 0.004 (p>0.05), suggesting that no link between breath ammonia and age could be determined from this population. Several volunteers with ages between the 20's and 40's appear to have above average ammonia levels while those over 50 years all had ammonia levels close to or below the mean level.

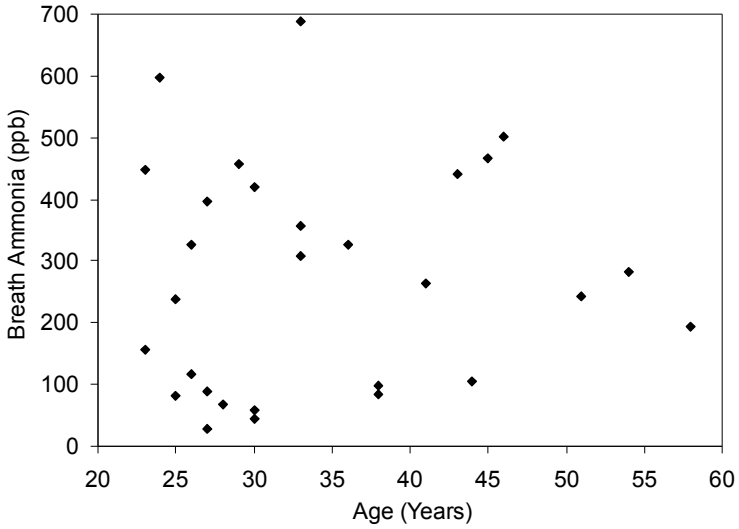

Figure 2.5 Relationship between age and mean oral breath ammonia (n=5) among a population of 29 volunteers.

Previous literature based on SIFT-MS have shown the coefficient of determination (R^2) between oral breath ammonia and age to be 0.18 over an age range of 7 to 18 years (n=200) [13], approximately 0.25 for an age range of 24 to 59 years (n=30) [12], and 0.50 among an age range between 4 and 83 years (n=17) [22] indicating that a small relationship may exist

for those populations. Other techniques focusing on spectrophotometric examination of exhaled breath condensate (ages 23 to 79 years) gave results similar to ours which indicated that age has no effect on ammonia levels [23].

2.3.5 Oral breath ammonia and body mass index

Mean oral breath ammonia levels were compared against body mass index (Fig. 2.6). Volunteer BMIs ranged between 17.51 kg/m^2 and 36.23 kg/m^2 with an average of 25.18 ±5 kg/m^2. The correlation was insignificant given an R^2 of 0.04 (p>0.05), suggesting that no link between breath ammonia and body mass index could be determined from this population. Previous publications using SIFT-MS technology have shown the coefficient of determination (R^2) between oral breath ammonia and BMI to be 0.004 for a range of 18.4 Kg/m^2 to 30.6 Kg/m^2 (n=30) [12], and 0.08 for a range from approximately 13 Kg/m^2 to 33 Kg/m^2 (n=200) [13] further emphasising the lack of significance between the two variables.

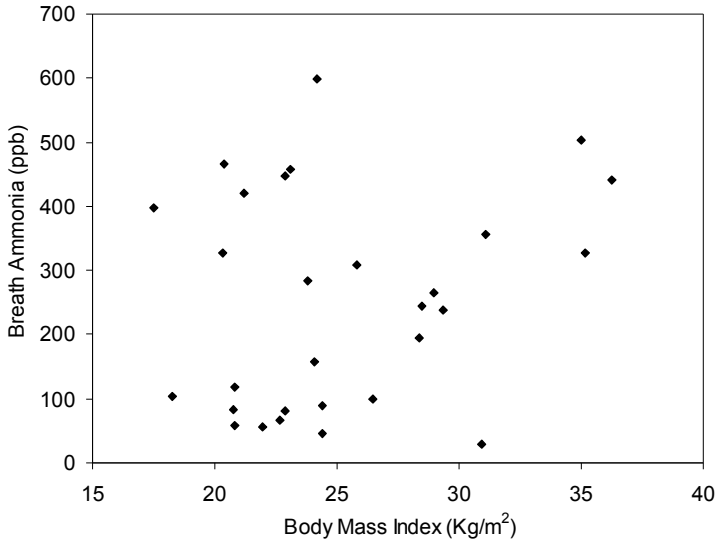

Figure 2.6 Relationship between body mass index and mean oral breath ammonia (n=5) from a population of 29 volunteers.

2.3.6 Daily variation in oral breath ammonia concentrations

The variation in oral breath ammonia levels were monitored over an eight hour working day for five consecutive days. As stated previously in Section 2.2.3, only two samples (one male and one female) were observed on each of the five days. Ammonia levels were measured at 10:00 h, 13:00 h (post-prandial) and 16:00 h. In both studies, there was a drop

in breath ammonia from the morning measurement to the mid-day measurement and then a progressive increase as the day continued (Fig. 2.7). Over the period of five days, the female volunteer expressed a mean breath ammonia of 205 ±12 ppb in the morning, 74 ±41 ppb at 13:00 h, and 202 ±152 ppb by the afternoon. The male volunteer generated a mean breath ammonia of 414 ±35 ppb in the morning, 275 ±95 ppb at 13:00 h, and exhaled 702 ±110 ppb by the afternoon. At 13:00 h, the ammonia level of the male decreased by 119 ppb while the female breath ammonia dropped by 111 ppb. Previous literature states that this decrease in ammonia may be a result of ingestion of food since the liver has a tendency to increase portal blood flow when eating [3]. As for the increase in ammonia afterwards, the male showed a difference of 439 ppb and the female changed by 140 ppb. This shows a significant increase, but the absolute value is still low. Literature has also proposed that such an increase may have been a result of purine nucleotide deamination and amino acid catabolism that occur during the physical processes that take place over the day [24].

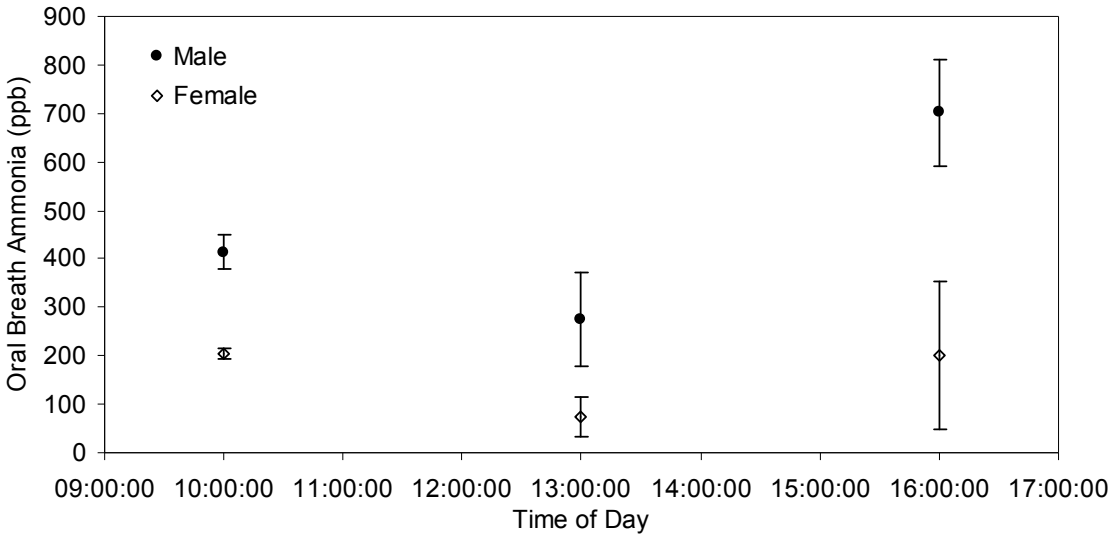

Figure 2.7 Comparison of the daily variation in oral breath ammonia for a male and female volunteer averaged over a period of 5 days. Volunteers fasted for 12 h until 10:00 h, and were tested again at 13:00 h, post-prandial. At 16:00 h, the volunteers gave further breath samples following their regular daily routine.

Furthermore, both gut bacteria and dietary contributions may demonstrate influential effects on ammonia production. Literature has stated that ammonia in the intestines could result from hydrolysis of urea via bacterial urease, or deamination of digested proteins and other nitrogenous substrates [25]. Some notable urease-producing intestinal organisms

mentioned by Vince *et al* include bacteroides, bifidobacteria, clostridia, *Proteus* spp, and *Klebsiella* spp. With proportion of these factors unique to the individual, logic would dictate that concentration of ammonia produced would either increase or decrease in relation.

2.3.7 Oral breath ammonia and nasal breath ammonia

Oral breath ammonia concentrations were consistently higher than those of nasal from both volunteers. For volunteer one, morning nasal exhalations (Fig. 2.8) gave a mean ammonia concentration of 38 ±9 ppb while oral exhalations were 210 ±24 ppb. Towards mid-day (post-prandial), the mean nasal breath ammonia level decreased to 26 ±2 ppb and the mean oral breath ammonia dropped to 64 ±4 ppb. Measurements taken in the afternoon displayed an increased mean nasal ammonia concentration of 57 ±6 ppb and mean oral ammonia at 553 ±75 ppb.

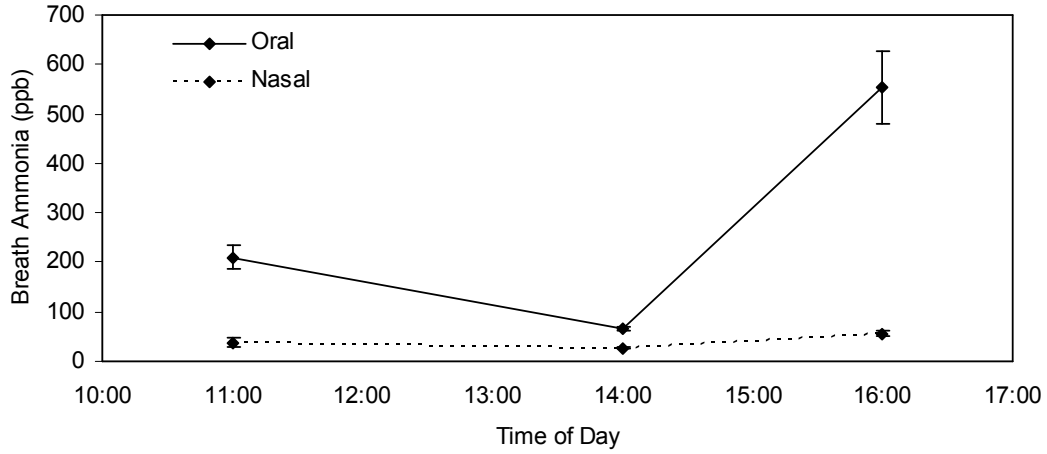

Figure 2.8 Comparison between the mean oral and mean nasal breath ammonia concentrations from volunteer one (n=5). Breath samples were taken in the morning (11:00 h), post-prandial (14:00 h), and in the afternoon (16:00 h).

From volunteer two (Fig. 2.9), the mean nasal breath ammonia concentration in the morning was 47 ±17 ppb along with an oral concentration of 246 ±25 ppb. By mid-day (post-prandial), the ammonia concentrations did not vary as much as those of volunteer one. The mean nasal breath ammonia recorded was 68 ±9 ppb while the mean oral ammonia was 253 ±29 ppb. Similar to volunteer one, measurements from the latter part of the day were higher. By the evening, volunteer two emitted a nasal ammonia concentration

of 65 ±9 ppb and an oral of 420 ±36 ppb. This display of nasal breath ammonia concentrations being lower than oral is similar to the results in other studies where measurement from nasal exhalations was shown to be preferable over oral. It was stated that a possible reason for the higher oral ammonia levels was due to bacteria and other compounds that reside there since bacteria are known to produce ammonia and are readily found in the saliva [26]. Furthermore, this may provide some reasoning as to why the standard deviation of the oral ammonia is so much larger than that of the nasal.

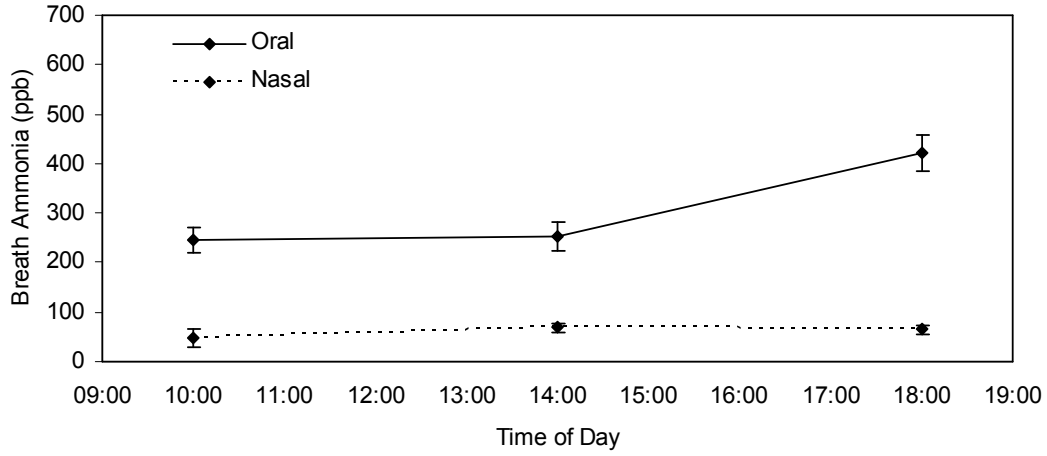

Figure 2.9 Comparison between the mean oral and mean nasal breath ammonia concentrations from volunteer two (n=5). Breath samples were taken in the morning (10:00 h), post-prandial (14:00 h), and in the evening (18:00 h).

2.4 Conclusions

Photoacoustic laser spectroscopy has the potential to be a viable tool for monitoring real-time concentrations of ammonia in human breath. Being able to extract an ammonia signal from flowing breath samples provided the advantage of collecting large amounts of data in a short period of time. Furthermore, the sensitivity and accuracy were highly supportive of the results found in previous literature. In a small cohort of 30 healthy human volunteers, breath ammonia concentrations were found to range from 29 ppb to 688 ppb which was broadly in line with other studies. However, no correlation between oral breath ammonia and oral breath carbon dioxide, gender, age or BMI was established. While monitoring daily routines, breath ammonia levels were shown to decrease until mid-day (post-prandial), but were followed by a large increase into the afternoon. The large variation in baseline levels was originally believed to be a result of a number of confounding factors

such as diurnal variation, inter-individual variation, food intake and metabolic activity, and the presence of significant levels of ammonia in oral breath from bacterial sources which would serve to obscure more subtle relationships. However, a comparison between nasal and oral breath ammonia appeared to imply that confounding factors may mostly exist in oral breath. Oral ammonia was consistently and significantly higher than nasal which may be pointing to the significance of oral bacterial contributions of ammonia as mentioned by Smith *et al.* [26] in previous literature. If so, this suggests that more appropriate ways of sampling are needed to avoid this unwanted contribution. Nasal breath sampling may assist with this. However, if monitoring of patients is the goal, issues of nasal congestion and comfort will need to be explored as well. More extensive studies with larger patient cohorts using nasal monitoring may add clarity to this preliminary study.

2.5 References

[1] Diskin, A.M., Spanel, P.and Smith, D., (2003), "Time Variation of Ammonia, Acetone, Isoprene and Ethanol in Breath: A Quantitative SIFT-MS Study Over 30 Days", *Physiological Measurement,* Vol.24 (1), pp. 107-119.

[2] Endre, Z.H., et al., (2011), "Breath ammonia and trimethylamine allow real-time monitoring of haemodialysis efficacy", *Physiological Measurement,* Vol.32 pp. 115-130.

[3] Smith, D., Spanel, P.and Davies, S., (1999), "Trace gases in breath of healthy volunteers when fasting and after a protein-calorie meal: a preliminary study", *Journal of applied physiology,* Vol.87 (5), pp. 1584-1588.

[4] Narasimhan, L.R., Goodman, W.and Patel, C.K.N., (2001), "Correlation of Breath Ammonia with Blood Urea Nitrogen and Creatinine During Hemodialysis", *Proceedings of the National Academy of Sciences of the United States of America,* Vol.98 (8), pp. 4617-4621.

[5] Harren, F.J.M., et al., (2000), "Photoacoustic Spectroscopy in Trace Gas Monitoring", *in AnonymousEncyclopedia of Analytical Chemistry,* John Wiley & Sons Ltd, pp. 2203-2226.

[6] Pushkarsky, M.B., et al., (2002), "Laser-based photoacoustic ammonia sensors for industrial applications", *Applied Physics B,* Vol.75 pp. 391-396.

[7] Patel, C.K.N. (1964), "Continuous-wave Laser Action on Vibrational-Rotational Transitions of CO2", *Physical Review,* Vol.136 (5A), pp. 1187-1194.

[8] Wang, C.and Sahay, P., (2009), "Breath Analysis Using Laser Spectroscopic Techniques: Breath Biomarkers, Spectral Fingerprints, and Detection Limits", *Sensors,* Vol.9 (10), pp. 8230-8262.

[9] Webber, M.E., Pushkarsky, M.and Patel, C.K.N., (2003), "Fiber-Amplifier-Enhanced Photoacoustic Spectroscopy with Near-Infrared Tunable Diode Lasers", *Applied Optics,* Vol.42 (12), pp. 2119-2126.

[10] Pranalytica, I. (2009) "Nephrolux Breath Ammonia Analyzer", *User Manual,* pp.1-32.

[11] Davies, A. and Moores, C., (2003)*, The Respiratory System - Basic Science and Clinical Conditions,* , Churchill Livingstone,.

[12] Turner, C., Španěl, P.and Smith, D., (2006), "A Longitudinal Study of Ammonia, Acetone and Propanol in the Exhaled Breath of 30 Subjects Using Selected Ion Flow Tube Mass Spectrometry, SIFT-MS", *Physiological Measurement,* Vol.27 (4), pp. 321-337.

[13] Enderby, B., et al., (2009), "Concentrations of Some Metabolites in the Breath of Healthy Children Aged 7-18 Years Measured Using Selected Ion Flow Tube Mass Spectrometry (SIFT-MS)", *Journal of Breath Research,* Vol.3 pp. 1-11.

[14] American Statistical Association. (1998), "What is a Survey?", *ASA Series: Section on Survey Research Methods,* pp. 1-8.

[15] Argyrous, G., (2005), "Inference Using Estimation and Confidence Intervals", *in AnonymousStatistics for Research,* (2nd ed.), SAGE Publications, pp. 242-253.

[16] Tortora, G.J., (2006), "Lung Volumes and Capacities; Exchange of Oxygen and Carbon Dioxide", *in AnonymousPrinciples of Anatomy and Physiology,* (11th ed.), John Wiley & Sons, Inc., New Jersey, pp. 868-870.

[17] Pleil, J.D.and Lindstrom, A.B., (1995), "Measurement of volatile organic compounds in exhaled breath as collected in evacuated electropolished canisters", *Journal of Chromatrography B,* Vol.665 pp. 271-279.

[18] Posner, J.B.and Plum, F., (1960), "The Toxic Effects of Carbon Dioxide and Acetazolamide in Hepatic Encephalopathy", *Journal of Clinical Investigation,* Vol.39 (8), pp. 1246-1258.

[19] Owen, E.E., Tyor, M.P.and Giordano, D., (1962), "The Effect of Acute Alkalosis on Renal Metabolism of Ammonia in Cirrhotics", *Journal of Clinical Investigation,* Vol.41 (5), pp. 1139-1144.

[20] Timmer, B., Olthuis, W.and Berg, A.v.d., (2005), "Ammonia Sensors and Their Applications – A Review", *Sensors and Actuators B,* Vol.107 (2), pp. 666-677.

[21] Zoli, M., et al., (1999), "Total and functional hepatic blood flow decrease in parallel with ageing", *Age and Ageing,* Vol.28 pp. 29-33.

[22] Španěl, P., Dryahina, K.and Smith, D., (2007), "Acetone, Ammonia and Hydrogen Cyanide in Exhaled Breath of Several Volunteers Aged 4 - 83 Years", *Journal of Breath Research,* (1), pp. L1-L4.

[23] Brooks, S.M., Haight, R.R.and Gordon, R.R., (2006), "Age Does Not Affect Airway pH and Ammonia as Determined by Exhaled Breath Measurements", *Lung,* Vol.184 pp. 195-200.

[24] Nybo, L., et al., (2005), "Cerebral ammonia uptake and accumulation during prolonged exercise in humans", *Journal of Physiology,* Vol.563 (1), pp. 285-290.

[25] Vince, A., et al., (1973), "Ammonia production by intestinal bacteria", *Gut,* Vol.14 (1), pp. 171-177.

[26] Smith, D., et al., (2008), "A Selected Ion Flow Tube Mass Spectrometry Study of Ammonia in Mouth- and Nose- Exhaled Breath and in the Oral Cavity", *Rapid Communications in Mass Spectrometry,* Vol.22 (6), pp. 783-789.

CHAPTER 3

A SYSTEM FOR THE CONTINUOUS GENERATION OF SIMULATED HUMAN BREATH SUPPLEMENTED WITH TRACE GASES

3.1 Introduction

Human breath is a complicated matrix where potential factors of interfering breath gases, temperature, and relative humidity (RH) levels can differ from individual to individual. As the study of human breath continues to increase in relevance for trace gas analysis, the development of a system capable of producing the necessary analyte gas concentrations combined with other breath elements (e.g. temperature and relative humidity) would prove to be a highly beneficial lab tool. There are numerous systems which have been developed for the purpose of breath simulation. However, most of these systems tend to focus on breathing patterns rather than actual exhalation of a humidified breath-simulating matrix containing trace gases indicative of a physiological function. They can serve the purpose of analysing gas exchange between blood and the tissue membrane of lungs [1], helping to instruct and provide practice for medical procedures [2], testing ventilatory devices [3], or demonstrating how respiration works in general [4]. However, such devices would not provide the variables needed for comparison of interferents in human breath. Alternatively, another option for breath simulation could be to examine the constituents of breath under controlled conditions in a static chamber. However, this would not simulate genuine physiological conditions of volume and flow rate. A current technology known as the Gas Calibration Unit (Ionimed Analytik GmbH, Austria) has shown potential for producing volatile organic compounds among humidified conditions [5], but the complexity of this technology makes it expensive by comparison to the system discussed in the present work and the use of ammonia gas in such a method was not previously observed.

In this chapter, a low-cost in-house system was developed to investigate the measurement and detection of trace gases and interferents commonly found in human breath during the sensor development stages. The device is composed of a number of integrated components which can facilitate the reproducible and measurable dilution of gaseous ammonia within a human breath analogue. It comprises a clinical respiratory humidifier to generate air at a fixed and continuous flow rate, temperature, and relative humidity comparable with normal human breath exhalate in combination with micro flow controllers for the supplementation of additional gases such as ammonia at physiologically relevant concentrations. Continuous flow allows the researcher to obtain as much sample as they require. In addition, the system was supplemented with sensors to monitor temperature, relative humidity, and volume flow rate. Gas concentrations were cross-validated using photoacoustic spectroscopic analysis of

the ammonia concentration correlated with gas concentrations calculated from first principles.

3.2 Materials and methods

3.2.1 Materials

A continuous air pump (SleepStyle^{TM}200 Series air flow system, Fisher and Paykel Healthcare, Auckland, NZ) was used to push air through the system and was monitored by way of a spirometer (EasyOne Model 2001, Fisher Biomedical Incorporated, FL, USA). Using a 56 cm extension of plastic tubing (Fisher and Paykel Healthcare, Auckland, NZ) with a diameter of 22 mm, the air pump was connected to the respiratory humidifier. The respiratory humidifier was composed of two components; the MR290 Autofeed humidification chamber (Fisher and Paykel Healthcare, Auckland, NZ) and the MR850 humidifier (Fisher and Paykel Healthcare, Auckland, NZ). An external 1 Litre sterile bag (Respicare Ltd, Dublin, Ireland) was the source of the 18.2 MΩ.cm^{-1} water (Millipore, MA, USA) entering the humidifier. From the humidifier is a 156 cm length of coil-heated plastic tubing (Fisher and Paykel Healthcare, Auckland, NZ). Attached to the tubing is an adaptor (Sigma-Aldrich Co., Ireland) connected to a fixed stainless the steel flow control regulator (0.3 or 0.5 L/min) (Specialty Gases Ltd, Kent, UK) of a 58 L ammonia cylinder (5 to 400 ppm) (Specialty Gases Ltd, Kent, UK) by way of a 45 cm length of 5 mm diameter nitrile tubing (Sigma-Aldrich Co., Ireland). Adapted to the end of the coil-heated tubing is a holding cap fabricated using ABSplus 3D printing (Dimension Inc, MN, USA). This cap holds a humidity sensor (HIH-4000 series, RS Components Ltd, Honeywell, UK) and a thermistor (NTC 198-927 series, RS Components Ltd, UK). A laptop (Sony, Ireland), data acquisition card (NI USB-6009, National Instruments, Berkshire, UK), and LabVIEW 8.6 software (National Instruments, Berkshire, U.K.) were used to acquire the humidity and temperature data. A schematic of the simulated breath system is shown in Fig. 3.1a and a photograph of the actual system in 3.1b.

3.2.2 Instrumentation

The PALS (Nephrolux^{TM}, Pranalytica Inc., CA, USA) discussed in Chapter 2 was utilised to quantify the ammonia concentrations during the calibration process. All flow rates were

correlated against ultrasound transit-time measurements using the EasyOne Model 2001 Spirometer (ndd Medical Technologies, MA).

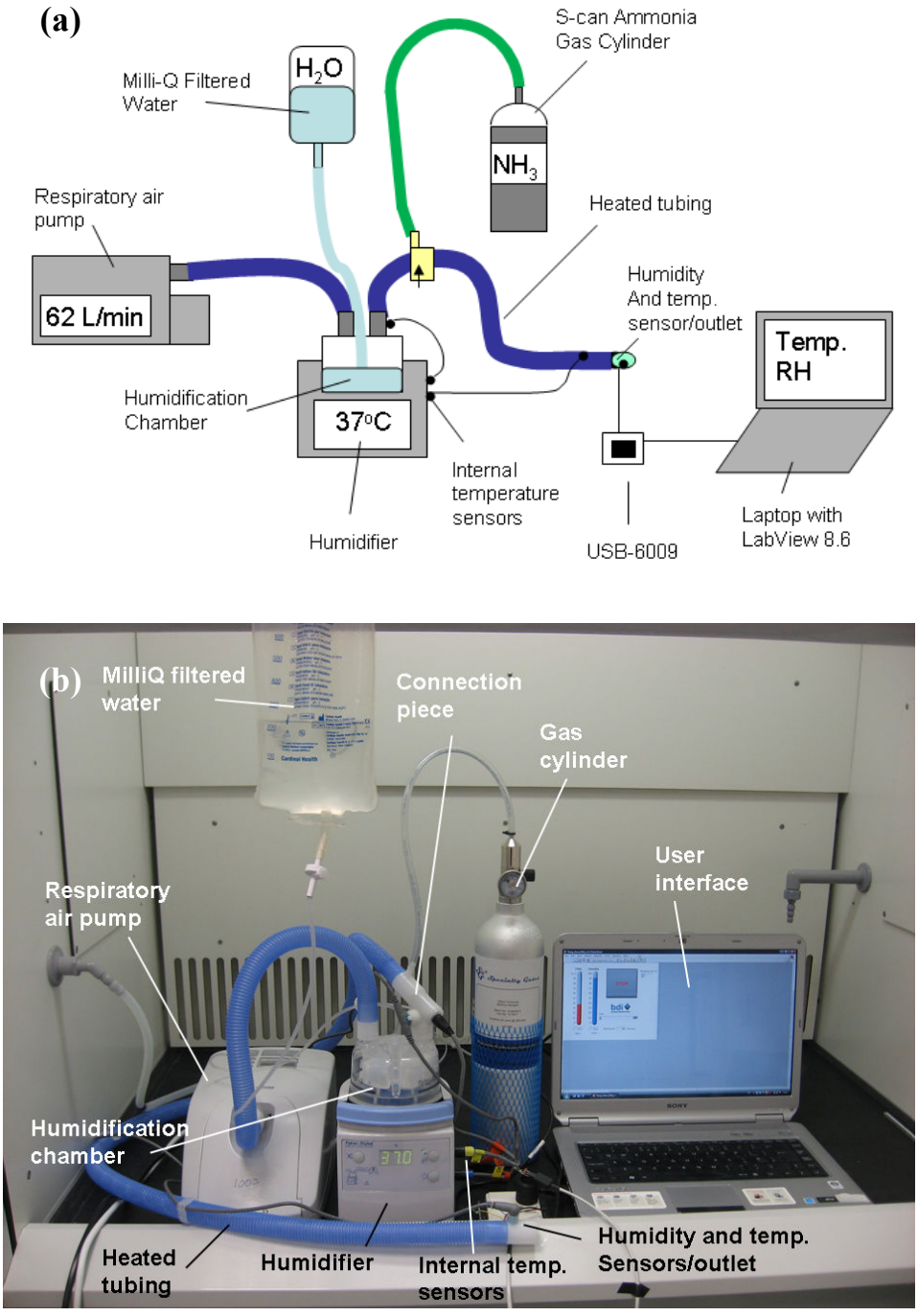

Figure 3.1 (a) Schematic and (b) photo of the simulated breath system. Atmospheric air is introduced via the respiratory air pump and mixed with water to create humidified air at a defined temperature. Ammonia gas is mixed with the turbulent flow of air to generate a controlled breath sample.

3.2.3 Air flow parameters

A continuous air pump supplies atmospheric air at a flow rate appropriate for human ventilation. It is typically used in attachment to continuous positive airway pressure (CPAP) machines to assist with obstructive sleep apnea [6]. This is capable of supplying flow rates of between 62.0 ±0.67 L/min and 83.9 ±0.47 L/min, depending on pressure settings and altitude and, for our application was set to supply air at a fixed flow rate of 62.0 ±0.67 L/min. Flow rates were independently monitored using a spirometer (Table 3.1).

3.2.4 Temperature and relative humidity measurements

The air pump connected to the respiratory humidifier pushed air through the system. The MR290 Autofeed humidification chamber introduced water into the air flow and the MR850 humidifier heated it. Combined together, these output warmed, humidified air in which the atmospheric air was heated to between 35 and 40^{o}C ±0.3^{o}C and humidified to approximately 98% RH. It is specified to create a humid environment in less than 30 minutes while maintaining a constant temperature. Internal temperature monitoring was monitored via the internal temperature probe, and an alarm was initiated when temperature levels exceeded the pre-set range [7]. The filtered water in the humidifier chamber was refilled using 18.2 MΩ.cm^{-1} water. The warmed, humidified air was then passed down the coil-heated plastic tubing. This was designed to reduce the build up of condensation within the tubing. While the internal temperature of the system was monitored by the temperature probes of the MR850 respiratory humidifier, the relative humidity and temperature of the expelled air were also monitored by way of a humidity sensor and a thermistor (Fig. 3.2a) which were placed in a flowing stream of the simulated breath at the end of the tubing using a holding cap (Fig. 3.2b). These were interfaced to a laptop via a data acquisition card and programmed using LabVIEW 8.6 software. The humidity sensor was capable of operating at temperatures between -40 and 85^{o}C whilst recording relative humidity from 0 to 100% with an accuracy of ±2.5% [8], and the thermistor performs over a temperature range of -55 to 250^{o}C [9]. It should be noted that ammonia is a corrosive substance and prolonged exposure to it might require regular replacement of the humidity sensor and thermistor.

(a)  (b) 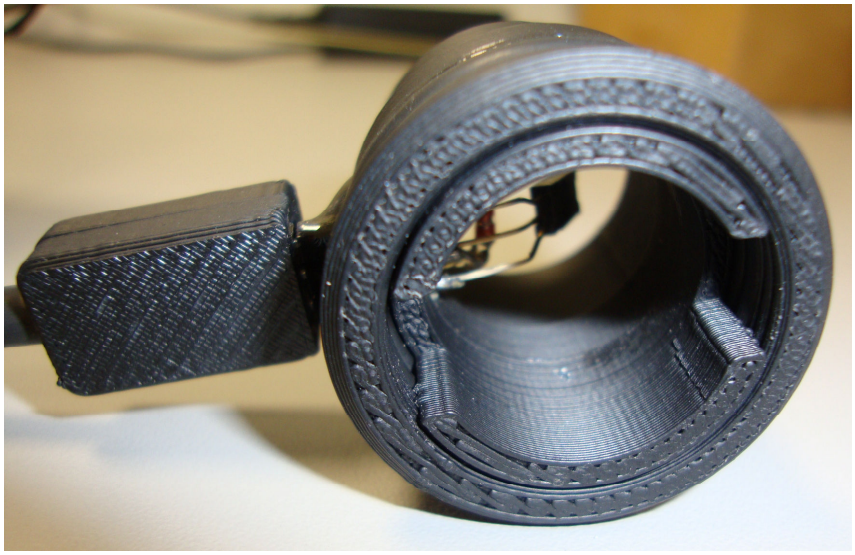

Figure 3.2 External humidity-temperature sensor: (a) Combining the HIH-4000 humidity sensor (black) and NTC 198-927 thermistor (red); (b) Attachment of the sensors within the ABS*plus* 3D cap.

3.2.5 Calibrations of ammonia gas

At the point at which the humidified air enters the plastic tubing, an adaptation piece allowed the injection of ammonia gas to join the flow of warmed, humidified air. To facilitate variation of the volume of ammonia applied to the system, and thus its concentration, fixed stainless steel flow control regulators (0.3 or 0.5 L/min) were used. Ammonia gas was supplied at concentrations between 5 and 400 ppm. The cylinders were connected to the connection piece via nitrile tubing. Beyond this intersection, the length of plastic tubing allowed for turbulent flow conditions that mix the added ammonia with the humidified air. The fluid dynamics of the humidified air with gaseous ammonia in the system were calculated to have a Reynolds number in excess of 11,000 (Appendix 2), indicating turbulent flow and, therefore, good mixing.

3.3 Results and discussion

3.3.1 Air flow parameters

This spirometer was capable of measuring with an accuracy of ±2% (volume), ±2% (flow), ±5% (maximum voluntary ventilation) and a resistance of approximately 18 $cmH_2O/L/min$ [10]. Maximum voluntary ventilation (MVV) was the key lung flow measurement used.

The MVV is a display of the maximum volume over a period of one minute and was used in comparisons between known human flow rates and the simulated system flow rates. Previous literature has shown the MVV in healthy human adults in the range between 29 and 190 L/min with a mean of 111 ±35 L/min (n=95) [11]. In a larger study, 2,247 volunteers categorized by age generated a low mean of 46 ±0 to a high mean of 120 ±25 L/min [12]. Since the relaxed MVV from the simulated breath system (i.e. 62.0 ±0.67 L/min) was within range of both studies, it was chosen for this preliminary study. By controlling the pressure and altitude settings of the SleepStyle^{TM}200 Series air flow system, the MVV could be adjusted accordingly with little deviation (Table 3.1). The flow rates of the simulated system were found to be comparable to the flow rates of human breath indicating that the flow rates produced are appropriate for the simulation of human breath flow, albeit of a constant flow rate.

Table 3.1 Flow rates from the simulated breath system (n = 3) as determined from spirometry measurements at a temperature of 38 ±0.3^{o}C and relative humidity of 96 ±1% (n = 216).

Pressure (cmH_2O)	Altitude (m)	MVV (L/min)
4	0	62.0 ±0.67
4	500	63.9 ±0.29
4	1,000	65.6 ±0.40
4	1,500	67.1 ±0.30
4	2,000	68.5 ±0.55
5	0	69.5 ±0.60
5	500	72.0 ±0.60
5	1,000	73.2 ±0.29
5	1,500	74.7 ±0.76
5	2,000	77.8 ±0.49
6	0	76.0 ±0.64
6	500	78.1 ±0.91
6	1,000	80.5 ±0.67
6	1,500	82.0 ±0.67
6	2,000	83.9 ±0.47

3.3.2 Temperature and relative humidity measurements

Previous literature has shown that human breath is exhaled at temperatures from approximately 32^{o}C to 37^{o}C [13][14]. Using its own internal temperature sensor, the MR850 monitors the internal environment in an attempt to maintain the air flow at a

constant temperature of 37°C. Under typical room temperature (approximately 21°C), the MR850 can maintain 37°C within ±0.5°C, but may vary more significantly under more extreme atmospheric conditions. At body temperature (i.e. 37°C), the relative humidity of human breath has been shown to range from approximately 91 to 96% [15]. The relative humidity of breath cannot reach 100% since this becomes the point at which it is no longer vapour, but is instead a condensate [16].

Humidity and temperature measurements were recorded at a flow rate of 62.0 ±0.67 L/min (n=3). Fig. 3.3 shows the averages of these three sets of readings. The initial humidity and temperature values generated by the simulated system were 51 ±7% RH and 21 ±1°C. From switch on, measurements from the external humidity sensor showed that the simulated breath system went from 51 ±7% RH to 91 ±3% RH in 530 seconds, then to 96 ±3% RH in 2,140 seconds, and the maximum pre-condensation point of 99 ±1% in 2,930 seconds. Temperature increased from 21 ±1°C to 32 ±1°C in 170 seconds, then to 37 ±1°C in 770 seconds, and reached a maximum of 38 ±1°C at 890 seconds which was maintained through 3,600 seconds. Condensation began to develop within the heated tubing after about 2,970 seconds which was corroborated by the humidity sensor reading above 99%. Due to the claims from previous literature, an equilibrium range from 91 to 96% relative humidity, and temperatures of 32 to 37°C were sought in the development of this simulated breath system. Thus, the purpose was to determine the time period over which the system would be operational within these parameters. Between 520 and 880 seconds, the system was at both the desired temperature (i.e. 32 to 37°C) and relative humidity (i.e. 91 to 96%). However, from 520 to 2,930 seconds, the system operated between 32 and 38 ±1°C and between 91 and 99 ±1% RH. This time could potentially be extended if the heating coils were increased to a temperature that could fully prevent condensation within the tubing without overheating the humidified air. Assuming that these maxima were suitable for simulated breath testing, the analytical measurements were performed within this window. If condensation did build up in the system, the system was switched off and the tubing cleaned and blow dried before reuse to remove condensate and prevent any trace gas build up in the condensate or on the tubing surfaces. Not doing so could result in contamination of future measurements by residual gases.

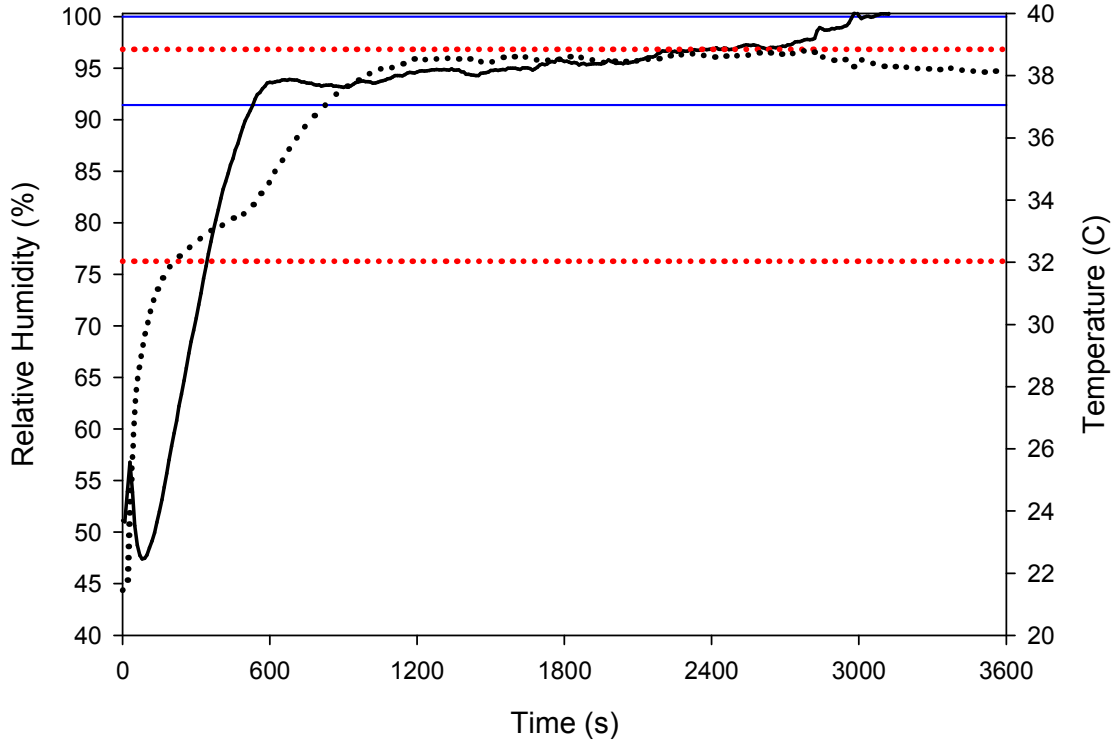

Figure 3.3 Measured operational temperature (dotted line) and relative humidity (solid line) of the simulated breath system from switch on (n = 3). Humidifier temperature setting: 37°C; Pressure and flow rate: 4 cmH_2O (measured MVV of 62 ±0.67 L/min); Initial system temperature: 21°C; Initial system humidity: 51% RH. Horizontal dotted and solid lines show lower and upper operational specification limits of temperature (32 to 39°C) and humidity (91 to 99% RH), respectively.

3.3.3 Calibrations of ammonia gas

The PALS instrument was developed for the quantification of ammonia in human breath. It is specified to detect ammonia as low as 1 ppb ±10% within 120 seconds [17]. A recent study using photoacoustic laser spectroscopy has shown that the ammonia breath values in a population of 30 normal human volunteers was in broad agreement with earlier studies using techniques such as SIFT-MS [18]. Exhaled breath from a healthy human adult contains ammonia concentrations from 50 to 2,000 ppb [19]. To produce and validate the concentrations of ammonia being delivered from the simulated breath system, a correlation was performed between calculated values and measured values using PALS. A total of 15 minutes per flowing sample was recorded. The first 10 minutes were used to ensure the

system had stabilized. Over the next five minutes, five samples were taken and averaged as the actual sample concentration. The calculated values were determined by way of introducing a known concentration of ammonia at a fixed flow rate into the known flow of humidified air (Appendix 3). For example, introduction of 50,000 ppb ammonia (v/v) at a flow rate of 0.3 L/min into the turbulent flow of simulated breath was calculated to generate a final concentration of 240.77 ppbv ammonia:

*((0.3 L/min / (62 L/min humidified air + 0.3 L/min NH_3 flow)) * 50,000 ppb NH_3 cylinder =*

240.77 ppbv NH_3 expected (Sample #7 in Table 3.2; Fig. 3.4) **(1)**

The measured concentrations obtained from PALS yielded a 0.9978 correlation with the calculated values over the measured range of approximately 0 to 3,000 ppbv (Table 3.2; Fig. 3.4), with a slope of 0.9374 and an intercept of 19 ppbv.

Table 3.2 Concentrations of calculated and measured ammonia (n = 5) in Fig. 3.4.

Calculated (NH_3 / ppbv)	Measured (NH_3 / ppbv)
0	0 ±0
24	18 ±1
40	40 ±2
80	92 ±3
120	121 ±15
200	218 ±2
241	245 ±8
400	392 ±6
482	460 ±10
800	755 ±7
963	984 ±21
1,445	1,368 ±11
1,600	1,576 ±7
1,926	1,919 ±20
2,400	2,175 ±26
3,200	2,993 ±10

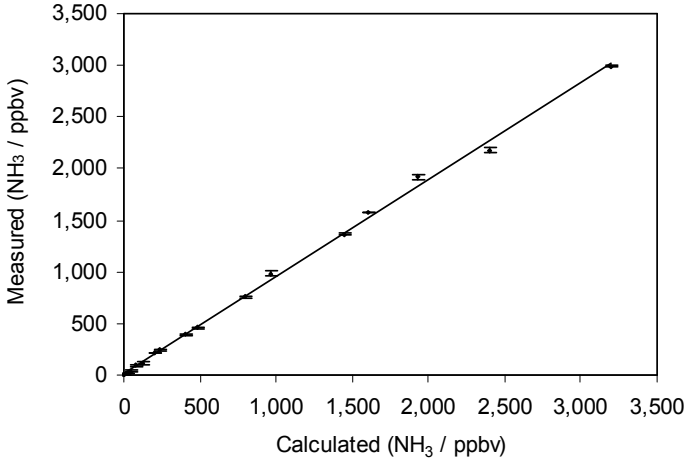

Figure 3.4 Calibration plot of ammonia concentrations. The calculated concentrations of ammonia compared against the measured concentrations (n=5) displayed by PALS (R^2 = 0.99). A slope and intercept of 0.9374 $ppbv^{-1}$ and 19.09 were generated.

This data suggests that, at low concentrations, there was a slight underestimation of the calculated value with respect to the measured value, whereas at higher concentrations, there appears to be an overestimation of the calculated value with respect to the measured value. This deviation from an ideal relationship may be due, either to discrepancies in the theoretical model of calculation and the system which does not derive the ideal ammonia concentrations calculated, or with analytical errors associated with the measurements determined from the photoacoustic spectrometer. Notwithstanding this, however, the two methodologies showed excellent correlation and comparability, cross-validating the two methods and demonstrating that the simulated breath system can be used to produce a continuous flow of simulated human breath, supplemented with known concentrations of trace gases, over a clinically useful range.

3.4 Conclusions

A system was developed which was capable of simulating human breath variables such as a flow rate with defined temperature and humidity. The system could be supplemented with known concentrations of a trace gas (i.e. ammonia) across the clinically relevant range for this gas in human breath from 18 to 2,993 ppbv which was corroborated using photoacoustic laser spectroscopy. The system can be used for controlled laboratory experiments which require observation of trace gas measurements among human breath interferents.

3.5 References

[1] Stefan Fischer, R.and Georg Matheis, B., (2007), "Artificial lung system and its use", Patent US 2007/0276508 A1.

[2] Lampotang, S., et al., (1996), "Self regulating lung for simulated medical procedures", Patent US005584701A.

[3] Barkalow, C.E., (1984), "Pneumatic lung analog for simulation of spontaneous breathing and for testing of ventilatory devices used with spontaneously breathing patients", Patent US 4,430,893.

[4] Owens, J.E., et al., (2005), "Mechanical Lungs", Patent US 6,910,896 B1.

[5] Singer, W., et al., (2007), "Dynamic gas dilution system for accurate calibration of analytical instruments such as PTR-MS", *Third international conference on proton transfer mass spec,* Vol.1 pp. 232-237.

[6] Fisher and Paykel Healthcare. (2009) "User Manual", *Sleep Style 200 CPAP,* pp.1-10.

[7] Fisher and Paykel Healthcare. (2005) "User Manual", *MR850 Respiratory Humidifier,* pp.1-62.

[8] Honeywell. (2005) "HIH-4000 Series", *Humidity Sensors,* pp.1-4.

[9] RS Components. (1999) "NTC Thermistors", *RS Data Sheet: Data Pack E,* .

[10] NDD Medical Technologies. (2004) "EasyOne Model 2001 Diagnostic Spirometer", *EasyOne Specifications,* .

[11] Kor, A.C., et al., (2004), "Prediction of the maximal voluntary ventilation in healthy adult Chinese subjects", *Respirology,* Vol.9 (1), pp. 76-80.

[12] Yokoyama, T.and Mitsufuji, M., (1972), "Statistical Representation of the Ventilatory Capacity of 2,247 Healthy Japanese Adults", *Chest,* Vol.61 (7), pp. 655-661.

[13] Popov, T.A., et al., (2007), "Evaluation of a Simple, Potentially Individual Device for Exhaled Breath Temperature Measurement", *Respiratory Medicine,* Vol.101 (10), pp. 2044-2050.

[14] Deng, C., et al., (2004), "Determination of Acetone in Human Breath by Gas Chromatography - Mass Spectrometry and Solid-Phase Microextraction with On-fiber Derivatization", *Journal of Chromatrography B,* Vol.810 (2), pp. 269-275.

[15] Zehentbauer, G., Krick, T.and Reineccius, G.A., (2000), "Use of Humidified Air in Optimizing APCI-MS Response in Breath Analysis", *Journal of Agricultural and Food Chemistry,* Vol.48 (11), pp. 5389-5395.

[16] Holloway, A.M.and Wayne, R.P., (2010), "Life and the atmosphere", *Atmospheric Chemistry,* pp. 80-98.

[17] Pranalytica, I. (2009) "Nephrolux Breath Ammonia Analyzer", *User Manual,* pp.1-32.

[18] Hibbard, T.and Killard, A.J., (2011), "Study of human baseline breath ammonia measurements using photoacoustic laser spectroscopy", *The Journal of Breath Research,* Vol.5 pp. 1-8.

[19] Aguilar, A.D., et al., (2008), "A Breath Ammonia Sensor Based on Conducting Polymer Nanojunctions", *IEEE Sensors Journal,* Vol.8 (3), pp. 269-273.

CHAPTER 4

DEVELOPMENT OF A METHOD FOR THE MEASUREMENT OF AMMONIA IN HUMAN BREATH USING INK-JET PRINTED POLYANILINE ELECTRODES

4.1 Introduction

Chapters 2 and 3 have managed to define the normal parameters of breath ammonia as well as create a system that produces ammonia within a breath-like matrix of commonly known physiological interferents. Using these as a control, assessment to define the behaviour and performance of in-house developed conducting polymer-based electrodes took place. Some conducting polymers which have demonstrated an affinity for gas sensing include polyaniline, polypyrrole, and polythiophene. The chemical structures (scheme 1) of these polymers are:

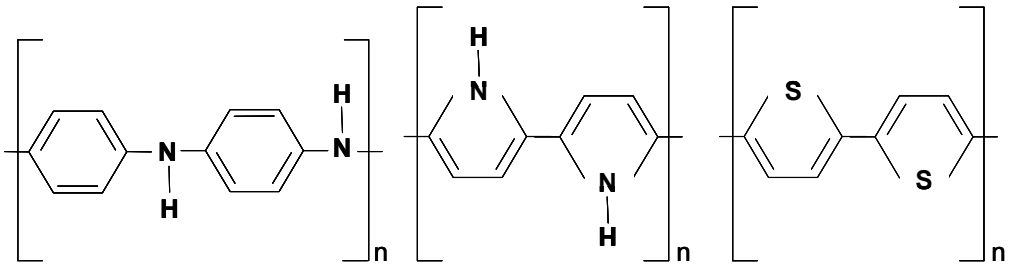

(1)

where (a) is polyaniline, (b) is polypyrrole, and (c) is polythiophene. Previous literature which utilised these polymers as films for gas-sensing electrodes indicated that detection of ammonia gas was possible via a change in resistance [1]. To isolate gaseous ammonia and quantify the concentration from breath in this chapter, polyaniline was the chosen sensing element. Polyaniline is a conducting polymer that has proven on numerous occasions to be effective in the detection and quantification of ammonia. The research of Wu *et al* observed the change in resistance resulting from interactions of ammonia concentrations from 10 to 1,000 ppm with polyaniline upon gold electrodes [2]. Using an optical approach, Jin *et al* observed changes in the absorption spectra as ammonia concentrations from 180 to 18,000 ppm flowed across a polyaniline film within a spectrometer system [3]. The reason polyaniline works so well is because the emeraldine state can be produced as either a salt or a base where the salt form is highly conductive due to its delocalised positive charge. When interaction takes place between analytes such as gaseous ammonia and protonated polyaniline, the polyaniline deprotonates to the base form [4] as shown in the following reaction diagram (scheme 2):

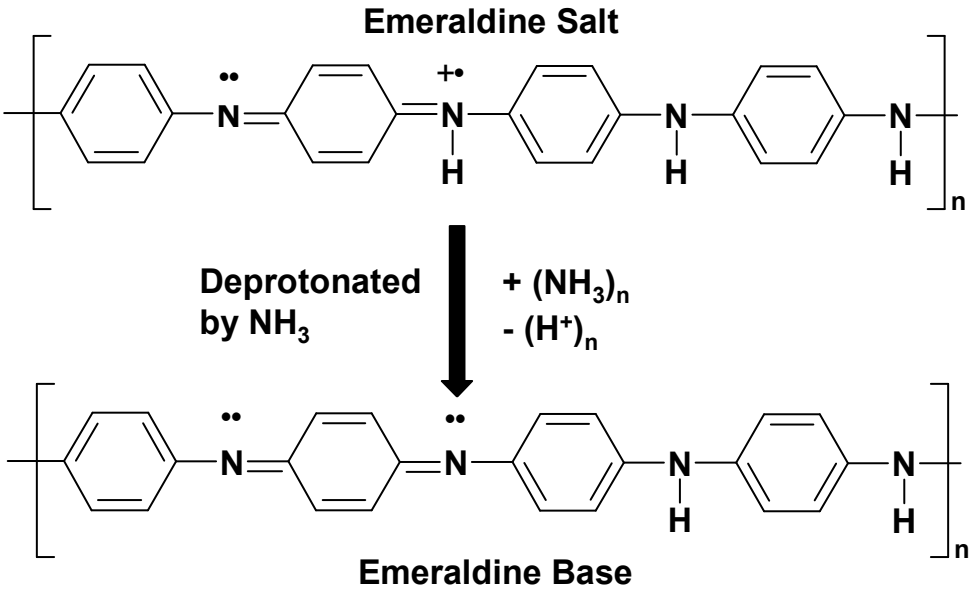

(2)

It is this deprotonation that causes changes in the observable conductive behaviour.

Though polyaniline exhibits the preferable conductive characteristics, it lacks the desired solubility in common solvents [5] that would be preferable for application to electrode-based analysis. However, the research of Li *et al* demonstrated how a colloidal suspension of polyaniline of nano-scale could be utilised for the purpose of deposition onto various substrates [6]. Among the more common methods of high resolution dispersion are micro-contact printing (μCP), ink-jet printing, screen printing, and offset printing. Each of these could be used in conjunction with substrates such as plastic, glass, laminates, and metal which provides the benefit of low cost production [7]. Of the printing techniques, ink-jet printing by way of piezoelectric drop-on-demand has displayed great promise. The picolitre volumes enable particularly thin layer production, and the multichannel assembly can be used to create simultaneous prints. Furthermore, since the printing method does not require direct contact with the substrate, damage to the dispersed polyaniline is prevented [8]. The combination of conducting polymers such as polyaniline with ink-jet printing for the purpose of sensor development is beginning to arise in reports, but research into applications for such areas as chemical sensing, biosensing, and other electronic devices still holds a challenge [5].

The Nanoparticle Technology Handbook defines a nanoparticle as being a particle between the range of 1 nm and 1 μm [9]. By this definition and the three-digit nanometre diameters

generated upon synthesis of the aforementioned polyaniline, the particles in this chapter have been termed polyaniline nanoparticles (nanoPANI). The nanoPANI was synthesised as an aqueous dispersion and piezoelectrically ink-jet printed onto the interdigitated silver electrode of a polyethylene terephthalate (PET) plastic substrate. It was previously verified that by observing the change in current from nanoPANI dispersion, analytes of interest such as ammonia could be detected between a range of 1 and 100 ppm [10]. Since the emeraldine salt form of polyaniline has proven to be conductive [11], detection and quantification by way of impedance, *Z*, (in units of ohms, Ω) was chosen to monitor the interaction between ammonia and nanoPANI. Polyaniline has been well studied using impedance spectroscopy. Research has shown the effects of utilising various electrode compositions [12], frequency analysis with focus on capacitive and inductive distortions [13], and the results of alternating current [14] and direct current [15]. However, the goal now is to isolate the signal specific to ammonia from the common physiological interferences that can arise in the stream of breath. By using a combination of nanoPANI-based silver electrodes and AC impedance, isolation and quantification of an ammonia gas signal in the necessary range of parts-per-billion (ppb) is shown to be possible among the matrix of human breath.

4.2 Materials and methods

4.2.1 Materials

Polyethylene terephthalate plastic (HiFi Industrial Film Ltd., UK) and Electrodag PF-410 silver ink (Acheson, Henkel Ireland Ltd., Ireland) were purchased and used as received. The nanoPANI consisted of deionised water (Veolia Water Solutions and Technologies, Ireland), dodecylbenzene sulphonic acid (Tokyo Chemical Industry UK Ltd., UK), ammonium persulfate (Sigma-Aldrich Co., Ireland), distilled aniline (Sigma-Aldrich Co., Ireland), and sodium dodecyl sulfate (Sigma-Aldrich Co., Ireland). Oxygen was provided by Air Products Ireland Ltd (Dublin, Ireland). Nitrogen was produced from in-house generators (DCU, Ireland). Carbon dioxide, ammonia, nitric oxide and hydrogen sulphide gases were supplied by Specialty Gases Ltd (Kent, UK).

4.2.2 Instrumentation

A DEK-248 screen printer (DEK International, Ireland) was used to print the silver ink onto the polyethylene terephthalate (PET) substrate. All ink-jet printing was performed using the Dimatix Drop Manager Ink-jet printer (FUJIFILM Dimatix Inc., Santa Clara, CA). Impedance measurements were conducted using a model 660C Series Electrochemical Analyser Workstation (CH Instruments Inc., Austin, TX). Simulated breath samples were generated using an in-house developed simulated breath system (Chapter 3, DCU, Ireland). Scanning electron microscopy (SEM) images were obtained with a Hitachi S3400 scanning electron microscope (Hitachi High Technologies America, Inc., U.S.A.) equipped with energy-dispersive X-ray spectroscopy (Oxford Inca EDX, Oxford Instruments, UK). Particle size distribution was performed using ImageJ software (ImageJ, NIH, USA). The UV-vis results were observed using a Lambda 900 UV/VIS/NIR spectrometer (PerkinElmer Inc., U.S.A.).

4.2.3 Electrode fabrication via screen printing

Using a DEK-248 screen printer consisting of a polyester screen with mesh thickness of 77T (filaments per cm) at 45^{o} to the print stroke, the silver electrodes were printed in-house via the method discussed in Crowley *et al* [16]. The commercial conductive silver ink was printed onto a 175 μm thick polyethylene terephthalate (PET) plastic substrate. Afterwards, the print was heat-treated at 150^{o}C for 30 minutes.

4.2.4 Polyaniline nanoparticle synthesis

Details of the polyaniline synthesis have been discussed previously [8][17]. In summary, nanoPANI was synthesised by adding 3.6 g of 0.25 M 90% dodecylbenzene sulfonic acid (DBSA) to 40 mL of deionised water. This was stirred at room temperature (20^{o}C) until the DBSA fully dissolved. To the DBSA solution, 0.36 g of ammonium persulfate (APS) was added and stirred until fully dissolved. This was followed by 0.6 mL of distilled aniline and allowed to mix for 150 min. After 150 min, 20 mL of 0.05 M sodium dodecyl sulphate (SDS) was added to the DBSA/APS/aniline solution which appeared thick and dark green in colour. The DBSA/APS/aniline/SDS solution was then centrifuged at 5,000 rpm for 30 minutes. The supernatant from the centrifuged solution was then poured into dialysis tubing

and dialysed against 0.05 M SDS for 2,880 min producing an aqueous ink-jet printable material.

4.2.5 Printing of nanoPANI via ink-jet

Previous work by Crowley *et al* [10] details the technique of ink-jet printed nanoPANI and the potential for detection of gaseous ammonia. In brief, preparation of the printer involved using a Norm-Jet Syringe combined with an Acrodisc polyvinylidene fluoride (PVDF) Syringe Filter (0.45 μm) and needle to inject nanoPANI into a Fuji Dimatix ink cartridge. The cartridge was placed into the Dimatix ink-jet printer where 10 nanoPANI layers were printed onto the silver electrodes. After printing 10 nanoPANI layers, the sheets of dry sensors were lightly rinsed with deionised water to remove any excess SDS that may reside. To ensure that the deionised water was fully removed, they were placed in a dry-heat oven at 70^{o}C for 30 minutes. Afterwards, the electrodes were cut from the PET sheet, and used for impedimetric analysis (Fig. 4.1).

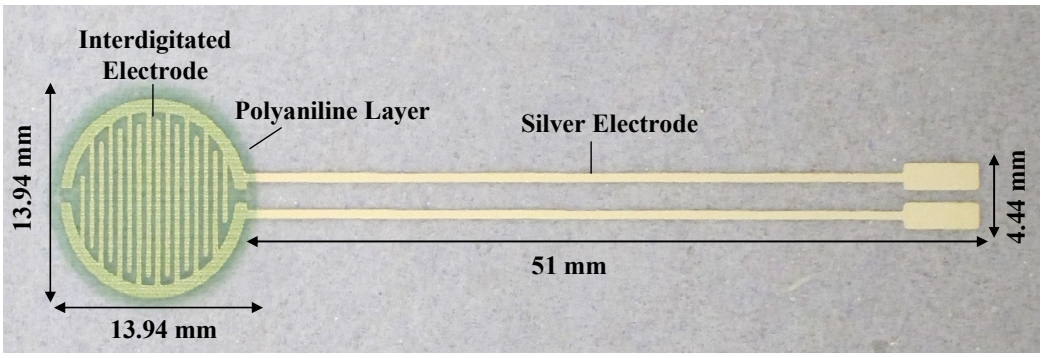

Figure 4.1 Design of interdigitated nanoPANI-based electrode.

4.2.6 Dispersion of nanoPANI upon electrodes

Observation of nanoPANI dispersal took place using SEM at 20 kV. The images were taken from between the interdigitated portion of a printed electrode that had been gold sputtered. Particle size distribution was obtained using ImageJ software.

4.2.7 Analysis of polyaniline formulation using energy-dispersive X-ray spectroscopy

Using EDX at 20 kV and x5k magnification, the formulation of polyaniline was assessed where a sample was added directly to an aluminium stub (with no carbon tab) and coated with chromium.

4.2.8 Electrode characterisation

The UV-vis spectrum was obtained from an aqueous dispersion made in our lab (1:50 dilution polyaniline in water) by way of monitoring the absorbance over a wavelength range from 300 nm to 1,300 nm. Using the spectra, distinctions were made between properly and improperly synthesised polyaniline. Resistive and capacitive characteristics of the nanoPANI modified IDEs were analysed over a frequency range of 1 to 100,000 Hz (5 mV rms) with and without ammonia exposure (n=3). Interdigitated electrodes (n=30) were then examined for their inter- and intra- electrode variability with reference to pure resistor stability and drift. Of these, 10 randomly chosen electrodes possessing different initial resistances were compared for reproducibility of the electrode behaviour.

4.2.9 Evaluation of the effect of pH

Solutions of pH 4, 6, 8, and 9 were used. The pH levels were indicated via universal litmus strips placed into the stream of exhaust from the simulated breath system during the first 1.6 min baseline period (before ammonia gas was turned on). With all parameters of humidity, temperature, flow rate, and sample length being the same as for previous protocols, the experiments were conducted where the electrodes were in the open environment in a fume hood. A concentration of 755 ppb ammonia was used for the measurements. The humidification chamber of the simulated breath system was changed for each of the four pH levels so as to reduce cross-contamination of solutions, and the water bags were changed for acid and base.

4.2.10 Interferent gases

Response of the electrodes to the percentile gases of breath (nitrogen, oxygen, carbon dioxide), as well as a few well-known volatile trace gases (nitric oxide, hydrogen sulphide, ammonia) was investigated for potential interferent effects. These potentially interferent gases were used at room temperature and contained no moisture. The first five minutes were used as a baseline with no exposure to the gases. Repeated exposure to the gas at flow rates of 0.3 L/min for 0.06 min intervals was followed by a rest of one minute until ten minutes were reached.

4.2.11 Temperature, humidity, and humidified ammonia

Using the simulated breath system discussed in Chapter 3, tests were performed to evaluate the effects of atmospheric air at room temperature (21 ±1^{o}C), atmospheric air (room humidity) at human breath temperature (37 ±1^{o}C), atmospheric air (with induced increase in humidity) at human breath temperature (37 ±1^{o}C, ≥90% RH), and atmospheric air (with induced increase in humidity) at human breath temperature containing ammonia (37 ±1^{o}C, ≥90% RH, 245 ±8 ppbv) on the ratio-metric impedimetric response of the nanoPANI-modified electrodes. Over a time span of 10 min, the first 1.67 min were used as a baseline with no exposure. At 1.68 min, the electrodes were exposed to a 62 ±0.67 L/min sample for repeated periods of 0.06 min every 1.67 min.

4.2.12 Quantification of ammonia

Using the simulated breath system discussed in Chapter 3, nanoPANI electrodes were exposed to samples (≥90% RH, 37 ±1^{o}C, 62 ±0.67 L/min) containing ammonia at concentrations from 40 ±2 ppbv to 2,175 ±26 ppbv (n=3) to observe the quantifiable ratio-metric impedance response (Z/Z_0) profile at 962 Hz. The initial 1.67 min were the baseline with no exposure to the gas. Beginning at 1.68 min, the electrodes were exposed to 0.06 min intervals of sample breath gas. This was repeated after the combined 0.25 min decrease in Z/Z_0 (humidity effect) and 0.25 min post-peak stabilisation resulting in one breath measurement every 0.5 min until 10 min was reached (~16 breaths).

4.3 Results and discussion

The current work is based upon the effective replication of a previously established formulation of polyaniline. The prior formulation which led to the current formulation was discussed in detail in the collaborative works of Ngamna *et al* [8] and Crowley *et al* [10], and correct replication of the formulation has been explained by way of comparable characteristic UV-visible spectra.

4.3.1 Reaction mechanism

The reaction that is expected to take place when gaseous ammonia interacts with the nanoPANI on the electrodes is:

$$1PAH^{+}DBSA^{-} + 1NH_3 \rightleftharpoons 1PA + 1DBSA^{-}\,NH_4^{+}$$

where PAH^+ is protonated (emeraldine) nanoPANI, PA is deprotonated (emeraldine) nanoPANI, NH_3 is gaseous ammonia, and NH_4^+ is ammonium [4]. Dodecylbenzene sulfonic acid ($DBSA^-$) provides the counter ion to balance the exchange of protons between nanoPANI and ammonia. As ammonia interacts with nanoPANI, the available protons on the nanoPANI are taken by the ammonia molecule. In doing so, ammonia converts to the more energetically favourable ammonium molecule [2]. This deprotonation of the nanoPANI causes a disturbance in the electrochemical signal displayed as an increase in impedance directly proportional to the concentration of ammonia. When the source of ammonia desists, the ammonium molecule reverts back to ammonia and protons which potentially returns the nanoPANI to its original status.

4.3.2 Dispersion of nanoPANI upon electrodes

When using ink-jet printing as the method of dispersion, it is necessary to use particles that are several orders of magnitude smaller than the diameter of the cartridge nozzle so as to prevent blockage [5]. Typically, the particles found in ink-jet inks range between approximately 100 nm to 400 nm [18], and the diameter of the nozzles in the Dimatix ink-jet printer were reported to be 20 μm [19]. Studies have shown that the size of the nanoparticles can increase or decrease depending on the ratio of aniline to either APS or DBSA [8]. This is an important observation, because the size can often affect dispersion as well as the conductive behaviour of the nanoparticles. For example, when the concentration of APS is increased in proportion to the aniline, secondary growth of the polymer particles takes place resulting in increased size. Along with the increased size, there would be an increase in overall conductivity. However, the increased size carries with it the difficulty of dispersing properly through the diameter of the cartridge nozzle. Inverse to the results of increased APS, an increase in DBSA with regard to aniline results in smaller particle sizes due to its ability to stabilise the dispersion. A decrease in particle size is favoured when using ink-jet printing, but the level of resistance tends to increase [8]. Hence, a balance must be found in order to generate a nanoparticle formulation which disperses easily by way of ink-jet printing while upholding a useable level of conductivity.

Shown via SEM (Fig. 4.2), the samples clearly consist of a continuous conductive printed film of polyaniline where some of the particles appear distinctly on top. By isolating the

more distinct particles, size distribution could be conducted which displayed a mean particle diameter of 382 ±33 nm (Table 4.1, n=23).

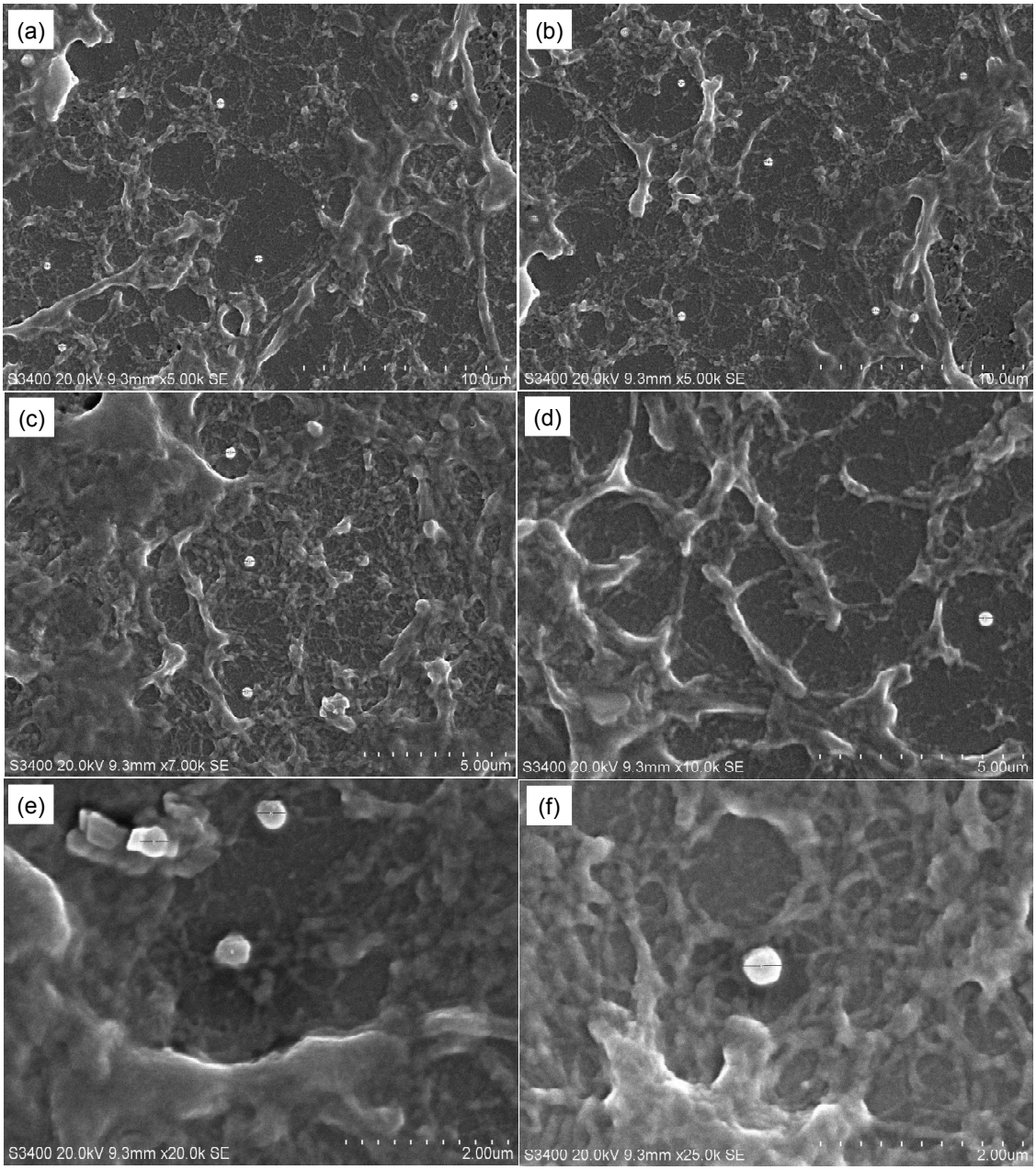

Figure 4.2 SEM images of printed polyaniline film obtained at magnifications of (a) x5K, (b) x5K, (c) x7K, (d) x10K, (e) x20K, (f) x25K.

Table 4.1 Size distribution of particles in Fig. 4.2

Particle	Diameter (nm)	Particle	Diameter (nm)	Particle	Diameter (nm)
a1	376	b1	395	c1	356
a2	397	b2	335	c2	397
a3	396	b3	373	c3	369
a4	436	b4	397	d1	364
a5	357	b5	432	e1	424
a6	395	b6	375	e2	350
		b7	452	e3	358
		b8	334	f1	387
		b9	335		

4.3.3 Analysis of polyaniline formulation using energy-dispersive X-ray spectroscopy

Use of EDX displayed the key elements which exist in the polyaniline formulation (Table 4.2; Figure 4.3). The spectrum of existing elements was measured at three locations of the polyaniline sample. It is expected to find contributions from the elements of the formulating components of deionised water (H_2O), dodecylbenzene sulphonic acid ($C_{18}H_{30}O_3S$), ammonium persulfate ($(NH_4)_2S_2O_8$), distilled aniline ($C_6H_5NH_2$), and sodium dodecyl sulfate ($CH_3(CH_2)_{11}OSO_3Na$). Of the components which were observed, contributions of carbon, oxygen, sodium, and sulphur were easily identified. The aluminium and trace amounts of copper were from the stub used to hold the sample. Silicon is s byproduct of the inner housing of the EDX system. Phosphorus was at such a low trace level that it is believed to be a false measure of the peek at that region of the spectrum more indicative of noise. Nitrogen is not indicated due to the limited range of sensitivity in EDX. Nitrogen can be absorbed by the matrix especially if large amounts of carbon are in the formulation. In other words, carbon's transmission absorbs that of nitrogen. It has also been indicated that the polymer film window on the detector would strongly absorb the nitrogen line acting as an interferent for that element (EDX user manual, DCU).

Table 4.2 EDX percentages of elements obtained from polyaniline formulation

Carbon (%)	60.86 ±3.7	**Silicon (%)**	0.07 ±0.0
Oxygen (%)	24.90 ±1.2	**Phosphorus (%)**	0.03 ±0.0
Sodium (%)	0.57 ±0.1	**Sulphur (%)**	11.03 ±2.6
Aluminium (%)	2.32 ±0.3	**Copper (%)**	0.25 ±0.0

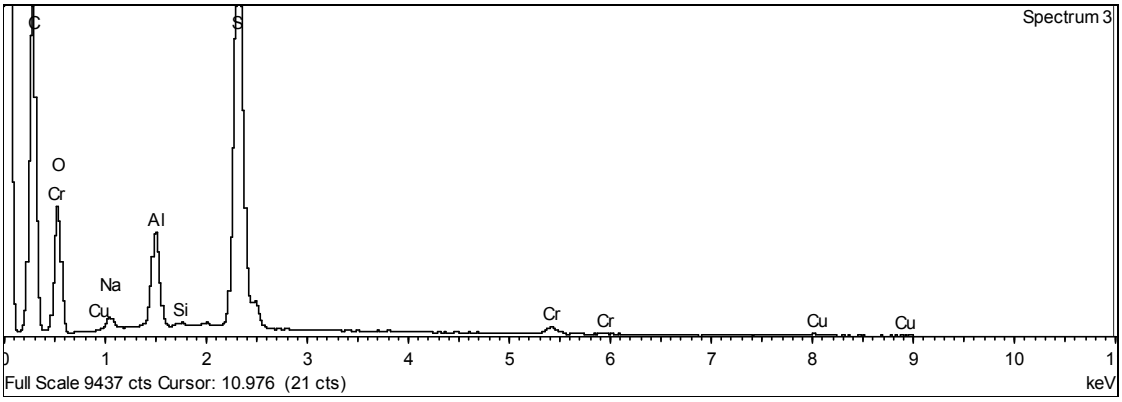

Figure 4.3 EDX spectrum of elements found in polyaniline formulation

4.3.4 Electrode characterisation

UV-visible spectra's were obtained for six different nanoPANI dispersions (Fig. 4.4) so as to demonstrate the difference between formulations which are effectively replicates of the previously established formulation [8] and those which are not. The nanoPANI labelled Batch 1 was a nano-dispersion created in our lab from the recipe described in this chapter. Batches 2 and 3 were also nano-dispersions from that same recipe by separate individuals in other labs at DCU. Batch 4 was from a dispersion made in our lab that was not uniform throughout and displayed obvious physical inconsistencies. Batches 5 and 6 were dispersions from other labs that also lacked uniformity. From this, the initial expectation was that Batches 1 - 3 would present similar spectra of useable nanoPANI while Batches 4 - 6 would display a significant difference indicative of a solution that would be discarded. In the case of the emeraldine salt form of polyaniline, it is characteristic of the energy transitional $\pi - \pi^*$ band to appear between 320 nm and 360 nm [20]. Hence, the six batches were normalised with respect to their individual maximas of this band between 344 nm and 351 nm. Following this, the π - polaron bands which were expected between 400 nm and 420 nm [20] were all seen at approximately 420 nm. The localised polaron bands should have been between 740 nm and 800 nm [20], but Batches 4 - 6 emerged between 757 nm and 818 nm which is a range falling outside the preferred limits. Batches 1 - 3 peaked between 756 nm and 766 nm providing similar results to those obtained in previous research [5, 8]. The higher intensity of the π - polaron bands seen in Batches 4 – 6 at 430 nm in addition to the decreased intensity of the localised polaron bands beginning at approximately 750 nm have been reported to be a result of doping level and formation of

polaron [20]. In this case, increased concentrations of APS in relation to aniline [8] are the likely reason, which would also explain the lack of uniformity seen in the dispersions of Batches 4 - 6.

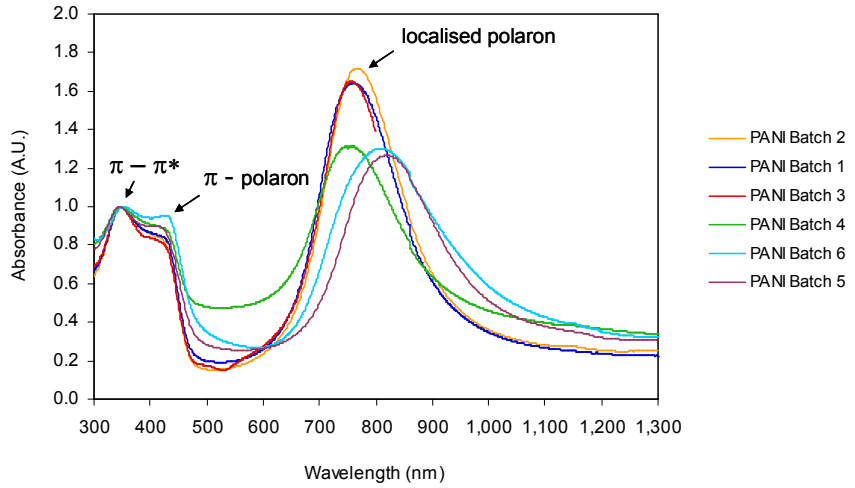

Figure 4.4 UV-vis spectra of nanoPANI aqueous dispersions. Batches 1 – 3 display the responses from properly synthesised nanoPANI. Batches 4 – 6 were the result of nanoPANI that was improperly synthesised.

To select a suitable frequency at which to operate the electrodes, the capacitive and resistive effects were observed over a range from 1 to 100,000 Hz (Fig. 4.5).

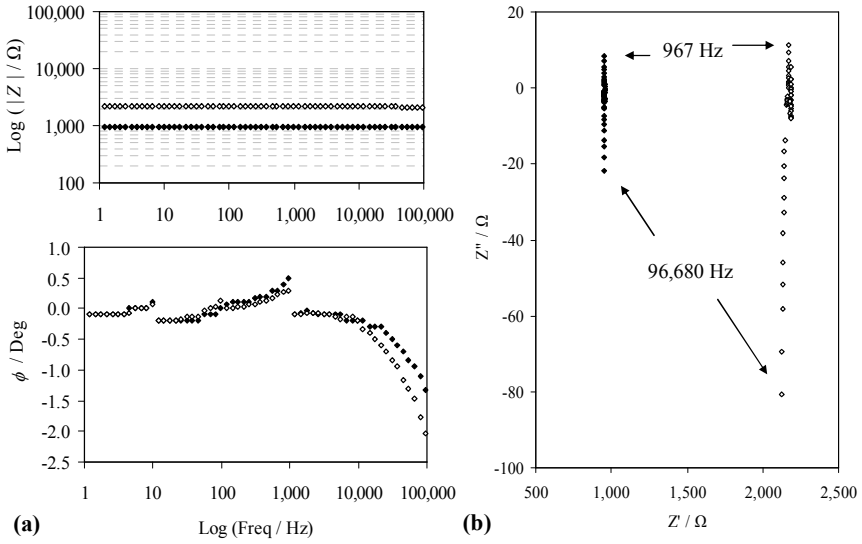

Figure 4.5 Impedimetric and phase behaviour of electrodes before (filled diamonds) and after (empty diamonds) exposure to 25 ppm ammonia. Results over the frequency range of 1 to 100,000 Hz were indicated by (a) Bode / phase and (b) Nyquist plots.

Bode plot data indicated that there was no significant change (955 ±1.33 Ω; n=3) in mean absolute impedance, $|Z|$, over the range of frequencies when no ammonia exposure took place (Fig. 4.5a). However, a noticeable capacitive effect did arise once the frequency went above 962 Hz. This was indicated by a slight decrease in impedance from 956 to 951 Ω, and a change in phase of -1.8^{o}. Using the same three electrodes, direct exposure to 25 ppm ammonia took place until a stable baseline was formed. Once stable, the frequency spectrum was recorded. The newly formed baseline displayed a higher mean $|Z|$ and deviation than without ammonia (2,166 ±17.8 Ω; n=3). As with the results without ammonia, a capacitive effect occurred after 962 Hz. The impedance decreased from 2,167 to 2,124 Ω, and phase displayed a change of -2.3^{o}. The Nyquist plot showed that once a frequency of 967 Hz was reached, a capacitive change occurred in the electrodes regardless of whether or not there was ammonia exposure (Fig. 4.5b). However, exposure to ammonia resulted in a larger change in capacitance as the frequency increased. The increase in capacitance seen beyond 962 Hz would not be favourable since it could essentially short-circuit the electrodes [21]. Hence, the critical frequency of 962 Hz was used for analysis in all subsequent measurements to ensure that the optimum resistive effects of the impedimetric measurements were still observed during ammonia interaction.

Using a sample of 30 electrodes printed from the same nanoPANI solution, examination of their baseline variability and drift at 962 Hz, 5 mV rms was performed. Measurements were taken over a 10 min period to reflect an adequate breath sampling period. The recorded baseline consisted of 121 data points which were averaged to create the intra-variable mean absolute impedance $|Z|$ and drift of that electrode's baseline. The drift was expressed as the deviation and absolute coefficient of variation of this mean over that time period. Of the 30 electrodes, the mean baseline ranged from 815 to 2,401 Ω with an inter-electrode baseline mean and standard deviation of 1,443.7 Ω and 478.2 Ω; 33% RSD. Over the 10 min, the intra-electrode drift varied from 1 to 33 Ω; 0.05% to 1.67% RSD. To compensate for the initial variation in baseline, 10 electrodes were analysed ratio-metrically based on their initial baseline impedance (Z_o) and then exposed to simulated breath ammonia (Z). Electrodes were repeatedly exposed to 0.06 min of simulated human breath (≥90% RH, 37 ±1^{o}C, 62 ±0.67 L/min) containing 245 ±8 ppbv ammonia as determined by photoacoustic laser spectroscopy (Chapter 3), followed by a gap of 0.25 min, and the difference between Z/Z_0 at 1.67 min and 10 min was evaluated which was determined to be 2.69 ±0.12 (4.46%

RSD, n=10). This suggested that the electrodes could be used without the need for extensive individual calibration other than initial ratio-metric baseline correction. Further measurements on the electrodes applied this methodology.

4.3.5 Evaluation of the effect of pH

The signal response as a result of pH is shown in Table 4.3 and Fig. 4.6. Of the solutions, the basic solutions initiate higher primary response signals and decreased quickly while the acidic demonstrated lower primary response signals. The behaviour has been demonstrated in previous literature where electrodes consisting of PANI films displayed an increase in resistance [22] or decrease in current [23] as deprotonation of the film takes place with increasing pH. However, the signals in Fig. 4.5 appear to decrease over time similar to the effect of increased water vapour. In addition, the closer the pH levels are to neutral, the more they stay around the baseline. The overall increase or decrease in pH constitutes less than ±0.1 change in *Z/Zo*, and though this will introduce a small error into the measurements, the error is towards the lower end of the measurement range.

Table 4.3 Signal response as a result of exposure to pH level.

pH	*Z/Zo* at 430 s	*Z/Zo* at 800 s
9	-0.06	-0.11
8	-0.02	-0.03
6	-0.01	-0.01
4	-0.07	-0.05

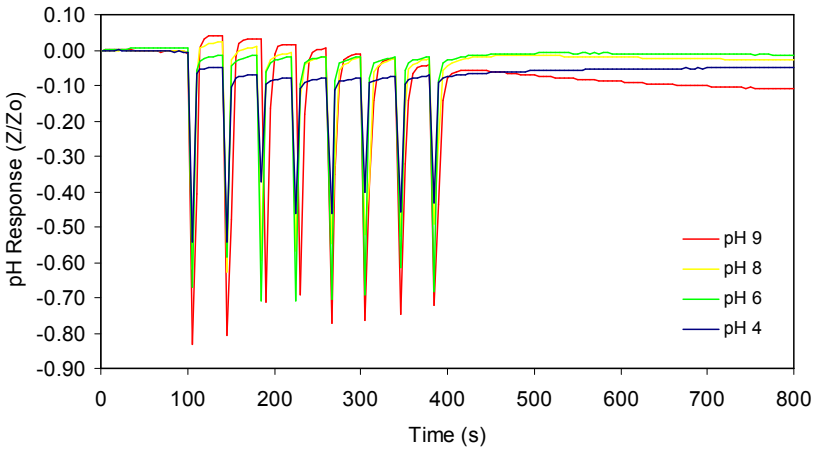

Figure 4.6 Response of electrodes to exposure of individual pH levels. The increase or decrease in pH constitutes a change of less than ±0.1 *Z/Zo*.

4.3.6 Evaluation of the effect of interferent gases

Carbon dioxide (99%), nitrogen (99%), hydrogen sulphide (25 ppm) and nitric oxide (25 ppm) showed no significant change in Z/Z_0 or phase responses from the electrodes despite the concentrations being well above those that would be realistically found in a human breath sample (Fig. 4.7). Oxygen (99%) displayed a negligible response in Z/Z_0 with no significant phase response. Ammonia (25 ppm) exhibited its well-established impedimetric response with an insignificant change in phase.

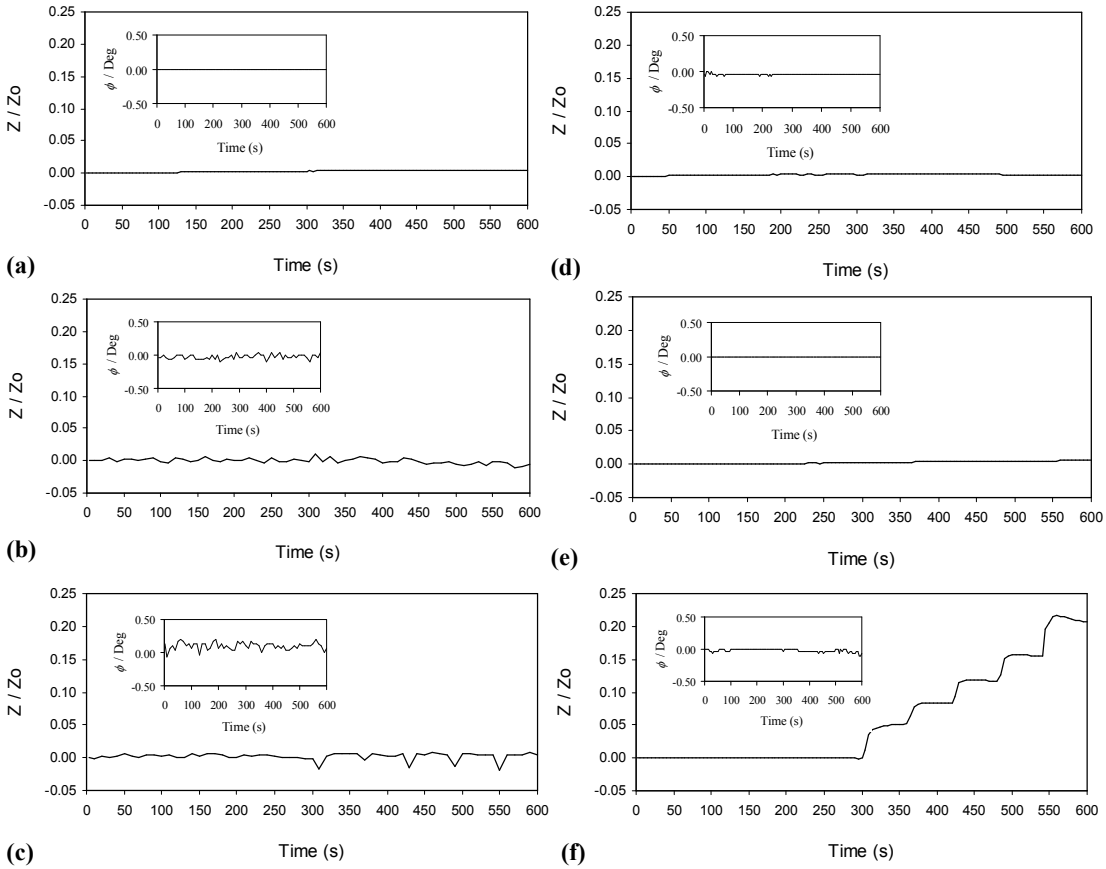

Figure 4.7 Ratio-metric impedance and phase (inset) responses to potential interferent gases in human breath: (a) 99% carbon dioxide, (b) 99% nitrogen, (c) 99% oxygen, (d) 25 ppm hydrogen sulphide, (e) 25 ppm nitric oxide, (f) 25 ppm ammonia.

The use of polyaniline in sensors for the detection of these gases has displayed varied results in other literature indicating that further research is still necessary. Previous literature has indicated that pure carbon dioxide caused an increase in conductivity when using the emeraldine base form of polyaniline [24]. The increased conductivity was shown

to be proportional to the increase in carbon dioxide. It was stated that the conversion of polyaniline from the base to the salt form resulting from the hydrolytic formation of carbonate ions during carbon dioxide's interaction with the base was the cause. However, this method was contradicted in other findings where the procedure led to poor sensing characteristics such as severe drift, shorter range of detection, and slower response time [25]. Research into the effects of gaseous nitrogen and oxygen on polyaniline was lacking, but studies using polyaniline as the conducting polymer of batteries displayed relevant comparisons [26]. In this work of Wu *et al*, it was demonstrated using a polyaniline-based battery that introduction of pure nitrogen gas caused a decrease in conductivity while oxygen increased conductivity. Though the results displayed were significant by comparison to the current work, they were the result of consistent flow and a signal only appearing after five minutes. Work with hydrogen sulphide in previous literature had shown significant increases or decreases in conductivity depending on the composition of the polyaniline [11]. The emeraldine salt form of polyaniline consistently showed weak responses to 100 ppm hydrogen sulphide. However, it was noticed that both base-treated polyaniline and copper chloride composite polyaniline displayed significant increases in conductivity. This behaviour was similar to previously discussed base-treated polyaniline and indicated that the polyaniline had been protonated to the salt form. Previous observations of 20 ppm nitric oxide on polyaniline films had shown an increase in resistance [27]. However, the response on their nine-layer film did not emerge until after a continuous flow of 20 s which was five times longer than that which was necessary for the research carried out on the 10-layer films assessed in this chapter. In observation of ammonia, there was a display of increased Z/Z_0 which was similar to the behaviour seen in other articles where polyaniline films were used. Using flows of ammonia gas on PANI films in a chamber headspace, research from Sengupta *et al* provided evidence of increased resistivity where concentrations of ammonia increased from 100 ppm to 750 ppm. [28]. The work of Du *et al* demonstrated how PANI films doped with 4-toluenesulfonic acid (TSA) display consistent increases in resistance where 50 ppm ammonia was observed as well as a progressive linear response from 5 ppm to 200 ppm [29]. In an article by Virji *et al*, a flow of 100 ppm ammonia onto a PANI film over 1,500 s also resulted in increased resistance [30]. From this, it was deduced that ammonia was the only major volatile compound of the tested common breath gases that would have a significant effect on the nanoPANI electrodes.

4.3.7 Evaluation of the effect of temperature, humidity, and humidified ammonia

Exposure of atmospheric air, warmed atmospheric air, warmed atmospheric air with induced humidity, and warmed atmospheric air with induced humidity and ammonia to the nanoPANI electrodes were examined to assess their potential interferent effects and characteristic behaviour (Fig. 4.8).

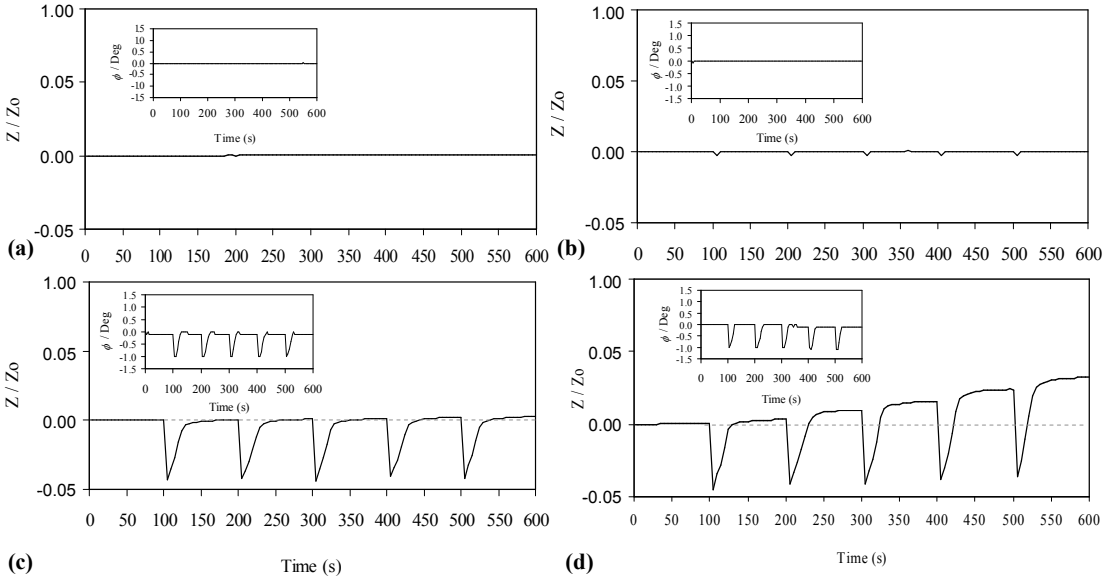

Figure 4.8 Interdigitated nanoPANI electrode response of ratio-metric impedance, Z/Z_0, and inset phase angle, ϕ, to 62 ±0.67 L/min of (a) room temperature atmospheric air, 21 ±1°C, (b) warmed atmospheric air, 37 ±1°C, (c) warmed humidified atmospheric air, 37 ±1°C, ≥90% RH, and (d) warmed humidified air with ammonia, 37 ±1°C, ≥90% RH, 245 ±8 ppbv.

Introduction of atmospheric air at room temperature to the electrodes resulted in no significant change in ratio-metric impedance, Z/Z_0, or phase angle, ϕ. Warmed atmospheric air comparable to human breath temperature was detected by the sensor with a very negligible and transient response to Z/Z_0, but no observable change in ϕ. These findings are similar to those produced in previous literature claiming slight changes in conductivity between the ranges of room temperature to approximately 60°C [10]. Warmed humidified air resulted in a significant transient decrease in Z/Z_0. Furthermore, there was a significant negative phase shift indicating a capacitive effect due to water vapour. As the water evaporated from the electrode after sampling, Z/Z_0 and the phase returned to their original

baselines in a characteristic, time-dependent manner. These effects were expected as it has been noted in published literature that both humidity and temperature can interfere with the conductivity of polyaniline electrodes [31]. The research of Wang *et al* went on to show how observations of the change in conductivity in a ratio-metrical manner (R/R_0), the effects of humidity and temperature could be isolated from those of gases such as ammonia. In humidified air at human breath temperature containing 245 ±8 ppbv of ammonia, the interaction of humidity with the electrodes again caused a negative phase shift and an initial decrease in Z/Z_0, similar to Fig. 4.8c, despite the simultaneous interaction of ammonia. However, upon recovery of the electrode from temperature and humidity fluctuation, an increase in the Z/Z_0 baseline could be observed, whereas an insignificant change in the phase angle was apparent. The insignificant change in the phase angle indicated that ammonia caused a resistive effect on the electrodes, and the capacitive effects were specific to water vapour. This suggested that the impedimetric response signature of ammonia on the electrodes could be differentiated from temperature and humidity components by time-dependent control of the sampling methodology, or through differential analysis of the changes in impedance and phase. For further work, a time-controlled breath sampling method was employed.

4.3.8 Quantification of ammonia in the presence of simulated human breath interferents

It was mentioned in the previous sections that literature has demonstrated how polyaniline could be used to detect gaseous ammonia and potentially quantify it. For the purpose of developing a quantitative measurement, the work of Kukla *et al* demonstrated that exposure of 100 ppm, 300 ppm, and 600 ppm ammonia to polyaniline films resulted in proportional increases in resistance [4]. This proportional increase in resistance could also be seen in the work of Liu *et al* where gaseous ammonia between 1 ppm and 50 ppm displayed proportional increases in resistivity [32]. Though the ranges shown in these articles were as low as parts-per-million, application for human breath would be insufficient since the necessary detection range is in parts-per-billion. Other studies have achieved detection and quantification in the parts-per-billion range by combining polyaniline with nanocomposites. Chang *et al* used polyaniline in combination with multi wall carbon nanotubes (MWCNTs) to see the effects of ammonia concentration on changes in current. It was noticed that gaseous ammonia over the range of 200 ppb to 25 ppm produced quantifiable readings where increases in concentration provided equal changes in the observed current [33].

Zhang *et al* showed how polyaniline in combination with single wall carbon nanotubes (SWCNTs) could be used to see a change in resistance proportional to ammonia concentrations between 50 ppb and 15 ppm [34]. In more recent literature, there have also been demonstrations that used composites such as titanium dioxide [35]. By combining polyaniline with titanium dioxide, Li *et al* were able to measure proportional changes in current to ammonia concentration from 25 ppb to 200 ppb. Assurance of higher sensitivity is a beneficial attribute of such nanocomposites, but there are also disadvantages. Synthesis of such materials as carbon nanotubes is a complex process which makes control of the chemical and electrical properties difficult [36]. This process also has a high tendency to generate composites with defects and impurities that are not easy to overcome. Furthermore, due to their hydrophobic attributes, they are difficult to disperse in most common solvents. The effort required to manufacture composites with the required characteristics also increases the production costs. The PANI films discussed in these other research were both capable of detecting ammonia at low concentrations as well as showing potential for quantification, but the gases studied were not immersed in matrices of interferents commonly found in breath. Hence, the effects of potential breath interferents were unknown. In the following work, using the nanoPANI electrodes allowed for low-concentration quantification of ammonia from among the simulated breath interferences discussed in the previous sections.

In Fig. 4.9, the response of the nanoPANI electrodes to simulated breath was observed.

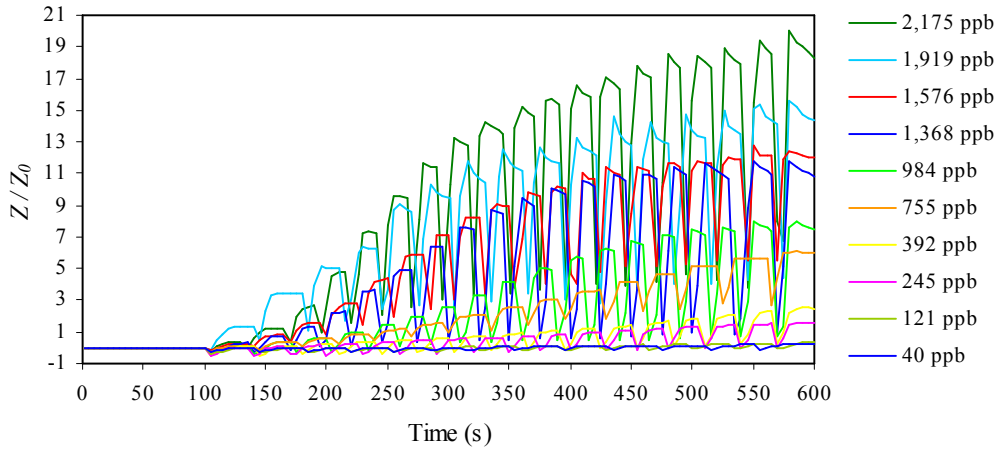

Figure 4.9 Ratio-metric impedance response (Z/Z_0) profile of simulated breath samples on nanoPANI electrode measured at 962 Hz. No exposure to the gas for 100 s formed the initial baseline. Beginning at 101 s, a 62 ±0.67 L/min exhalation of four seconds from the simulated breath system flowed onto the electrode. This was repeated after the combined 15 s decrease in Z/Z_0 due to humidity and 15 s post-peak stabilisation resulting in approximately one breath measurement every 30 s until 600 s was reached.

The behaviour was similar to that which was observed in Fig. 4.8d. There was an initial decrease in Z/Z_0 in response to temperature and humidity. This was followed by recovery of the electrode (indicated by an increase in Z/Z_0) upon return to atmospheric conditions. During this recovery, the response appeared to be cumulative because with each successive addition, there was a proportional increase in Z/Z_0. In other words, with each simulated breath, the specific number of expelled ammonia molecules interacted with the proportionally available number of protonated nanoPANI sites. Hence, a change-consistent step-like increase in Z/Z_0 with each exposure was observed. This also implied that there were more sites available for the next breath exposure since a lack of increase in Z/Z_0 would have been indicative of complete nanoPANI saturation. Thus, after a specified number of simulated breaths per cumulative sample time, the change in Z/Z_0 could be interpreted as a level which was proportional to the ammonia concentration. The concentrations observed were quantifiable over the tested range of 40 ±2 ppbv to 2,175 ±26

ppbv. Peak responses were then extracted from the data in Fig. 4.9 and plotted to determine the effect of breath number over the sampling time on range and linearity (Fig. 4.10).

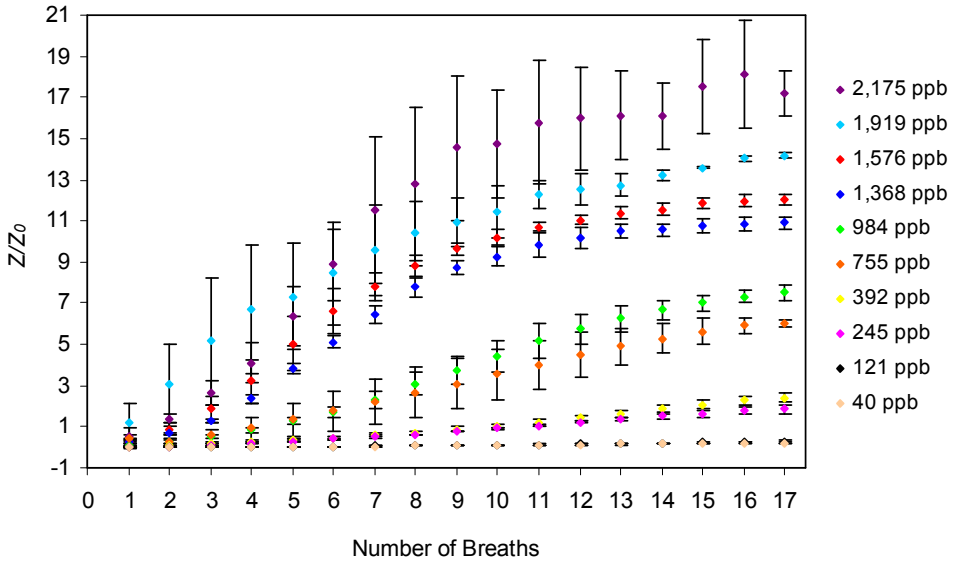

Figure 4.10 Change in Z/Z_0 observed on nanoPANI electrodes (n=3) for each ammonia concentration at 0.5 min increments where breath one was at 2.16 min and breath 17 was from the post-peak stabilisation at 10 min.

Immediately noticeable in Fig. 4.10 is that the standard deviation of Z/Z_0 increases with increasing ammonia concentration. This was exptected since with an increasing number of ammonia molecules, there would be increased competition for the remaining available protonated nanoPANI sites. Using the changes in Z/Z_0 observed for each concentration, calibration curves were obtained every 0.5 min from 2.16 min (breath 1) to 10 min (breath 17) to demonstrate the effect of increasing sample numbers on the correlative response (Table 4.4; Fig. 4.11). For the range from 40 ±2 ppbv to 2,175 ±26 ppbv, the response of Z/Z_0 to ammonia was found to increase in linearity with an increased number of breath samples. The correlation coefficient was found to be 0.5583 for the first breath, but showed improvement by breath 17 with a correlation of 0.9963.

Table 4.4 Correlations of the relationship between the impedance response ratio (Z/Z_0) and breath ammonia concentrations (Fig. 4.10) with respect to breath sample number.

Breath Number	Correlation (R^2)	Breath Number	Correlation (R^2)
1	0.5584	9	0.9698
2	0.6475	10	0.9788
3	0.7102	11	0.9837
4	0.8083	12	0.9882
5	0.9257	13	0.9901
6	0.9529	14	0.9942
7	0.9604	15	0.9920
8	0.9694	16	0.9923
		17	0.9963

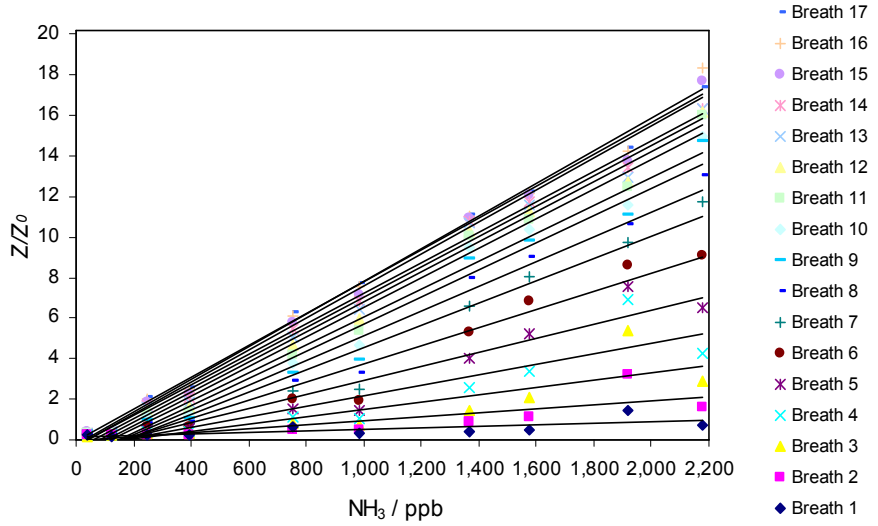

Figure 4.11 Relationship between the impedance response ratio (Z/Z_0) and simulated breath ammonia concentrations demonstrating an increase in linearity with increased sample number.

The ratio-metric responses at breath 17 (10 min) (Table 4.5; Fig. 4.12) generated a slope and intercept of 0.0079 $ppbv^{-1}$ and -0.28, respectively. Based on this data and the maximum intra-electrode baseline drift variability determined earlier (1.67%), a theoretical limit of detection of approximately 6.3 ppbv could be determined (S/N=3), and a linear dynamic range was observed from 40 ±2 ppbv to 2,175 ±26 ppbv. As discussed in Chapter 1, the physiological range of human breath ammonia is approximately 50 ppb to 2,000 ppb which conveys that the electrode detection limits encompass the relevent range for expected human breath measurements.

Table 4.5 Ammonia concentrations and ratio-metric (Z/Z_0) results from breath 17 (600 s). *Concentration determined by correlation with PALS (Chapter 3, Section 3.3.3).

*NH_3 / ppbv (n=5)	Z/Z_0 (n=3)	Z/Z_0 RSD (%)
40 ±2	0.20 ±0.01	3.72
121 ±15	0.30 ±0.02	6.60
245 ±8	1.86 ±0.21	11.22
392 ±6	2.42 ±0.21	8.55
755 ±7	6.06 ±0.17	2.77
984 ±21	7.51 ±0.40	5.30
1,368 ±11	10.89 ±0.31	2.84
1,576 ±7	12.05 ±0.27	2.20
1,919 ±20	14.19 ±0.17	1.17
2,175 ±26	17.20 ±1.10	6.41

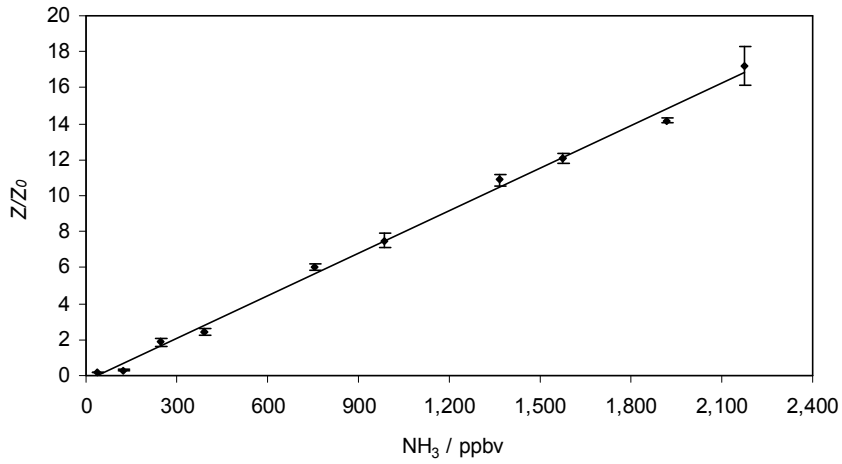

Figure 4.12 Relationship between ammonia concentration and change in Z/Z_0 after 17 breath samples (R^2 = 0.9963). A slope and intercept of 0.0079 $ppbv^{-1}$ and -0.2852 were generated.

4.4 Conclusions

An electrode based on an inkjet-printed film of a previously established nanoPANI formulation was used as the basis of an ammonia breath sensor. Physical characterisation of the nanoPANI displayed nanoparticles with a mean particle diameter of 382 ±33 nm that generated a UV-vis spectrum similar to those of previous works. Bode and Nyquist analysis identified the optimum frequency for measurements to be 962 Hz, 5 mV rms. Variability and drift of the electrodes was demonstrated to be low with an intra-variability of 0.05 to 1.67% RSD. From this, an impedimetric method of detection based on ratio-metric

impedance (Z/Z_0) measurements was established. Additionally, pH levels between 5 and 9 resulted in a change of signal behaviour less than ±0.1 *Z/Zo*. Observations of potential interferent gases as well as effects of temperature and humidity conveyed that the only significant factors were ammonia gas and humidity. Ammonia gas induced an increase in Z/Z_0 while humidity caused a decrease. An analytical technique utilising cumulative sampling of breaths over a particular duration of time was chosen for detection and quantification of ammonia from among the simulated breath interferents. Using this method generated a 0.9963 correlation across the analytical range of 40 ±2 ppbv to 2,175 ±26 ppbv (LOD=6.3 ppbv) which was appropriate for diagnostic applications of breath monitoring technology.

4.5 References

[1] Radhakrishnan, S.and Deshpande, S.D., (2002), "Conducting polymers functionalized with phthalocyanine as Nitrogen Dioxide Sensors", *Sensors,* Vol.2 (1), pp. 185-194.

[2] Wu, S., et al., (2000), "Ammonia sensitivity of polyaniline films via emulsion polymerization.", *European Polymer Journal,* Vol.36 pp. 679-683.

[3] Jin, Z., Su, Y.and Duan, Y., (2001), "Development of a polyaniline-based optical ammonia sensor", *Sensors and Actuators B,* Vol.72 pp. 75-79.

[4] Kukla, A.L., Shirshov, Y.M.and Piletsky, S.A., (1996), "Ammonia sensors based on sensitive polyaniline films", *Sensors and Actuators B,* Vol.37 pp. 135-140.

[5] Morrin, A., et al., (2008), "The fabrication and characterization of inkjet-printed polyaniline nanoparticle films", *Electrochimica Acta,* Vol.53 pp. 5092-5099.

[6] Li, G., Martinez, C.and Semancik, S., (2005), "Controlled electrophoretic patterning of polyaniline from a colloidal suspension", *Journal of the American Chemical Society,* Vol.127 pp. 4903-4909.

[7] Parashkov, R., et al., (2005), "Large area electronics using printing methods", *IEEE,* Vol.93 (7), pp. 1321-1329.

[8] Ngamna, O., et al., (2007), "Inkjet printable polyaniline nanoformulations", *Langmuir,* Vol.23 (16), pp. 8569-8574.

[9] Hosokawa, M., (2007), "Size effect and properties of nanoparticles", in *M. Hosokawa, K. Nogi, M. Naito, et al, eds., Nanoparticle Technology Handbook,* (1st ed.), 1, Elsevier, The Netherlands, pp. 5.

[10] Crowley, K., et al., (2008), "Fabrication of an ammonia gas sensor using inkjet-printed polyaniline nanoparticles", *Talanta,* Vol.77 pp. 710-717.

[11] Crowley, K., et al., (2008), "Fabrication of chemical sensors using inkjet printing and application to gas detection", *IEEE Sensors,* pp. 13-16.

[12] Sezai Sarac, A., Ates, M.and Kilic, B., (2008), "Electrochemical impedance spectroscopy study of polyaniline on platinum, glassy carbon, and carbon fiber microelectrodes", *International Journal of Electrochemical Science,* Vol.3 pp. 777-786.

[13] Horvat-Radosevic, V.and Kvastek, K., (2007), "Analysis of high-frequency distortions in impedance spectra of conducting polyaniline film modified Pt-electrode measured with different cell configurations", *Electrochimica Acta,* Vol.52 pp. 5377-5391.

[14] Krishantha, D.M.M., et al., (2006), "AC impedance analysis of polyaniline-montmorillonite nanocomposites", *Ionics,* Vol.12 pp. 287-294.

[15] Hui, D., et al., (2004), "Impedance spectroscopy studies on doped polyanilines", *Journal of Optoelectronics and Advanced Materials,* Vol.6 (3), pp. 817-824.

[16] Crowley, K., et al., (2010), "Fabrication of polyanilline-based gas sensors using piezoelectric inkjet and screen printing for the detection of hydrogen sulfide", Vol.10 pp. 1426.

[17] Moulton, S.E., et al., (2004), "Polymerisation and characterisation of conducting polyaniline nanoparticle dispersions", *Current Applied Physics,* Vol.4 pp. 402-406.

[18] Magdassi, S.and Moshe, M.B., (2003), "Patterning of organic nanoparticles by ink-jet printing of microemulsions", *Langmuir,* Vol.19 pp. 939-942.

[19] Azucena, O., et al., (2008), "Inkjet printing of passive microwave circuitry", *IEEE,* pp. 1075-1078.

[20] Kim, B., et al., (2001), "Synthesis and characterization of polyaniline nanoparticles in SDS micellar solutions", *Synthetic Metals,* Vol.122 pp. 297-304.

[21] Baumgartner, R.N., Chumlea, W.C.and Roche, A.F., (1988), "Bioelectric impedance phase angle and body composition", *The American Journal of Clinical Nutrition,* Vol.48 pp. 16-23.

[22] Cadenas, J.L.and Hu, H., (1998), "Chemically stable conducting polyaniline composite coatings", *Solar Energy Materials and Solar Cells,* Vol.55 (1), pp. 105-112.

[23] Homma, T., et al., (2012), "Electrochemical polymerization of aniline in the presence of poly(acrylic acid) and characterization of the resulting films", *Polymer,* Vol.1 (1), pp. 223-228.

[24] Ogura, K.and Shiigi, H., (1999), "A CO_2 sensing composite film consisting of base-type polyaniline and poly (vinyl alcohol)", *Electrochemical and solid-state letters,* Vol.2 (9), pp. 478-480.

[25] Irimia-Vladu, M.and W. Fergus, J., (2006), "Suitability of emeraldine base polyaniline-PVA composite film for carbon dioxide sensing", *Synthetic Metals,* Vol.156 pp. 1401-1407.

[26] Wu, A., Venancio, E.C.and MacDiarmid, A.G., (2007), "Polyaniline and polypyrrole oxygen reversible electrodes", *Synthetic Metals,* Vol.157 pp. 303-310.

[27] Xie, D., et al., (2002), "Fabrication and characterization of polyaniline-based gas sensor by ultra-thin film technology", *Sensors and Actuators B,* Vol.81 pp. 158-164.

[28] Sengupta, P.P., Barik, S.and Adhikari, B., (2006), "Polyaniline as a gas-sensor material", *Materials and manufacturing processes,* Vol.21 pp. 263-270.

[29] Du, Z., et al., (2012), "Ammonia gas detection based on polyaniline nanofibers coated on interdigitated array electrodes", *Journal of Materials Science: Materials in Electronics,* Vol.22 (4), pp. 418-421.

[30] Virji, S., et al., (2004), "Polyaniline nanofiber gas sensors: Examination of response mechanisms", *Nano Letters,* Vol.4 (3), pp. 491-496.

[31] Wang, J., et al., (2004), "Electrochemically fabricated polyaniline nanoframework electrode junctions that function as resistive sensors", *Nano Letters,* Vol.4 (9), pp. 1693-1697.

[32] Liu, M., et al., (2009), "Manufacture of a polyaniline nanofiber ammonia sensor integrated with a readout circuit using the CMOS-MEMS Technique", *Sensors,* Vol.9 pp. 869-880.

[33] Chang, Q., et al., (2008), "Preparation of gold/polyaniline/multiwall carbon nanotube nanocomposites and application in ammonia gas detection", *Journal of Materials Science,* Vol.43 pp. 5861-5866.

[34] Zhang, T., et al., (2006), "Electrochemically functionalized single-walled carbon nanotube gas sensor", *Electroanalysis,* Vol.18 (12), pp. 1153-1158.

[35] Li, Y., et al., (2011), "Fabrication of polyaniline/titanium dioxide composite nanofibers for gas sensing application", *Materials Chemistry and Physics,* Vol.129 pp. 477-482.

[36] Panhuis, M.i.h. (2006), "Caron nanotubes: enhancing the polymer building blocks for intelligent materials", *Journal of Materials Chemistry,* Vol.16 (36), pp. 3598-3605.

CHAPTER 5

DEVELOPMENT OF A DEVICE FOR MEASURING BREATH AMMONIA (AmBeR)

5.1 Introduction

The provision of real-time point-of-care diagnostics in a non-invasive manner is a major goal of modern biomedical diagnostics. There are several routes to non-invasive or minimally invasive measurements, and among the most attractive is exhaled breath. The sample size of human breath is typically a few hundred millilitres where the concentration of ammonia can be in the low parts-per-billion. This concentration is much lower than other common breath gases such as carbon dioxide and oxygen which means the method of ammonia detection must be highly sensitive and selective [1]. Furthermore, devising a system that can assist with processing and control of the breath ammonia sample to facilitate effective measurement would be necessary to achieve this goal.

Over the years, there have been several methods and devices developed for the purpose of breath ammonia detection. Some of the most sensitive devices for selectively detecting and quantifying ammonia have relied upon techniques such as mass spectrometry which would not be suitable for miniaturisation or integration and, therefore, have proven unsuitable for point-of-care instrumentation that would be easily portable for clinical use. An example would be devices based on selected ion flow tube mass spectrometry (SIFT-MS) such as the Profile 3 [2] which at 120 kg and £130,000 would not be useful as a point of care system. Melker *et al* utilised the concept of the electronic nose which was capable of detecting gases based on pattern recognition [3]. However, using electronic nose technology tends to utilise sensors that are only capable of recognition, but are not capable of quantifying breath ammonia. Boga *et al* developed a method whereby a tube was lined with Michler's hydrol which would react with exhaled breath [4]. Michler's hydrol is an indicating agent that utilises a visible change in colour upon the presence of exhaled ammonia. This method could be used as an indicator, but also lacked the ability to quantify breath ammonia. Furthermore, the use of an indicating agent so close to the mouth could raise issues of toxicity in a clinical setting. Suslick *et al* discussed a different device that also relied on a visual method of detection where an indicator dye was used [5]. Techniques which have attempted to simplify the method of detection by removing interferences such as breath humidity have also been attempted. Hamilton *et al* created a device which used sodium hydroxide to remove the water vapour from the breath as it passed through the system [6]. The dehydrated sample containing ammonia would then interact with a sensor. However, use of desiccants is not ideal for clinical development as the potential for

exposure to the patient would be too high. Furthermore, a desiccant would add complexity to the technology whereby it would need to be regenerated on a regular basis. Stepping away from attempts to segregate ammonia from the other constituents of breath, others have proposed merely collecting the alveolar portion of breath with the assumption that the sample will contain the highest concentration of breath ammonia. The work of Baghdassarian demonstrated a breath sampling device which utilised an internal monitor for detection of CO_2 concentrations within breath samples [7]. The purpose of monitoring CO_2 was to indicate when alveolar breath emerged, and with it the gaseous metabolites from blood (e.g. ammonia). The concentration of CO_2 varies from person to person, but previous research has suggested that approximately 3.3 ±0.9 % (v/v) would be an appropriate value to indicate when a sample contained alveolar breath [8]. While the device was good for isolation of alveolar breath, it did not demonstrate the ability to quantify ammonia concentrations in real-time. Furthermore, the system demonstrated no means of reducing effects from humidity which is a well-known interferent in gas measurements [9]. Olthuis *et al* showed a device that could not only detect ammonia, but also quantify it by combining a sample volume of the gas with purified water to form ammonium ions [10]. The concentration of ammonium ions formed in the water was quantified using an electrolyte conductivity sensor [11] providing an indication of the original ammonia concentration. The advantage of using such a technique was that a sample of gas could be concentrated into a smaller volume of liquid suitable for miniaturised devices [1]. However, whether or not the structure of the technology was simple enough to be suitable as a re-usable point-of-care device used in real-time monitoring of patients was not demonstrated.

Although these examples demonstrate a number of methods which show potential for development into breath gas monitoring devices, there is currently still no suitable analyser for use in clinical analysis [1]. The requirements of being non-invasive, point-of-care, low cost, easy to use, and providing real-time results have not been fulfilled. The ammonia sensor demonstrated in Chapter 4 has the potential to form the basis of a system for measuring breath ammonia. However, to achieve this, it too must interact with the breath sample in a defined and appropriate fashion to account for, or prevent interference from a number of variables such as sample flow rate, volume, temperature and humidity. Thus, a breath monitoring system was developed based on the ammonia sensor to achieve this

control for the purpose of developing a non-invasive real-time point-of-care clinical monitoring device for breath ammonia.

5.2 Materials and methods

5.2.1 Materials

Disposable spirettes (831204A) were provided by NDD Medical Technologies, MA. Bacterial / viral filter mouthpiece (02129 NS, DEAS Breathing Solutions, Italy), T-junction valves fitted with one-way directional flow passive valve diaphragms (4476, Respironics Respiratory Drug Delivery UK Ltd., UK), and 22 mm internal diameter ethyl vinyl acetate (EVA) corrugated flexible tubing (001405, Cardinal Health, USA) were all approved with CE0123 certification. The air-cushioned face masks were sourced from Pranalytica, CA, U.S.A. as an accessory of their breath analysing photoacoustic laser system, the Nephrolux^{TM}. A manually operated two-way valve (651160, 25 mm I.D.) was purchased from Yamitsu, UK. A custom-built electrode housing was fabricated by Parsec Ltd., Ireland. A model SG40281B1-0000-Q99 DC12 V fan (4934354) was purchased from Sunonwealth Electric Machine Industry Co., Ltd., Taiwan. A 12 V universal power supply (EA-PS 1501 T) was purchased from Elektro-Automatik GmbH and Co., Germany. The power supply was later modified so as to have the speed controls integrated within the system enclosure and was connected to the mains. Axial fan finger guard (5440374), power supply chassis socket (505-1637), potentiometer P16A (118-413), panel mounted switch (710-9299), SRBP strip board (433-832), PVC equipment wire (356-527), ceramic capacitors (653-0024), and carbon resistors (707-7745 and 707-7760) were all purchased from Radionics, Ltd. The interdigitated electrodes were fabricated according to Chapter 4, Section 4.2.

5.2.2 Instrumentation

Impedance measurements were performed using a model 660C Series Electrochemical Analyser Workstation (CH Instruments Inc., TX, USA). Human breath ammonia measurements were performed with a Nephrolux^{TM} photoacoustic laser spectrometer system (Pranalytica, USA). Air flow measurements were made using a spirometer (EasyOne Model 2001, Fisher Biomedical Incorporated, FL, USA).

5.2.3 Generation of simulated breath samples

Ammonia sensor baseline measurements were taken in atmospheric air (21 ±1^{o}C and 51 ±7% RH) prior to the application of simulated and human breath samples. Simulated breath samples (62 ±0.7 L/min air flow at a temperature of 37 ±1^{o}C and relative humidity ≥ 90%, with or without ammonia) were generated using the system described in Chapter 3.

5.2.4 Measurement of ammonia

A new ammonia electrode (fabricated according to Chapter 4) was used for each set of measurements and subsequently disposed of. Electrodes were exposed to simulated breath for defined periods. Experiments were performed to investigate the impact of breath interferences (e.g. temperature and humidity) and the nature of the breath sampling interface on the sensor response to ammonia. These included investigations of the configuration of the sample collection measurement chamber, the orientation to the sensor, and the control of sample flow rate and volume across the sensor (Sections 5.2.5 through 5.2.8). Ammonia was measured impedimetrically at 962 Hz, 0 V initial bias, 5 mV amplitude, and a 5 s sampling rate, as established in Chapter 4.

5.2.5 Effect of the measurement chamber design on sensor impedance response characteristics

Plastic spirettes (22 mm internal diameter and 152 mm length) were used as the tubing through which the simulated breath samples were supplied to the sensor. A variety of tubing designs were evaluated for their effect on the sensor response to simulated breath containing ammonia (see Section 5.3.1).

5.2.6 Effect of sensor orientation in the measurement chamber on impedance response characteristics

The response characteristics of the sensor with regard to its configuration within the sample measurement chamber were investigated. The sensor was oriented in a number of configurations with respect to the chamber and impedance responses to ammonia were measured.

5.2.7 Evaluation of a three-stage sampling methodology

A preliminary breath measurement prototype was designed consisting of two parts. The first was a breath sample collection chamber of defined volume (79 to 225 ml) with passive inlet and outlet T-junction diaphragm valves. The inlet valve was connected to a face mask or anti-bacterial / viral mouthpiece. The outlet was connected to a second passive T-junction valve. The second part was a measurement chamber consisting of a length of tubing housing the ammonia sensor and the fan.

Simulated breath samples were first collected in the sample collection chamber for 4 seconds during sensor baseline measurement. Following collection, samples were drawn from the sample collection chamber through the measurement chamber containing the sensor at a flow rate of approximately 110.8 ±0.7 L/min using the miniaturised fan by manually connecting the two sections together. Fresh atmospheric air was allowed to pass across the electrode through the measurement chamber before and after breath sampling.

5.2.8 Effect of flow-rate and volume on electrode signal behaviour

The effect of the flow rate of breath and atmospheric air across the electrode assembly on the electrode signal behaviour was investigated. Rates from approximately 90 to 128 L/min were mediated by controlling the applied voltage to a miniaturised fan and recording the flow rates through the measurement chamber using a spirometer. Sample collection chambers of varying volumes from approximately 79 to 225 ml were employed to evaluate the impact of sample volume on sensor responses.

5.2.9 Final prototype assembly

A prototype breath ammonia measurement system (AmBeR) was assembled based on the outcomes of earlier experimental work. This consisted of the breath sample collection chamber with passive inlet and outlet T-junction valves, and face mask. This was connected to a custom-built electrode holder and fan assembly (measurement chamber) via a manually operated two-way valve to alternate flow across the electrode between the sample collection chamber, and atmospheric air, as required.

5.2.10 Calibration using simulated breath ammonia

Calibration of the system was performed by sequential application of eight simulated breath samples for each of the ammonia concentrations ranging from 40 ±2 to 2,993 ±10 ppbv (n=3). From this data, comparisons with human breath measurements were made.

5.2.11 Evaluation of the AmBeR system in normal human breath samples

A cohort of 10 healthy human volunteers was locally recruited following institutional ethical approval (Appendix 4). The method of breath analysis was the same as that previously described in Chapter 2. To summarise, volunteers who claimed to have no breathing abnormalities answered a questionnaire to provide biometric information such as their gender, ethnicity, age and BMI. The volunteers then provided oral breath samples via PALS and the AmBeR system. One individual provided multiple breath samples (n=7) for an intra-individual variability study.

5.2.12 Retrospect on sensor lifetime and robustness

Using AmBeR, electrode stability was observed over six-months using data from six individuals who displayed similar breath ammonia concentrations (651 ±36 ppbv). Stability and robustness of the electrodes at month six were compared to month. This included assessment of baseline drift, and overall signal response to similar breath ammonia concentrations.

5.3 Results and discussion

The development of the sensor in Chapter 4 for measuring ammonia in simulated breath samples at clinically relevant concentrations indicated that the sensor had the appropriate measurement capabilities to make it useful in a diagnostic application. However, many challenges in measuring real breath samples such as how to control the interaction of a breath sample with the sensor in such a way as to provide responses from the electrode that were not influenced by other factors still had to be addressed. Some of these known factors were issues such as the volume and flow rate profile of the breath sample, and constituents of the breath sample such as temperature and humidity. Research focussed on investigating these issues and establishing appropriate solutions to bring about a viable breath sampling methodology and an associated sampling system.

5.3.1 Effect of the measurement chamber design on sensor impedance response characteristics

As demonstrated in Chapter 4, Section 4.3.5, humidity had the effect of causing a decrease in Z/Z_0, while ammonia resulted in an increased Z/Z_0 response. However, that study was performed in a 'ventilated' environment in which the humidified sample was able to quickly dissipate and mix with atmospheric air. In that case, the increase in Z/Z_0 from ammonia only occurred upon cessation of flow of the humidified sample which, in turn, allowed for the moisture to disperse from the electrode surface. This would appear to indicate that if a stagnant layer of moisture were to build up on the electrode surface, the resulting decrease in Z/Z_0 could potentially block or reduce the characteristic increase in Z/Z_0 from ammonia. Hence, the more 'enclosed' the environment around the sensor, the greater the interference that might be expected from the trapped humidity. Thus, it was critical to evaluate this aspect of the breath measurement process on the behaviour of the sensor.

To enable breath samples to be passed over the surface of the electrode, an appropriate form of tubing was required. To avoid any further complicated variations in pressure and linear flow velocities of the breath samples, the diameter of the flow tubing used for the samples was kept as constant as possible. In this regard, spirette tubes are widely used in medical technology to sample breath for lung capacity measurements, or to allow the administration of therapeutic agents such as gases or nebulised drugs [12]. Therefore, disposable spirettes were selected as an excellent human-to-device interface as they have already been developed and optimised for this purpose. The spirettes were of a cylindrical configuration with dimensions of 22 mm diameter and 152 mm length [13]. A diameter of 22 mm is the minimum diameter commonly observed in spirometry. Initially, electrodes were positioned horizontally within the end of the spirette at the mid-point between the top and bottom of the chamber. The spirette inlet and outlet were either left entirely open to the atmosphere (ventilated) or were sealed by passive diaphragm valves (non-ventilated) (Fig. 5.1), and their impact on the impedimetric response from simulated breath ammonia samples was evaluated. The passive flow valves consisted of flexible diaphragms that would allow air to pass through the system until the flow of air ceased, at which point, the valves would close and trap a sample of the simulated breath within the chamber.

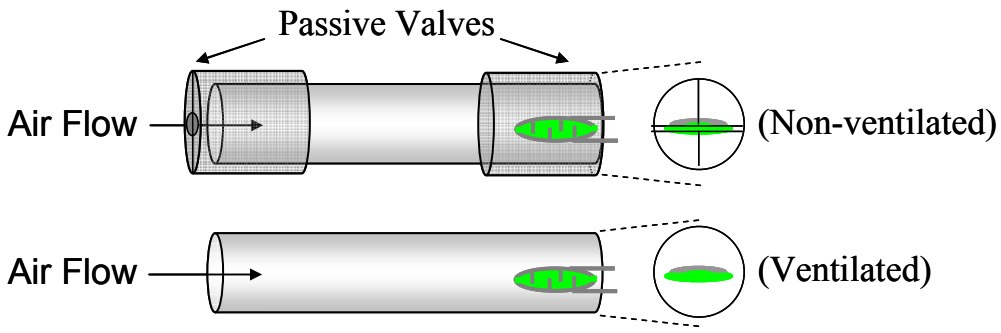

Figure 5.1 Diagram of ventilated and non-ventilated measurement chambers used to compare effects of simulated breath on the electrodes.

The ventilated set-up, however, contained no valves to close off the flow of air. In doing so, the simulated breath would pass across the electrode followed by dissipation of the sample into the open atmosphere once the flow had ceased. Fig. 5.2 shows the response from warmed, humidified air containing 245 ±8 ppbv of ammonia. The non-ventilated system resulted in a permanent decrease in Z/Z_0 where neither a recovery to the original baseline, nor a quantifiable reading from ammonia was evident. The lack of a significant flow through resulted in flow stagnation and vapour condensation which was observed on the walls of the non-ventilated chamber, and by a thin film of liquid on the sensor. With the ventilated system, however, the characteristic initial decrease in Z/Z_0 due to humidity was seen, followed by a subsequent increase in Z/Z_0 above the baseline due to ammonia, similar to the behaviour observed in Chapter 4. By allowing release of the sample to the open atmosphere, efficient dissipation of the vapour could occur, allowing the electrode to recover from humidity effects. Conversely, trapping the sample within the confines of the sensor resulted in elevated interference from humidity in the sample which masked the sensor's response to ammonia. Thus, further studies were performed in the 'open' ventilated configuration.

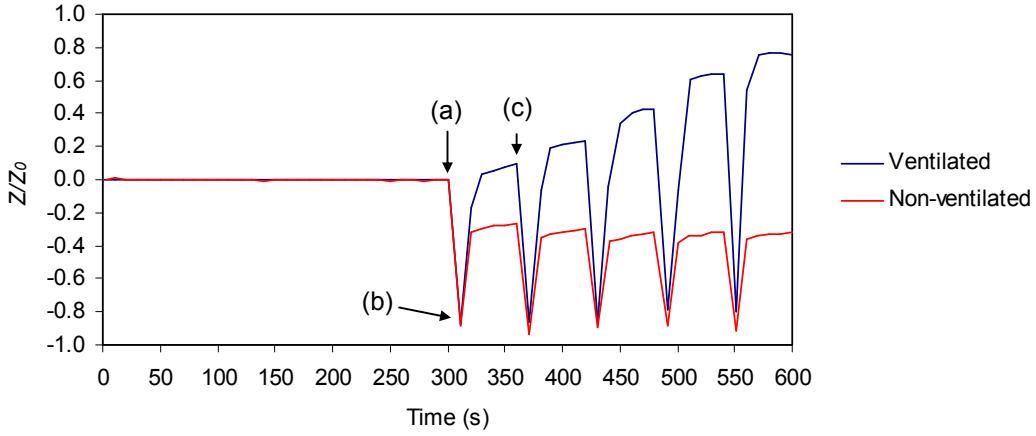

Figure 5.2 Evaluation of the effect of the measurement chamber design on the sensor impedance response to simulated breath containing 245 ±8 ppbv ammonia. Sample was applied to the chamber (a) for a period of 10 s (b), followed by the next pulse of sample which was 50 s later (c). The cycle was repeated five times.

5.3.2 Effect of sensor orientation relative to the measurement chamber on impedance response characteristics

The position of the sensor relative to the chamber was also investigated with the sensor being positioned either perpendicular or parallel with the air flow in different regions of the chamber (Fig. 5.3). The diameters of the nanoPANI electrode and chamber were approximately 14 and 22 mm, respectively, allowing sample and air flow to pass over and around the electrode. Configurations 1 through 4 were parallel to the flow of air where 1 was set at the base of the chamber, 2 at approximately a quarter ways from the base, 3 at three-quarters of the way, and 4 in close contact with the top of the chamber. Configuration 5 was perpendicular to the flow of air. The 62 ±0.7 L/min flow of air from the simulated breath system was consistent with atmospheric conditions (21 ±1^{o}C and 51 ±7% RH) whereby a 50 s input of 755 ±7 ppbv ammonia took place after a 100 s baseline consisting only of the atmospheric air flow. Since the purpose of the experiment was to optimise sensor response to ammonia, elevated humidity was not employed.

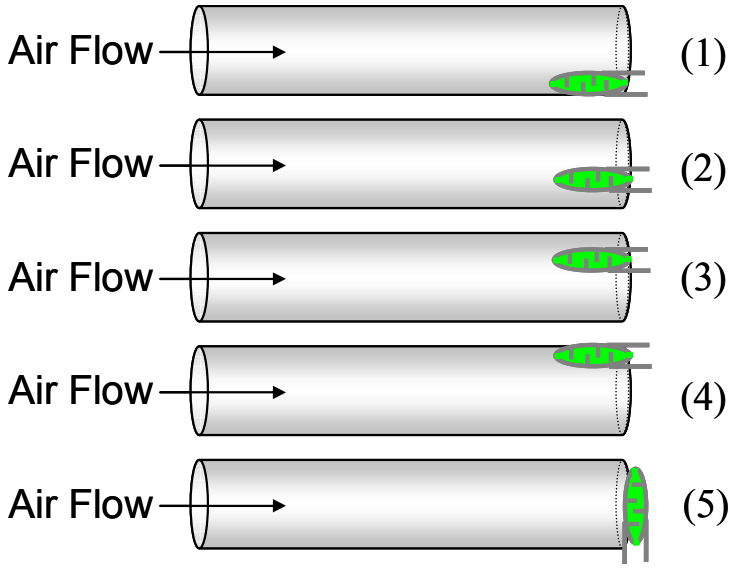

Figure 5.3 Configurations of electrode within the measurement chamber. With the nanoPANI in parallel to the flow of air and exposed upwards, the approximate percentage chamber diameter from the base of the chamber: (1) 0%, (2) 25%, (3) 75%, (4) 100%, and (5) perpendicular to the chamber exit.

All configurations showed an increase in Z/Z_0 upon exposure to the flow of atmospheric air from the simulated breath system (Fig. 5.4). However, configuration 5 displayed the greatest response from the sensor. This was observed by the largest increase in Z/Z_0 as well as a notable recovery towards the baseline due to good ventilation at the surface following sample application. With regard to the parallel flow configurations, 1 showed the highest response and the fastest recovery although 2 was quite similar, as both were exposed to adequate sample headspace to ensure no reduction in signal due to convective limitations at the electrode. Configuration 3 showed a significantly weaker ammonia signal due to further headspace limitation, but still had good sensor recovery showing good convective ventilation at the electrode. However, configuration 4 showed further inhibition of signal response to ammonia due to the significantly reduced headspace and flow conditions close to the chamber wall, and also had slower recovery showing reduced convective efficiency in removing ammonia from the sensor. Transport of ammonia to the electrode was most efficient when the electrode was perpendicular (configuration 5) due to the improved mass transport characteristics. This demonstrated the difference between a configuration at which a turbulent, infinite layer was flowing parallel to a surface, and a perpendicular configuration more akin to a wall-jet which flows perpendicular to the surface. Wall-jet

type configurations have found use in assessment of electrode kinetics via electrochemical flow through detectors for liquid chromatography and flow-injection [14]. In addition, previous studies of hollow fibre membranes have demonstrated how perpendicular flow dynamics through the membranes have higher mass transfer coefficients than parallel flows [15, 16]. Sengupta *et al* examined this phenomenon for the purpose of more efficiently removing and adding gases to aqueous solutions. Results from the previous literature as well as those observed in the current study suggested that perpendicular flow would allow more of the analyte to react with the electrode surface over time than in parallel flows. Furthermore, the ratio of the nanoPANI sensor diameter to the diameter of the sample collection measurement chamber was sufficient to allow the largest change in Z/Z_0 making configuration 5 the chosen configuration for use in future experiments.

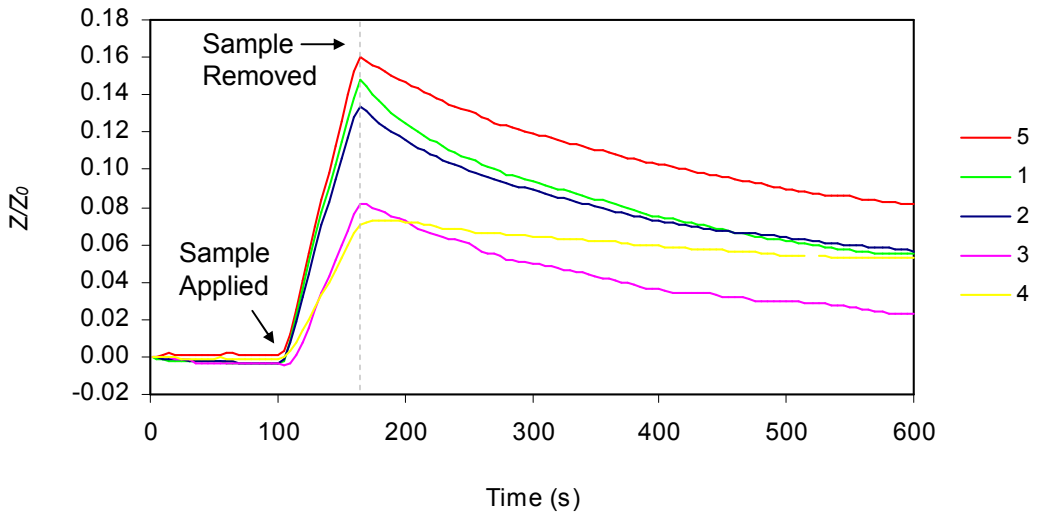

Figure 5.4 Comparison of the effect of 755 ±7 ppbv ammonia sample over 50 s on various electrode configurations as seen in Figure 5.3 where the approximate percentage of the chamber diameter from the bottom of the chamber was: (1) ~ 0%, (2) 25%, (3) 75%, (4) ~ 100%, and (5) perpendicular to the chamber exit.

5.3.3 Investigation of methods to displace sample from the sensor surface

In Section 5.3.1, it was observed that the electrodes did not generate the typical increase in Z/Z_0 upon exposure to ammonia if the moisture from the breath sample was allowed to condense on the electrode since the increasing presence of moisture masked the impedimetric behaviour of ammonia. Thus, in order to prevent the final fraction of breath

from remaining in contact with, and potentially condensing on the electrode, a method was developed to ensure that the entire breath sample would flow across the electrode, and be fully displaced from it when the breath was complete. This displacement could be brought about in two ways; either displacement of the sample with atmospheric air, or by using a defined gas supply that does not contain ammonia. Since responses from the ammonia sensor to atmospheric air had already been shown to be stable with low background signals, and that the addition of a means of providing defined gas supplies via a cylinder would add undesirable complexity to the measurement system, it was decided to use atmospheric air to displace the breath sample. This method of breath sample displacement had been shown to be effective in previous works for the collection of alveolar gases [17, 18]. This would require the application of a force to bring about this displacement and would, as a consequence, result in air flow.

It has been shown here (Sections 5.3.6 and 5.3.7), and in other related work that several variables including sample flow rate (linear flow velocity) across the sensor will affect its response characteristics [19]. It is also well-established that exhaled breath samples are not linear in terms of flow rate and are not consistent in terms of volume [20]. There are multiple potential solutions to this issue which could include the constant monitoring of flow velocity and sample volume, or by controlling the flow rates and volumes of the sample gasses. Given that it was now a design requirement to introduce a mechanism to remove the breath sample from the electrode, it was decided that the most appropriate technological solution was one that brought about the alternating application of a human breath sample and atmospheric air of defined volume and flow rate to the electrode. As a consequence of this, a breath measurement prototype was developed and referred to as the **Am**monia **Bre**ath Monito**r** (AmBeR), which utilised this approach.

5.3.4 Preliminary AmBeR system design and optimisation

Based on the design requirements defined, a preliminary, manually operated breath sampling device was assembled and configured with the ammonia sensors. A schematic and photograph of the system are shown in Fig. 5.5. The system now consisted of two major sub-systems; the sample collection chamber and the measurement chamber.

5.3.5 Sample collection chamber

The sample collection chamber was initially composed of a 37 cm length of flexible plastic cylindrical tubing typically used for respiratory systems, with an internal diameter of 22 mm and an initial volume of 250 ml which is approximately half the volume of an average human breath [21]. By employing a sampling volume of some fraction of the average human breath, it would be more likely to ensure collection of representative, undiluted samples from those who could only provide smaller sample volumes. Furthermore, use of a chamber volume some fraction of the average human breath would ensure that the sample remaining within the chamber after a full exhalation consisted of the end tidal volume of the breath. The end tidal volume consists of the alveolar breath which comes from exchange between the breath gases and blood [7], and is likely to provide the best quality sample. In addition, initial breath exhalate from the buccal cavity (mouth) would not be sampled and would, thus, be likely to reduce interference from ammonia generated from oral bacteria observed previously [22, 23].

The sample collection chamber possessed an entry port for breath exhalation via a facemask. This was connected to the passive T-junction diaphragm valves to allow exhalation of the breath sample to the sample chamber, inhalation of atmospheric air by the subject without removal of the mask, and passage of atmospheric air through the sample collection chamber during measurement. However, for initial evaluation, the inlet valve for the drawing of atmospheric air remained closed off, effectively making it a one-way valve (1). The outlet of the sample collection chamber was also connected to a similar valve arrangement. Two exit ports were available where one was for passage of the sample across the electrode, while the other allowed excess breath sample to overflow the sample collection chamber. Again, for preliminary evaluation, these outlets could also be sealed off manually. The work of Murnick *et al* also made use of a breath displacement method for isolation of alveolar gases which required manual opening and closing of the chamber when capturing the samples [24]. This method effectively displaced the sample, but it was designed to capture breath samples at designated time intervals. Doing so had the disadvantage of not determining when the complete flow of breath had ended which could have led to inconsistencies in sample volumes among individuals of various lung capacities.

5.3.6 Measurement chamber

The measurement chamber was fabricated using a 35 mm length of 22 mm diameter tubing in which the ammonia electrode was housed according to the outcome of experiments in Section 5.3.2 and positioned perpendicular to the sample flow. This was positioned 33 mm upstream from a miniature fan that would be used to draw the breath and air samples across the electrode. The fan speed, and therefore flow rate, could be controlled by the applied voltage and calibrated using spirometry.

5.3.7 Operation of the sample collection and measurement system

A manual operational methodology was adopted for initial system evaluation. A baseline signal from the sensor was first established using atmospheric air which was drawn through the initially detached measurement chamber assembly and across the electrode by the fan. For initial evaluation, the fan was operated at 10 V DC, which resulted in a flow rate of approximately 110.8 ±0.7 L/min. Following this, a simulated breath sample containing 245 ±8 ppbv of ammonia was applied to the sample chamber entry port for 4 s. The sample flowed through the collection chamber displacing the air present within by forcing the excess to exit via the open valve (2). The sample chamber exit port remained sealed during this period, and was then opened to allow attachment of the measurement chamber assembly to draw the breath sample from the sample collection chamber across the electrode, followed by a portion of atmospheric air. This was allowed to proceed for a period of 0.33 min. The excess breath outlet (2) was sealed off during this period. Following this, the measurement chamber assembly was detached from the sample exit port. The seal from the excess breath outlet (2) was removed and used to seal the sample chamber exit. Finally, the measurement chamber assembly was detached from the sample collection chamber and the process repeated.

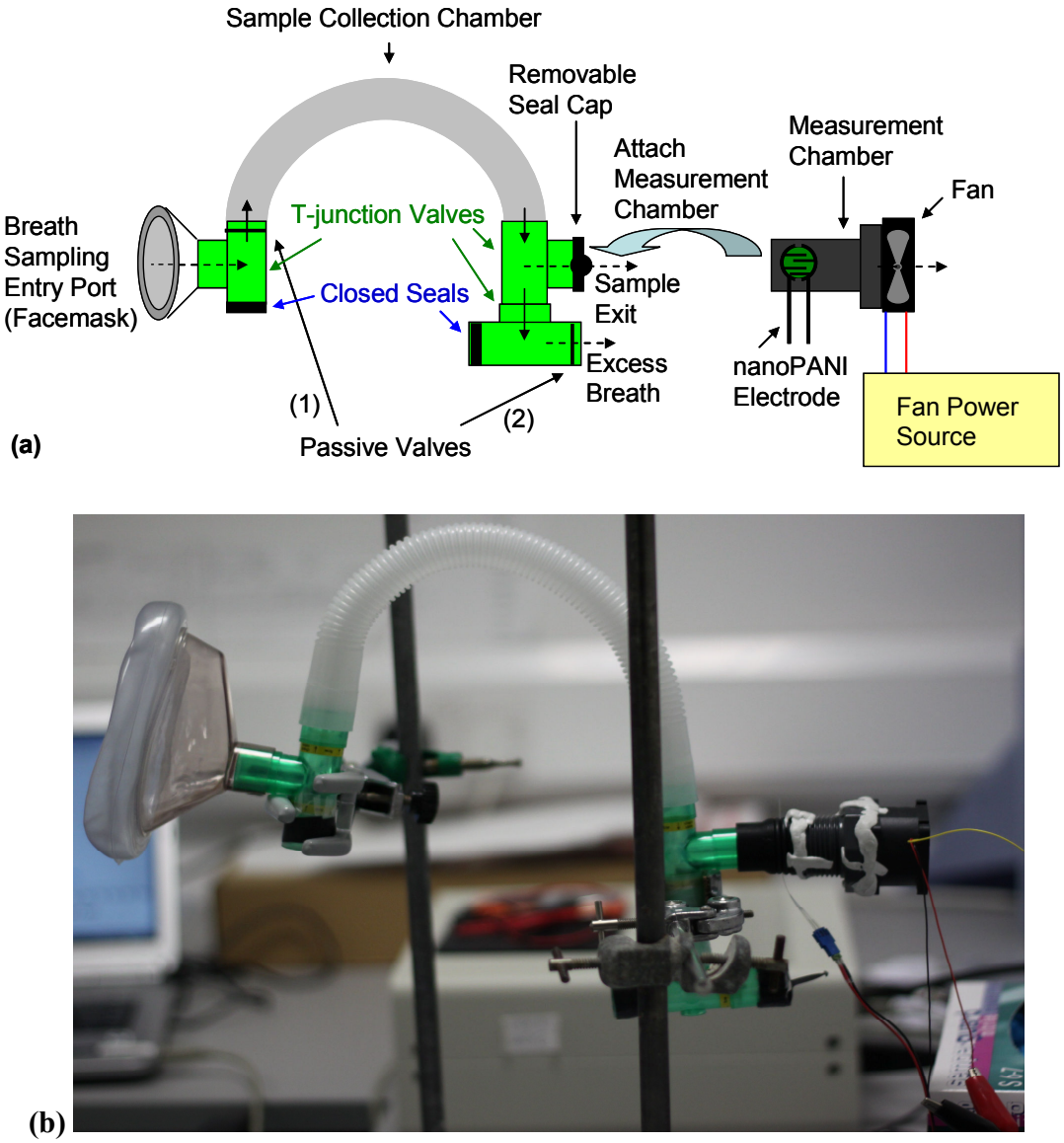

Figure 5.5 (a) Schematic and (b) photograph of the preliminary ammonia breath monitor system.

The impedance responses from the sensor for this experiment are shown in Fig. 5.6. The responses demonstrated the typical initial decrease in Z/Z_0 for 0.33 min when the humidity from a breath sample interacted with the sensor (Fig. 5.6b to c). At this point, the Z/Z_0 response increased gradually over the next 0.16 min followed by a more rapid increase with the flow of atmospheric air (Fig. 5.6c to d). The increase in Z/Z_0 was noticeable once the measurement chamber assembly was detached from the sample exit port since a stronger flow of air was obtained. There was slight air flow resistance within the sample collection chamber resulting from the passive valve diaphragms in the T-junction valve assemblies 1

and 2 which weakened the flow of atmospheric air being drawn behind the breath sample and across the electrode. Once the increasing response (Z/Z_0) of the electrode displayed a stable plateau, the sampling process repeated. The same behaviour was observed with all five samples, and displayed similarities to the behaviour seen in Chapter 4. The transition of interactions between breath sample and atmospheric air on the electrode not only demonstrated that the stagnant layer formed from sample humidity could be removed from the electrode following initial interaction, but that the technique had potential for use as the sampling methodology to generate an ammonia response from humidified breath samples within a device-type set-up.

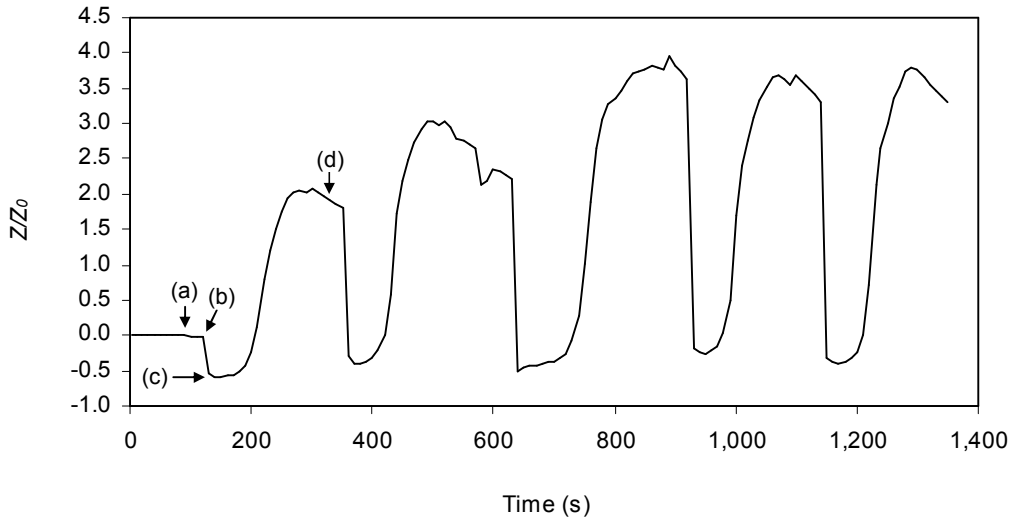

Figure 5.6 Impedance response ratio of the ammonia sensor to alternating application of a sample of simulated breath and atmospheric air (n=5). (a) Time at which a simulated breath sample containing 245 ±8 ppbv ammonia was applied to the sample collection chamber; (b) point of attachment of the measurement chamber assembly to the sampling chamber drawing breath sample across the electrode; (c) point of detachment of the measurement chamber assembly from the sampling chamber drawing atmospheric air across the electrode; (d) time at which second simulated breath sample containing ammonia was applied to the sample collection chamber.

As was observed, the process of removing the sample exit seal and attaching the sensor flow chamber assembly for each breath sample contributed to variability in the measurements. In order to efficiently automate the switch from sample collection to sample measurement, a manually operated two-way valve was installed to allow redirection of the

flow across the electrode with the measurement chamber assembly permanently attached to the sampling system (Fig. 5.7). One port of the valve was connected to the sample collection chamber, while the second was connected to the source of atmospheric air, and the third was connected to the measurement chamber assembly.

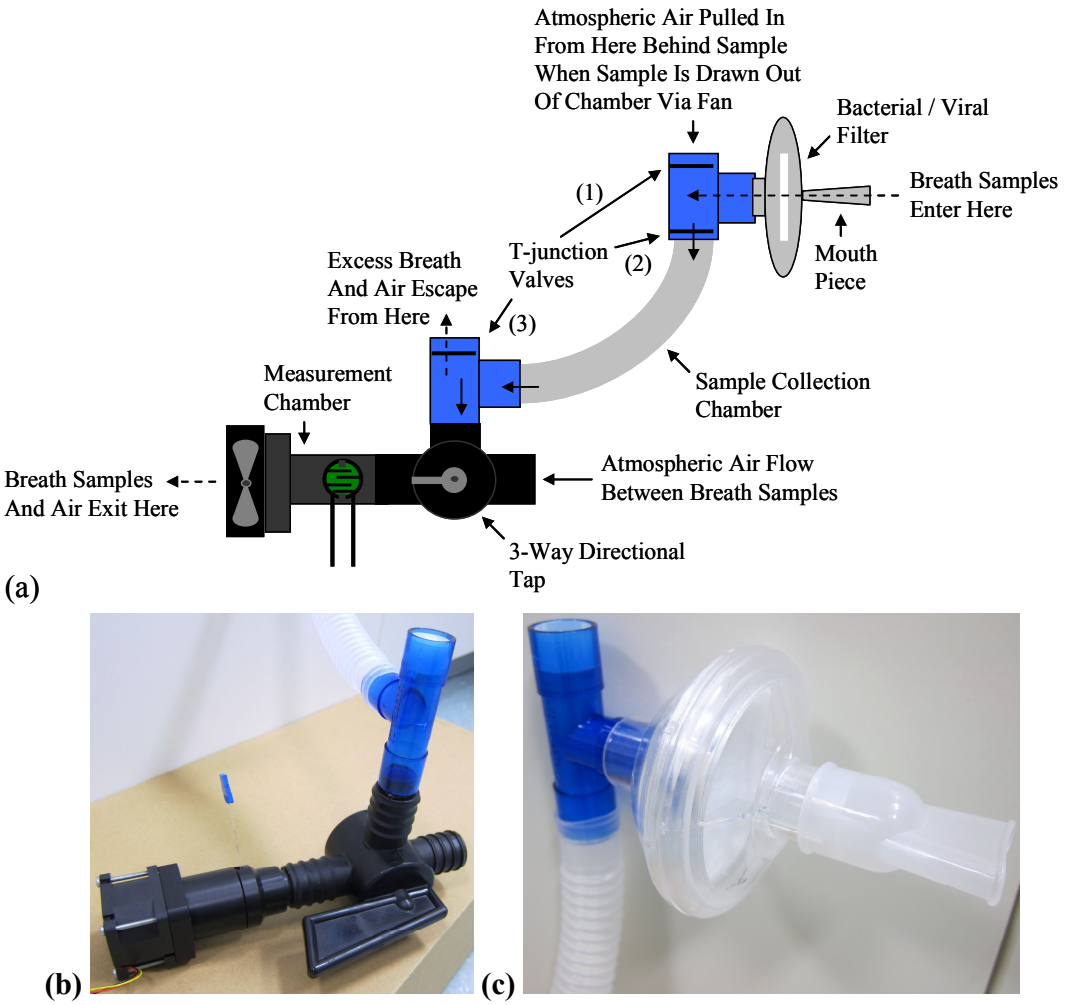

Figure 5.7 (a) Schematic of breath ammonia measurement prototype incorporating manually operated, two-way valve and bespoke measurement chamber housing. (b) Photos of tap and measurement chamber assembly, and (c) the mouth-piece with a bacterial / viral filter.

The sampling flow chamber was also upgraded to flexible corrugated ethyl vinyl acetate (EVA) cylindrical tubing that was approved for clinical usage (CE0123). The measurement chamber assembly was also upgraded from a temporary plastic housing to a bespoke housing that connected the fan and sensor to the valve (Fig. 5.7b). The CE-marked tubing

for the sample collection chamber was available in lengths of 23, 37, 51, and 65 cm which equated to volumes of 79, 128, 176, and 225 ml. For initial system evaluation, the 37 cm tubing was selected (128 ml) which was approximately half the volume used in previous experiments (i.e. 250 ml) and a quarter the volume of a normal exhalation (i.e. 500 ml). The system was also augmented with the addition of a CE0123-approved mouth piece with filter to avoid microbial contamination (Fig. 5.7c). In terms of operation, exhaled breath samples could enter the sample collection chamber while atmospheric air was being passed across the electrode through the measurement chamber. This revised assembly was tested with three samples of simulated breath ammonia at 40 ±2, 121 ±15 and 392 ±6 ppbv. As before, simulated breath samples of 4 s duration were applied to the sample collection chamber while the sensor was undergoing baseline measurement with atmospheric air. Once the baseline was complete, the valve was switched to allow the sample (followed by a plug of atmospheric air) to be drawn from the sample collection chamber and across the electrode for 10 s via the fan at a setting of 10 V. The sampling time was reduced from the previously used 20 s to 10 s since it was evident that the typical response behaviour could still be achieved in this time period, so reducing overall measurement time. After the sample was drawn out of the chamber, the tap was switched back to its original position where air was drawn directly from the atmosphere. This allowed another breath to be sampled in the collection chamber while fresh atmospheric air passed across the electrode through the measurement chamber. Once the Z/Z_0 from the sample had levelled off, the process was repeated until three readings at each concentration were taken (Fig. 5.8).

As seen in the previous data, each sample concentration displayed an initial decrease in Z/Z_0 due to humidity, followed by an increase in Z/Z_0 due to ammonia, which typically reached a plateau after 20 s. The method resulted in a response to ammonia that was capable of distinguishing concentrations of ammonia in the low ppbv concentration range, and the responses did not suffer from interference due to humidity. The changes in Z/Z_0 were lower than those derived in the previous design, most probably due to the reduction in the quantity of breath sampled. However, the responses were consistent and reproducible due to the effective systemisation of the breath sampling interface.

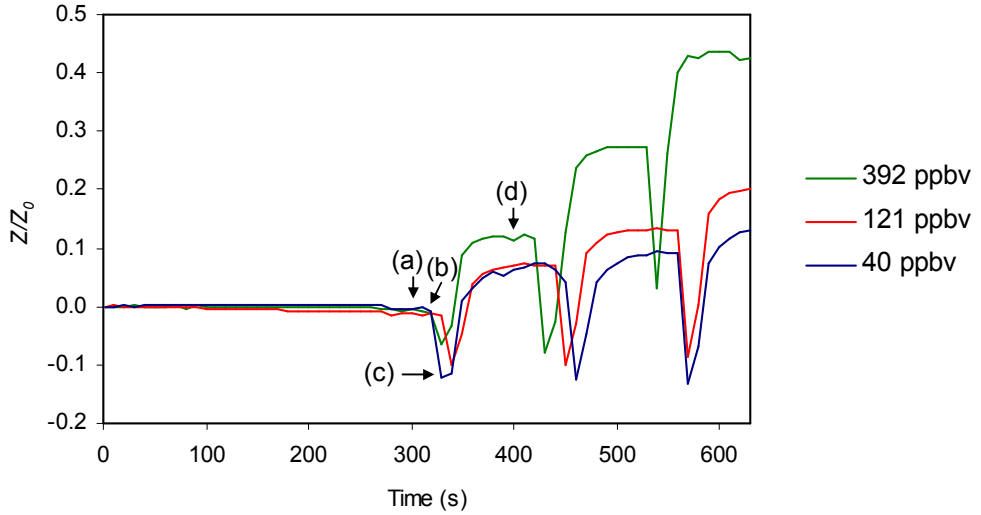

Figure 5.8 Evaluation of ammonia sensor impedance responses to simulated breath ammonia samples using the breath sample collection chamber with a manually operated tap in conjunction with the measurement chamber assembly. Simulated breaths of 4 s duration containing 40 ±2, 121 ±15, or 392 ±6 ppbv ammonia were (a) applied to the sampling chamber and (b) upon switching the tap, the samples followed by atmospheric air were drawn from the sample collection chamber for 10 s across the electrode (c) followed by switching the tap back to its original position allowing air to be drawn directly from the atmosphere until a stable baseline was observed, and (d) addition of the next sample to the collection chamber (n=3).

5.3.8 Effect of flow-rate across the electrode on impedance response

The effect of the flow rate across the electrode on impedance response was assessed. The fan speed could be adjusted by control of the applied voltage, operating across the range of 8 to 12 V which resulted in flow rates from approximately 90 to 128 L/min (Table 5.1). Flow rates were measured with a spirometer at the interface between the sampling chamber and the manually operated valve. The responses from a simulated breath containing 755 ±7 ppbv ammonia and a sample chamber volume of 128 ml were investigated (Fig. 5.9). As established, simulated breath samples filled the sampling chamber, and after establishment of the sensor baseline, the simulated breath sample was drawn from the sampling chamber through the measurement chamber across the electrode at a range of flow rates. After measurement, the valve was again switched back to draw air directly from the atmosphere

across the electrodes for a period of 20 s which was found in Fig. 5.8 to be sufficient to derive a stable baseline response to ammonia. It was observed that the Z/Z_0 signal decrease characteristic of the presence of humidity was greater at lower flow rates. This observation appears broadly in line with earlier observations that have indicated that rapid dissipation of the humid breath sample from the sensor surface reduces this effect. Thus, passage of sample at higher flow rates reduced this effect. In addition, higher flow rates also brought about an increase in the ammonia response. This can be explained due to improved mass transport at the electrode surface. The gas flow impinging on the electrode results in the formation of a stagnant layer at the electrode surface which is flow rate dependent. Increasing the flow rate has the effect of reducing this stagnant layer and increasing mass transport to the electrode surface. Due to the specific nature of this study, though, there is a lack of exact comparative literature on flow rates of ammonia interacting with polyaniline films. However, this flow rate dependent behaviour can be observed in literature which focuses on the flow rate interaction between other carrier gases and polyaniline. For example, Draman *et al* observed the effects of oxygen gas flow rate on response in sulphonic acid-doped polyaniline by way of fluorescence quenching [25]. Assessment of oxygen flow from 0.25 to 2.00 mL/s also resulted in an increased response with an increase in flow rate demonstrating the effect of increased mass transport.

A flow rate of 110.8 ±0.7 L/min was chosen for further studies since the humidity effect was sufficiently decreased in comparison to lower flow rates (90.1 ±0.4 L/min and 101.0 ±0.4 L/min), while the increased Z/Z_0 due to ammonia was comparable to that at higher flow rates (119.90 ±0.8 L/min and 127.50 ±0.8 L/min) and while having the advantage of reducing power consumption from 12 V to 10 V. For a point-of-care device intended to be used in clinical diagnostics, lower power consumption will no doubt prove to be beneficial.

Table 5.1 Relationship between fan voltage, flow rates, and the change in Z/Z_0 using simulated breath samples containing 755 ±7 ppbv of ammonia and a sampling chamber volume of 128 ml.

Fan Voltage (V)	Flow Rate (L/min)	Z/Z_0
8	90.1 ±0.4	0.08
9	101.0 ±0.4	0.09
10	110.8 ±0.7	0.12
11	119.9 ±0.8	0.13
12	127.5 ±0.8	0.15

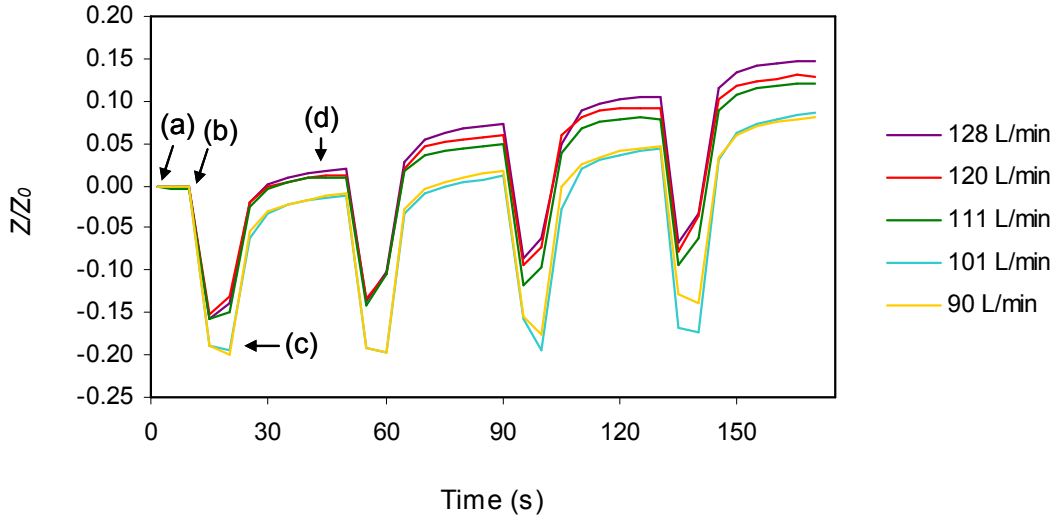

Figure 5.9 Investigation of the effect of sample flow rate on sensor response (Z/Z_0). A simulated breath sample containing 755 ±7 ppbv ammonia within a sampling chamber volume of 128 ml was used. The samples were (a) applied to the sampling chamber 10 s before baseline completion, and (b) upon switching the valve were drawn across the electrode for 10 s (c) followed by switching to atmospheric air for 20 s, whereupon (d) the next sample entered the collection chamber (n=4).

5.3.9 Effect of sample collection chamber volume on electrode signal behaviour

As already discussed, having control over the volume of breath sampled would ensure that any inconsistencies in human exhalation volumes were accounted for and the actual volume sampled was always known. In addition, errors due to insufficient sample and interferences due to oral ammonia would be reduced. An assessment of the effect of sample volume was made using the available tubing volumes from 79 to 225 ml which represented fractions of a normal breath sample of approximately 16 to 45% (Table 5.2). Using simulated breath samples containing 245 ±8 ppbv of ammonia at a flow rate of 110.8 ±0.7 L/min (n=4), the characteristic increase in Z/Z_0 was observed for each sampling chamber volume (Fig. 5.10).

Table 5.2 Relationship between the sampling chamber volume and the change in Z/Z_0 using four sequential simulated breath samples containing 245 ±8 ppbv of ammonia and a fan flow rate of 110.8 ±0.7 L/min.

Sample Collection Chamber Length (cm)	Volume (ml)	Z/Z_0
23	79	0.07
37	128	0.05
51	176	0.02
65	225	0.01

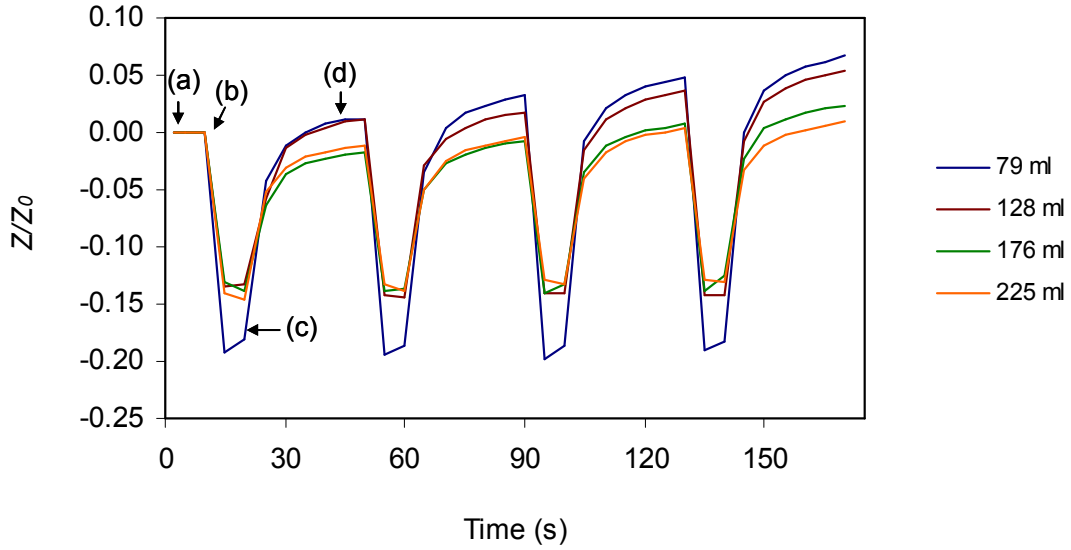

Figure 5.10 Investigation of the effect of sample collection chamber volume on the ammonia sensor impedance response using simulated breath samples containing 245 ±8 ppbv of ammonia and a flow rate of 110.8 ±0.7 L/min. The samples were: (a) applied to the sampling chamber 10 s before baseline completion, and (b) upon switching the valve, they were drawn across the electrode for 10 s (c) followed by atmospheric air for 20 s, whereupon (d) the next sample entered the collection chamber (n=4).

The results exhibited an inverse proportionality between volume and signal. Larger volumes of 176 and 225 ml displayed less of an increase in Z/Z_0 than did the smaller two volumes (79 and 128 ml). Furthermore, the smallest sampling chamber (79 ml) showed the greatest initial decrease in Z/Z_0 which would indicate the most significant signal contribution from humidity as demonstrated earlier (Chapter 4, Section 4.3.5). The inverse proportionality observed can be explained by the Fundamental Flow equation which is a representation of the fluid dynamics of air through a tube [26]. The equation is as follows:

$$Q = 1.1494 \times 10^{-3} (T_b / P_b) [(P_1^2 - P_2^2) / GT_f LZf]^{-0.5} D^{2.5} \quad \textbf{(1)}$$

where Q is the gas flow rate (L/min*1.44), f is the friction factor (unitless), T_b is the base temperature (^{o}C+274.15), P_b is the base pressure (kPa, air = ˜101 kPa), P_1 is the upstream pressure (kPa, air = ˜101 kPa), P_2 is the downstream pressure (kPa, air = ˜101 kPa), G is the gravity on the gas (unitless, air = 1.00), T_f is the average temperature of the flowing gas (^{o}C+274.15), L is the length of the tube (cm*10^{-5}), Z is the gas compressibility factor at the flowing temperature (unitless), and D is the internal diameter of the tube (mm). This formula could potentially be used to make predictions of Q within the system, but the friction factor and gas compressibility factor are values that must be found through experimentation where the friction is the effect of the ratio between the inner-most corrugation and the outer-most wall over the length of each tube, and the compressibility of a particular flowing gas is dependent upon the pressure and temperature measured within the tube at each time of flow. The Fundamental Flow equation states that when air passes through a cylindrical vessel such as the chamber used in this study for sample collection, the flow rate is affected by several factors. If the gravity, compressibility factor, and/or temperature of the gas increase, the flow rate will decrease. These variables have remained constant within the collection chamber, though, and so are not relevant factors. If the diameter of the tube were to increase, the flow rate would increase proportionally. However, the diameter of the chamber also remained constant resulting in no effect on the air flow. The Fundamental Flow equation also states that for a given pressure, and assuming the other variables (i.e. temperature, gravity, etc.) remain constant, the flow rate of air through the tube will decrease with an increase in tube length. The key factor behind this phenomenon is the friction between the gas and the walls of the chamber tubing [26]. With an increased amount of surface area from the increased length of the collection chamber comes an increased amount of friction between the gas and the tube surface as well as a reduction in pressure [27, 28]. The friction is further increased by the corrugated structure of the chamber wall. Hence, the shorter length of tubing used to assess smaller volumes resulted in a faster flow rate of ammonia gas. This compliments the results found in Section 5.3.6 which showed an increase in signal response (Z/Z_0) with an increase in flow rate, and hence, improved mass transport of the ammonia gas. Experimental evidence using spirometry to measure a continuous flow of simulated breath (62 ±0.7 L/min, 37

±1°C, ≥ 90% RH, 245 ±8 ppbv ammonia) through each sample collection chamber length supported this observation (Table 5.3).

Table 5.3 Relationship between the sample collection chamber volume and flow rate of sample exiting the collection chamber using four sequential simulated breath samples containing 245 ±8 ppbv of ammonia and an entry fan flow rate of 62 ±0.67 L/min.

Sample Collection Chamber Length (cm)	Volume (ml)	Flow Rate At Exit (L/min)
23	79	51.9 ±0.3
37	128	50.7 ±0.2
51	176	49.5 ±0.2
65	225	48.5 ±0.1

The sampling chamber volume of 128 ml was chosen for use in future studies since it demonstrated a lower Z/Z_0 change to humidity compared with the 176 and 225 ml chambers as well as a higher response to ammonia than either 176 or the 225 ml chambers. Furthermore, an assessment of patient comfort – which is necessary for use in clinical diagnostics – also indicated that the length of the 37 cm sampling chamber would allow adequate flexibility for patients to reach the breath sampler while undergoing haemodialysis.

5.3.10 Final AmBeR prototype system assembly and analytical validation

Based on preliminary experiments, the optimised system comprised of a sampling chamber volume of 128 ml and a fan setting of 10 V with a flow rate of 110.8 ±0.7 L/min. The measurement chamber and three-way tap were enclosed within a hinged plastic housing and the sample collection chamber was made external to the housing as it would be a semi-disposable component and so be simpler to replace in this configuration, while also allowing a flexible interface with the patient. The fan was modified so as to have the speed controls mounted on the casing with lead-outs for mains power supply and impedance instrumentation. An axial fan finger guard was added to the exhaust port of the fan for safety. The ammonia sensor was mounted perpendicular to the air flow path between the manually-operated valve and the fan. A schematic and photographs of the final breath ammonia monitoring system (AmBeR) are shown in Figure 5.11.

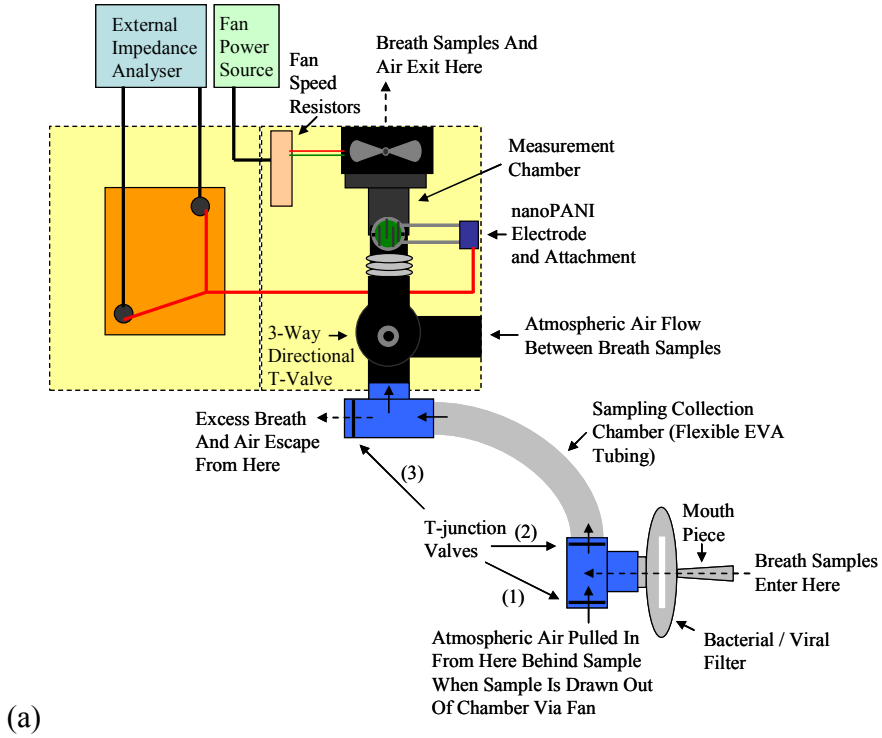

(a)

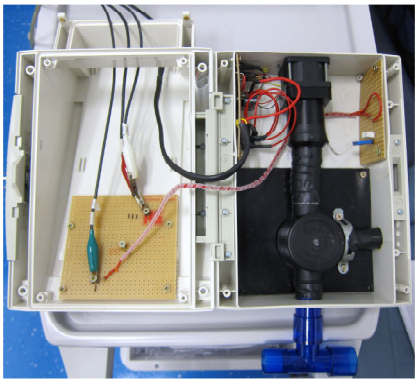

(b)

(c)

(d)

Figure 5.11 Final AmBeR design prototype. (a) Schematic of the device and air flow direction, (b) photograph showing internal assembly, (c) photograph of disposable sampling chamber portion, and (d) photograph of final assembled prototype.

5.3.11 Calibration of AmBeR using simulated breath ammonia

The response characteristics (Z/Z_0) of the ammonia sensor in the assembled AmBeR prototype system to eight consecutive simulated breath samples containing ammonia in the range of 40 ±2 to 2,993 ±10 ppbv are illustrated in Fig. 5.12. Simulated breath samples were collected as described in Section 5.3.6. As seen in several earlier observations, the characteristic signal decrease due to the presence of humidity followed by an increase upon removal of the sample was evident with each breath sample. Furthermore, the increase in Z/Z_0 due to ammonia was seen to be quantitative and cumulative over this clinically relevant analytical range. This cumulative response characteristic suggests that the interaction of ammonia with the electrode was following a process dominated by the rate of association of ammonia with the polyaniline. It further indicates that the nanoPANI film was below saturation levels whereby many nanoPANI sights were still available for interaction with ammonia molecules. Binding is thus limited by the mass of ammonia molecules arriving at the surface. Furthermore, the recovery towards the initial baseline suggests that the rate of dissociation was much slower than the rate of association indicating that the process was not in equilibrium. This slow rate of dissociation hinders the possibility of the sensors being utilised as a re-usable component. However, previous studies have indicated that the short-term application of heating to between 104 and 107^{o}C could have potential in sensor recovery [29]. Kukla *et al* performed such a technique to remove ammonium residue from PANI films and found that in PANI exposed to ammonia between 100 and 600 ppm, almost complete restoration to the initial baseline was possible. However, examination of thermal effects on polyaniline using infrared spectroscopy was performed by Trchová *et al* and demonstrated that heat treatment can cause degradation of the PANI chain, resulting in decreased conductivity [30]. Thus, even if the nanoPANI could be recovered to the original baseline, duplicate exposures to ammonia may generate inconsistent conductive responses.

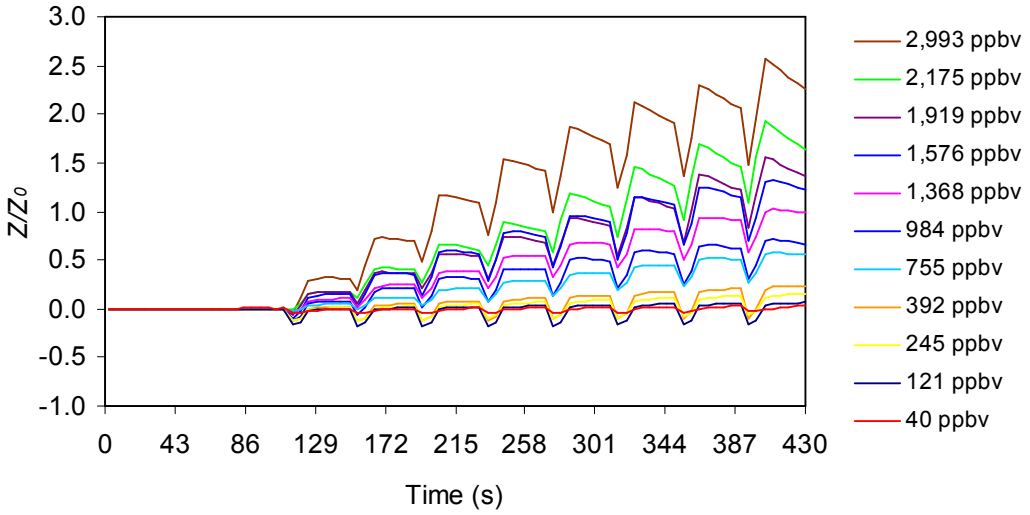

Figure 5.12 Impedance response ratio (*Z/Zo*) responses of nanoPANI electrodes to sequential application of simulated breath samples containing 40 ±2 to 2,993 ±10 ppbv of ammonia measured using the AmBeR breath ammonia monitoring system.

Similar to the work of Prasad *et al* which involved observation of the kinetics between ammonia and polyaniline-based films, the rate of dissociation appears to become greater as more ammonia binds to the film [31]. This was evidenced by the steepening of the dissociation component of the curve at higher ammonia concentrations. Prasad explained that higher concentrations of ammonia result in larger amounts of chemisorbed ammonia which leads to a higher rate of desorption. However, it has been demonstrated on numerous accounts that desorption of ammonia does not indicate that polyaniline will completely recover to its original baseline value [32, 33] which further verifies that polyaniline-based electrodes are at their optimum sensitivity during initial interaction with ammonia.

The peak breath responses obtained after eight consecutive simulated breath samples were plotted against breath sample number (Fig. 5.13). By the eighth breath, the coefficient of variation of the signal response (Z/Z_0, n=3 from three different electrodes) had increased from 0.0843 at 40 ppbv to 0.1728 at 2,993 ppbv, but did not increase proportionally. This could in part be due to the increased standard deviations previously observed at higher concentrations from the simulated breath system (Table 3.2). However, as described in previous literature, it is more likely that the higher concentrations of ammonia cause an increase in competition for available active nanoPANI sites [31], therefore causing greater variability.

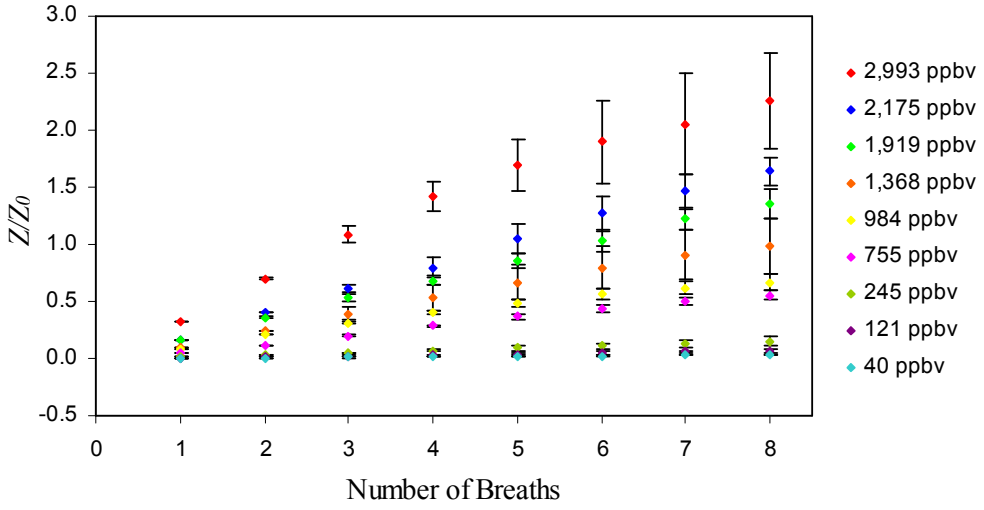

Figure 5.13 Relationship between impedance response ratio (Z/Z_0) and breath sample number for sequential additions of simulated breath samples to the AmBeR device. Error bars indicate standard deviation (n=3).

The relationship between Z/Z_0 and ammonia concentration for each accumulated breath sample number was determined (Table 5.4 and Fig. 5.14). It could be seen that the coefficient of determination increased with the number of breath samples. It should also be noted that changes in response could be identified for a single breath. However, at lower breath sample number, it was difficult to quantify ammonia concentration due to the lower sensitivities obtained. Slopes demonstrated an increase from 0.00010 (breath 1) to 0.00076 $ppbv^{-1}$ (breath 8), and calibrations for all accumulated breath sample numbers resulted in good linear fitting which improved significantly with the numbers of breaths sampled from 0.9687 (breath 1) to 0.9975 (breath 8).

Table 5.4 Relationship between the impedance response ratio (Z/Z_0) and breath ammonia concentrations with respect to breath sample number.

Breath Number	Slope ($ppbv^{-1}$)	R^2
1	0.00010	0.9687
2	0.00022	0.9743
3	0.00034	0.9689
4	0.00044	0.9675
5	0.00054	0.9808
6	0.00062	0.9883
7	0.00069	0.9960
8	0.00076	0.9975

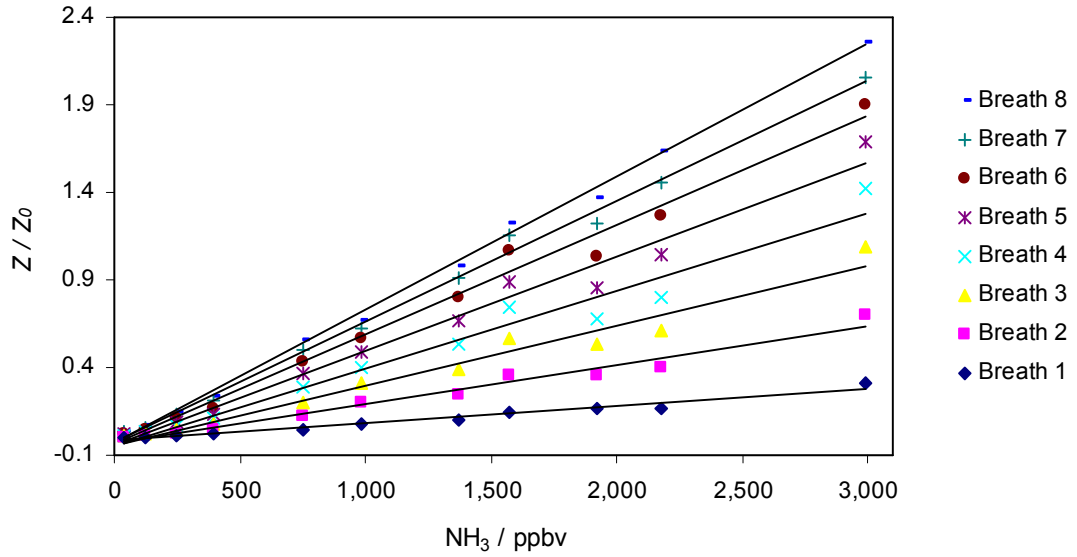

Figure 5.14 Effect of breath sample number on the relationship between the impedance response ratio (Z/Z_0) and breath ammonia concentration determined using the AmBeR device.

In the case of the responses after eight breaths, these generated a slope and intercept of 0.00076 $ppbv^{-1}$ and -0.0354, respectively (Table 5.5 and Fig. 5.15). Based on this data, and the maximum intra-electrode baseline drift variability data determined in Chapter 4 (1.67%), a theoretical limit of detection of approximately 65.9 ppbv could be determined (S/N=3). The actual linear dynamic range observed, though, was from 40 ±2 to 2,993 ±10 ppbv (although the system may have proven linear above this value, this was not tested during this research). As discussed previously, human breath ammonia typically falls between the physiological range of approximately 50 ppbv to 2,000 ppbv. This demonstrated that the AmBeR system's operational range was within that required for human diagnostic breath measurements. The RSD (%) values were higher than expected, but as mentioned earlier, this may be due to the standard deviations previously observed from the simulated breath system (Table 3.2). This could also suggest that the sensors may require more complex calibration procedures than just simple baseline correction as well as further fabrication optimisation. With many of the deviations being of a smaller magnitude, it is clear that improvements are possible.

Table 5.5 Ammonia concentrations and impedance response (Z/Z_0) results after eight breath samples. *Concentration of ammonia determined by PALS (Chapter 3, Section 3.3.3).

*PALS (NH_3 / ppbv, n=5)	AmBeR (Z/Z_0, n=3)	AmBeR (Z/Z_0, RSD %)
40 ±2	0.0318 ±0.0027	8.4
121 ±15	0.0641 ±0.0155	24.1
245 ±8	0.1490 ±0.0554	37.2
392 ±6	0.2372 ±0.0228	9.6
755 ±7	0.5553 ±0.0631	11.4
984 ±21	0.6659 ±0.1249	18.8
1,368 ±11	0.9831 ±0.2631	26.8
1,576 ±7	1.2242 ±0.2641	21.6
1,919 ±20	1.3620 ±0.1169	8.6
2,175 ±26	1.6373 ±0.1347	8.2
2,993 ±10	2.2594 ±0.3905	17.3

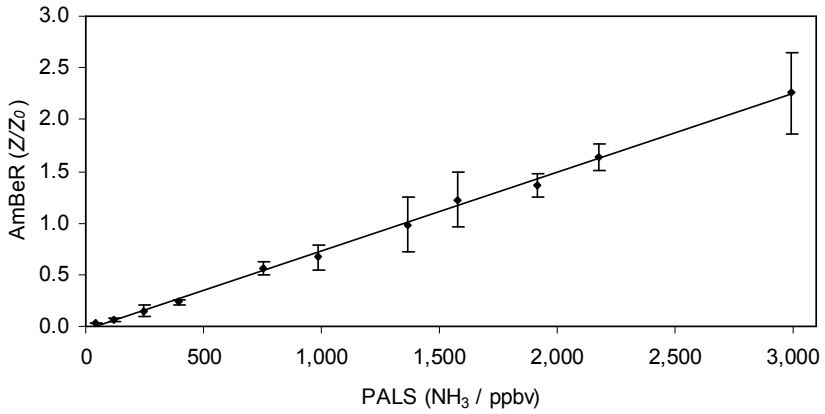

Figure 5.15 Relationship between ammonia concentration (as determined by PALS) and impedance response (Z/Z_0) after eight sequential breath samples using AmBeR (R^2 = 0.9975, n=3). Slope = 0.00076 $ppbv^{-1}$ and intercept = -0.0354.

5.3.12 Evaluation of the AmBeR system in normal human breath samples

Having demonstrated the AmBeR system in simulated breath samples, it was evaluated using breath samples from normal healthy human volunteers (n=10) including repeated evaluation of a single volunteer over a period of three days (n=7). There were five female and five male volunteers, and the average body mass index provided from nine of these volunteers was 23.72 kg/m^2 (range from 17.64 to 31.25 kg/m^2). The mean age of the population was 35 years (range from 24 to 52 years). Of these volunteers, six identified themselves as ethnically Irish, three Americans, and one Maltese. The sampling was performed using both the AmBeR device and PALS whereby the AmBeR device was used

directly after PALS. Sampling with PALS involved breathing continuously into the system for five minutes (n=3) while sampling with AmBeR was performed by way of taking eight breath samples in the same way as in Section 5.3.6, again replacing the sensor with a new one for each set of measurements. Table 5.6 and Fig. 5.16a show the relationship between the concentration of ammonia in the human breath population samples as determined by PALS and the values of Z/Z_0 derived from the AmBeR system. PALS indicated that the mean oral breath ammonia of the 10 volunteers was 226 ppbv (ranging from 22 to 583 ppbv), while the average inter-individual deviation was 14 ppbv (n=3). The population data yielded a slope of 0.00066 $ppbv^{-1}$ and an intercept of 0.079, with Pearson correlation coefficient of r=0.9980 (p<0.01), indicating excellent correlation with PALS in a normal human population. The ammonia concentrations were within the range of values previously determined for normal human subjects (Chapter 2, Section 2.3.1). The mean oral breath ammonia of the individual volunteer tested was 96 ppbv (ranging from 66 to 147 ppbv) with an intra-sample deviation of 25 ppbv (n=3) (Fig. 5.16b and Table 5.6). This yielded a slope of 0.00069 $ppbv^{-1}$ and an intercept of -0.011, with Pearson correlation coefficient of r=0.9640 (p<0.01), again showing excellent correlation with PALS. Both population and individual data demonstrated similar response sensitivity (<8% RSD) to that determined using simulated breath (Fig. 5.15) indicating good agreement between simulated and real breath samples as well as the capability to quantify human breath ammonia concentrations.

Table 5.6 Ammonia concentrations in real human breath samples as measured by the PALS and AmBeR systems displaying a normal human breath sample from 10 volunteers, and 7 normal human breaths from one volunteer.

Normal Breath From 10 Volunteers			Normal Breath From A Single Volunteer		
PALS (ppbv) (n=3)	**AmBeR (Z/Z_0)**	**AmBeR (ppbv)**	**PALS (ppbv) (n=3)**	**AmBeR (Z/Z_0)**	**AmBeR (ppbv)**
22 ±5	0.08	53	66 ±22	0.04	6
53 ±1	0.09	76	83 ±10	0.04	6
84 ±12	0.12	110	85 ±8	0.04	8
102 ±14	0.17	182	91 ±14	0.05	19
112 ±2	0.16	166	98 ±5	0.06	32
163 ±8	0.21	233	101 ±16	0.06	32
217 ±7	0.23	251	147 ±1	0.09	72
451 ±27	0.37	443			
477 ±50	0.43	520			
583 ±29	0.44	528			

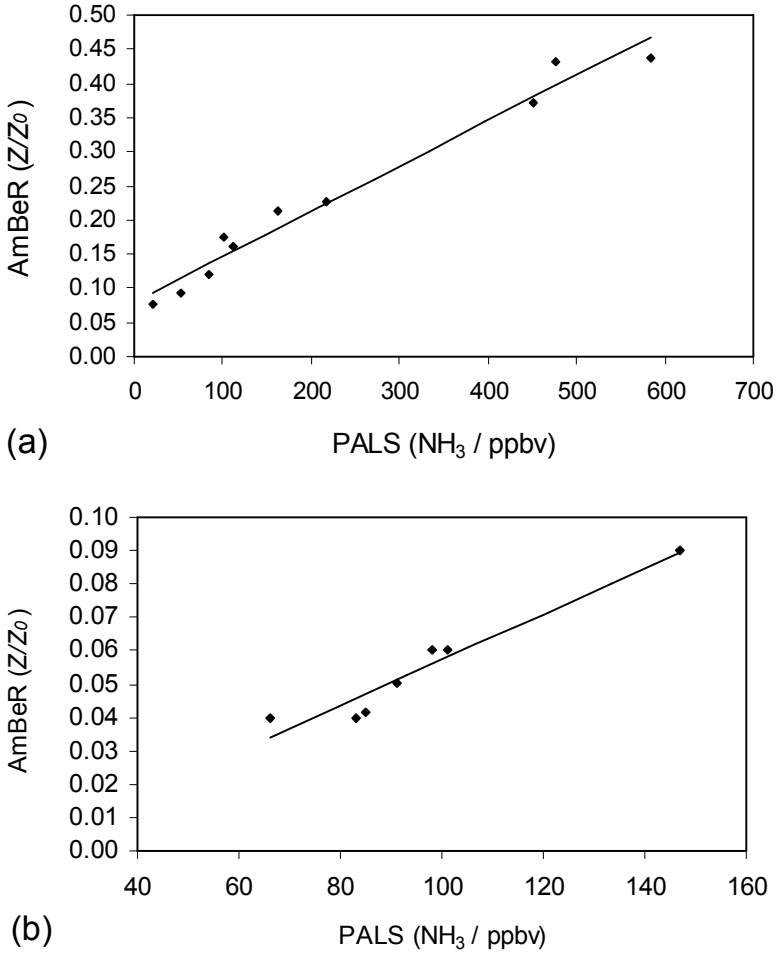

Figure 5.16 Relationship between AmBeR (Z/Z_0) and PALS (NH_3/ppbv) (a) a normal human breath sample from 10 volunteers (r=0.9980, p<0.01), and (b) 7 normal human breaths from one volunteer (r=0.9640, p<0.01).

Table 5.6 and Fig. 5.17 show the relationship between the concentration of ammonia in the human breath samples as determined by PALS and the concentration of ammonia derived from AmBeR via conversion of the Z/Z_0 values using the simulated breath calibration established in Fig. 5.15. The population showed a positive bias towards the AmBeR responses across the measurement range with a slope and intercept of 0.8749 $ppbv^{-1}$ and 58.11. (Table 5.6 and Fig. 5.17a). The population data had a Pearson correlation coefficient of r=0.9860 (p<0.01). By comparison to the population mean oral breath ammonia concentration of 226 ppbv indicated by PALS, AmBeR provided a mean of 256 ppbv (ranging from 53 to 528 ppbv). The intra-individual correlation had a slope and intercept of 0.9034 $ppbv^{-1}$ and -61.94 with a Pearson correlation coefficient of r=0.9678 (p<0.01).

There was a bias towards PALS in the intra-individual data. By comparison to the mean oral breath ammonia concentration of 96 ppbv from the individual volunteer indicated by PALS, AmBeR displayed a mean of 25 ppbv (ranging from 6 to 72 ppbv).

The reason for the bias is not clear. However, it demonstrates that there may be a small bias in the response between simulated breath samples, as derived in Fig. 5.15, versus real breath samples due to, as yet, undetermined interferents. However, this bias could be removed by direct calibration against PALS or even SIFT-MS using real samples as opposed to simulated breaths.

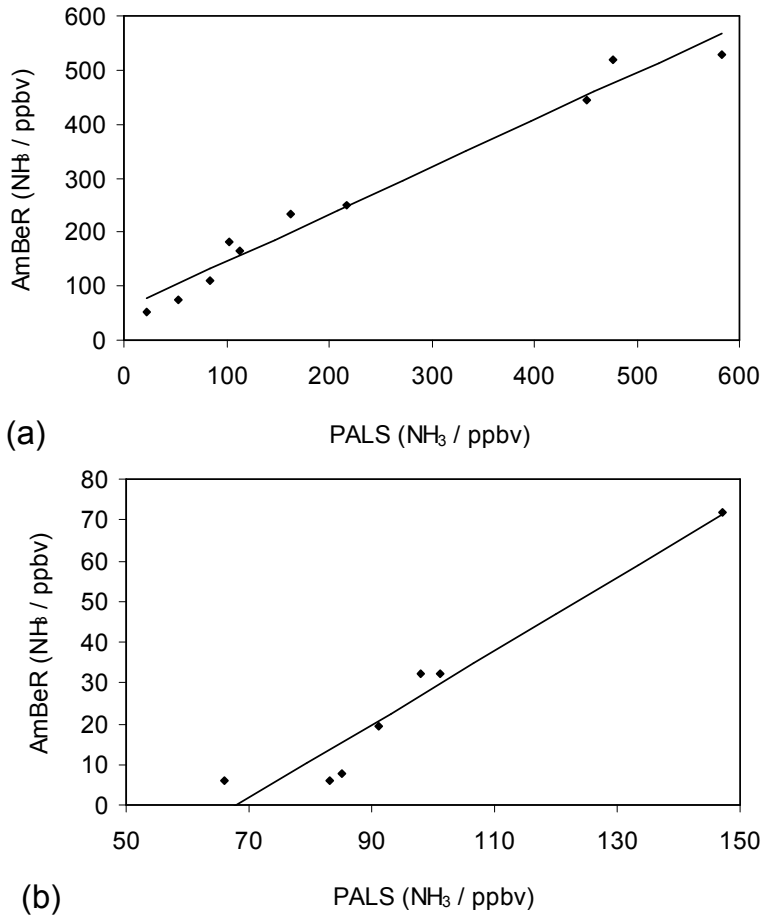

Figure 5.17 Relationship between AmBeR (NH_3/ppbv), calculated based on simulated breath samples, and PALS (NH_3/ppbv). The data represents (a) a normal human breath sample from 10 volunteers (r=0.9860, p<0.01), and (b) 7 normal human breaths from one volunteer (r=0.9678, p<0.01).

In comparison to other recent devices for the measurement of ammonia, the AmBeR system demonstrated great potential for application in clinical diagnostics. Timmer *et al* proposed a technology involving miniaturised gas samplers for detection of ambient ammonia. This involved transfer of the ammonia gas to solution and its sequential acidification and basification, before measurement using simple conductivity. As a result, the system required many liquid supply lines and pumps and was not suitable for diagnostic application. In addition, they only demonstrated the capability of determining ammonia at concentrations from 600 to 9,400 ppb [34], and 300 to 9,800 ppb [35] which did not reach the minimum required for human breath measurements. Furthermore, the assessments were performed in air rather than actual breath or a breath-like matrix. This could leave many unanswered questions about potential interferences such as breath humidity or temperature, sample volume and flow rate, etc. Aguilar *et al* described a device based on conducting polymer nanojunctions and demonstrated a sensor which responded to concentrations of ammonia from 10 ppb to 1 ppm including data from both ammonia gas and human breath ammonia [36]. However, the technique used samples collected in Tedlar bags among dilutant air which would make real-time human breath sampling impossible. Furthermore, the device was relatively complex with integration of a sodium hydroxide filter required to minimise humidity. Integrated desiccants such as this could pose problems where issues of toxicity may come into question with regard to point-of-care clinical monitoring via oral sampling, or regeneration of the desiccant component. A further device which consisted of a metal oxide-based nanosensor (i.e. MoO_3) displayed potential for measuring human breath since it was portable and capable of detecting ammonia gas as low as 50 ppb [37]. However, Gouma *et al* were only able to assess 50 ppb and 100 ppb, and no actual human breath measurement was performed. In this case, it is not known if it would be suitable for clinical patients whose breath ammonia concentrations could range from 50 to several thousand ppb. Furthermore, in each example, the methods were not validated against a standard method.

5.3.13 Retrospect on sensor lifetime and robustness

A preliminary six-month observation of electrode stability was performed using the data from individuals who displayed similar breath ammonia concentrations (651 ±36 ppbv, n=6) via AmBeR (Table 5.7 and Fig. 5.18). Stability and robustness of the electrodes at month six are comparable to that which was observed at month one where original baseline

drift is 0.00 ±0.01, and overall signal response to similar breath ammonia concentrations display similar response behaviours.

Table 5.7 Sensor responses to similar human breath ammonia concentrations of 651 ±36 ppbv (n=6) via a batch of polyaniline-based electrodes printed prior to the initial indicated date and observed over duration of approximately six months.

Trial Date	Z/Zo	Abs. NH_3 (ppbv)
Oct 22, 2011	0.50	611
Dec 8, 2011	0.52	638
March 27, 2012	0.54	664
April 3, 2012	0.56	690
April 5, 2012	0.50	611
April 6, 2012	0.56	690

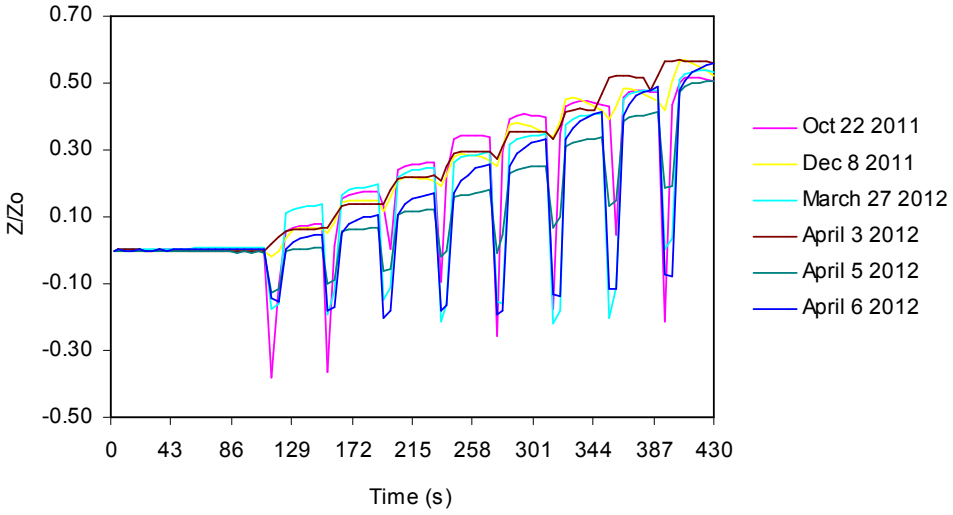

Figure 5.18 Observation of behaviour from polyaniline-based electrodes (n=6) printed prior to the initial indicated date and utilised over duration of approximately six months. Similar concentrations of human breath ammonia (651 ±36 ppbv) were observed upon each electrode. The baseline drift from 0 to 100 s was 0.00 ±0.01 overall.

5.4 Conclusions

Experimental observations showed that nanoPANI sensor responses to humidity could be controlled by careful design of the sensor/sampling interface with additional dynamic control of the sampling process. Further studies demonstrated the relationships between sample flow rates and sample volumes on the dynamics of interaction of ammonia in breath

with the polyaniline sensor. These findings led to the design and method of operation of a breath sampling interface having a sample flow rate of 110 L/min and a sample volume of 128 ml. The device was calibrated over the range of 40 ±2 and 2,993 ±10 ppbv using simulated breaths. Detection and quantification of ammonia concentrations from normal human breath showed a 0.9860 correlation between the resulting AmBeR device and the commercial PALS system in the population and a 0.9678 in the intra-individual correlation. The bias observed could be due to interferences. Six month stability assessment of the electrodes displayed a baseline drift of 0.00 ±0.01 indicating robust fabrication. Utilising the combination of nanoPANI electrodes and impedance analysis within the prototype sampling system established that this system had potential for further clinical testing.

5.5 References

[1] Timmer, B.H., et al., (2006), "Selective low concentration ammonia sensing in a microfluidic lab-on-a-chip", *IEEE Sensors Journal,* Vol.6 (3), pp. 829-835.

[2] Smith, D.and Spanel, P., (2010), "Selected ion flow tube mass spectrometry, SIFT-MS; new horizons in real time air and breath analysis", *Spectroscopy Europe,* Vol.22 (4), pp. 21-24.

[3] Melker, R.J., et al., (2007), "System and method for monitoring health using exhaled breath", FL/U.S.A. Patent No. US 2007/0167.

[4] Boga, R.B.and MacDonald, J.G., (2005), "Method and device for detecting ammonia odors and helicobacter pylori urease infection", SC, U.S.A. Patent No. US 2005/0084977 A1.

[5] Suslick, K.S., et al., (2005), "Method and apparatus for detecting ammonia from exhaled breath", NJ/U.S.A. Patent No. US 2005/0171449.

[6] Hamilton, L.H., (1990), "Noninvasive diagnosis of gastritis and duodenitis", Wis/U.S.A. Patent No. 4,947,861.

[7] Baghdassarian, O., (2003), "Alveolar breath collection device and method", U.S.A. Patent No. US 6,582,376.

[8] Dolch, M.E., et al., (2008), "Molecular breath-gas analysis by online mass spectrometry in mechanically ventilated patients: a new software-based method of CO_2-controlled alveolar gas monitoring", *Journal of Breath Research,* Vol.2 pp. 037010.

[9] Wang, J., et al., (2004), "Electrochemically fabricated polyaniline nanoframework electrode junctions that function as resistive sensors", *Nano Letters,* Vol.4 (9), pp. 1693-1697.

[10] Olthuis, W., Van Uitert, I.and van den berg, A., (2008), "Device for measuring the ammonia content in a gas mixture", U.S.A. Patent No. WO 2008/056985.

[11] Timmer, B., et al., (2002), "Optimization of an electrolyte conductivity detector for measuring low ion concentrations", *Lab Chip,* Vol.2 pp. 121-124.

[12] Walters, J.A.E., et al., (2006), "Stability of the EasyOne ultrasonic spirometer for use in general practice", *Respirology,* Vol.11 pp. 306-310.

[13] Spirometry consumables, Intermedical (UK) Limited, [online], http://www.intermedical.co.uk/products/Lung+Function/Spirometry+Consumables (Accessed February 24, 2012).

[14] Karyakin, A.A., Karyakina, E.E.and Gorton, L., (1998), "The electrocatalytic activity of Prussian blue in hydrogen peroxide reduction studied using a wall-jet electrode with continuous flow", *Journal of Electroanalytical Chemistry,* Vol.456 pp. 97-104.

[15] Sengupta, A., et al., (1998), "Large-scale application of membrane contactors for gas transfer from or to ultrapure water", *Separation and purification technology,* Vol.14 (1), pp. 189-200.

[16] Zheng, J., et al., (2005), "Shell side mass transfer in a transverse flow hollow fiber membrane contactor", *Journal of membrane science,* Vol.261 (1), pp. 114-120.

[17] Ryan, D.F.,and Williams, A.N., (1975), "Alveolar gas trap and method of use", U.S.A. Patent No. 3,858,.

[18] Delente, J.J., (1993), "Apparatus and method for collecting human breath samples", U.S.A. Patent No. 5,211,.

[19] Chen, Z.and Adams, M.A., (1998), "A metallic cobalt electrode for the indirect potentiometric determination of calcium and magnesium in natural waters using flow injection analysis", *Talanta,* Vol.47 pp. 779-786.

[20] Ringel, E., (2008), "Pulmonary Diagnostic Testing", in *D.K. Onion, ed., The Little Black Book of Pulmonary Medicine,* (1st ed.), Jones and Bartlett Publishers, LLC, MA, U.S.A., pp. 82.

[21] Sherwood, L., (2010)*, Human physiology: From cells to systems,* , Yolanda Cossio,.

[22] Amano, A., et al., (2002), "Monitoring Ammonia to Assess Halitosis", *Oral Surgery Oral Medicine Oral Pathology,* Vol.94 (6), pp. 692-696.

[23] Smith, D., et al., (2008), "A Selected Ion Flow Tube Mass Spectrometry Study of Ammonia in Mouth- and Nose- Exhaled Breath and in the Oral Cavity", *Rapid Communications in Mass Spectrometry,* Vol.22 (6), pp. 783-789.

[24] Murnick, J.G.and Cronenberg, R.A., (1994), "Breath collection devices", U.S.A. Patent No. 5,361,.

[25] Draman, S.F.S., Daik, R.and Musa, A., (2009), "Synthesis and fluorescence spectroscopy of sulphonic acid-doped polyaniline when exposed to oxygen gas", *International Journal of Chemical and Biological Engineering,* Vol.2 (3), pp. 112-119.

[26] Menon, E.S., (205), "General Flow Equation", in *C. Carelli andM. Hecht, eds., Gas Pipeline Hydraulics,* (1st ed.), 1, CRC Press, FL, U.S.A., pp. 33-35.

[27] Schwankl, L. andPrichard, T.(1999), "Delivery Pipeline", *in Drip Irrigation in the Home Landscape,* (1st ed.), 1, ANR Publications, CA, U.S.A., pp. 17.

[28] Post, S., (2012), "Energy loss due to friction", in *T. Sliter, ed., Applied and computational fluid mechanics,* (1st ed.), 1, Jones and Bartlett Learning, MA, U.S.A., pp. 212-213.

[29] Kukla, A.L., Shirshov, Y.M.and Piletsky, S.A., (1996), "Ammonia sensors based on sensitive polyaniline films", *Sensors and Actuators B,* Vol.37 pp. 135-140.

[30] Trchova, M., et al., (2004), "FTIR spectroscopic and conductivity study of the thermal degradation of polyaniline films", *Polymer degradation and stability,* Vol.86 (1), pp. 179-185.

[31] Prasad, G.K., et al., (2005), "Ammonia sensing characteristics of thin film based on polyelectrolyte templated polyaniline", *Sensors and Actuators B,* Vol.106 pp. 626-631.

[32] Jin, Z., Su, Y.and Duan, Y., (2001), "Development of a polyaniline-based optical ammonia sensor", *Sensors and Actuators B,* Vol.72 pp. 75-79.

[33] Hong, K.H., Oh, K.W.and Kang, T.J., (2003), "Polyaniline-nylon 6 composite fabric for ammonia gas sensor", *Journal of Applied Polymer Science,* Vol.92 pp. 37-42.

[34] Timmer, B., Olthuis, W.and van den Berg, A., (2004), "Sampling small volumes of ambient ammonia using a miniaturised gas sampler", *Lab Chip,* Vol.4 pp. 252-255.

[35] Timmer, B.H., et al., (2004), "Miniaturized Measurement System for Ammonia in Air", *Analytica Chimica Acta,* Vol.507 (1), pp. 137-143.

[36] Aguilar, A.D., et al., (2008), "A Breath Ammonia Sensor Based on Conducting Polymer Nanojunctions", *IEEE Sensors Journal,* Vol.8 (3), pp. 269-273.

[37] Gouma, P., et al., (2010), "Nanosensor and breath analyser for ammonia detection in exhaled human breath", *IEEE Sensors Journal,* Vol.10 (1), pp. 49-53.

CHAPTER 6

CLINICAL EVALUATION OF AmBeR IN A HAEMODIALYSIS PATIENT COHORT

6.1 Introduction

Throughout the world, national renal registries provide reports conveying the statistics of patients in need of treatment for kidney failure. The United States Renal Data System (USRDS) has recorded the prevalence of end stage renal disease for approximately 40 countries dating as far back as 1998 [1]. The trends observed by the USRDS show that the rate of prevalence has slowed down in some countries while others continue to remain stable or increase. Countries which have registered patient numbers above 10,000 (per million) since 1998 include Australia, Canada, Japan, Taiwan, and the United States. As of 2009, the number in Australia has increased by 57%, in Canada by 53%, in Japan by 66%, in Taiwan by 48%, and in the United States by 62% [1]. The causes of renal failure vary from person to person where conditions could arise from medical, surgical, traumatic, obstructive, or obstetric issues [2]. However, the main cause is acute tubular necrosis, which is responsible for approximately 80% of cases related to renal failure [3]. With this condition, the renal tubular epithelial cells use extremely large amounts of energy to process glomerular filtrate which results in the cells undergoing necrosis [4].

The current treatment for kidney failure is haemodialysis. Even though haemodialysis machines have become more compact and simple since the 1960s, this is a therapy that is still both complicated and inconvenient for those involved [5]. In haemodialysis, blood flows out of the body by way of an arterial access point and into a dialyser. Within the dialyser are semi-permeable membranes upon which blood and dialysate flow counter-currently. The blood consists of an excess of metabolic wastes and electrolytes, and the dialysate contains an electrolyte composition typical of normal blood which is closely matched to the particular composition of the individual patient [6]. Equilibration of these electrolytes takes place by their diffusion across the semi-permeable membrane from a higher concentration to a lower concentration. Metabolic wastes (e.g. urea and creatinine) and excess water also pass from the blood and into the dialysate through the membrane via osmotic and hydrostatic pressures thereby decreasing blood concentrations and removing waste outside of the body [6]. The flow of dialysate maintains the concentration of these species at a level close to zero on the dialyser side, so maintaining the maximum concentration gradient and most efficient removal of wastes from the blood. Haemodialysis patients, on average, undergo treatment three days a week for a period of approximately four hours to remove excess fluids, minerals, and wastes from the blood [7]. The

effectiveness of their dialysis is determined by the urea reduction ratio (URR), reduction of creatinine, and / or calculation of clearance (Kt/V) [8]. Use of the URR gives the percentage of urea cleared from the blood during dialysis by using the calculation:

$$(\text{pre-dialysis urea} - \text{post-dialysis urea}) / \text{pre-dialysis urea}) * 100 \quad \textbf{(1)}$$

where the concentration of urea is in mmol/L. A URR of at least 65% is sought during these sessions. However, the actual reduction achieved may vary each time [9]. Creatinine is a waste product generated from muscle metabolism that is cleared from the blood by the kidneys and which also acts as a good indicator of renal function [10]. Kt/V is a unitless ratio resulting from the amount of blood cleared of urea (K*t) divided by the urea distribution volume (V). In this case, K is measured in units of L/hour, t is hours, and V is approximately the volume (litres) equivalent to the total body water [8]. Monitoring of clearance usually only takes place once a month [9]. Hence, the result is a cumulative one, and the results per individual dialysis session are often unknown [7].

Since its creation in 1976, continuous ambulatory peritoneal dialysis (CAPD) has developed as an alternative to haemodialysis which has allowed patients to remove wastes and fluids from their blood while at home rather than at a clinic [11]. The process works by allowing dialysate to enter from the outside of the body through the peritoneum of the abdomen via a catheter. The peritoneum is utilised as the semi-permeable membrane across which blood electrolytes and metabolic wastes diffuse [6]. The dialysate fluid is retained in the body for approximately 4 to 5 hours with each session and can be repeated up to five times in a day [12].

Both haemodialysis and CAPD are technologies that could benefit from the use of a real-time, point-of-care monitoring device that was capable of indicating reductions in blood nitrogen levels. By having a portable device that utilises the non-invasive aspects of breath, the patient and clinicians would have a convenient way of determining end points or efficacy in every dialysis session [13]. It could also reduce the need for blood testing. It has been established in previous literature that patients with renal dysfunction have higher concentrations of ammonia in their blood than do healthy individuals [14]. Often, an increase in blood ammonia levels is attributed to dysfunction in the liver's ability to convert ammonia into urea. However, in circumstances where the liver is functioning properly, but ammonia is still elevated, the condition is a result of uremic behaviour [15]. Briefly,

proteins and amino acids are naturally broken down throughout the body resulting in the generation of metabolic byproducts such as ammonia. Ammonia is then converted into urea by the liver and removed from the blood via the kidneys. However, if the kidneys can no longer remove urea from the blood, the normal dynamic between blood urea and ammonia is altered. An increased concentration of blood urea recycles back into the body (e.g. via the gastrointestinal tract) and is acted upon by the colonic bacteria and mucosal enzymes (e.g. urease) that previously broke down the proteins and amino acids resulting in production of more blood ammonia [15]. In circumstances where ammonia levels in the blood are higher than those found in the air, the ammonia can diffuse out of the blood and into the lungs [16]. It could, therefore, be predicted that, as byproducts of nitrogen metabolism (e.g. urea) are being removed from the patient during dialysis, the concentration of ammonia exhaled in the breath would decrease proportionally. As a consequence, breath ammonia could be a surrogate measurement for blood nitrogen levels.

In this chapter, haemodialysis patients were selected to assist with preliminary evaluation of the AmBeR system. This study assessed the correlation between the values of ammonia determined by the AmBeR system and PALS in breath samples from haemodialysis patients. In addition, observations of the correlation between breath ammonia levels in haemodialysis patients as obtained by AmBeR and other measures of blood nitrogen (e.g. urea and creatinine) and clearance (Kt/V) were made.

6.2 Materials and methods

6.2.1 Instrumentation

The ammonia sensor and AmBeR device described in Chapters 4 and 5 were used to quantify ammonia concentrations in patient breath samples. Impedance measurements of the AmBeR device were conducted using a model 660C Series Electrochemical Analyser Workstation (CH Instruments Inc., Austin, TX). Measurement of breath ammonia using photo-acoustic laser spectroscopy, PALS, (Nephrolux^{TM}, Pranalytica, USA) was used as the standard method for comparison with the AmBeR device. Renal profiles of nitrogen levels from urea and creatinine were measured from heparinised blood samples in the St. Vincent's University Hospital biochemistry laboratory. Tests of the blood urea and blood creatinine samples were processed using the Roche chemistry analyser (Modular P, Roche Diagnostics, Ireland).

6.2.2 Methods

A cohort of 20 haemodialysis patients were recruited following ethical approval at St. Vincent's University Hospital (Appendix 5). Patients were excluded if they had conditions related to cognitive impairment, or were clinically unstable. These patients typically undergo dialysis three days a week for a minimum of three hours each day. Informed consent was obtained from each patient. Breath ammonia, blood urea nitrogen, blood creatinine, gender, age, and BMI were recorded. For breath sampling, volunteers were asked to provide samples using the AmBeR device and PALS. Pre- and post-dialysis measurements using both devices (PALS and AmBeR) were performed on four patients while measurements with the AmBeR system alone were performed on the full patient cohort. Some patients were measured repeatedly on multiple visits. The sampling method for PALS was the same as that used with the healthy volunteers in Chapter 2, Section 2.2.2 and Chapter 5, Section 5.3.12, while the sampling method for the AmBeR device was the same as that used with healthy volunteers in Chapter 5, Section 5.3.12. Correlations were based on the equation determined in Fig. 5.15 which consisted of a slope and intercept of 0.00076 ppbv and -0.0354 ppbv, respectively, from calibrations with simulated breath. The data obtained for normal volunteers in Chapters 2 and 5 served as normal controls for comparison with the haemodialysis patient breath samples in this chapter. Blood urea concentrations were determined using urease and glutamate dehydrogenase (GIDH) in combination with α-ketoglutarate and nicotinamide adenine dinucleotide (NADH), with measurement of the resulting NAD^+ at 340 nm as follows [17]:

$$\text{Urea} + 2\,H_2O \xrightarrow{\text{Urease}} 2\,NH_4^+ + CO_3^{2-}$$

$$NH_4^+ + \alpha\text{-ketoglutarate} + \text{NADH} \xrightarrow{\text{GIDH}} \text{L-glutamate} + NAD^+ + H_2O$$

Blood creatinine concentrations were measured with a rate-blanked and compensated alkaline picrate colorimetric assay (11875418, Roche Diagnostics, Ireland) based on the Jaffe method [18]. Standardisations for urea and creatinine measurements in the chemistry analyser were performed using standard reference material 909b (SRM-909b), and isotope dilution mass spectrometry (IDMS). SRM-909b was developed by The National Institute of Standards and Technology (NIST) from lyophilised human serum to provide known concentrations of analytes (i.e. urea and creatinine) for standardisation purposes [19]. In

IDMS, a known concentration of an isotope of the analyte is added to the sample among the natural isotopes, whereby the changes in isotopic ratios are monitored via mass-spectrometry [20]. The changes in ratios are directly related to the concentration of analytes in the sample, and allow for quantification of the original analytes.

6.2.3 Methodology for statistical and numerical calculations

Assessment of relationships was performed using the Pearson correlation coefficient (r). Statistical significance (*p*) of that relationship was interpreted using SPSS statistical software package (IBM SPSS Statistics Version 19, IBM Co., U.S.A.) for Windows Vista, where the level of significance of the correlation was indicated as either <0.01 or <0.05 (two-tailed). Absolute breath ammonia reduction was the subtraction of post-dialysis ammonia from pre-dialysis ammonia, where the significance was found using a two-tailed paired t-test. Breath ammonia reduction ratios were calculated from the previously discussed equation 1. Calculations of Kt/V were performed using Finesse® Dialysis Data Acquisition and Management software with FinProDB (Fresenius Medical Care, Ireland). All data assessments were performed post-hoc.

6.3 Results and discussion

6.3.1 Correlation of breath ammonia concentrations between AmBeR and PALS

Eight breath ammonia samples were taken using PALS immediately followed by AmBeR. Four samples were pre-dialysis and four were post-dialysis (Table 6.1 and Fig. 6.1). This yielded a Pearson correlation coefficient of 0.97 ($p<0.01$). With a slope and intercept of 0.9287 ppbv and -39 ppbv, respectively there was a slight bias towards PALS. This could be an indication that PALS is sensitive to unknown metabolites of which AmBeR is not. Hence, further clinical analysis was performed with the AmBeR device.

Pre-dialysis measurements were comparable to the levels of 1,500 to 2,000 ppb stated in previous literature which are indicative of renal dysfunction and, hence, high blood nitrogen levels [9]. The post-dialysis measurements were similar to those observed from healthy volunteers in previous chapters (Chapter 2, Section 2.3.1, and Chapter 5, Section 5.3.12) as well as in previous literature which employed laser spectroscopy to assess the breath ammonia of seven haemodialysis patients, indicating that a range from

approximately 200 to 300 ppb should be expected [9]. These concentrations suggest that blood metabolite concentrations had returned to a healthy state over the period of dialysis.

Table 6.1 Pre-dialysis (n=4) and post-dialysis (n=3) breath ammonia concentrations obtained from four haemodialysis patients using both AmBeR and PALS (n=7). Negative values are indicated by (-).

Volunteer (number)	Dialysis (Pre / Post)	PALS (ppbv)	AmBeR (ppbv)
1	Pre	1,030	1,203
	Post	16	-
2	Pre	2,442	2,230
	Post	39	72
3	Pre	774	335
	Post	186	98
4	Pre	678	506
	Post	282	322

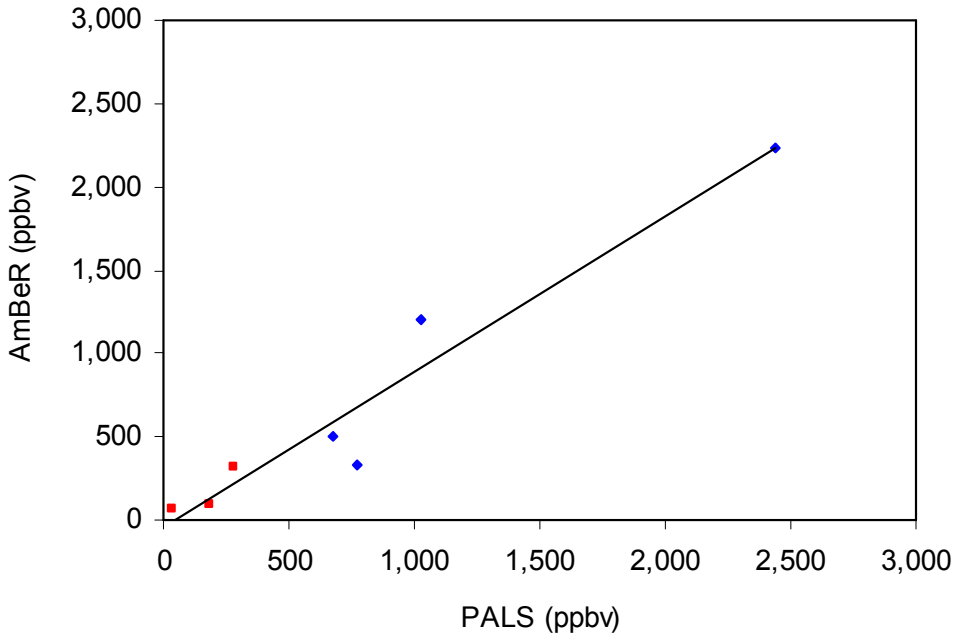

Figure 6.1 Pre-dialysis (blue diamond) and post-dialysis (red square) breath ammonia concentrations measured using AmBeR and PALS (n=7). The progression displayed a slope and intercept of 0.9287 ppbv and -39.73 ppbv, respectively (r=0.97, p<0.01).

6.3.2 Pre- and post-dialysis measurements of breath ammonia, blood urea nitrogen, and blood creatinine in the haemodialysis patient cohort

Breath ammonia and blood nitrogen levels for dialysis patients have been shown to vary over large ranges depending on their level of renal dysfunction. In other words, this bias in readings can be the result of variable blood metabolite concentrations resulting from differences among the individual patient kidney functions, and their ability to remove nitrogenous waste [21]. For example, patients who have higher renal function are able to produce larger volumes of urine, and do not require the level of restrictions (e.g. dietary, etc.) that anuric patients do. This would imply that a larger variety of metabolites could exist at any given time in those with higher renal function since they are permitted to consume a larger variety of substances. In addition, the lengths of dialysis sessions as well as the time between sessions are often inconsistent among those in the population. Fluid weight gain between the midweek intervals would be less than after the longer weekend interval adding inconsistencies to the metabolic output observed during that period [21].

The methods of analysis of breath samples have also been shown to have an impact on the concentrations of ammonia observed. For example, it has been shown that the use of Tedlar bags to collect breath samples could result in a 1.5 to 2-fold decrease in breath ammonia concentration by comparison to measurements obtained from direct breath interaction to the sensing element [14]. This is due to the fact that ammonia is highly soluble in water, and Tedlar bags have potential for build up of condensation from breath on the surface of the bags. With greater condensation, it is expected that ammonia concentrations would decrease due to absorption.

The breath ammonia levels measured using AmBeR along with blood urea nitrogen, blood creatinine, corresponding reduction ratios, and Kt/V values from all 51 volunteer samples are compiled in Table 6.2. The observed patient cohort (n=20) had a mean age of 63 years (ranged 36 to 91 years). There were ten female and ten male volunteers. The mean body mass index was 25.79 kg/m^2 (ranged 17.58 to 32.42 kg/m^2). Of these patients, 11 were willing to perform repeated correlative measurements of breath ammonia and blood nitrogen resulting in a complete population sample count of 51. Reductions in breath ammonia, blood urea nitrogen, and blood creatinine concentrations were observed in all patient samples following dialysis.

Table 6.2 Summary of pre- and post-dialysis breath ammonia concentrations as measured with the AmBeR device, blood urea nitrogen, blood creatinine, corresponding reduction ratios, and Kt/V for a cohort of 20 haemodialysis patients (n=51). Negative values are indicated by (-).

Volunteer (number)	Dialysis (Pre/Post)	Abs. NH_3 (ppbv)	Abs. Urea (mmol/L)	Abs. Cre (μmol/L)	NH_3 RR (%)	Urea RR (%)	Cre RR (%)	Kt/V (A.U.)
1	Pre	638	33.7	866				
	Post	98	9.3	279	84.64	72.40	67.78	1.19
2	Pre	624	18.7	863				
	Post	164	6.2	357	73.72	66.84	58.63	1.16
3	Pre	1,203	25.5	1,020				
	Post	-	6.3	337	-	75.29	66.96	1.36
4	Pre	2,230	29.0	1,137				
	Post	72	7.6	359	96.77	73.79	68.43	1.32
5	Pre	335	24.8	1,257				
	Post	98	7.2	507	70.75	70.97	59.67	1.29
6	Pre	835	21.5	683				
	Post	519	9.0	340	37.84	58.14	50.22	0.79
7	Pre	1,532	15.9	359				
	Post	611	5.8	154	60.12	63.52	57.10	0.95
8	Pre	506	24.3	551				
	Post	322	9.0	229	36.36	62.96	58.44	0.90
9	Pre	1,309	31.5	959				
	Post	164	8.0	311	87.47	74.60	67.57	1.50
10	Pre	282	21.1	392				
	Post	85	7.6	156	69.86	63.98	60.20	0.93
11	Pre	1,322	13.1	789				
	Post	730	5.4	387	44.78	58.78	50.95	0.91
12	Pre	1,690	19.0	995				
	Post	1,138	9.7	576	32.66	48.95	42.11	0.69
13	Pre	1,361	20.3	649				
	Post	-	4.6	206	-	77.34	68.26	1.09
14	Pre	164	12.3	470				
	Post	19	4.2	187	88.41	65.85	60.21	0.98
15	Pre	1,138	23.0	705				
	Post	480	8.0	299	57.82	65.22	57.59	1.09
16	Pre	743	21.3	630				
	Post	480	8.6	285	35.40	59.62	54.76	N/A
17	Pre	1,559	28.9	509				
	Post	572	10.1	230	63.31	65.05	54.81	1.01
18	Pre	940	23.2	586				
	Post	388	7.4	231	58.72	68.10	60.58	1.04
19	Pre	1,085	21.4	684				
	Post	98	5.4	225	90.97	74.77	67.11	1.25
20	Pre	440	30.2	920				
	Post	72	8.3	280	83.64	72.52	69.57	1.15
21	Pre	2,243	17.6	642				
	Post	190	6.8	276	91.53	61.36	57.01	0.94

Volunteer (number)	Dialysis (Pre/Post)	Abs. NH3 (ppbv)	Abs. Urea (mmol/L)	Abs. Cre (μmol/L)	NH3 RR (%)	Urea RR (%)	Cre RR (%)	Kt/V (A.U.)
22	Pre	1,401	35.0	1,420				
	Post	19	7.7	396	98.64	78.00	72.11	1.54
23	Pre	874	26.6	912				
	Post	480	7.7	323	45.08	71.05	64.58	1.36
24	Pre	664	30.8	1,470				
	Post	85	9.6	517	87.20	68.83	64.83	1.16
25	Pre	1,098	25.0	1,050				
	Post	177	6.2	309	83.88	75.20	70.57	1.51
26	Pre	967	19.9	545				
	Post	-	4.3	161	-	78.39	70.46	1.46
27	Pre	874	22.4	751				
	Post	414	7.2	284	52.63	67.86	62.18	1.02
28	Pre	1,072	19.8	623				
	Post	32	4.7	206	97.01	76.26	66.93	1.44
29	Pre	901	19.2	710				
	Post	72	4.6	224	92.01	76.04	68.45	1.53
30	Pre	993	21.3	1,079				
	Post	440	4.6	354	55.69	78.40	67.19	1.48
31	Pre	677	18.1	593				
	Post	282	5.2	212	58.35	71.27	64.25	1.13
32	Pre	1,217	16.4	597				
	Post	45	5.1	248	96.30	68.90	58.46	1.13
33	Pre	940	18.7	554				
	Post	85	4.5	175	90.96	75.94	68.41	1.39
34	Pre	1,282	14.7	563				
	Post	217	5.1	240	83.07	65.31	57.37	1.02
35	Pre	2,164	25.6	1,150				
	Post	85	4.6	293	96.07	82.03	74.52	1.72
36	Pre	493	8.8	325				
	Post	19	2.5	133	96.15	71.59	59.08	1.20
37	Pre	690	16.3	536				
	Post	32	3.9	165	95.36	76.07	69.22	1.37
38	Pre	559	23.2	815				
	Post	138	6.2	253	75.31	73.28	68.96	1.18
39	Pre	282	23.2	1,151				
	Post	32	6.7	415	88.65	71.12	63.94	1.31
40	Pre	611	20.2	843				
	Post	164	5.2	291	73.16	74.26	65.48	1.46
41	Pre	388	32.9	786				
	Post	-	7.6	226	-	76.90	71.25	1.39
42	Pre	598	23.9	969				
	Post	32	4.4	302	94.65	81.59	68.83	1.62
43	Pre	835	20.2	823				
	Post	480	4.8	249	42.51	76.24	69.74	1.51
44	Pre	1,217	15.6	535				
	Post	151	5.3	231	87.59	66.03	56.82	1.06
45	Pre	690	14.2	475				
	Post	-	3.5	157	-	75.35	66.95	1.36
46	Pre	295	31.0	847				
	Post	59	7.4	240	80.00	76.13	71.66	1.31

Volunteer (number)	Dialysis (Pre/Post)	Abs. NH3 (ppbv)	Abs. Urea (mmol/L)	Abs. Cre (μmol/L)	NH3 RR (%)	Urea RR (%)	Cre RR (%)	Kt/V (A.U.)
47	Pre	756	20.0	504				
	Post	85	5.4	179	88.76	73.00	64.48	1.32
48	Pre	717	23.4	750				
	Post	164	5.6	210	77.13	76.07	72.00	1.28
49	Pre	677	15.9	623				
	Post	59	4.6	213	91.29	71.07	65.81	1.25
50	Pre	611	25.0	754				
	Post	72	8.1	271	88.22	67.60	64.06	1.08
51	Pre	690	13.8	556				
	Post	-	2.8	149	-	79.71	73.20	1.36

6.3.3 Pre- and post-dialysis measurements of breath ammonia in the haemodialysis patient cohort

Breath ammonia measurements had a pre-dialysis population mean of 930 ±483 ppbv (ranged 164 to 2,243 ppbv, n=51) and a post-dialysis mean of 227 ±236 ppbv (ranged 19 to 1,138 ppbv, n=45). Fig. 6.2 represents the difference between pre- and post-dialysis breath ammonia measurements demonstrating the link between blood and breath metabolites. SPSS analysis of the correlation between the two-data sets generated a two-tailed $p<0.05$ displaying a high level of significance in the difference between pre- and post-dialysis measurements.

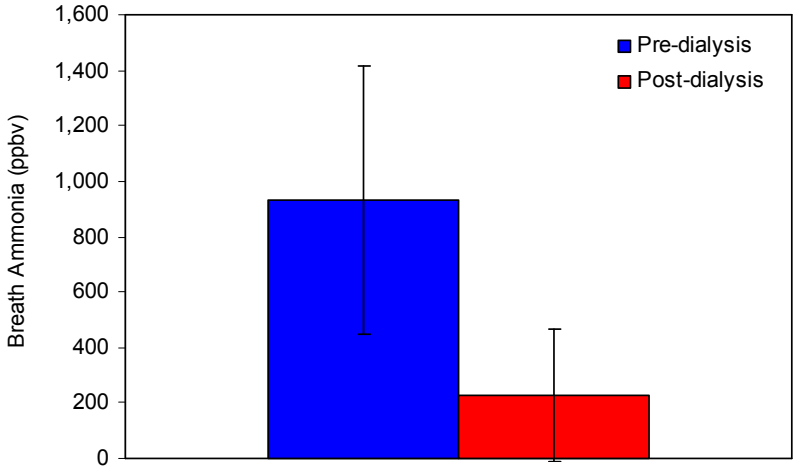

Figure 6.2 The mean pre-dialysis (930 ±483 ppbv, n=51) and post-dialysis (227 ±236 ppbv, n=45) breath ammonia measurements in the haemodialysis population ($p<0.05$) as determined by the AmBeR system.

These concentration ranges were comparable with the results obtained in previous literature. For example, Narasiman *et al* conducted a study on a cohort of haemodialysis patients (n=7) using laser spectroscopy whereby breaths were sampled directly rather than pre-collected [9]. The concentration range measured among those patients showed a decrease from approximately 2,000 to 200 ppb following haemodialysis. Furthermore, as in Section 6.3.1, the post-dialysis breath ammonia concentrations were similar to the levels observed in healthy volunteers (Chapter 2, Section 2.3.1 and Chapter 5, Section 5.3.12). However, as mentioned earlier, different studies have indicated a wide range of potential concentrations. Endre *et al* observed oral breath ammonia concentrations from two cohorts of haemodialysis patients as measured using SIFT-MS [13]. Group A (n=15) were from a hospital unit, and group B (n=5) were undergoing home dialysis. Samples from group A were pre-collected in Tedlar bags and generated breath ammonia concentrations from 370 to 9,210 ppb while group B measurements were collected by way of direct breath exhalations from the patients through a mouthpiece into the heated inlet of the SIFT-MS resulting in breath ammonia concentrations from 270 to 10,900 ppb. Group B displayed a slightly higher concentration range which could be either attributed to the bias in population sizes, or in the use of Tedlar bags by group A. Davies *et al* also used SIFT-MS with a cohort of 26 CAPD patients [14]. Breath samples were either collected in volumes of 3 litres in Tedlar bags, or directly into the device. A concentration range from 820 to 14,700 ppb was observed for this population.

6.3.4 Pre- and post-dialysis measurements of blood urea nitrogen in the haemodialysis patient cohort

Both breath ammonia and blood urea nitrogen concentrations were found to decrease from pre- to post-dialysis. Blood urea nitrogen pre-dialysis had a mean of 22 ±6 mmol/L (range of 9 to 35 mmol/L), and reduced to a mean of 6 ±2 mmol/L (range of 3 to 10 mmol/L) in post-dialysis measurements (Fig. 6.3). Analysis of this difference using a paired *t*-test displayed a t-statistic of 23.00 (two-tailed, $p<0.01$). Literature has suggested that blood urea nitrogen concentrations indicative of renal failure are approximately 10 mmol/L [22] to 13.2 mmol/L [23]. These values which indicate the boundary between healthy and non-healthy concentrations coincide with what was found in the patients in this work. The observed patient group had a pre-dialysis mean that was higher than these indicated references, while the post-dialysis mean was well within the indicated healthy range.

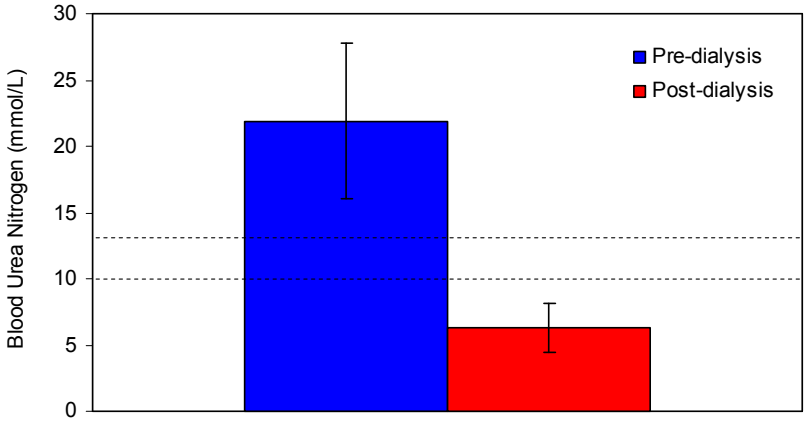

Figure 6.3 The mean pre-dialysis (22 ±6 mmol/L) and post-dialysis (6 ±2 mmol/L) blood urea nitrogen measurements in the haemodialysis population (p<0.01, n=51). Dashed lines designate the approximate range (10 to 13.2 mmol/L) indicative of renal failure [22, 23].

The relationship between the absolute concentrations of breath ammonia and blood urea nitrogen was studied. This was found to have a Pearson correlation coefficient of 0.61 (p<0.01, n=96) (Fig. 6.4). The correlation r=0.61 is not very strong, but the strength of significance, p<0.01, among the measurements demonstrates enough potential for continued assessment in clinical applications to take place. In comparison to previous literature, the work by Davies *et al* which used SIFT-MS with 26 CAPD patients, displayed a correlation between breath ammonia and blood urea nitrogen of 0.49 (p<0.01) [14]. This lower correlation could be due to a difference between CAPD and haemodialysis techniques. However, a review by Gokal *et al* has stated that variations among these techniques are minimal, and therefore, unlikely to be the cause of the difference [24]. Another more likely possibility is that population size has affected the statistical assessment since the cohort observed by Davies *et al* was smaller.

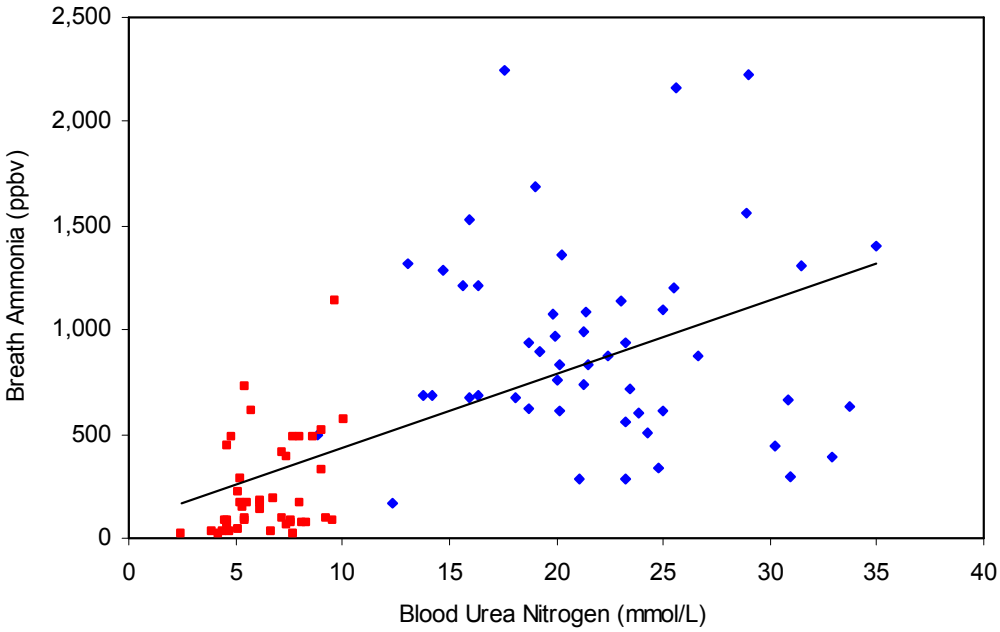

Figure 6.4 Pre-dialysis (blue diamond) and post-dialysis (red square) of absolute breath ammonia and blood urea nitrogen concentrations (n=96). The regression displayed a slope and intercept of 35.57 ppbv and 78.56 ppbv, respectively, with r=0.61 (p <0.01).

6.3.5 Pre- and post-dialysis measurements of blood creatinine in the haemodialysis patient cohort

Pre-dialysis measurements of blood creatinine had a mean of 764 ±261 μmol/L (ranged from 325 to 1,470 μmol/L) and a post-dialysis concentration mean of 302 ±96 μmol/L (ranged from 133 to 576 μmol/L) (Fig. 6.5). Blood creatinine concentrations indicative of renal failure range from approximately 141 μmol/L [23] to 250 μmol/L [22]. As with the blood urea nitrogen measurements, the observed patients had pre-dialysis blood creatinine means that were higher than the values indicated for renal failure. However, the post-dialysis mean was marginally above the cut-off for normal creatinine. Analysis of these two means using a paired t-test yielded a t-statistic of 18.58, and a two-tailed p<0.01 demonstrating a significant difference between the pre- and post-dialysis creatinine levels.

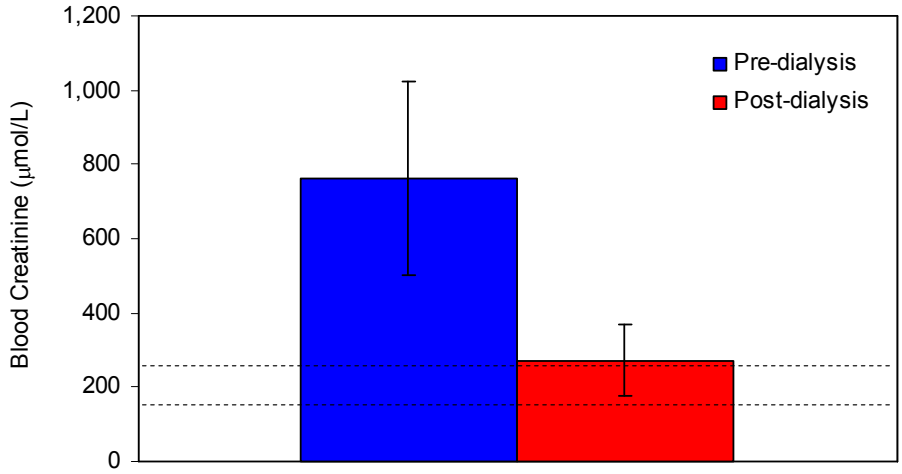

Figure 6.5 The mean pre-dialysis (764 ±261 µmol/L) and post-dialysis (302 ±96 µmol/L) blood creatinine measurements in the haemodialysis population (p<0.01, n=51). Dashed lines designate the approximate range (141 to 250 µmol/L) indicative of renal failure [22, 23].

The relationship between the absolute concentrations of breath ammonia and blood creatinine had a Pearson correlation coefficient of 0.60 (p<0.01, n=96) (Fig. 6.6) which was very similar to the 0.61 value previously determined with blood urea nitrogen. It was stated by Ishida *et al* that the lower correlations found with creatinine could be directly related to differences in muscle mass among individuals in the population since creatinine is a byproduct from muscle metabolism. A bias would exist where those with more muscle would generate higher amounts of creatinine even if other factors (e.g. weight, etc.) were the same [7]. Furthermore, in the work of Davies *et al*, the cohort of 26 CAPD patients generated a poor and statistically insignificant correlation of 0.22 (p>0.1) via SIFT-MS which was lower than the 0.49 (p<0.01) observed with blood urea [14]. In addition, the data shown in Fig. 6.6 suggests a near comparable correlation between breath and urea and creatinine. As mentioned previously, the differences between this data and that found in previous literature could be due to the statistical variations in accordance with cohort size as SIFT-MS should not suffer from the introduction of sampling errors.

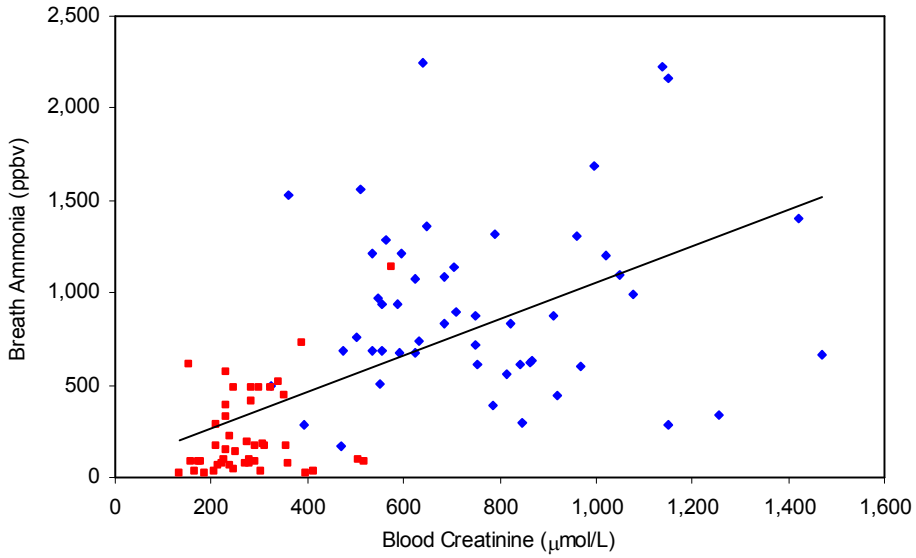

Figure 6.6 Pre-dialysis (blue diamond) and post-dialysis (red square) of breath ammonia and blood creatinine levels using the AmBeR device (n=96). The progression displayed a slope and intercept of 0.9895 ppbv and 68.70 ppbv, respectively, with r=0.60 (p<0.01).

6.3.6 Comparison of pre- and post-dialysis measurements of blood urea and blood creatinine in the haemodialysis patient cohort

The laboratory results for absolute blood urea and creatinine were compared with one another to see if there was a relationship between these two blood nitrogen species (Fig. 6.7). This yielded a Pearson correlation of 0.88 (p<0.01) demonstrating a strong relationship. These two species have been examined in previous literature, and are well known to have a good correlation. For example, Davies *et al* found a correlation of 0.63 (p<0.01) between blood urea and creatinine in 26 CAPD patients via SIFT-MS [14], and Lesaffer *et al* employed high performance liquid chromatography (HPLC) analysis yielding a correlation of 0.51 (p<0.01) between the removed blood urea and creatinine of 10 haemodialysis patients [25]. Both correlations were lower than that found in this work, again potentially as a result of the difference in sample sizes. Nonetheless, the relationship was evident in all cases. A slight bias existed towards creatinine as indicated by the intercept of 83.56 μmol/L.

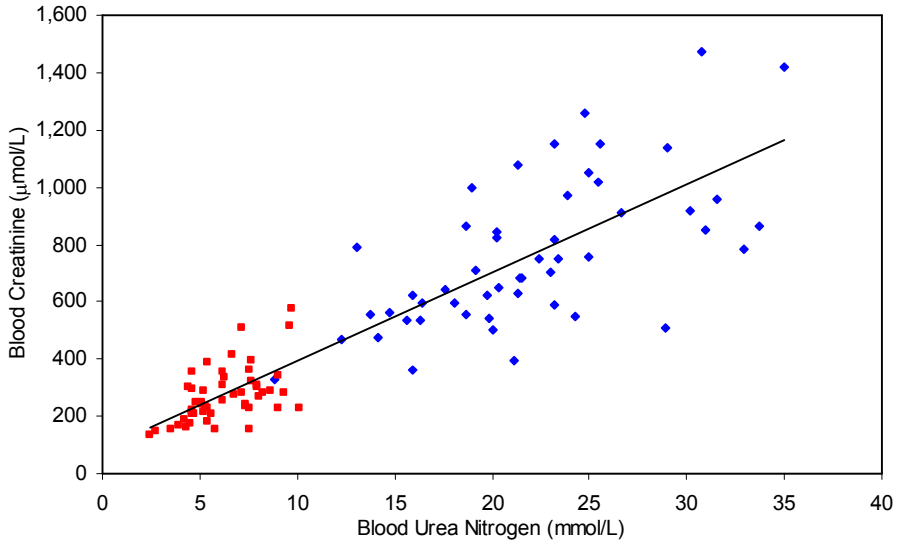

Figure 6.7 Pre-dialysis (blue diamond) and post-dialysis (red square) of blood creatinine and blood urea nitrogen concentrations (n=102). The regression displayed a slope and intercept of 30.82 µmol/L^{-1} and 83.56, respectively, r=0.88 (p<0.01).

6.3.7 Correlation of breath ammonia reduction ratios with blood urea and blood creatinine reduction ratios in the haemodialysis patient population

The population data established in Figs. 6.4 and 6.6 did not yield very strong correlations between breath ammonia and either blood urea nitrogen or creatinine. It has already been discussed that additional patient-specific variables may make it difficult to establish a strong population correlation. Thus, other approaches were investigated to see whether better relationships could be established between breath ammonia and blood nitrogen levels that could eliminate such subject-specific variables. One approach to this was to investigate reduction ratios in breath ammonia, urea, and creatinine as such ratios only take into account the overall change in levels pre- and post-dialysis, rather than the absolute concentrations. However, the relationship between the reduction ratios from pre- to post-dialysis breath ammonia and blood urea concentrations yielded a Pearson correlation coefficient of 0.60 (p<0.01, n=45) (Fig. 6.8). This value was closely in line with those determined for the relationship between absolute concentrations. This data again suggested that there was a link between blood urea nitrogen levels and breath ammonia levels, but that the correlation could be masked by additional, patient-specific variables such as the

previously mentioned differences in renal function, body mass, and perhaps simultaneous influences such as oral ammonia (e.g. bacteria) [21, 26].

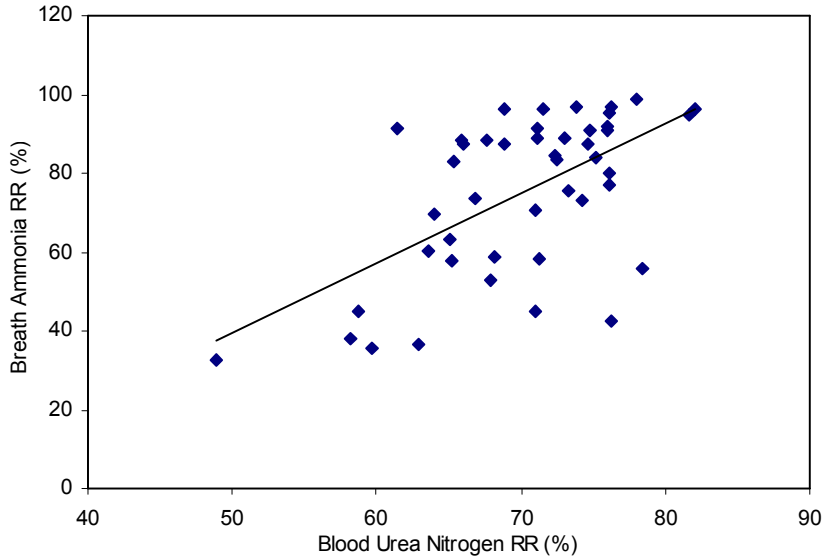

Figure 6.8 Relationship of breath ammonia and blood urea reduction ratios for the haemodialysis patient population (r=0.60, p<0.01, n=45).

The relationship between the reduction ratios from pre- to post-dialysis breath ammonia and blood creatinine concentrations had a Pearson correlation coefficient of 0.55 (p<0.01) (Fig. 6.9). This was a slightly lower correlation in comparison to the previously observed urea reduction ratio (r=0.60). No indications of relationships with creatinine reduction ratios could be found in previous literature.

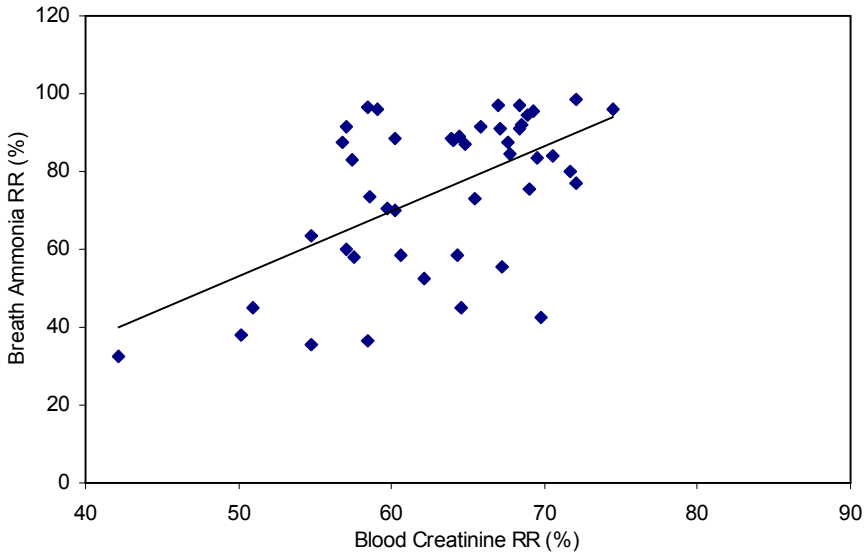

Figure 6.9 Relationship of breath ammonia and blood creatinine reduction ratios for the haemodialysis patient population (r=0.55, p<0.01, n=45).

The relationship between the reduction ratios from pre- to post-dialysis blood creatinine and urea concentrations had a Pearson correlation coefficient of 0.94 (p<0.01) (Fig.6.10) showing the strong link between the blood nitrogen species and the consistency from one patient to the next. However, it is worth noting that the range observed is indicative of individual metabolic behaviour. In other words, each patient has a reduction ratio that was unique to themselves and varied from levels in excess of 85% to levels lower than 45%. Narasimhan *et al* also showed that the reductions could potentially be different from person to person [9]. While observing four haemodialysis patients, Narasimhan *et al* found a significant bias among the blood samples. Pre- to post-dialysis measurements showed a 15% greater reduction in the blood urea for three of the four patients suggesting that differences exist in how the other patient's body processed the nitrogenous compounds [9], and further demonstrated the need for a real-time monitoring technique to assist with such variation.

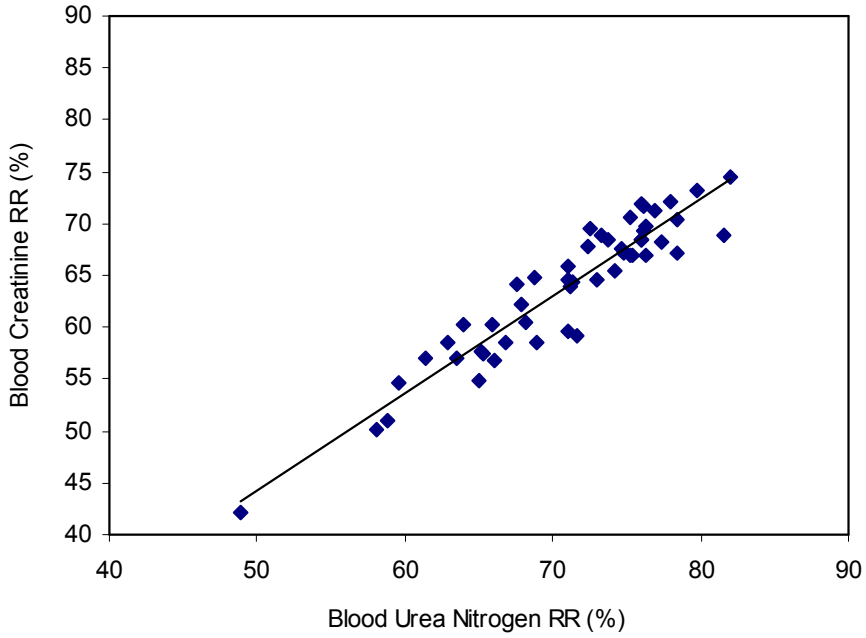

Figure 6.10 Relationship of blood creatinine reduction ratios and blood urea nitrogen reduction ratios for the haemodialysis patient population (r=0.94, p<0.01, n=51).

As was discussed earlier, a decrease of 65% in the URR is typically sought to ensure adequate dialysis. Here, this equated to a concomitant breath ammonia reduction of approximately 63% of the pre-dialysis value. If using 65% reduction in creatinine, this would equate to a reduction in breath ammonia of approximately 80%. This may suggest that urea and creatinine levels diminish at different rates than breath ammonia levels where urea is faster and creatinine is potentially slower. However, previous research by Lévesque *et al* demonstrated through case studies of haemodialysis patients (n=2) that blood metabolites were removed at similar rates [27, 28]. Blood-side clearances such as these are calculated using a standard method which is detailed by Leypoldt *et al* [29]. To summarise, concentrations (e.g. mmol/L or μmol/L) of the nitrogenous compounds are monitored at the arterial blood inlet, the venous blood outlet, and the dialysate outlet. Comparison of the blood-side with dialysate-side clearances (blood minus dialysate) is then used to calculate the overall clearance flow rate (ml/min) of the particular nitrogenous compounds [29, 30]. Observations in one patient took place at four hourly increments of a four hour dialysis session, and resulted in averaged clearance rates of approximately 261 ml/min for ammonia, 263 ml/min for urea, and 200 ml/min for creatinine [27]. The study was repeated in a second haemodialysis patient and clearance rates were found to be approximately 290

ml/min for ammonia, 352 ml/min for urea, and 180 ml/min for creatinine [28]. The urea in those studies was cleared from the blood faster than ammonia, but creatinine was cleared at a slower rate. Urea was cleared from the blood 2 ml/min faster than ammonia in the first patient and 62 ml/min faster in the second patient. However, creatinine was cleared from the blood 61 ml/min slower than ammonia in the first patient and 110 ml/min slower in the second patient. Hence, with the diversity of the results, it is not likely that the dialysis clearance rate of nitrogenous compounds is initiating the difference between reductions in breath ammonia and both blood nitrogen species.

However, one potential reason is that urea and creatinine measurements come from samples which are taken directly from the source (i.e. blood) while the ammonia is sampled from an intermediate source (i.e. breath) which must abide by the rate of gas exchange via the lungs. This could cause a slight delay in the measurements from blood-to-breath whereby the complete ammonia load generated in the blood has not yet diffused into the alveolar air by the time measurements are taken. In other words, to exhale gaseous ammonia, the ammonia molecules in the blood which are flowing through the capillaries of lung alveoli must move from their position of higher concentration to that of lower concentration in the atmosphere. This makes it necessary for the partial pressure between the capillary blood and the alveolar air to initiate diffusion allowing ammonia molecules to bypass the tissue. This would occur more slowly than sampling directly from the blood as with urea and creatinine nitrogen giving the appearance of delayed ammonia clearance [31].

Another possible reason could be related to the rebound of nitrogenous compounds in the blood of patients after dialysis. Patients with elevated blood nitrogen levels have potential for rapid reaccumulation of ammonia in the blood upon cessation of dialysis which could give the appearance of less ammonia reduction via dialysis clearance as detected by way of the breath [32]. This is due to ongoing catabolism of nitrogenous compounds within the blood [33]. Kooman *et al* described the phenomenon of increased nitrogenous waste as being a result of one of three key factors [34]. First, within 0.25 to 0.33 min after dialysis, access recirculation could occur whereby dialysed blood from the venous line returns to the arterial line [35] causing a narrowing of blood vessel walls (vessel stenosis) [36]. Second, during the first minute or two after dialysis, cardiopulmonary recirculation takes place [34]. This is where the purified blood which is returning from the dialyser to the body is rapidly returned to the dialyser thereby reducing the efficiency of dialysis by reducing the

concentration of metabolites at the dialyser inlet [37]. Third, up to 30 and 60 minutes after dialysis, disequilibrium of the nitrogenous wastes throughout the body could exist due to the concentration gradients between intra- and extra-cellular spaces derived from resistance of cell membranes to transport of the nitrogenous wastes [34] whereby reaccumulation would arise from the intra-cellular space. Rajpoot *et al* described three examples of this in haemodialysis patients [38]. In their patient C, ammonia decreased from 639 to 150 μmol/l during dialysis with a rebound to 360 mmol/l measured over the six hours after dialysis. In their patient D, ammonia decreased from 650 to 270 μmol/l during dialysis followed by an increase to 389 μmol/l as measured over three hours. A follow up dialysis session of patient D was performed, and the ammonia concentration further decreased from 389 to 200 μmol/l during dialysis. This was followed by an ammonia rebound to 254 μmol/l as measured over the next seven hours. This rapid rebound of nitrogenous compounds in the blood could, therefore, result in a post-dialysis breath measurement consisting of higher blood ammonia levels than that which was measured during dialysis. This would result in the measurement of a smaller ammonia reduction from pre- to post-dialysis, and give the appearance that ammonia has a slower rate of clearance than other nitrogenous compounds.

6.3.8 Relationship between Kt/V and absolute breath ammonia reduction, breath ammonia reduction ratio, and blood urea nitrogen reduction ratios in the haemodialysis patient population

It has already been shown that population statistics of the correlation between breath ammonia and blood nitrogen levels was less than satisfactory. Attempts to compensate for patient-specific factors using reduction ratios did not improve this. Kt/V is a unitless ratio used to determine clearance rates of urea from blood during dialysis [39]. In this way, it takes into account individual differences in body fluid volume which can impact clearance rates and which might partly account for inter-individual variations. While current guidelines request a urea reduction ratio of 65% in haemodialysis, a Kt/V of at least 1.20 is sought [40]. However, due to potential rebound of nitrogenous compounds at the end of dialysis, this number could be overestimated by as much as 0.15 to 0.20 of the true value. To compensate, a calculation is often performed to equilibrate the Kt/V measurement, where 1.00 becomes the optimum value [40]. A higher Kt/V, indicative of higher dialysis efficiency, is well known to decrease mortality risks [41], and is therefore a key goal of

each dialysis session. As mentioned in Section 6.3.2, variations in the internal fluids among individuals in a haemodialysis population can result in a range of metabolite concentrations within. Thus, additional correlations were performed between Kt/V and absolute breath ammonia reduction, breath ammonia reduction ratio, and blood urea nitrogen reduction ratio to determine if variations in volume clearance rate might account for the variations seen in earlier correlations.

The correlation between the absolute breath ammonia reduction and Kt/V of 44 patient samples (only 44 of the 51 patient samples could be measured due to lack of post-dialysis breath ammonia measurements for 6 patients, and no haematocrit data for one patient) displayed a Pearson correlation coefficient of 0.25, and was not significant (p=0.102) (Fig. 6.11), indicating that use of Kt/V to correlate with absolute breath ammonia reduction would not be beneficial. In the case of the SIFT-MS data of Endre *et al* generated from their group B (n=5, home dialysis patients), this yielded a 0.34 (p<0.01) correlation between the change in breath ammonia during dialysis and Kt/V, which was significant [13]. The difference observed could again potentially be due to population size, but this is uncertain.

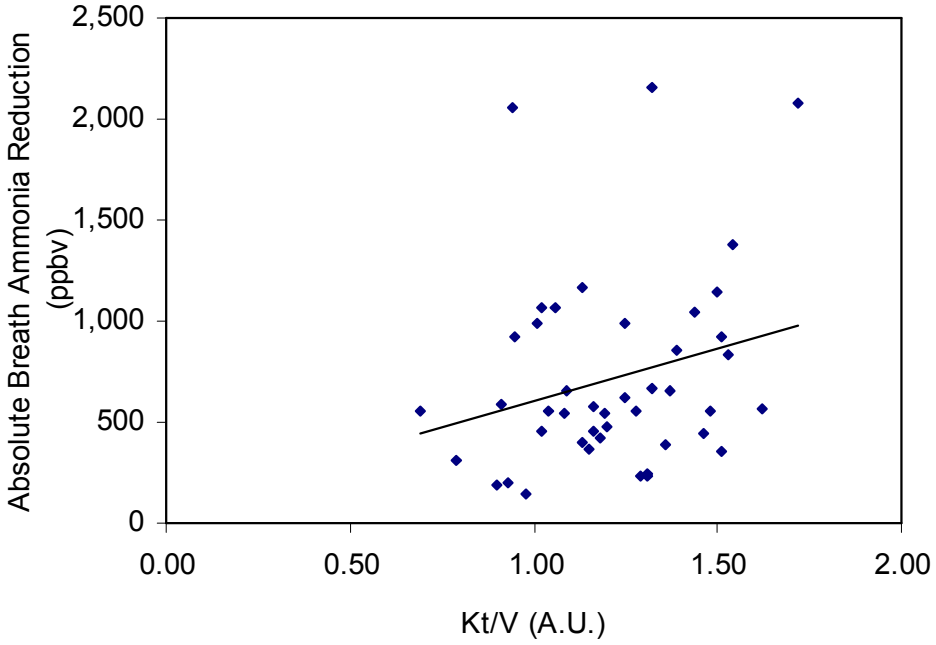

Figure 6.11 Relationship between absolute breath ammonia reduction and Kt/V for the haemodialysis patient population samples (r=0.25, p=0.102, n=44).

Breath ammonia reduction ratios of the 44 patient samples displayed a Pearson correlation of 0.50 (p<0.01) with Kt/V indicating a stronger relationship (Fig. 6.12). Endre *et al* also showed a slight increase in this relationship with a correlation of 0.38 (p<0.01) [13]. This makes sense since both breath ammonia reduction ratio and Kt/V consider the fraction of metabolites removed from the whole of a particular volume, while the absolute reduction shown earlier is just a difference calculated of the metabolites being removed during dialysis where volume is not taken into account.

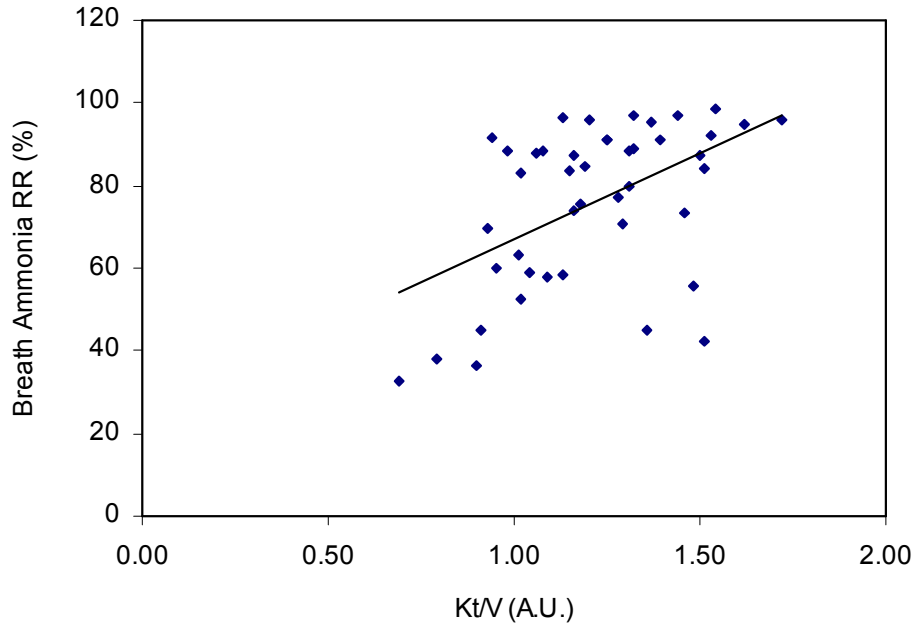

Figure 6.12 Relationship between breath ammonia reduction ratio and Kt/V for the haemodialysis patient population samples (r=0.50, p<0.01, n=44).

The relationship between Kt/V and blood urea reduction ratio yielded a Pearson correlation coefficient of 0.93 (p<0.01) (Fig. 6.13). This correlation was significantly higher than between the Kt/V and absolute breath ammonia reduction (r=0.25) and breath ammonia reduction ratio (r=0.50) indicating that use of Kt/V to correlate with blood urea reduction ratios would be useful. This further corroborates the fact that Kt/V is meant to yield measurements associated with the urea reduction ratio, and would be expected to demonstrate a significant correlation with that ratio [42].

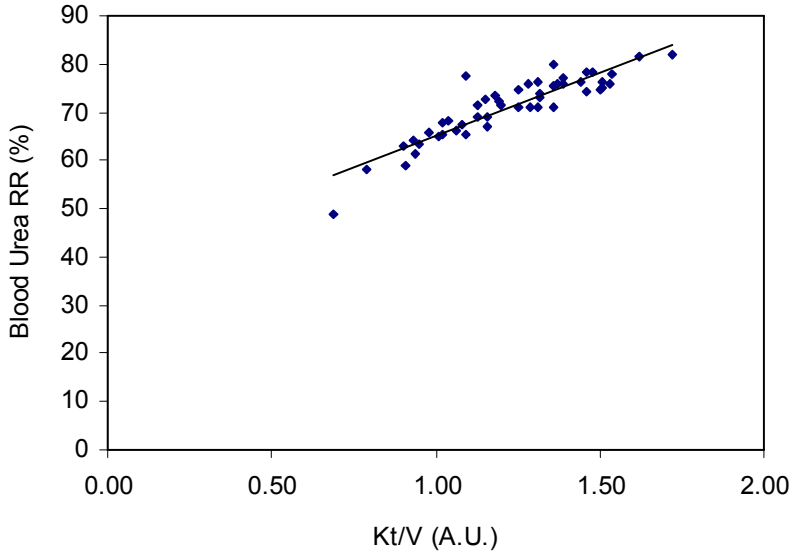

Figure 6.13 Relationship between blood urea nitrogen reduction ratio and Kt/V for the haemodialysis patient population samples (r=0.93, p<0.01, n=44).

6.3.9 Intra-individual correlations of breath ammonia and blood urea nitrogen levels

Thus far, any population-based correlations, using either absolute values or looking at changes and ratios did not yield strong correlations between breath ammonia and blood nitrogen levels. As a result, focus was switched to looking at the relationship between breath ammonia and blood nitrogen on a patient-by-patient basis. Several patients were willing to perform repeated correlative measurements of breath ammonia and blood nitrogen (Table 6.3).

Table 6.3 Summary of pre- and post-dialysis absolute breath ammonia concentrations (as measured with the AmBeR device), blood urea nitrogen, and blood creatinine for haemodialysis patients (n=11). Negative values are indicated by (-).

Volunteer (Number)	Dialysis (Pre/Post)	Absolute NH_3 (ppbv)	Absolute Urea (mmol/L)	Absolute Cre (µmol/L)
1	Pre	874	22.4	751
	Post	414	7.2	284
	Pre	690	16.3	536
	Post	32	3.9	165
2	Pre	1,098	25.0	1,050
	Post	190	6.2	309
	Pre	611	20.2	843
	Post	164	5.2	291

Volunteer (Number)	Dialysis (Pre/Post)	Absolute NH3 (ppbv)	Absolute Urea (mmol/L)	Absolute Cre (μmol/L)
3	Pre	1,203	25.5	1,020
	Post	-	6.3	337
	Pre	1,072	19.8	623
	Post	32	4.7	206
	Pre	861	23.9	969
	Post	32	4.4	302
4	Pre	335	24.8	1,257
	Post	98	7.2	507
	Pre	664	30.8	1,470
	Post	85	9.6	517
	Pre	282	23.2	1,151
	Post	32	6.7	415
5	Pre	2,230	29.0	1,137
	Post	72	7.6	359
	Pre	1,401	35.0	1,420
	Post	19	7.7	396
	Pre	2,164	25.6	1,150
	Post	85	4.6	293
6	Pre	835	21.5	683
	Post	519	9.0	340
	Pre	967	19.9	545
	Post	-	4.3	161
	Pre	559	23.2	815
	Post	138	6.2	253
	Pre	717	23.4	750
	Post	164	5.6	210
7	Pre	1,361	20.3	649
	Post	-	4.2	206
	Pre	1,085	21.4	684
	Post	98	5.4	225
	Pre	677	18.1	593
	Post	282	5.2	212
	Pre	940	18.7	554
	Post	85	4.5	175
8	Pre	545	40.5	970
	Post	59	10.1	293
	Pre	638	33.7	866
	Post	98	9.3	279
	Pre	440	30.2	920
	Post	72	8.3	280
	Pre	388	32.9	786
	Post	-	7.6	226
	Pre	295	31.0	847
	Post	59	7.4	240

Volunteer (Number)	Dialysis (Pre/Post)	Absolute NH3 (ppbv)	Absolute Urea (mmol/L)	Absolute Cre (μmol/L)
9	Pre	1,309	31.5	959
	Post	164	5.4	311
	Pre	874	26.6	912
	Post	480	7.7	323
	Pre	993	21.3	1,079
	Post	440	4.6	354
	Pre	835	20.2	823
	Post	480	4.8	249
	Pre	677	15.9	623
	Post	59	4.6	213
10	Pre	1,690	19.0	995
	Post	1,138	9.7	576
	Pre	2,243	17.6	642
	Post	190	6.8	276
	Pre	1,217	16.4	597
	Post	45	5.1	248
	Pre	1,282	14.7	563
	Post	217	5.1	240
	Pre	1,217	15.6	535
	Post	151	5.3	231
11	Pre	940	23.2	586
	Post	388	7.4	231
	Pre	901	19.2	710
	Post	72	4.6	224
	Pre	493	8.8	325
	Post	19	2.5	133
	Pre	690	14.2	475
	Post	-	3.5	157
	Pre	756	20.0	504
	Post	85	5.4	179

The relationship between the absolute concentrations of breath ammonia and blood urea nitrogen are shown in Fig. 6.14. It can be seen that the correlation between breath ammonia and blood urea nitrogen ranged from 0.82 to 0.96 with *p*-values of <0.01 and <0.05, indicating strong correlation and good statistical significance in all cases. The fact that the correlations for all intra-individual data were strong with good statistical significance suggests that the relationship between breath ammonia and blood urea levels remain reasonably consistent between dialysis sessions for a particular individual and so the correlation is not utterly dependent on the dynamics of a single dialysis event. It was also obvious that the relationship between breath ammonia and blood urea varied considerably from patient to patient as evidenced by the slopes (ranging from 15.70 to 122.59 ppbv).

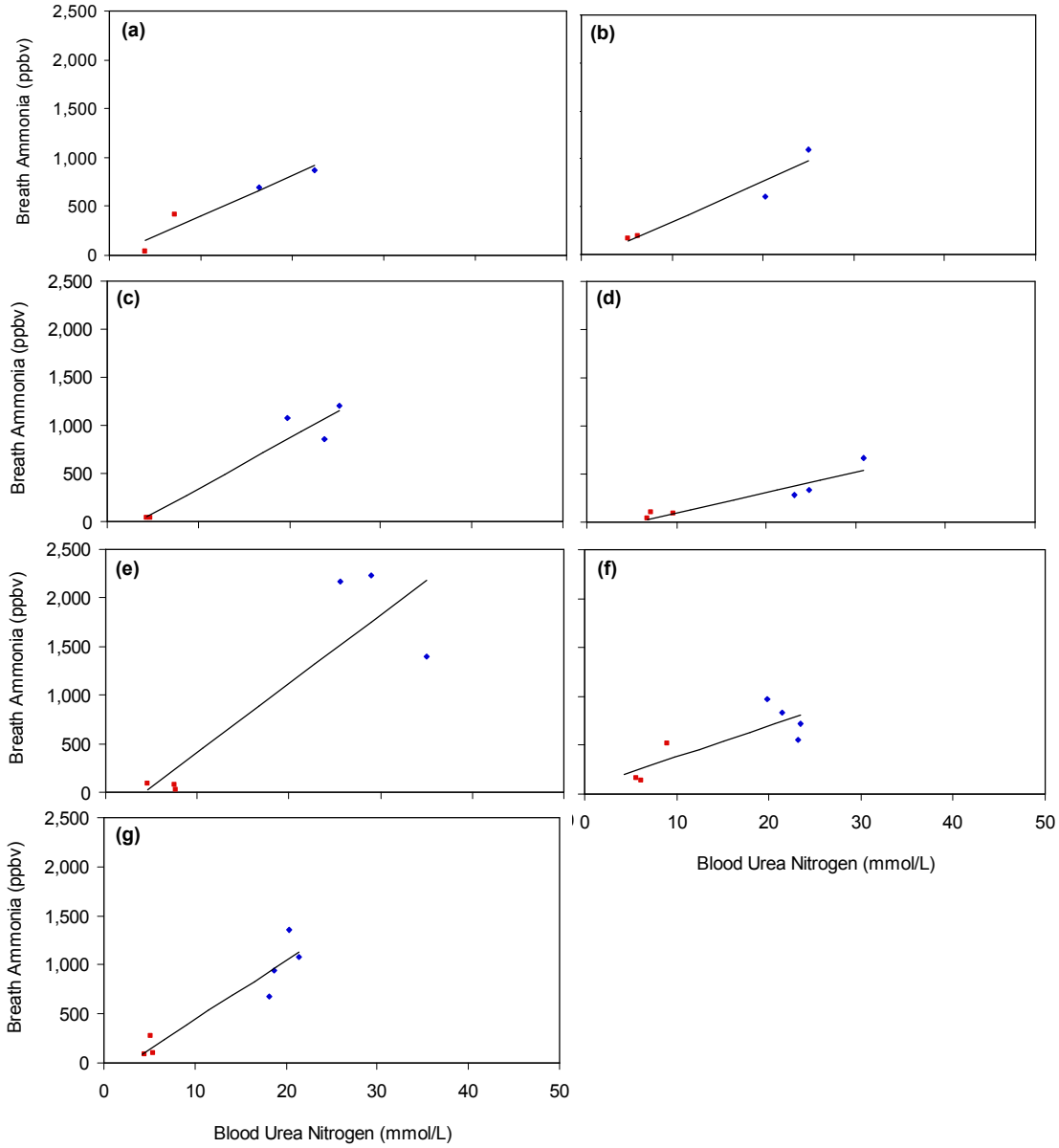

Figure 6.14 (a-g) Pre-dialysis (blue diamond) and post-dialysis (red square) of intra-individual absolute breath ammonia and blood urea nitrogen concentrations: (a) Volunteer 1: r=0.96, p<0.05, n=4 (b) Volunteer 2: r=0.96, p<0.05, n=4 (c) Volunteer 3: r=0.96, p<0.01, n=5 (d) Volunteer 4: r=0.94, p<0.01, n=6 (e) Volunteer 5: r=0.88, p<0.05, n=6 (f) Volunteer 6: r=0.82, p<0.05, n=7 and (g) Volunteer 7: r=0.94, p<0.01, n=7.

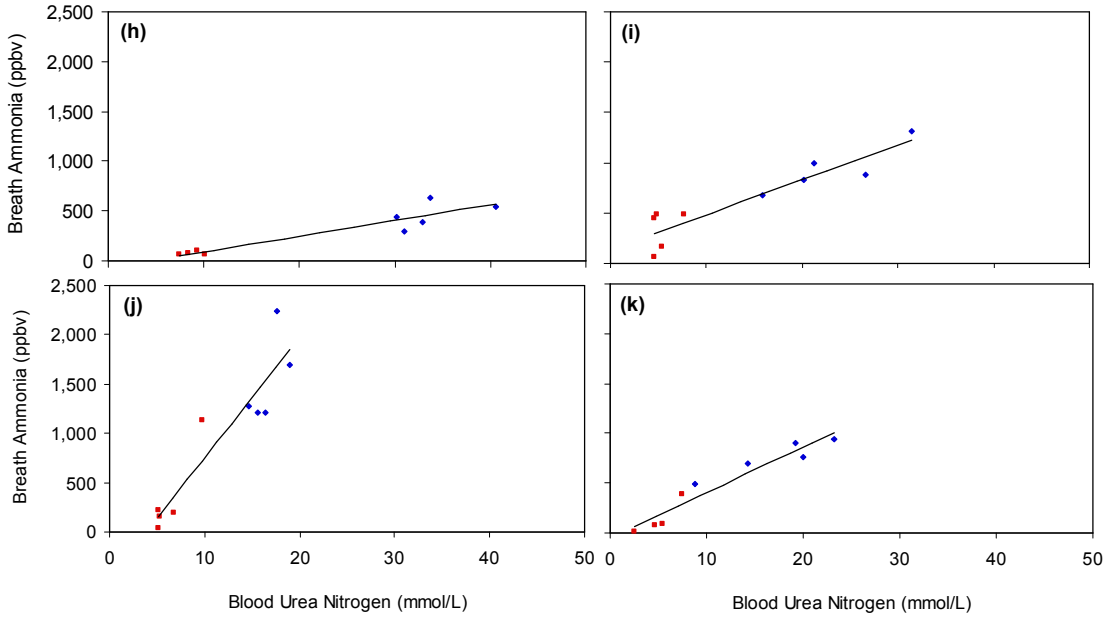

Figure 6.14 (h-k) Pre-dialysis (blue diamond) and post-dialysis (red square) of intra-individual absolute breath ammonia and blood urea nitrogen concentrations: (h) Volunteer 8: r=0.93, p<0.01, n=9 (i) Volunteer 9: r=0.86, p<0.01, n=10 (j) Volunteer 10: r=0.93, p<0.01, n=10 and (k) Volunteer 11: r=0.96, p<0.01, n=9.

Furthermore, the relationship between breath ammonia and blood urea appears to be reasonably linear for each individual. All these facts suggest that there would appear to be a defined relationship between breath ammonia and blood urea nitrogen levels that was specific to each individual. The reasons for this specific relationship are, as yet, undetermined, but again probably relate to patient-specific factors. For example, Volunteer 8 (Fig. 6.14 h) yielded pre-dialysis urea concentrations in excess of 30 mmol/L, while only registering ammonia levels of approximately 440 ppbv, and Volunteer 10 (Fig. 6.14 j) had a pre-dialysis breath ammonia level of 2,243 ppbv with a urea level of 17.6 mmol/L. This is an obvious display of the unique physiological factors associated with each individual.

It should be noted that individually these relationships were based on small sample sets. However, the number of volunteers and the strength and consistency of the correlations across all samples strengthens their validity. It can be seen that the correlations were much improved over the population correlations, suggesting the possibility that tracking changes in an individual's levels may be more effective than using population correlations. The population data had potential for bias since comparisons were made inter-individual, and

the unique physiology of each patient could have interfered with the correlations observed in other patients. With the intra-individual assessment, the unique behaviour is only being compared against itself which would greatly reduce bias. The values were comparable to the 0.95 correlation (n=6) seen within the individual haemodialysis patient observed in the previous research of Narasimhan *et al* [9]. In that study, the six measurements observed in the individual were made over the period of a single dialysis session following the reduction of blood constituents from pre- to post-dialysis rather than over separate sessions as performed in this work. However, the correlations in both experiments between the decrease in breath ammonia and the decrease in nitrogenous blood metabolites demonstrate how non-invasive breath ammonia measurements could provide a real-time measure of blood nitrogen levels within an individual.

6.3.10 Intra-individual correlations of breath ammonia and blood creatinine levels

The relationship between the absolute concentrations of breath ammonia and blood creatinine begins in Fig. 6.15. The correlation between breath ammonia and blood creatinine had a wider range than that with urea going from 0.71 to 0.97 with *p*-values of <0.01 and <0.05, once again displaying a strong correlation with good statistical significance. Volunteer 6 (Fig. 6.15f), however, displayed a non-significant relationship ($p=0.074$) between breath ammonia and blood creatinine. The reason for this result is unidentified, but is likely the cause of an unknown interferent given that the other correlations were strong. Furthermore, the results were similar to that of Narasimhan *et al* where laser spectroscopic measurements of breath ammonia displayed a correlation of 0.83 (n=6) with blood creatinine over the duration of a dialysis session in an individual haemodialysis patient [9]. As with the urea correlations, the good statistical significance among the intra-individual data suggests that the relationship between breath ammonia and blood creatinine levels remain reasonably consistent between dialysis sessions. In addition, the behaviour observed by the slopes (ranging from 0.47 to 2.64 ppbv) was similar to that seen with urea analysis where the relationship varied from person to person suggesting patient-specific factors are involved. The previously discussed Volunteer's 8 (Fig. 6.15 h) and 10 (Fig. 6.15 j) yielded pre-dialysis creatinine concentrations in excess of 500 μmol/L, yet Volunteer 8 only expressed breath ammonia concentrations of approximately 400 ppbv in this region while Volunteer 10 was over 900 ppbv on all accounts again demonstrating individual specificity.

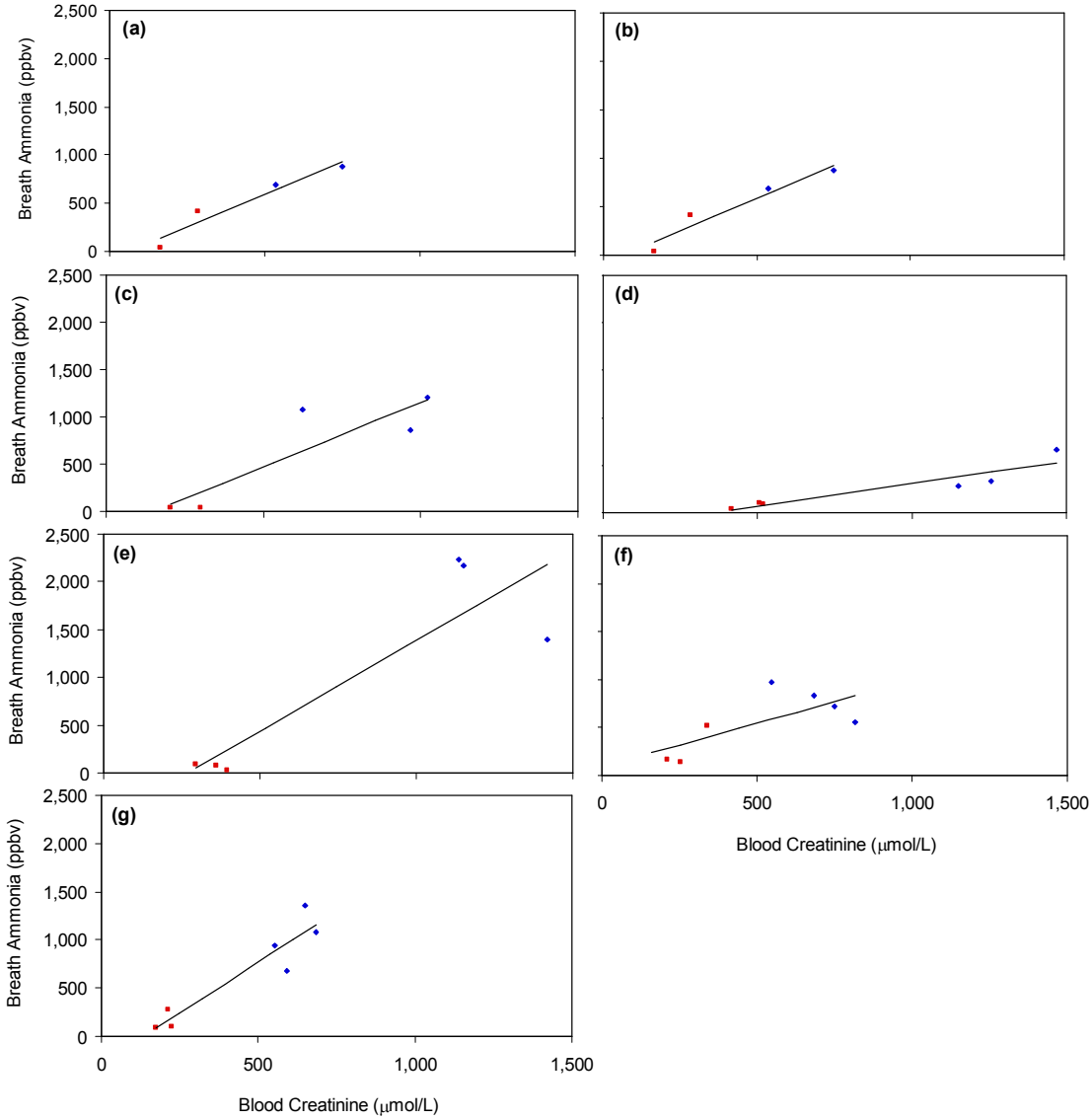

Figure 6.15 (a-g) Pre-dialysis (blue diamond) and post-dialysis (red square) of intra-individual absolute breath ammonia and blood creatinine concentrations: (a) Volunteer 1: r=0.96, *p*<0.05, n=4 (b) Volunteer 2: r=0.97, *p*<0.05, n=4 (c) Volunteer 3: r=0.89, *p*<0.05, n=5 (d) Volunteer 4: r=0.93, *p*<0.01, n=6 (e) Volunteer 5: r=0.88, *p*<0.05, n=6 (f) Volunteer 6: r=0.71, *p*=0.074, n=7 and (g) Volunteer 7: r=0.94, *p*<0.01, n=7.

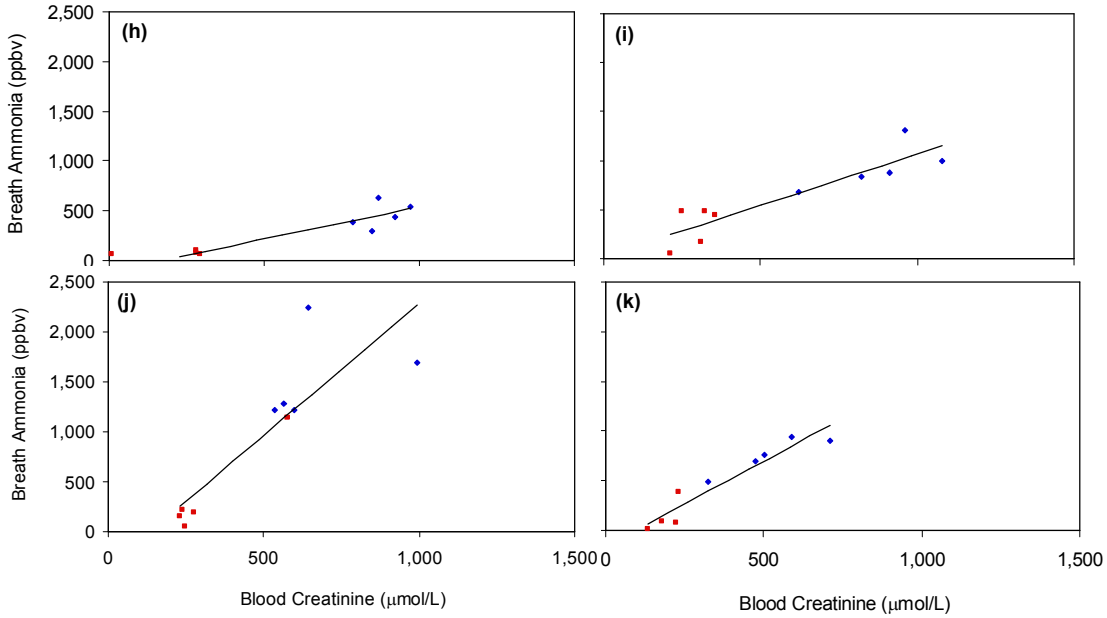

Figure 6.15 (h-k) Pre-dialysis (blue diamond) and post-dialysis (red square) of intra-individual absolute breath ammonia and blood creatinine concentrations: (h) Volunteer 8: r=0.92, *p*<0.01, n=9 (i) Volunteer 9: r=0.85, *p*<0.01, n=10 (j) Volunteer 10: r=0.86, *p*<0.01, n=10 and (k) Volunteer 11: r=0.95, *p*<0.01, n=9.

6.3.11 Intra-individual correlations of blood creatinine and blood urea levels

The relationship between the absolute concentrations of blood urea and creatinine begins in Fig. 6.16. The correlation between blood urea nitrogen and creatinine ranged from 0.90 to 1.00 with *p*-values of <0.01 and <0.05, indicating strong correlation and good statistical significance. The variation previously seen in the slopes also existed between blood urea and creatinine (ranging from 23.84 to 43.71 μmol/L), but not as much as between blood and breath. It is also worth noting that the relationship between blood urea and creatinine appears to be reasonably linear among the individuals suggesting that the relationship between blood urea nitrogen and creatinine levels displays similar behaviour from person to person. Although, slight variations do exist as exemplified by the previously mentioned Volunteer 8 (Fig. 6.16 h) yielded pre-dialysis urea concentrations in excess of 30 mmol/L, while registering creatinine levels of approximately 1,000 μmol/L, and Volunteer 10 (Fig. 6.16 j) had a pre-dialysis creatinine level close to 1,000 μmol/L where urea concentrations were only at approximately 20 mmol/L.

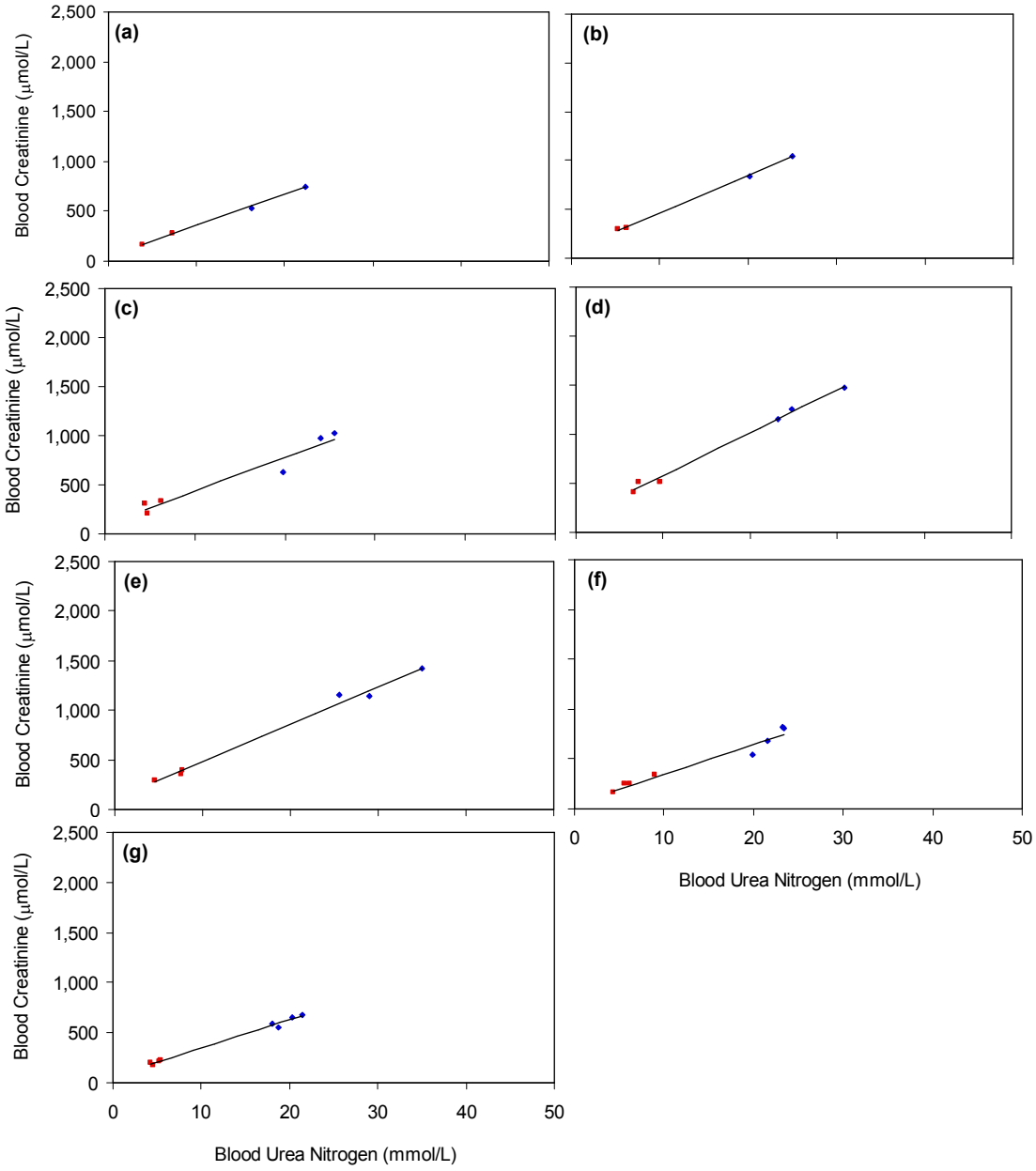

Figure 6.16 (a-g) Pre-dialysis (blue diamond) and post-dialysis (red square) of intra-individual blood creatinine and blood urea concentrations: (a) Volunteer 1: r=1.00, p<0.01, n=4 (b) Volunteer 2: r=1.00, p<0.01, n=4 (c) Volunteer 3: r=0.97, p<0.01, n=6 (d) Volunteer 4: r=1.00, p<0.01, n=6 (e) Volunteer 5: r=1.00, p<0.01, n=6 (f) Volunteer 6: r=0.98, p<0.01, n=8 and (g) Volunteer 7: r=1.00, p<0.01, n=8.

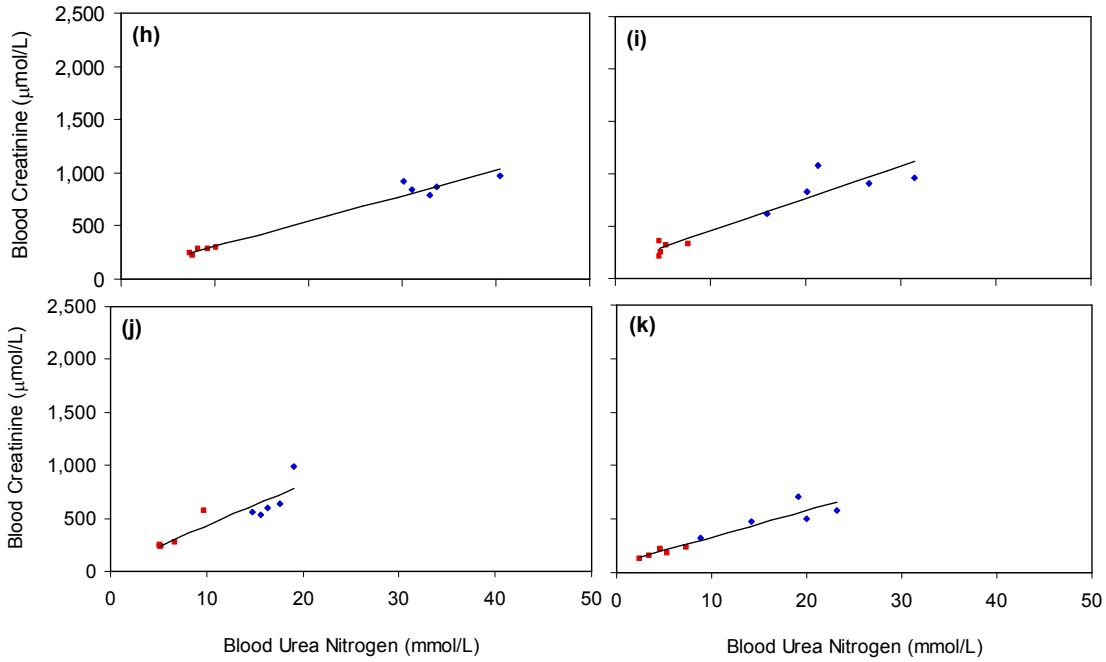

Figure 6.16 (h-k) Pre-dialysis (blue diamond) and post-dialysis (red square) of intra-individual blood creatinine and blood urea concentrations: (h) Volunteer 8: r=0.99, *p*<0.01, n=10 (i) Volunteer 9: r=0.94, *p*<0.01, n=10 (j) Volunteer 10: r=0.90, *p*<0.01, n=10 and (k) Volunteer 11: r=0.95, *p*<0.01, n=10.

By comparison to the population data, the improved correlations observed between breath ammonia, blood urea, and blood creatinine within individuals demonstrates a higher level of consistency among intra-individual samples. It is likely that the metabolic and physiological characteristics (e.g. kidney function, muscle mass, etc.) unique to the individuals would result in greater consistency in blood and breath measurement behaviour than would inter-individual comparisons among a population. This is demonstrated by the variations in individual slopes which signify metabolic behaviour unique to each person. In addition, the Pearson correlations found between breath ammonia and blood urea nitrogen were within a slightly smaller range than with blood creatinine suggesting that a more consistent and potentially stronger relationship may exist between breath ammonia and blood urea.

6.4 Conclusions

The AmBeR breath ammonia system was shown to yield excellent correlation with PALS (r=0.97, p<0.01, n=7) with regard to breath ammonia measurements in haemodialysis

patients and so was evaluated for its ability to further correlate with both blood urea nitrogen and blood creatinine levels. A significant difference between pre- and post-dialysis breath ammonia levels was identified. However, population correlations between absolute breath ammonia and blood urea (r=0.61, p<0.01, n=96), and blood creatinine (r=0.60, p<0.01, n=96) levels suggested the presence of patient-specific variables that reduced the correlative relationship between blood nitrogen and breath ammonia. Furthermore, this negative impact on correlations could also be seen between breath ammonia reduction ratios and blood urea reduction ratios (r=0.60, p<0.01, n=45), and blood creatinine reduction ratios (r=0.55, p<0.01, n=45). Comparison of Kt/V with breath ammonia reduction ratios (r=0.50, p<0.01, n=44), and blood urea reduction ratios (r=0.93, p<0.01, n=44) demonstrated similar correlations to the previous results, but did not reduce patient-specific variations. A urea reduction ratio of 65% equated to a breath ammonia reduction ratio of approximately 63% of the pre-dialysis value. Studies on the intra-individual correlations between absolute breath ammonia and blood urea nitrogen and blood creatinine yielded correlation coefficients ranging from 0.82 to 0.96, and 0.71 to 0.97, respectively. Although, further trials will be necessary to confirm these correlations, the data suggests that the AmBeR system has the potential to aid clinicians and patients in monitoring haemodialysis in a non-invasive manner following patient-specific calibration of the device.

6.5 References

[1] United States Renal Data System: 2011 USRDS Annual Data Report, Vol. 2, USRDS, [online], http://www.usrds.org/atlas.aspx (Accessed April 2, 2012).

[2] Renal Association., (2002), "Acute Renal Failure", *in Treatment of adults and children with renal failure: standards and audit measures,* (3rd ed.), 1, Royal College of Physicians, London, pp. 137.

[3] Maher, J.F., (1989), "Causes of acute renal failure, general work up of patients", in *J.F. Maher, ed., Replacement of renal function by dialysis: a textbook of dialysis,* (3rd ed.), 1, Kluwer Academic Publishers, Holland, pp. 617.

[4] McConnell, T.H., (2007), "Acute tubular necrosis", in *D.B. Troy andD.L. Knighten, eds., The nature of disease: Pathology for the health professions,* (1st ed.), Lippincott Williams and, MD, U.S.A., pp. 499.

[5] National Institutes of Health, The. (2006), "Treatment Methods for Kidney Failure", *National Kidney and Urologic Diseases Information Clearinghouse,* pp. 1-28.

[6] Lippincott Williams and Wilkins., (2007), "How haemodialysis works", in *J.D. Kowalak andJ. Munden, eds., Visual nursing: A guide to diseases, skills, and treatments,* (1st ed.), 1, Lippincott Williams and Wilkins, PA, U.S.A., pp. 284.

[7] Ishida, H., et al., (2008), "The Breath Ammonia Measurement of the Hemodialysis with a QCM-NH3 Sensor", *Bio-medical Materials and Engineering,* Vol.18 (2), pp. 99-106.

[8] Daugirdas, J.T. and Ing, T.S., (1994)*, Handbook of dialysis,* (Second ed.), Little, Brown and Company, Boston, New York, Toronto, London.

[9] Narasimhan, L.R., Goodman, W.and Patel, C.K.N., (2001), "Correlation of Breath Ammonia with Blood Urea Nitrogen and Creatinine During Hemodialysis", *Proceedings of the National Academy of Sciences of the United States of America,* Vol.98 (8), pp. 4617-4621.

[10] Dwinnell, B.G. andAnderson, R.J.(1999), "Diagnostic evaluation of the patient with acute renal failure", in *T. Berl andJ.V. Bonventre, eds., Atlas of Diseases of the Kidney,* (1st ed.), 1, Wiley-Blackwell, pp. 202.

[11] Wu, G., Kim, D.and Oreopoulos, D.G., (1985), "The efficacy and adequacy of continuous ambulatory peritoneal dialysis", *The Ulster Medical Journal,* Vol.54 pp. S48-S61.

[12] Warady, B.A., Schaefer, F.and Alexander, S.R.(2012), "Peritoneal Dialysis", in *B.A. Warady, F. Schaefer and S.R. Alexander, eds., Pediatric Dialysis,* (2nd ed.), 1, Springer, New York, pp. 7.

[13] Endre, Z.H., et al., (2011), "Breath ammonia and trimethylamine allow real-time monitoring of haemodialysis efficacy", *Physiological Measurement,* Vol.32 pp. 115-130.

[14] Davies, S., Spanel, P.and Smith, D., (1997), "Quantitative Analysis of Ammonia on the Breath of Patients in End-Stage Renal Failure", *Kidney International,* Vol.52 (1), pp. 223-228.

[15] Schrier, R.W., (2007), "Diagnosis of uremic encephalopathy", in *L. McAllister, L. Bierig, K. Barrett, et al, eds., Diseases of the kidney and urinary tract,* (8th ed.), 3, Lippincott Williams and, PA, U.S.A., pp. 2461.

[16] Timmer, B., Olthuis, W.and Berg, A.v.d., (2005), "Ammonia Sensors and Their Applications – A Review", *Sensors and Actuators B,* Vol.107 (2), pp. 666-677.

[17] Urea Test Principle: Kinetic UV Test, Roche Diagnostics, [online], http://www.roche-applied-science.com/custom-biotech/docs/IB_TechnicalFlyers/urea_testing_flyer_march11.pdf (Accessed May 19, 2012).

[18] Chromy, V., Rozkosna, K.and Sedlak, P., (2008), "Determination of serum creatinine by Jaffe method and how to calibrate to eliminate matrix interference problems", *Clinical Chemistry and Laboratory Medicine,* Vol.46 (8), pp. 1127-1133.

[19] Phinney, C.S., et al., (1998), "Definitive method certification of clinical analytes in lyophilized human serum: NIST Standard Reference Material (SRM) 909b", *Fresenius Journal of Analytical Chemistry,* Vol.361 (1), pp. 71-80.

[20] Watters Jr., R.L., et al., (1997), "Protocol for isotope dilution using inductively coupled plasma-mass spectrometry (ICP-MS) for the determination of inorganic elements", *Metrologia,* Vol.34 (1), pp. 87-96.

[21] Denhaerynck, K., et al., (2007), "Prevalence and consequences of nonadherence to hemodialysis regimens", *American Journal of Critical Care,* Vol.16 (3), pp. 222-235.

[22] Morgan, D.B., Carver, M.E.and Payne, R.B., (1977), "Plasma creatinine and urea: creatinine ratio in patients with raised plasma urea", *British Medical Journal,* Vol.2 pp. 929-932.

[23] Bowker, L.K., et al., (1992), "Raised blood urea in the elderly: a clinical and pathological study", *Postgraduate Medical Journal,* Vol.68 pp. 174-179.

[24] Gokal, R., et al., (1999), "Outcomes in peritoneal dialysis and haemodialysis - a comparative assessment of survival and quality of life", *Nephrology Dialysis Transplantation,* Vol.14 (6), pp. 24-30.

[25] Lesaffer, G., et al., (2000), "Intradialytic removal of protein-bound uraemic toxins: role of solute characteristics and of dialyser membrane", *Nephrology Dialysis Transplantation,* Vol.15 pp. 50-57.

[26] Amano, A., et al., (2002), "Monitoring Ammonia to Assess Halitosis", *Oral Surgery Oral Medicine Oral Pathology,* Vol.94 (6), pp. 692-696.

[27] Levesque, R., et al., (1999), "Haemodialysis for severe hyperammonaemic coma complicating urinary diversions", *Nephrology Dialysis Transplantation,* Vol.14 (1), pp. 458-461.

[28] Levesque, R., et al., (2000), "Haemodialysis for severe hyperammonaemic coma complicating urinary diversions", *Nephrology Dialysis Transplantation,* Vol.15 (1), pp. 1101.

[29] Leypoldt, J.K., et al., (1997), "Hemodialyzer mass transfer-area coefficients for urea increase at high dialysate flow rates", *Kidney International,* Vol.51 (1), pp. 2013-2017.

[30] Leypoldt, J.K.and Cheung, A.K., (1999), "Effect of low dialysate flow rate on hemodialyzer mass transfer area coefficients for urea and creatinine", *Home Hemodialysis International,* Vol.3 (1), pp. 51-54.

[31] Sherwood, L., (2010)*, Human physiology: From cells to systems,* (8th ed.), Yolanda Cossio, CA, U.S.A.

[32] Warady, B.A., Schaefer, F.and Alexander, S.R.(2012), "Inborn errors of metabolism", in *B.A. Warady, F. Schaefer and S.R. Alexander, eds., Pediatric dialysis,* (2nd ed.), 1, Springer, New York, pp. 769.

[33] Collen, J.F., et al., (2008), "Hemodialysis for hyperammonemia associated with ornithine transcarbamylase deficiency", *The Application of Clinical Genetics,* Vol.1 (1), pp. 1-5.

[34] Kooman, J.P., van der Sande, Frank M.and Leunissen, K.M.L., (2001), "Kt/V: finding the tree within the woods", *European Renal Association-European Dialysis and Transplant Association,* Vol.16 (1), pp. 1749-1752.

[35] Sherman, R.A.and Kapoian, T., (1997), "Recirculation, Urea disequilibrium, and Dialysis Efficiency: Peripheral Arteriovenous Versus Central Venovenous Vascular Access", *American Journal of Kidney Diseases,* Vol.29 (4), pp. 479-489.

[36] Schneditz, D., Kaufman, A.M.and Levin, N., (2003), "Surveillance of access function by the blood temperature monitor", *Seminars in Dialysis,* Vol.16 (6), pp. 483-487.

[37] Henrich, W.L., (2009), "Approach to hemodialysis kinetic modelling", in *W.L. Henrich, ed., Principles and practice of dialysis,* (4th ed.), 1, Lippincott Williams and Wilkins, pp. 83.

[38] Rajpoot, D.K.and Gargus, J.J., (2004), "Acute hemodialysis for hyperammonemia in small neonates", *Pediatrics and Nephrology,* Vol.19 (1), pp. 390-395.

[39] Gotch, F.A.and Sargent, J.A., (1985), "A mechanistic analysis of the National Cooperative Dialysis Study (NCDS)", *Kidney International,* Vol.28 (1), pp. 526-534.

[40] Eknoyan, G., et al., (2002), "Effect of dialysis dose and membrane flux in maintenance hemodialysis", *The New England Journal of Medicine,* Vol.347 (25), pp. 2010-2019.

[41] Fourtounas, C., et al., (2006), "Causes of impaired delivery of hemodialysis prescription", *Artificial Organs,* Vol.30 (11), pp. 878-891.

[42] Ahmad, S., (2009), "Current methods of measuring dialysis dose", in *M. Knowles, ed., Manual of clinical dialysis,* (2nd ed.), Springer, U.S.A., pp. 81-83.

CHAPTER 7
OVERALL CONCLUSIONS AND FUTURE WORK

7.1 Overall conclusions

The concentrations of breath ammonia in a healthy cohort measured via PALS were comparable to those of previous literature, and defined normal baseline analytical measurements. Inter-individual comparisons between oral breath ammonia and biometric parameters of oral breath carbon dioxide, gender, age, and BMI displayed insignificant correlations. Observations of changes in breath ammonia over the course of daily routines revealed a pattern of decline at mid-day followed by an increase in the afternoon. Orally exhaled breath had consistently higher concentrations of ammonia than did nasally exhaled breath.

The system developed to simulate breath for sensor characterisation studies generated continuous flowing samples at human levels of flow rate, temperature, humidity, and trace gas ammonia levels, which were validated using a number of measurement tools (e.g. PALS, thermistor, spirometer).

The ammonia sensing element (nanoPANI interdigitated electrode) displayed an intra-electrode variability of 0.05 to 1.67%. Observations of potential interferent gases as well as effects of temperature and humidity established that the only significant factors in the response of the sensor were ammonia gas, humidity, and temperature. Correlations of ammonia gases over the range of 40 ±2 ppbv to 2,175 ±26 ppbv demonstrated a correlation of 0.99 with a limit of detection of 6.3 ppbv.

A breath sampling system (AmBeR) was thus developed consisting of a breath sampling interface, sample measurement chamber with integrated nanoPANI-based ammonia sensor connected to an impedance analyser, and integrated into a housing to allow the system to be used at the point-of-care. A correlation of ammonia concentration with PALS of 0.99 with a LOD of 65.9 ppbv over the range of 40 ±2 to 2,993 ±10 ppbv was established in simulated breath samples. In addition, quantification of ammonia concentrations from normal human breath showed a 0.9860 correlation between the resulting AmBeR device and the commercial PALS system in the population, and a 0.9678 in the intra-individual correlation

A correlation of 0.97 was also established for ammonia breath concentrations in haemodialysis patients between AmBeR and PALS. A significant difference between pre- and post-dialysis breath ammonia and blood metabolite levels was also observed in these

patients. Population statistics displayed intermediate levels of correlation (r=0.54 to 0.65) between breath ammonia and blood nitrogen concentrations. However, intra-individual responses displayed higher correlations (r=0.78 to 0.97) between breath ammonia and blood nitrogen levels, establishing the prospect for AmBeR to be used in assisting with clinical decision support in this, or related applications.

7.2 Future works

The breath ammonia data collected from healthy volunteers using PALS was based on a small cohort (n=30). Tests on a larger population, both local and internationally, would provide stronger statistical analysis of ammonia levels in the breath of the normal population. It is well known that different cultures have unique diets, and various countries often have unique environments, which can all potentially influence metabolic input and output. Also, it would be of interest to examine the breath of volunteers who indicate no internal kidney dysfunction, but have been fasting, have asthma, are on specific diets, are smokers, drink alcohol, use medications, or play sports regularly.

A brief assessment of the effect of medication on breath ammonia levels as measured using PALS was made following administration of a normal dose of paracetamol. Breath ammonia levels appeared to increase over time subsequent to paracetamol consumption, and were monitored via PALS every 30 minutes (Fig. 7.1). Further studies could investigate whether the administration of this and other drugs have a transient effect on liver function that results in a change in the ability to process nitrogen. Such a technique might allow investigation of drug liver toxicity. In addition, assessment of increased blood sugar (e.g. glucose) and the effect on breath ammonia also took place (Fig. 7.2). Over the duration of three hours after injection of a glucose bolus into the blood stream, breath ammonia concentrations were continuously monitored displaying a steady increase from approximately 200 to 400 ppb. The resulting changes discussed here are merely anecdotal, as there was no additional investigation or controls performed. However, they show that there could be potential for future studies using AmBeR to monitor breath in other applications such as human physiology/sports science, etc. Such variables would apply to a real-world situation and may help to discriminate against potential interferences that were not observed previously.

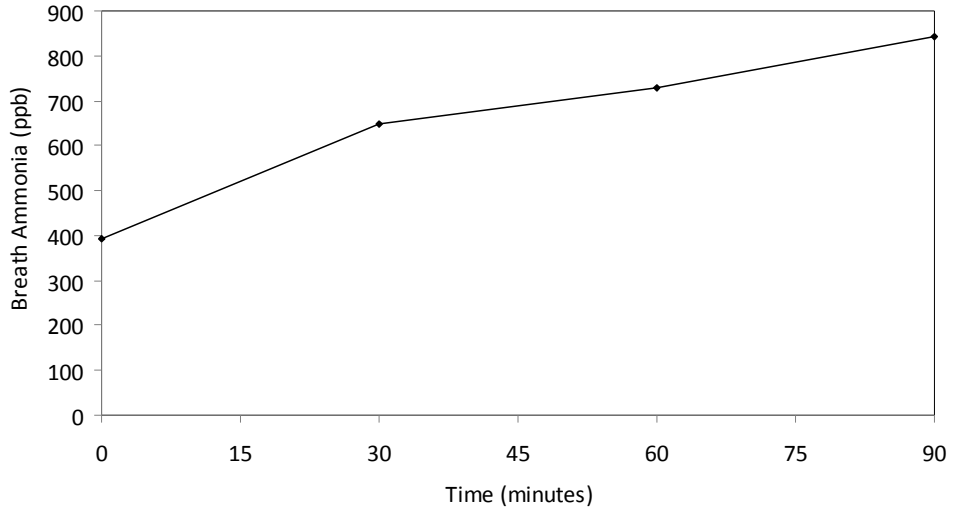

Figure 7.1 Effect on breath ammonia over time following paracetamol ingestion.

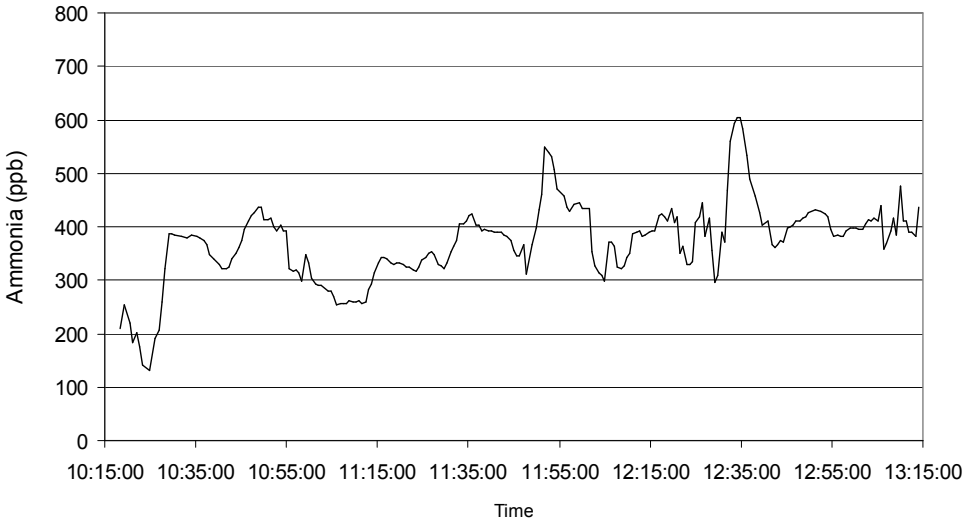

Figure 7.2 Effect of glucose bolus injection on breath ammonia concentration over time.

The ammonia sensor was also briefly studied for its potential use in other applications apart from breath. In addition to breath samples, responses to urine were carried out for the purpose of investigating urinary incontinence. The experimental set-up shown in Fig. 7.3 shows the configuration of three sensors (A, B, and C) in relation to a urine sample. According to the results in Fig. 7.4, the vapour response from urine suggested that the further away the sensor was from the urine, the less the response. Hence, sensor A

displayed a week change in conductivity since exposure to vapour was weakest, while sensor C displayed the largest change due to direct interaction with the urine. This was important since it indicated that vapour could be detected over a given distance and a sensor would not have to be in direct contact with the sample. Such a system of disposable sensors could have applications in assisted living to improve the quality of life for those suffering from this condition, while also assisting in better targeting the needs of patients.

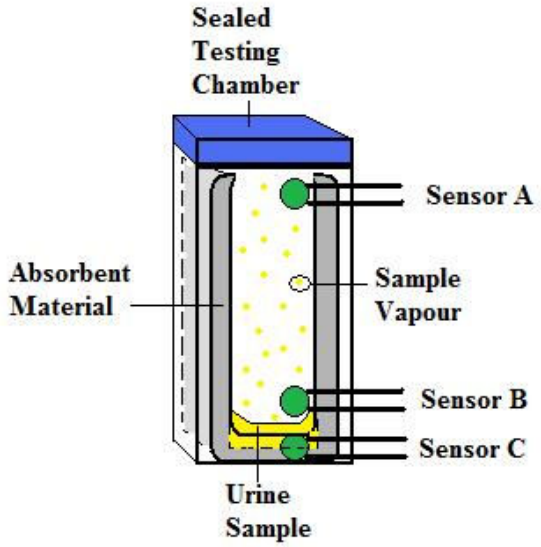

Figure 7.3 Experimental set-up for urine analysis.

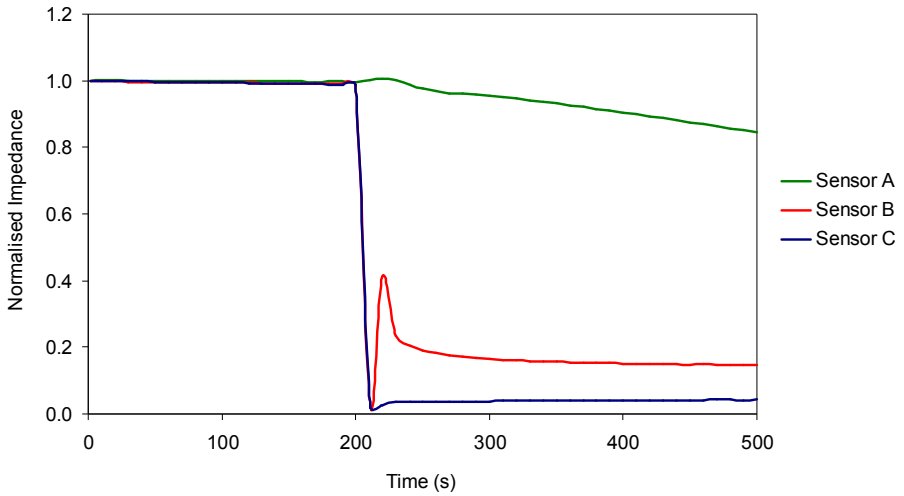

Figure 7.4 Examination of optimum distance of sensors from urine sample via impedance.

The simulated breath system assisted with studies of the major interferents in breath. One possible future direction in its development might be integration of multiple gases simultaneously. For example, the nanoPANI electrodes did not show significant affects from CO_2 in Chapter 4, but this gas could demonstrate interferent effects if combined with some of the other thousands of gases found in breath, or be an interferent in another sensor type. In addition, the system developed here used constant, continuous gas flow, which was extremely useful for sensor development. However, it did not represent a breath in terms of the flow rate profile during exhalation. Inclusion of such a pulsed breath method would enable the instrument to simulated human breath more realistically, which may be important for other applications. This system may have limited value since other similar versions are commercially available such as the Gas Calibration Unit (Ionimed Analytik GmbH, Austria), but perhaps the simplicity of the simulated breath instrument may prove more beneficial in some applications.

The primary focus of the development of the ammonia sensor should be on further optimisation of nanoPANI fabrication and production so as to improve sensor reproducibility. In addition, with portability being a key dynamic in diagnostics, assessment of miniaturisation and design development could make it easier to insert and remove the electrode from the device and allow further miniaturisation of the system. It would be of interest to observe the effects that these changes have on signal behaviour as well. The modification process could also involve replacement of silver ink with inks of lower cost such as carbon. Perhaps carbon could be ink-jet printed instead of screen-printed which may simplify the manufacturing process. Methods could be developed to increase sensitivity using composite mixtures (e.g. silver, gold, MWCNT, SWCNT), or a new chemistry all together which utilises the current methods but allows the sensors to detect gases other than ammonia. Development of better methods for exclusion of interference from humidity such as use of PTFE membranes on the nanoPANI film or new impedance measurement techniques which compensate for these interferences could also be pursued. A study of the shelf-life where electrodes are stored in both air and modified atmosphere packaging should also be performed to ensure adequate product shelf-life. A closer look at the kinetic nature of the interaction of ammonia with the polymer film should be taken to assess whether or not quick recovery would be possible could increase the potential for reuse of the electrodes.

For the future of the AmBeR device, further simplification is recommended to make it potentially hand-held. The impact of miniaturisation would need to be studied so as to see the effect on measurement characteristics. Complete systems integration with inbuilt electronics consisting of a display screen, minimal controls for ease-of-use, and further automation should be performed. This should also include an interface for the simple insertion and removal of sensors from the system. Automation could utilize pressure sensors that detect the beginning and end of exhalation, and automatic control of valves and flow controls. Furthermore, addition of a CO_2 sensor could assist with confirmation of alveolar samples which would assist in progression towards single breath analysis rather than multi-breath. Integration and optimisation of the impedance measurement electronics would also be a key development.

With regards to the application of AmBeR in haemodialysis, examination of a larger clinical cohort would provide a better understanding of limitations in both the AmBeR system and in the relationship between breath and blood nitrogen levels. Furthermore, rather than just observing pre- and post-dialysis, it would be beneficial to observe metabolic behaviour throughout, and after haemodialysis. A direct comparison of breath ammonia with blood ammonia is also lacking in the literature and may demonstrate better correlations than breath ammonia and blood urea nitrogen. Further development of intra-individual calibrations should be attempted to see if this would have clinical benefit. Collaborations with a wider number of dialysis units would also be an important next step since the parameters currently observed may not transfer to other countries where diets, environments, and daily routines vary. In addition, focus on monitoring of effects from other ammonia-based conditions such as transplants, liver dysfunction, *Helicobacter pylori*, and hepatic encephalopathy may open the route to assisting with a wider population of patients. If efforts were made to modify the chemistry of the sensing element, there may also be potential for monitoring of other breath gases (e.g. acetone) which would lead to assistance with other conditions such as diabetes.

7.3 Challenges

Certain challenges arose during the conduct of this work. Instances which involved human trials always required ethical approval. The process took several months in both the university and hospital trials due to the fact that committees which oversee applications

meet only a few times a year. Applications and timelines should have been assessed more thoroughly before beginning the project. Furthermore, when attempting to find volunteers for trials, it was not always easy to find the required population number. Hence, plans should have been made to schedule the volunteer cohorts months in advance. With the clinical volunteers, candidates were unwilling to commit to the trials unless a doctor provided direct introductions on a regular basis. In addition, since the clinical trials involved doctors, nurses, technicians, patients, and even personal assistants of the patients, there was little organisation. With so many people involved, regular meetings which engage everyone associated should have been better established. The result was that schedules became confused, samples were forgotten, and much needed time was lost. Regarding equipment, the most vital pieces failed at key moments. To name just a few from this project, lap tops were not always compatible with the required software, experiments had to be repeated regularly due to potentiostats freezing in the middle of a reading, the PALS system malfunctioned at the beginning of the clinical trials resulting in a six month loss due to repair and maintenance, and the internal construction of AmBeR had leaks which required regular sealing. All of these were challenges which could be overcome with time, but with studies involving clinical trials, loss of a key component such as PALS resulted in a lack of data for correlations between AmBeR and PALS.

APPENDIX

Appendix 1

DCU Research Ethics Committee: Notification Form for Low-Risk Projects

Project Title:

Breath Monitoring: Non-invasive Sample Collection and Analysis

Project Dates:

February 1, 2009 – January 31, 2012

Applicant Name and Email:

Troy Hibbard (troy.hibbard2@mail.dcu.ie)

If a student applicant, please provide the following:

Level of Study: PhD

Supervisor Name and Email: Dr. Tony Killard (Tony.Killard@dcu.ie)

1. A lay description of the proposed research

Currently, the methods for monitoring dysfunction of the human liver and kidneys rely on elaborate testing techniques. In development of these techniques, research has shown that impairment of the liver and kidneys can be detected by analyzing breath ammonia. Thus, having a sensor that can provide accurate readings would prove advantageous. The eventual goal is to develop a non-invasive breath ammonia sensor that can provide readings in real-time at the point-of-care. In order to do this, data must be recorded from healthy human subjects to determine normal baseline trends. Volunteers will be asked to provide breath samples at specified times over the period of the project. Breath samples will be taken and measured by a non-invasive ammonia breath monitoring system which investigators will establish. Once sufficient data is collected, it will be used as a reference for future clinical trials. When the clinical juncture of the project is reached, notification will be sent to the ethics committee again for further approval.

2. Details of the proposed methodology

Initially, suitable volunteers will be recruited by the methods mentioned in the following section titled "3. Details of the means by which potential participants will be recruited". Suitable volunteers are defined in the Plain Language Statement which is attached within this application. Once volunteers are recruited, they will be asked to provide breath samples at designated times during the project. Before each designated breath sampling, volunteers will be asked to fill out a questionnaire. This questionnaire serves the purpose of informing the investigator of possible reasons for abnormal data fluctuations (if any

exist). A copy of the questionnaire has been attached to this application and the anonymity of the information is discussed in section titled "4. How the anonymity of the participants will be respected". The time involved per volunteer is relatively short. The method for providing a breath sample is by breathing into a safe and approved interface similar to the image in *Figure 1. Interface for sample collection of oral breath ammonia*.

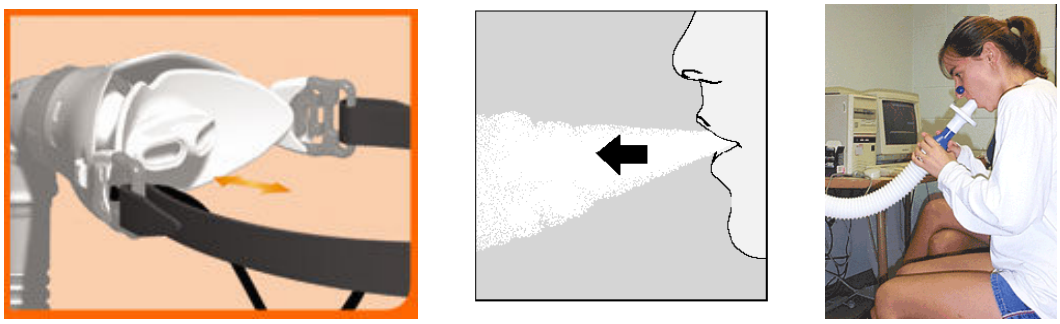

Figure 1. Interface for sample collection of oral breath ammonia (http://www.fphcare.com/osa/Oracle452.asp)

Breath samples will be taken using three different interfaces. The amount of breath samples taken will depend on the volunteer's comfort and willingness. Volunteers will be comfortably seated during the breath test and advised to rest and recover following the test. Each breath only takes a matter of seconds to produce. The three different interfaces are nasal, oral (front of mouth), and oropharyngeal (back of mouth). Using three different interfaces serves the purpose of analyzing possible physiological interferences to alveolus ammonia. It is of interest to measure the breath ammonia that originates only from the lungs. However, the human mouth is a source of bacteria that can produce ammonia gas. This oral bacterial gas can interfere with the ammonia gas from the lungs. Measuring ammonia concentrations through nasal and oropharyngeal (back of mouth) interfaces is expected to bypass the interference from the oral (front of mouth) ammonia. Furthermore, to have data that shows the difference between the oral (front of mouth) ammonia and other ammonia, specific volunteers will be asked to refrain from brushing their teeth for up to seven days before sampling. Not brushing for up to seven days is expected to increase the bacteria of the mouth to a level that will be distinguishable from that of the lungs. This technique has been approved by dental consultants of the St. James Hospital Ethics Committee as discussed in the section titled "6. Approvals that have been sought or secured from other sources". The ammonia breath concentration will be measured by an instrumental ammonia sensor known as the Pranalytica Nephrolux (http://www.pranalytica.com/nephrolux.html). For measurements of breath flow rates and volumes, a modified spirometer with added temperature and humidity sensors will also be used. Regular "follow ups" will be performed to answer any questions that the volunteers may have.

3. Details of the means by which potential participants will be recruited

A document containing our requirements for volunteers will be written from the Plain Language Statement. The document will reflect the purpose of the study, variables of preference (age ranges, etc.), time involved, risk assessment, and potential benefits to the volunteers. This document will be circulated by methods of brochures, campus flyers, emails, and in-person discussions. Volunteers will be sought on the campus of Dublin City University, and will not include vulnerable groups (children, etc.).

4. How the anonymity of the participants will be respected

All volunteers will be associated with a number. The data recorded from each volunteer will be labeled with respect to the variables tested rather than the volunteer's identity. Any personal information recorded for purposes of contacting the volunteer will be used only for that purpose. No personal information of the volunteers will be made public in any way.

5. The risks that researchers and / or participants may be exposed to

No abnormal testing will be performed. Abnormal is defined as any risks that may arise outside of everyday life. However, as with any breathing test, specific risks and discomforts may apply. The risks involved in this test may include fainting. Every effort will be made to minimize risks by selecting only those who fit the criteria written in the Plain Language Statement and by creating a safe and comfortable environment in the test location. Volunteers will be given time to rest and recover as needed.

6. Approvals that have been sought or secured from other sources

Since select volunteers will be asked to refrain from brushing their teeth for up to seven days, an inquiry was submitted to dental consultants of the St. James Hospital Ethics Committee. The question concerns whether or not lack of brushing for up to seven days could cause any ethical issues. Ethical issues in this case are defined as anything that causes dental health problems. The following is the email response from the dental consultants of St. James Hospital Ethics Committee in regards to this matter**:**

-----Original Message-----
From: O Mahony, Aisling (Consultant Restorative Dentistry)
Sent: 10 March 2009 09:05
To: Info
Subject: RE: Dental Ethics Question - Dublin City University

Hi,
I cannot see any ethical issue with this. It will certainly result in some gingivitis which is reversible. The only problem might be to exclude people with a history of or with active periodontal disease. This is obviously a personal opinion only. So a complete bill of health (dental) from their gdp might be in order.
AIsling

-----Original Message-----
From: Info
Sent: 02 March 2009 13:04
To: McKiernan, Eamonn (Consultant Orthodontist); O Mahony, Aisling (Consultant Restorative Dentistry)
Subject: FW: Dental Ethics Question - Dublin City University

-----Original Message-----
From: troy.hibbard2@mail.dcu.ie [troy.hibbard2@mail.dcu.ie]
Sent: 02 March 2009 12:25
To: Info
Subject: Dental Ethics Question - Dublin City University

Hello,
My name is Troy Hibbard and I am a current PhD researcher at Dublin City University. If it is possible, I was hoping that you would be able to answer a question that I have about dental ethics. I previously contacted the Irish Dental Association, and they informed me that there is an ethical committee at St James's Hospital which can give quick approval to such studies. We are researching breath ammonia levels and require that volunteers stop brushing their teeth anywhere from 5 days to one week. Would this time frame be acceptable or would there be any ethical issues? If so, do you have any recommendations on how to go about approaching the ethical issues, or perhaps who to ask? I greatly appreciate your time and assistance.
Regards,
Troy Hibbard
Dublin City University

Aisling O'Mahony recommended that we inquire about the dental background of the volunteers that will be asked to refrain from brushing. This inquiry will take place in the attached questionnaire labeled "DCU Breath Analysis Questionnaire". In relation to the criteria of section "5. The risks that researchers and / or participants may be exposed to", a risk assessment was asked for from Fisher & Paykel. Fisher & Paykel is the company that we intend to purchase the nasal, oral and oropharyngeal interfaces from. Since these interfaces will make physical contact with the volunteer, the risks should be acknowledged. Fisher & Paykel responded with the following email stating that risks have already been assessed by their company and there is no need to provide a copy for ethical proposal**:**

Date: Monday, March 2, 2009 3:29 PM
From: Emma Duckworth <Emma.Duckworth@fphcare.co.nz>
To: troy.hibbard2@mail.dcu.ie
cc: Stephen Stanley <Stephen.Stanley@fphcare.co.uk>
Subject: RE: Fisher & Paykel Healthcare Website Enquiry

Hello Troy,

Thanks you for providing me with further information. Unfortunately we cannot give out our risk assessment data. Once we have products approved for release then it means they have completed the risk assessment process. In my research experience, we have never had to provide risk assessment data on a released product that is already for sale - only on

products that are still in development for use in clinical investigations. However, I am not familiar with the Irish system so this may be a requirement. Perhaps providing the Instructions for use of each product would suffice as the Investigators Brochure for these products in your Clinical Investigation, which may help. I have certainly used them for this in Clinical Investigations in the past. For price estimates I have copied in one of my Irish colleagues who will be able to assist you with this. Please let me know if I can help more.

Best regards,
Emms
Emma Duckworth
Clinical Research Manager – OSA
Fisher & Paykel Healthcare
Phone +64 9 5740123 ext 8754

-----Original Message-----
From: troy.hibbard2@mail.dcu.ie [mailto:troy.hibbard2@mail.dcu.ie]
Sent: Thursday, 26 February 2009 1:49 a.m.
To: Emma Duckworth
Subject: Re: Fisher & Paykel Healthcare Website Enquiry

Hello Emma,

Thanks for getting back to me and sorry for the lack of details. The interfaces are needed for a current Clinical Research Investigation. We are in the first phases of collecting data on breath. In order to do this, though, we still need the interfaces for people to breathe into. However, ethical protocols require that we have a risk assessment available before breath sampling can take place. The reason that I asked for information on various interfaces is because we are going to be collecting data from various methods (nasal and oral). If there is anything else that you have questions about, please let me know.

Thanks for your assistance,

Troy

Hello Troy,

Thank you for your recent enquiry via the Fisher & Paykel Healthcare website. I need to ask a few more questions before I will be able to help you out. Do you require this information for a Clinical Research Investigation or simply for the use of our products within your clinical setting? If you could provide me with a little more information I will see how we can help.

Best regards,
Emms

Emma Duckworth
Clinical Research Manager – OSA
Fisher & Paykel Healthcare
Phone +64 9 5740123 ext 8754

Mobile +64 21 538499

-----Original Message-----

From: troy.hibbard2@mail.dcu.ie [mailto:troy.hibbard2@mail.dcu.ie]
Sent: Sunday, 22 February 2009 1:49 a.m.
To: Info
Subject: Fisher & Paykel Healthcare
Web Site : General enquiry (21 February 2009 05:48)
Name: Troy Hibbard
E-mail: troy.hibbard2@mail.dcu.ie
Subject: General
Country: Ireland
Company Name: Biomedical Diagnostics Institute
Position: PhD student researcher
Hospital Name: BDI of DCU
Product Enquiring About: OSA Interfaces
Comments:

Hello,

My name is Troy Hibbard and I am a current PhD researcher at Dublin City University. We are interested in purchasing several of the interfaces in regards to the nasal and oral. Due to protocol of human use, though, it is necessary to ask for a risk assessment of the equipment before being able to use them. Would it be possible for you to send a risk assessment form for the OSA Interfaces? The specific ones we are interested in are the Opus360, FlexFit405, FlexFit406, FlexFit407, Zest, and the Oracle452. Your time and assistance are greatly appreciated!

Thank you,

Troy Hibbard

---

7. Confirmation that the following forms are attached to this document:

Informed Consent Form (yes/no):

Yes

Plain Language Statement (yes/no):

Yes

Dublin City University - Informed Consent Form

Research Study Title: Breath Monitoring: Non-invasive Sample Collection and Analysis

University Department: Biomedical Diagnostics Institute *and* School of Chemical Sciences

Investigators: Dr. Tony Killard, Dr. Karl Crowley, Zahra Shahbazian, and Troy Hibbard

Before agreeing to participate in this research study, it is important that you read the explanation of this study. This statement describes the purpose, procedures, benefits, alternative procedures, risks, and precautions of the program. Also described is your right to withdraw from the study at any time. No guarantees or assurances can be made as to the results of the study.

Purpose of the research

To collect and analyse breath samples for ammonia concentrations. The data collected will serve to develop a sensor specific to assisting dialysis patients who have excretory dysfunctions.

Confirmation of requirements as highlighted in the Plain Language Statement

Participant – please complete the following (Circle Yes or No for each question)

1. Have you read (or had read to you) the Plain Language Statement? Yes / No
2. Do you understand the information provided? Yes / No
3. Have you had an opportunity to ask questions and discuss this study? Yes / No
4. Have you received satisfactory answers to all your questions? Yes / No
5. Are you aware that your participation will involve a questionnaire? Yes / No

Statement of voluntary involvement

Participants may withdraw from the Research Study at any point. There will be no penalty for withdrawing before all stages of the Research Study have been completed.

Confidentiality of data

All information gathered from the study will remain confidential and kept in a locked facility. Participant's individual data will not be disclosed outside of the testing personnel without each participant's written permission. However, Dublin City University may review the study data without written consent. The results of this study may be published for scientific purposes, and participant's identity will not be revealed.

Benefits to participants

Although there are no direct benefits to the people in this study, possible benefits include better sensor technology for dialysis patients.

Risks to participants

No abnormal testing will be performed. Abnormal is defined as any risks that may arise outside of everyday life. However, as with any breathing test, specific risks and discomforts may apply. The risks involved in this test may include fainting. Every effort will be made to minimize risks by selecting only those who fit the criteria written in the Plain Language Statement and by creating a safe and comfortable environment in the test location. Volunteers will be given time to rest and recover as needed. It is the participant's responsibility to inform the study investigator if they feel dizzy, ill-feeling or other symptoms during the breath sampling procedure.

Alternative Procedures

Since this study does not involve specific treatments or procedures, there are no alternative methods at this time.

Signature

I have read and understood the information in this form. My questions and concerns have been answered by the researchers, and I have a copy of this consent form. Therefore, I consent to take part in this research project.

Participants Signature: _____

Name (Block Capitals): _____

Witness: _____

Date: _____

Dublin City University – Plain Language Statement

Research Study Title: Breath Monitoring: Non-invasive Sample Collection and Analysis

University Department: Biomedical Diagnostics Institute *and* School of Chemical Sciences

Investigators: Dr. Tony Killard, Dr. Karl Crowley, Zahra Shahbazian, and Troy Hibbard

What involvement in the Research Study will require

I. Human volunteers will be expected to fulfill the requirements of "normalcy". Normalcy is defined as having the following characteristics:

1. Age range between 18 and 60 years

2. Have no known respiratory (breathing, etc.) or digestive (stomach, etc.) complications

3. Not a daily tobacco smoker

4. Do not consume excessive quantities of alcohol (21 units for men / 14 units for women – per week)

II. Volunteers will be asked to fill out an Informed Consent Form to confirm they understand the project. Volunteers will also be asked to fill out a short questionnaire (10 to 15 "check-box" questions) to help associate the data with the volunteer.

III. Volunteers will be asked to provide breath samples by breathing into a sensor. Specific volunteers may be asked if they would be willing to refrain from brushing their teeth for up to seven days. Once a schedule has been agreed upon between the volunteer and the investigator, the sampling can begin. The amount of samples required per volunteer is as follows:

1. Oral (front of mouth) – Up to 10 breaths (more if volunteer is willing)

2. Oropharyngeal (back of mouth) – Up to 10 breaths (more if volunteer is willing)

3. Nasal (from nose) – Up to 10 breaths (more if volunteer is willing)

IV. The preferred schedule is once a week for 1-2 months before 12 noon (lunch). This schedule can be modified according to the necessity of the volunteer. Times before lunch are preferred since food and beverages may modify data.

Risks to participants

No abnormal testing will be performed. Abnormal is defined as any risks that may arise outside of everyday life. However, as with any breathing test, specific risks and discomforts may apply. The risks involved in this test may include fainting. Every effort will be made to minimize risks by selecting only those who fit the criteria written in the Plain Language Statement and by creating a safe and comfortable environment in the test location. Volunteers will be given time to rest and recover as needed. It is the participant's responsibility to inform the study investigator if they feel dizzy, ill-feeling or other symptoms during the breath sampling procedure.

Benefits to participants

Although there are no direct benefits to the people in this study, possible indirect benefits include better sensor technology for dialysis patients.

Confidentiality of data

All information gathered from the study will remain confidential and kept in a locked facility. Participant's individual data will not be disclosed outside of the testing personnel without each participant's written permission. However, Dublin City University may review the study data without written consent. The results of this study may be published for scientific purposes, and participant's identity will not be revealed.

Is data to be destroyed after a minimum period?

All data being recorded is non-sensitive. No clinical assessments or diagnoses will be made that would reflect the volunteers associated with this research study. With this, there is no need to destroy the data.

Statement of voluntary involvement

Participants may withdraw from the Research Study at any point. There will be no penalty for withdrawing before all stages of the Research Study have been completed.

*** If participants have concerns about this study and wish to contact an independent person, please contact:**

The Secretary, Dublin City University Research Ethics Committee, c/o Office of the Vice-President for Research, Dublin City University, Dublin 9. Tel 01-7008000

DCU Breath Analysis Questionnaire

A. Please write your information on the lines, and put a check mark (X) in the box next to the gender that qualifies.

Volunteer Number:

_____

Gender: Male ☐

Female ☐

Age:

_____

Occupation:

_____

B. For the following questions, please put a check mark (X) in the box next to the answers. If any of the questions are unclear, please feel free to ask an investigator to clarify.

1) In the past month, I have suffered from the following symptoms:

** Please check all boxes that apply*

Difficulty Breathing	☐	Excessive Sneezing	☐
Excessive Coughing	☐	Stomach Pain	☐
Rhinitis (Runny Nose)	☐	Sinus Pain	☐

2) In the past week, the amount of tobacco products I smoked was:

*An example of "amount" would be associated with 1 cigarette (not 1 pack).

0 – 5 ☐

6 – 10 ☐

11 – 15 ☐

16 + ☐

3) In the past week, I believe I was exposed to secondary smoke:

* An example of "exposed" would be if the smoke was noticeably being inhaled.

0 – 5 times ☐

6 – 10 times ☐

11 – 15 times ☐

16 times + ☐

4) In the past week, I consumed an alcoholic beverage (ex: 1 glass = 1 time):

0 – 5 times ☐

6 – 10 times ☐

11 – 15 times ☐

16 times + ☐

5) In the past week, I consumed a sugar-based beverage (ex: Cola, Energy Drinks, Sports Drinks, etc.):

0 – 5 times ☐

6 – 10 times ☐

11 – 15 times ☐

16 times + ☐

6) I receive a professional dental evaluation:

More than "one time every year" ☐

One time every year ☐

One time every two years ☐

Less than "one time every two years" ☐

7) My regular oral cleaning routine is:

I brush my teeth more than twice a day ☐

I brush my teeth twice a day ☐

I brush my teeth less than twice a day ☐

I use other methods ☐

8) I have had dental complications in the past (ex: oral diseases, gingivitis, etc.):

Yes ☐

No ☐

9) Please rank the following food groups in the order of what you believe you eat the most to what you eat the least (on a regular basis):

* *What you eat the most = 1 ; What you eat the least = 5*

Grains ☐

Vegetables ☐

Fruits ☐

Milk ☐

Meat / Beans ☐

10) In the last six hours I have eaten and / or drank the following items:

_____

11) I am currently on a medication that affects my breathing and / or digestion:
Yes ☐
No ☐

DCU

Dublin City University
Ollscoil Chathair Bhaile Átha Cliath

Offiice of the Vice-President for Research
Dublin 9, Ireland

Dr. Tony Killard
Biomedical Diagnostics Institute and School of Chemical Sciences

31st March 2009

REC Reference: DCUREC/2009/048

Proposal Title: **Breath Monitoring: Non-invasive Sample Collection and Analysis**

Applicants: Dr. Tony Killard, Dr. Karl Crowley, Ms. Zahra Shabazian, Mr. Troy Hibbard

Dear Tony,

This research proposal qualifies under our Notification Procedure, as a low-risk project. Therefore, the DCU Research Ethics Committee approves this research proposal. Should substantial modifications to the research protocol be required at a later stage, a further submission should be made to the REC.

Yours sincerely,

pp Fiona Brennan

Mr. Brian Trench
Chair
DCU Research Ethics Committee

DCU
Office of the Vice-President
for Research

Telephone 353 (0)1 700 8000
Facsimile 353 (0)1 700 8002

Appendix 2

Reynolds number for a humidified air stream containing gaseous ammonia

Reference (Re Formula): http://www.engineeringtoolbox.com/reynolds-number-d_237.html

Note: Dynamic viscosity used is the average of the three gas viscosities.

Definition: A dimensionless number that gives a ratio of inertial forces to viscous forces in flow conditions. In this case, within a pipe or tube.

Laminar: Re < 2300
Transient: 2300 < Re < 4000
Turbulent: 4000 < Re

Reynolds (Re) = (pVD) / (μ)

p = Gas density, Kg/m^3
V = Mean velocity, m/s
D = Diameter of pipe, m
μ = Dynamic viscosity of gas, Pa.s

Calculated Reynolds number of (air + ammonia gas + water vapour) =

((2.65 Kg/m^3)(2.735 m/s)(0.022 m)) / (0.0000142 Pa.s) = **11,228.91 = Turbulent Flow**

II. Gas Density (p, Kg/m^3)

Online Calculated Densities:

Reference (Densities): http://www.engineeringtoolbox.com/gas-density-d_158.html

Note: Reference densities were at 20^oC and 1atm.

Air 1.205 Kg/m^3
Water (vapour) 0.804 Kg/m^3
Ammonia (gas) 0.717 Kg/m^3

My Calculated Densities:

Reference (Ideal Gas Law):
http://www.indiana.edu/~geog109/topics/10_Forces&Winds/GasPressWeb/PressGasLaws.html

Ideal Gas Law (PV = nRT) => (Pressure x Volume = Moles x Gas Constant x Temperature)

Converted for Density (P = nRT / V) => (P / RT = n / V) => (Density = p = n / V)

Air	1.199 Kg/m^3
Water (vapour)	0.746 Kg/m^3
Ammonia (gas)	0.705 Kg/m^3

Air + Water + Ammonia (summed molecular weights; same original volume) = **2.65 Kg/m^3**

Air (Molecular Weight, g/mol, Kg/mol)

Reference (Molecular Weight): DCU chem. lab manual periodic table

Reference (Gas Percentages): http://scifun.chem.wisc.edu/chemweek/pdf/airgas.pdf

Nitrogen (N_2) 14.00674 x 2 = 28.0134 g/mol at 78.08% of air
0.7808 x 28.0134 = 21.87286272 g/mol
Oxygen (O_2) 15.9994 x 2 = 31.9988 g/mol at 20.95% of air
0.2095 x 31.9988 = 6.7037486 g/mol
Argon (Ar) 39.984 g/mol at 0.93% of air
0.0093 x 39.984 = 0.3718512 g/mol
Carbon Dioxide (CO_2) 12.0107 + (15.9994 x 2) = 44.0095 g/mol at 0.033% of air
0.00033 x 44.0095 = 0.014523135 g/mol
Neon (Ne) 20.1797 g/mol at 0.0018% of air
0.000018 x 20.1797 = 0.0003632346 g/mol
Helium (He) 4.002602 g/mol at 0.00052% of air
0.0000052 x 4.002602 = 0.0000208135304 g/mol
Methane (CH_4) 12.0107 + (1.00794 x 4) = 16.04246 g/mol at 0.0002% of air
0.000002 x 16.04246 = 0.00003208492 g/mol
Krypton (Kr) 83.798 g/mol at 0.00011% of air
0.0000011 x 83.798 = 0.0000921778 g/mol
Nitrogen (I) Oxide (N2O) (14.00674 x 2) + 15.9994 = 44.01288 g/mol at 0.00005% of air
0.0000005 x 44.01288 = 0.00002200644 g/mol
Hydrogen (H_2) 1.00794 x 2 = 2.01588 g/mol at 0.00005% of air
0.0000005 x 2.01588 = 0.00000100794 g/mol
Xenon (Xe) 131.293 g/mol at 0.0000087% of air
0.000000087 x 131.293 = 0.000011422491 g/mol
Ozone (O_3) 15.9994 x 3 = 47.9982 g/mol at 0.000001% of air
0.00000001 x 47.9982 = 0.000000479982 g/mol

Air Molar Mass =

(21.87286272 + 6.7037486 + 0.3718512 + 0.014523135 + 0.0003632346 + 0.0000208135304 + 0.00003208492 + 0.0000921778 + 0.00002200644 + 0.00000100794 + 0.000011422491 + 0.000000479982) = 28.96352888 g/mol = **0.02896352888 Kg/mol**

Ammonia (NH_3) Molar Mass 14.00674 + (1.00794 x 3) =

17.03056 g/mol = **0.01703056 Kg/mol**

Water (H_2O) Vapour Molar Mass (1.00794 x 2) + 15.9994 =

18.01528 g/mol = **0.01801528 Kg/mol**

Air Density = Molar Mass / Volume =

((Kg/mole)(1 mole / 24.15 L Perfect Gas Constant)(L/m^3)) =
((0.02896352888 Kg/mole)(1 mole / 24.15 L)(1 L / 0.001 m^3) =
1.199317966 Kg/m^3

Ammonia (gas) Density = Molar Mass / Volume =

((Kg/mole)(1 mole / 24.15 L Perfect Gas Constant)(L/m^3)) =
((0.01703056 Kg / mole)(1 mole / 24.15 L)(1 L / 0.001 m^3) =
0.705199171 Kg/m^3

Water (vapour) Density = Molar Mass / Volume =

((Kg/mole)(1 mole / 24.15 L Perfect Gas Constant)(L/m^3)) =
((0.01801528 Kg/mole)(1 mole / 24.15 L)(1 L / 0.001 m^3) =
0.745974327 Kg/m^3

Air + Ammonia (gas) + Water (vapour) Density = Molar Mass / Volume =

(0.02896352888 Kg/mol + 0.01703056 Kg/mol + 0.01801528 Kg/mol) =
((Kg/mole)(1 mole / 24.15 L Perfect Gas Constant)(L/m^3)) =
((0.06400936888 Kg/mole)(1 mole / 24.15 L)(1 L / 0.001 m^3)) =
2.65049 Kg/m^3

III. Flow velocity per concentration (V, m/s)

Reference: I calculated these myself from previously shown work attached at the end.

Note: Pressure setting from air blower of main flow is 4 cmH_2O, and velocities from *velocity at concentration* were used for final calculation.

<u>1) Humidified air (Control = No ammonia):</u>

Flow Rates and Concentration
62.0 L/min
Velocity at this Concentration
Velocity within tube (m/s) = Airflow (m^3/s) / Internal surface area of tube (m^2)
62.0 L/min to m^3/s convert: (62.0 L/min)(0.00001667 constant) = 0.00103354 m^3/s
Area = (pi)(radius^2) = (3.14)((0.011 m)^^{2}) = 0.00037994 m^2
Velocity = (0.00103354 m^3/s) / (0.00037994 m^2) = 2.72 m/s

2) Humidified air + 24.08 ppb (0.0161 mg/m^3) NH_3:

Flow Rate (Ammonia, Humidified Air)
0.3 L/min flow ammonia into main flow of 62.0 L/min.
0.3 L/min + 62.0 L/min = 62.3 L/min main flow
Ammonia Concentration
(0.3 L/min / 62.3 L/min)(Initial 5,000 ppb NH_3 cylinder concentration) = Final 24.08 ppb NH_3
ppm = ((mg/m^3)(Kelvin constant + temperature ^oC))/((proportionality constant)(gas molecular weight))
Final 24.08 ppb NH_3 / 1000 = 0.0241 ppm = ((X mg/m^3)(273.15 + 37^oC))/((12.187)(17.03 g/mol))
Step 1: (12.187)(17.03g/mol) = 207.54461 g/mol => 207.54461 (0.0241 ppm) = 4.9971
Step 2: 4.9971 / 310.15^oC = 0.0161 mg/m^3
Velocity at this Concentration
Velocity within tube (m/s) = Airflow (m^3/s) / Internal surface area of tube (m^2)
Airflow: 62.3 L/min to m^3/s convert: (62.3 L/min)(0.00001667 constant) = 0.001038541 m^3/s
Internal Surface Area = (pi)(radius^2) = (3.14)((0.011 m)^2) = 0.00037994 m^2
Velocity = (0.001038541 m^3/s) / (0.00037994 m^2) = 2.73 m/s

3) Humidified air + 40.00 ppb (0.026766 mg/m^3) NH_3:

Flow Rate (Ammonia, Humidified Air)
0.5 L/min flow ammonia into main flow of 62.0 L/min.
0.5 L/min + 62.0 L/min = 62.5 L/min main flow
Ammonia Concentration
(0.5 L/min / 62.5 L/min)(Initial 5,000 ppb NH_3 cylinder concentration) = Final 40.00 ppb NH_3
ppm = ((mg/m^3)(Kelvin constant + temperature ^oC))/((proportionality constant)(gas molecular weight))
Final 40.00 ppb NH_3 / 1000 = 0.04 ppm = ((X mg/m^3)(273.15 + 37^oC))/((12.187)(17.03 g/mol))
Step 1: (12.187)(17.03g/mol) = 207.54461 g/mol => 207.54461 (0.04 ppm) = 8.3017844
Step 2: 8.3017844 / 310.15^oC = 0.026766 mg/m^3
Velocity at this Concentration
Velocity within tube (m/s) = Airflow (m^3/s) / Internal surface area of tube (m^2)
Airflow: 62.5 L/min to m^3/s convert: (62.5 L/min)(0.00001667 constant) = 0.001041875 m^3/s
Internal Surface Area = (pi)(radius^2) = (3.14)((0.011 m)^2) = 0.00037994 m^2
Velocity = (0.001041875 m^3/s) / (0.00037994 m^2) = 2.74 m/s

4) Humidified air + 80.00 ppb (0.053533 mg/m^3) NH_3:

Flow Rate (Ammonia, Humidified Air)
0.5 L/min flow ammonia into main flow of 62.0 L/min.
0.5 L/min + 62.0 L/min = 62.5 L/min main flow
Ammonia Concentration

(0.5 L/min / 62.5 L/min)(Initial 10,000 ppb NH_3 cylinder concentration) = Final 80.00 ppb NH_3
ppm = ((mg/m^3)(Kelvin constant + temperature ^oC))/((proportionality constant)(gas molecular weight))
Final 80.00 ppb NH_3 / 1000 = 0.08 ppm = ((X mg/m^3)(273.15 + 37^oC))/((12.187)(17.03 g/mol))
Step 1: (12.187)(17.03g/mol) = 207.54461 g/mol => 207.54461 (0.08 ppm) = 16.60356
Step 2: 16.60356 / 310.15^oC = 0.053533 mg/m^3
Velocity at this Concentration
Velocity within tube (m/s) = Airflow (m^3/s) / Internal surface area of tube (m^2)
Airflow: 62.5 L/min to m^3/s convert: (62.5 L/min)(0.00001667 constant) = 0.001041875 m^3/s
Internal Surface Area = (pi)(radius^2) = (3.14)((0.011 m)^^{2}) = 0.00037994 m^2
Velocity = (0.001041875 m^3/s) / (0.00037994 m^2) = 2.74 m/s

5) Humidified air + 120.39 ppb (0.08055 mg/m^3) NH_3:

Flow Rate (Ammonia, Humidified Air)
0.3 L/min flow ammonia into main flow of 62.0 L/min.
0.3 L/min + 62.0 L/min = 62.3 L/min main flow
Ammonia Concentration
(0.3 L/min / 62.3 L/min)(Initial 25,000 ppb NH_3 cylinder concentration) = Final 120.39 ppb NH_3
ppm = ((mg/m^3)(Kelvin constant + temperature ^oC))/((proportionality constant)(gas molecular weight))
Final 120.39 ppb NH_3 / 1000 = 0.12038 ppm = ((X mg/m^3)(273.15 + 37^oC))/((12.187)(17.03 g/mol))
Step 1: (12.187)(17.03g/mol) = 207.54461 g/mol => 207.54461 (0.120385 ppm) = 24.985
Step 2: 24.985 / 310.15^oC = 0.08055 mg/m^3
Velocity at this Concentration
Velocity within tube (m/s) = Airflow (m^3/s) / Internal surface area of tube (m^2)
Airflow: 62.3 L/min to m^3/s convert: (62.3 L/min)(0.00001667 constant) = 0.001038541 m^3/s
Internal Surface Area = (pi)(radius^2) = (3.14)((0.011 m)^^{2}) = 0.00037994 m^2
Velocity = (0.001038541 m^3/s) / (0.00037994 m^2) = 2.73 m/s

6) Humidified air + 200.00 ppb (0.1297 mg/m^3) NH_3:

Flow Rate (Ammonia, Humidified Air)
0.5 L/min flow ammonia into main flow of 62.0 L/min.
0.5 L/min + 62.0 L/min = 62.5 L/min main flow
Ammonia Concentration
(0.5 L/min / 62.5 L/min)(Initial 25,000 ppb NH_3 cylinder concentration) = Final 200.00 ppb NH_3
ppm = ((mg/m^3)(Kelvin constant + temperature ^oC))/((proportionality constant)(gas molecular weight))
Final 200.00 ppb NH_3 / 1000 = 0.2 ppm = ((X mg/m^3)(273.15 + 37^oC))/((12.187)(17.03 g/mol))
Step 1: (12.187)(17.03g/mol) = 207.54461 g/mol => 207.54461 (0.2 ppm) = 41.5089

Step 2: 41.5089 / 310.15^{o}C = 0.13383 mg/m^3
Velocity at this Concentration
Velocity within tube (m/s) = Airflow (m^3/s) / Internal surface area of tube (m^2)
Airflow: 62.5 L/min to m^3/s convert: (62.5 L/min)(0.00001667 constant) = 0.001041875 m^3/s
Internal Surface Area = (pi)(radius^2) = (3.14)((0.011 m)^^{2}) = 0.00037994 m^2
Velocity = (0.001041875 m^3/s) / (0.00037994 m^2) = 2.74 m/s

<u>7) Humidified air + 240.77 ppb (0.1611 mg/m^3) NH_3:</u>

Flow Rate (Ammonia, Humidified Air)
0.3 L/min flow ammonia into main flow of 62.0 L/min.
0.3 L/min + 62.0 L/min = 62.3 L/min main flow
Ammonia Concentration
(0.3 L/min / 62.3 L/min)(Initial 50,000 ppb NH_3 cylinder concentration) = Final 240.77 ppb NH_3
ppm = ((mg/m^3)(Kelvin constant + temperature ^{o}C))/((proportionality constant)(gas molecular weight))
Final 240.77 ppb NH_3 / 1000 = 0.2407 ppm = ((X mg/m^3)(273.15 + 37^{o}C))/((12.187)(17.03 g/mol))
Step 1: (12.187)(17.03g/mol) = 207.54461 g/mol => 207.54461 (0.2407 ppm) = 49.97
Step 2: 49.97 / 310.15^{o}C = 0.1611 mg/m^3
Velocity at this Concentration
Velocity within tube (m/s) = Airflow (m^3/s) / Internal surface area of tube (m^2)
Airflow: 62.3 L/min to m^3/s convert: (62.3 L/min)(0.00001667 constant) = 0.001038541 m^3/s
Internal Surface Area = (pi)(radius^2) = (3.14)((0.011 m)^^{2}) = 0.00037994 m^2
Velocity = (0.001038541 m^3/s) / (0.00037994 m^2) = 2.73 m/s

<u>8) Humidified air + 400.00 ppb (0.26766 mg/m^3) NH_3:</u>

Flow Rate (Ammonia, Humidified Air)
0.5 L/min flow ammonia into main flow of 62.0 L/min.
0.5 L/min + 62.0 L/min = 62.5 L/min main flow
Ammonia Concentration
(0.5 L/min / 62.5 L/min)(Initial 50,000 ppb NH_3 cylinder concentration) = Final 400.00 ppb NH_3
ppm = ((mg/m^3)(Kelvin constant + temperature ^{o}C))/((proportionality constant)(gas molecular weight))
Final 400.00 ppb NH_3 / 1000 = 0.4 ppm = ((X mg/m^3)(273.15 + 37^{o}C))/((12.187)(17.03 g/mol))
Step 1: (12.187)(17.03g/mol) = 207.54461 g/mol => 207.54461 (0.4 ppm) = 83.017
Step 2: 83.017 / 310.15^{o}C = 0.26766 mg/m^3
Velocity at this Concentration
Velocity within tube (m/s) = Airflow (m^3/s) / Internal surface area of tube (m^2)
Airflow: 62.5 L/min to m^3/s convert: (62.5 L/min)(0.00001667 constant) = 0.001041875 m^3/s
Internal Surface Area = (pi)(radius^2) = (3.14)((0.011 m)^^{2}) = 0.00037994 m^2
Velocity = (0.001041875 m^3/s) / (0.00037994 m^2) = 2.74 m/s

9) Humidified air + 481.54 ppb (0.32187 mg/m^3) NH_3:

Flow Rate (Ammonia, Humidified Air)
0.3 L/min flow ammonia into main flow of 62.0 L/min.
0.3 L/min + 62.0 L/min = 62.3 L/min main flow
Ammonia Concentration
(0.3 L/min / 62.3 L/min)(Initial 100,000 ppb NH_3 cylinder concentration) = Final 481.54 ppb NH_3
ppm = ((mg/m^3)(Kelvin constant + temperature ^oC))/((proportionality constant)(gas molecular weight))
Final 481.54 ppb NH_3 / 1000 = 0.481 ppm = ((X mg/m^3)(273.15 + 37^oC))/((12.187)(17.03 g/mol))
Step 1: (12.187)(17.03g/mol) = 207.54461 g/mol => 207.54461 (0.481 ppm) = 99.828
Step 2: 99.828 / 310.15^oC = 0.32187 mg/m^3
Velocity at this Concentration
Velocity within tube (m/s) = Airflow (m^3/s) / Internal surface area of tube (m^2)
Airflow: 62.3 L/min to m^3/s convert: (62.3 L/min)(0.00001667 constant) = 0.001038541 m^3/s
Internal Surface Area = (pi)(radius^2) = (3.14)((0.011 m)^2) = 0.00037994 m^2
Velocity = (0.001038541 m^3/s) / (0.00037994 m^2) = 2.73 m/s

10) Humidified air + 800.00 ppb (0.53533 mg/m^3) NH_3:

Flow Rate (Ammonia, Humidified Air)
0.5 L/min flow ammonia into main flow of 62.0 L/min.
0.5 L/min + 62.0 L/min = 62.5 L/min main flow
Ammonia Concentration
(0.5 L/min / 62.5 L/min)(Initial 100,000 ppb NH_3 cylinder concentration) = Final 800.00 ppb NH_3
ppm = ((mg/m^3)(Kelvin constant + temperature ^oC))/((proportionality constant)(gas molecular weight))
Final 800.00 ppb NH_3 / 1000 = 0.8 ppm = ((X mg/m^3)(273.15 + 37^oC))/((12.187)(17.03 g/mol))
Step 1: (12.187)(17.03g/mol) = 207.54461 g/mol => 207.54461 (0.8 ppm) = 166.03
Step 2: 83.017 / 310.15^oC = 0.53533 mg/m^3
Velocity at this Concentration
Velocity within tube (m/s) = Airflow (m^3/s) / Internal surface area of tube (m^2)
Airflow: 62.5 L/min to m^3/s convert: (62.5 L/min)(0.00001667 constant) = 0.001041875 m^3/s
Internal Surface Area = (pi)(radius^2) = (3.14)((0.011 m)^2) = 0.00037994 m^2
Velocity = (0.001041875 m^3/s) / (0.00037994 m^2) = 2.74 m/s

11) Humidified air + 963.08 ppb (0.64446 mg/m^3) NH_3:

Flow Rate (Ammonia, Humidified Air)
0.3 L/min flow ammonia into main flow of 62.0 L/min.
0.3 L/min + 62.0 L/min = 62.3 L/min main flow
Ammonia Concentration

(0.3 L/min / 62.3 L/min)(Initial 200,000 ppb NH_3 cylinder concentration) = Final 963.08 ppb NH_3
ppm = ((mg/m^3)(Kelvin constant + temperature ^oC))/((proportionality constant)(gas molecular weight))
Final 963.08 ppb NH_3 / 1000 = 0.963 ppm = ((X mg/m^3)(273.15 + 37^oC))/((12.187)(17.03 g/mol))
Step 1: (12.187)(17.03g/mol) = 207.54461 g/mol => 207.54461 (0.963 ppm) = 199.88
Step 2: 199.88 / 310.15^oC = 0.64446 mg/m^3
Velocity at this Concentration
Velocity within tube (m/s) = Airflow (m^3/s) / Internal surface area of tube (m^2)
Airflow: 62.3 L/min to m^3/s convert: (62.3 L/min)(0.00001667 constant) = 0.001038541 m^3/s
Internal Surface Area = (pi)(radius^2) = (3.14)((0.011 m)^^{2}) = 0.00037994 m^2
Velocity = (0.001038541 m^3/s) / (0.00037994 m^2) = 2.73 m/s

12) Humidified air + 1,444.62 ppb (0.96670 mg/m^3) NH_3:

Flow Rate (Ammonia, Humidified Air)
0.3 L/min flow ammonia into main flow of 62.0 L/min.
0.3 L/min + 62.0 L/min = 62.3 L/min main flow
Ammonia Concentration
(0.3 L/min / 62.3 L/min)(Initial 300,000 ppb NH_3 cylinder concentration) = Final 1,444.62 ppb NH_3
ppm = ((mg/m^3)(Kelvin constant + temperature ^oC))/((proportionality constant)(gas molecular weight))
Final 1,444.62 ppb NH_3 / 1000 = 1.444 ppm = ((X mg/m^3)(273.15 + 37^oC))/((12.187)(17.03 g/mol))
Step 1: (12.187)(17.03g/mol) = 207.54461 g/mol => 207.54461 (1.444 ppm) = 299.82
Step 2: 299.82 / 310.15^oC = 0.96670 mg/m^3
Velocity at this Concentration
Velocity within tube (m/s) = Airflow (m^3/s) / Internal surface area of tube (m^2)
Airflow: 62.3 L/min to m^3/s convert: (62.3 L/min)(0.00001667 constant) = 0.001038541 m^3/s
Internal Surface Area = (pi)(radius^2) = (3.14)((0.011 m)^^{2}) = 0.00037994 m^2
Velocity = (0.001038541 m^3/s) / (0.00037994 m^2) = 2.73 m/s

13) Humidified air + 1,600 ppb (1.07067 mg/m^3) NH_3:

Flow Rate (Ammonia, Humidified Air)
0.5 L/min flow ammonia into main flow of 62.0 L/min.
0.5 L/min + 62.0 L/min = 62.5 L/min main flow
Ammonia Concentration
(0.5 L/min / 62.5 L/min)(Initial 200,000 ppb NH_3 cylinder concentration) = Final 1,600.00 ppb NH_3
ppm = ((mg/m^3)(Kelvin constant + temperature ^oC))/((proportionality constant)(gas molecular weight))
Final 1,600.00 ppb NH_3 / 1000 = 1.6 ppm = ((X mg/m^3)(273.15 + 37^oC))/((12.187)(17.03 g/mol))
Step 1: (12.187)(17.03g/mol) = 207.54461 g/mol => 207.54461 (1.6 ppm) = 332.07

Step 2: 332.07 / 310.15^{o}C = 1.07067 mg/m^3
Velocity at this Concentration
Velocity within tube (m/s) = Airflow (m^3/s) / Internal surface area of tube (m^2)
Airflow: 62.5 L/min to m^3/s convert: (62.5 L/min)(0.00001667 constant) = 0.001041875 m^3/s
Internal Surface Area = (pi)(radius^2) = (3.14)((0.011 m)^^{2}) = 0.00037994 m^2
Velocity = (0.001041875 m^3/s) / (0.00037994 m^2) = 2.74 m/s

14) Humidified air + 1,926.16 ppb (1.28883 mg/m^3) NH_3:

Flow Rate (Ammonia, Humidified Air)
0.3 L/min flow ammonia into main flow of 62.0 L/min.
0.3 L/min + 62.0 L/min = 62.3 L/min main flow
Ammonia Concentration
(0.3 L/min / 62.3 L/min)(Initial 400,000 ppb NH_3 cylinder concentration) = Final 1,926.16 ppb NH_3
ppm = ((mg/m^3)(Kelvin constant + temperature ^{o}C))/((proportionality constant)(gas molecular weight))
Final 1,926.16 ppb NH_3 / 1000 = 1.926 ppm = ((X mg/m^3)(273.15 + 37^{o}C))/((12.187)(17.03 g/mol))
Step 1: (12.187)(17.03g/mol) = 207.54461 g/mol => 207.54461 (1.926 ppm) = 399.73
Step 2: 399.73 / 310.15^{o}C = 1.28883 mg/m^3
Velocity at this Concentration
Velocity within tube (m/s) = Airflow (m^3/s) / Internal surface area of tube (m^2)
Airflow: 62.3 L/min to m^3/s convert: (62.3 L/min)(0.00001667 constant) = 0.001038541 m^3/s
Internal Surface Area = (pi)(radius^2) = (3.14)((0.011 m)^^{2}) = 0.00037994 m^2
Velocity = (0.001038541 m^3/s) / (0.00037994 m^2) = 2.73 m/s

15) Humidified air + 2,400.00 ppb (1.60601 mg/m^3) NH_3:

Flow Rate (Ammonia, Humidified Air)
0.5 L/min flow ammonia into main flow of 62.0 L/min.
0.5 L/min + 62.0 L/min = 62.5 L/min main flow
Ammonia Concentration
(0.5 L/min / 62.5 L/min)(Initial 300,000 ppb NH_3 cylinder concentration) = Final 2,400.00 ppb NH_3
ppm = ((mg/m^3)(Kelvin constant + temperature ^{o}C))/((proportionality constant)(gas molecular weight))
Final 2,400.00 ppb NH_3 / 1000 = 2.4 ppm = ((X mg/m^3)(273.15 + 37^{o}C))/((12.187)(17.03 g/mol))
Step 1: (12.187)(17.03g/mol) = 207.54461 g/mol => 207.54461 (2.4 ppm) = 498.10
Step 2: 498.10 / 310.15^{o}C = 1.60601 mg/m^3
Velocity at this Concentration
Velocity within tube (m/s) = Airflow (m^3/s) / Internal surface area of tube (m^2)
Airflow: 62.5 L/min to m^3/s convert: (62.5 L/min)(0.00001667 constant) = 0.001041875 m^3/s
Internal Surface Area = (pi)(radius^2) = (3.14)((0.011 m)^^{2}) = 0.00037994 m^2
Velocity = (0.001041875 m^3/s) / (0.00037994 m^2) = 2.74 m/s

16) Humidified air + 3,200.00 ppb (2.14135 mg/m^3) NH_3:

Flow Rate (Ammonia, Humidified Air)
0.5 L/min flow ammonia into main flow of 62.0 L/min.
0.5 L/min + 62.0 L/min = 62.5 L/min main flow
Ammonia Concentration
(0.5 L/min / 62.5 L/min)(Initial 400,000 ppb NH_3 cylinder concentration) = Final 3,200.00 ppb NH_3
ppm = ((mg/m^3)(Kelvin constant + temperature ^oC))/((proportionality constant)(gas molecular weight))
Final 3,200.00 ppb NH_3 / 1000 = 3.2 ppm = ((X mg/m^3)(273.15 + 37^oC))/((12.187)(17.03 g/mol))
Step 1: (12.187)(17.03g/mol) = 207.54461 g/mol => 207.54461 (3.2 ppm) = 664.14
Step 2: 664.14 / 310.15^oC = 2.14135 mg/m^3
Velocity at this Concentration
Velocity within tube (m/s) = Airflow (m^3/s) / Internal surface area of tube (m^2)
Airflow: 62.5 L/min to m^3/s convert: (62.5 L/min)(0.00001667 constant) = 0.001041875 m^3/s
Internal Surface Area = (pi)(radius^2) = (3.14)((0.011 m)^^{2}) = 0.00037994 m^2
Velocity = (0.001041875 m^3/s) / (0.00037994 m^2) = 2.74 m/s

Average of eight velocities (humid air with ammonia):

(2.73 + 2.74 + 2.73 + 2.74 + 2.73 + 2.74 + 2.73 + 2.74 +2.73 + 2.74 + 2.73 + 2.74 + 2.73 + 2.74 + 2.73 + 2.74) / 16 **= 2.735 m/s**

IV. Internal diameter of tubing (D, m)

Reference: I used digital callipers on spirette tube = **0.022 m**

V. Dynamic viscosity of gas (μ, Pa.s)

Reference: http://www.complore.com/viscosity-gases

Reference (Water vapour): http://www.thermexcel.com/english/tables/vap_eau.htm

Note: Dynamic viscosity of water vapour was taken from density of 0.75 Kg/m^3 of link since this is similar to the 0.745 Kg/m^3 calculated in the density section of this document.

Sutherlands Formula: $\mu = \mu_0 \cdot ((T_0 + C)/(T + C)) \cdot (T/T_0)^{3/2}$

μ_0 = Reference viscosity at reference temperature
T_0 = Reference temperature in Kelvin
T = Input temperature in Kelvin (273 + 37^oC)
C = Sutherlands constant for particular gas

Variable	Air	Ammonia (Gas)	Water (Vapour)
μ_0	0.00001827 Pa.s	0.00000982 Pa.s	-
T_0	291.15 K	293.15 K	-
C	120 K	370 K	-
T	310 K	310 K	-
μ	0.0000192 Pa.s	0.0000104 Pa.s	0.0000130 Pa.s

Average Viscosity: (0.0000192 Pa.s + 0.0000104 Pa.s + 0.0000130 Pa.s) / 3 = 0.0000426 Pa.s / 3 = **0.0000142 Pa.s**

Appendix 3

Ammonia calculations for expected concentrations

(NH_3 flow rate / Sum of flow rates)(Initial NH_3 Concentration) = Expelled NH_3 Concentration (ppb)

NH_3 Flow Rates (L/min)	Humid Air Flow Rates (L/min)	Sum of Flow Rates (L/min)	Initial NH_3 Concentration (ppb)	Expelled NH_3 Concentration (ppbv)
0.30	62.00	62.30	5,000	24.08
0.50	62.00	62.50	5,000	40.00
0.30	62.00	62.30	10,000	48.15
0.50	62.00	62.50	10,000	80.00
0.30	62.00	62.30	25,000	120.39
0.50	62.00	62.50	25,000	200.00
0.30	62.00	62.30	50,000	240.77
0.50	62.00	62.50	50,000	400.00
0.30	62.00	62.30	100,000	481.54
0.50	62.00	62.50	100,000	800.00
0.30	62.00	62.30	200,000	963.08
0.50	62.00	62.50	200,000	1,600.00
0.30	62.00	62.30	300,000	1,444.62
0.50	62.00	62.50	300,000	2,400.00
0.30	62.00	62.30	400,000	1,926.16
0.50	62.00	62.50	400,000	3,200.00

Appendix 4

Healthy Volunteers Ethics Approval

---------- Forwarded message ----------
From: Fiona Brennan<Fiona.Brennan@dcu.ie>
Date: Thu, May 5, 2011 at 11:09 AM
Subject: RE: Ethical Approval - Troy Hibbard
To: Troy Hibbard<troy.hibbard2@mail.dcu.ie>

Hi Troy - if this is part of the same project, and no changes have been made either to the methodology or the documentation being provided to the next cohort of participants, then the ethics approval will stand.

Kind regards, Fiona.

Fiona Brennan
Research Officer
Office of the VP for Research
Invent Building
Dublin City University

-----Original Message-----
From: Troy Hibbard [mailto:troy.hibbard2@mail.dcu.ie]
Sent: 05 May 2011 10:19
To: Fiona Brennan
Subject: Ethical Approval - Troy Hibbard

Dear Fiona,

I have attached a pdf of the ethical approval you sent to us in 2009. The experiments were low-risk non-invasive measurements of breath from volunteers. We will be conducting the exact same experiments with volunteers again soon. If I recall correctly, the approval lasts for the duration of the project which is from January 2009 to January 2012. However, I do not have written documentation stating the approval duration. Is this correct about the duration of the ethical approval given that the procedures are still just breath sampling from volunteers?

Thank you for your time,
Troy

Appendix 5

St. Vincent's University Hospital ethics approval

St. Vincent's Healthcare GROUP LIMITED

UCD DUBLIN

Ethics and Medical Research Committee
ELM PARK, DUBLIN 4
Tel. (01) 2214117 Fax (01) 2214428
email: joan.mcdonnell@ucd.ie or jacinta.mcmanus@ucd.ie

14th September, 2011

Professor A. Watson,
Consultant Nephrologist,
St. Vincent's University Hospital,
Elm Park,
D. 4.

Re: A clinical study on Breath Ammonia Diagnostics involving Haemodialysis Patients.
Application Form. Protocol 2011. Revised PIL/Consent vs 2. Breath Analysis Q.A.

Dear Professor Watson,

Thank you for the revised PIL/Consent and questionnaire that were requested prior to granting full ethical approval at the Ethics and Medical Research Committee meeting held on Wednesday 7th September, 2011 at which the above study was reviewed.

Following review of the revised documents, this study is now granted full ethical approval.

Yours sincerely,

Dr. B. Kirby,
Chairman,
Ethics & Medical Research Committee

cc Mr F. Fleming, National Centre for sensor research, D.C.U.

ELM PARK, DUBLIN 4
DEPARTMENT OF NEPHROLOGY, ST. VINCENT'S UNIVERSITY HOSPITAL

PARTICIPANT INFORMATION AND CONSENT FORM

STUDY TITLE:
A clinical study on breath ammonia diagnostics involving haemodialysis patients

NAME OF PRINCIPAL INVESTIGATOR:
Collaboration:
Prof. Alan Watson (St. Vincent's University Hospital)
Prof. Anthony J. Killard (Dublin City University)

WHAT IS THE PURPOSE OF THIS STUDY?
The aim of the study is to establish whether there is potential for a point-of-care breath ammonia analyser. The analyser is to be used in measuring ammonia levels in the breath of haemodialysis patients with the potential to assist in the treatment and management of patients with kidney disease.

WHY HAVE I BEEN CHOSEN?
You have been chosen because your specific condition could provide valuable information on how to improve current treatment methods.

WHAT WILL HAPPEN IF I VOLUNTEER?
Your participation is entirely voluntary. If you initially decide to take part you can subsequently change your mind without difficulty. This will not affect your future treatment in any way. If you agree to participate, you will be requested to donate breath samples during your regularly scheduled dialysis, and complete an *optional* questionnaire.

You will be asked to provide breath samples by breathing into a machine for approximately 10 minutes.

No additional time and/or visits are required.

ARE THERE ANY BENEFITS FROM MY PARTICIPATION?
You will not benefit directly from taking part in this study, but the information we will obtain may provide further knowledge of this condition.

ARE THERE ANY RISKS INVOLVED IN PARTICIPATING?
As with the normal breathing process, specific risks and discomforts may include dizziness, weakness and sweating. Every effort will be made to minimize risks by creating a safe and comfortable environment in the test location. The equipment that comes into contact with you (mouthpiece, etc.) contains a bacterial / virus filter and is disposed of after use. You will be given

time to rest and recover as needed. It is the participant's responsibility to inform the study investigator if they feel dizzy, ill, or have other symptoms during the breath sampling procedure.

WHAT HAPPENS IF I DO NOT AGREE TO PARTICIPATE?

If you decide not to participate in this study your treatment will not be affected in any way.

CONFIDENTIALITY

Your identity will remain confidential. A study number will identify you. Your name will not be published or disclosed to anyone.

COMPENSATION

Your doctors are adequately insured by virtue of their participation in the clinical indemnity scheme.

WHO IS ORGANISING AND FUNDING THIS RESEARCH?

This research has been organised by the technicians of St. Vincent's University Hospital and Dublin City University under the supervision of the previously acknowledged principle investigators. No additional funding is required since this study is part of a continuous project which has already been established through Enterprise Ireland.

Will I be paid for taking part in this study?

There is no option for payment during this study.

Will my expenses be covered for taking part in this study?

This study will be conducted during already scheduled dialysis and will not result in additional expenses.

HAS THIS STUDY BEEN REVIEWED BY AN ETHICS COMMITTEE?

The St. Vincent's Healthcare Group, Ethics and Medical Research Committee have reviewed and approved this study.

CONTACT DETAILS

Prof. Alan Watson
Department of Nephrology
SVUH
Ph: (01) 2214493

PLEASE TICK YOUR RESPONSE IN THE APPROPRIATE BOX

- I have read and understood the Participant Information YES □ NO □
- I have had the opportunity to ask questions and discuss the study YES □ NO □
- I have received satisfactory answers to all my questions YES □ NO □
- I have received enough information about this study YES □ NO □
- I understand that I am free to withdraw from the study at any time without giving a reason and without this affecting my future medical care YES □ NO □
- I agree to take part in the study YES □ NO □

Participant's Signature: _____ Date: _____

Participant's Name in print: _____

Investigator's Signature: _____ Date: _____

Investigator's Name in print: _____